NASA/TM-20210017131

Compass Final Report: Nuclear Electric Propulsion (NEP)-Chemical Vehicle 1.2

Steven R. Oleson, Laura M. Burke, Lee S. Mason,
Elizabeth R. Turnbull, and Steven McCarty
Glenn Research Center, Cleveland, Ohio

Anthony J. Colozza
HX5, LLC, Brook Park, Ohio

James E. Fittje
Science Applications International Corporation, Brunswick, Ohio

John T. Yim
Glenn Research Center, Cleveland, Ohio

Michael Smith
Oak Ridge National Laboratory, Oak Ridge, Tennessee

Thomas W. Packard
HX5, LLC, Brook Park, Ohio

Brandon T. Klefman
Glenn Research Center, Cleveland, Ohio

John Z. Gyekenyesi
HX5, LLC, Brook Park, Ohio

Brent F. Faller
Glenn Research Center, Cleveland, Ohio

Paul C. Schmitz
Power Computing Solutions Inc., Avon Lake, Ohio

David A. Smith
HX5, LLC, Brook Park, Ohio

Lucia Tian, Caroline R. Austin, W. Peter Simon,
Christopher R. Heldman, Onoufrios Theofylaktos, Christine L. Schmid,
Thomas J. Parkey, and Natalie J. Weckesser
Glenn Research Center, Cleveland, Ohio

Lee A. Jackson
HX5, LLC, Brook Park, Ohio

An Erratum was added to this report May 2023.

September 2021

NASA STI Program . . . in Profile

Since its founding, NASA has been dedicated to the advancement of aeronautics and space science. The NASA Scientific and Technical Information (STI) Program plays a key part in helping NASA maintain this important role.

The NASA STI Program operates under the auspices of the Agency Chief Information Officer. It collects, organizes, provides for archiving, and disseminates NASA's STI. The NASA STI Program provides access to the NASA Technical Report Server—Registered (NTRS Reg) and NASA Technical Report Server—Public (NTRS) thus providing one of the largest collections of aeronautical and space science STI in the world. Results are published in both non-NASA channels and by NASA in the NASA STI Report Series, which includes the following report types:

- TECHNICAL PUBLICATION. Reports of completed research or a major significant phase of research that present the results of NASA programs and include extensive data or theoretical analysis. Includes compilations of significant scientific and technical data and information deemed to be of continuing reference value. NASA counter-part of peer-reviewed formal professional papers, but has less stringent limitations on manuscript length and extent of graphic presentations.

- TECHNICAL MEMORANDUM. Scientific and technical findings that are preliminary or of specialized interest, e.g., "quick-release" reports, working papers, and bibliographies that contain minimal annotation. Does not contain extensive analysis.

- CONTRACTOR REPORT. Scientific and technical findings by NASA-sponsored contractors and grantees.

- CONFERENCE PUBLICATION. Collected papers from scientific and technical conferences, symposia, seminars, or other meetings sponsored or co-sponsored by NASA.

- SPECIAL PUBLICATION. Scientific, technical, or historical information from NASA programs, projects, and missions, often concerned with subjects having substantial public interest.

- TECHNICAL TRANSLATION. English-language translations of foreign scientific and technical material pertinent to NASA's mission.

For more information about the NASA STI program, see the following:

- Access the NASA STI program home page at http://www.sti.nasa.gov

- E-mail your question to help@sti.nasa.gov

- Fax your question to the NASA STI Information Desk at 757-864-6500

- Telephone the NASA STI Information Desk at 757-864-9658

- Write to:
  NASA STI Program
  Mail Stop 148
  NASA Langley Research Center
  Hampton, VA 23681-2199

NASA/TM-20210017131

Compass Final Report: Nuclear Electric Propulsion (NEP)-Chemical Vehicle 1.2

Steven R. Oleson, Laura M. Burke, Lee S. Mason,
Elizabeth R. Turnbull, and Steven McCarty
Glenn Research Center, Cleveland, Ohio

Anthony J. Colozza
HX5, LLC, Brook Park, Ohio

James E. Fittje
Science Applications International Corporation, Brunswick, Ohio

John T. Yim
Glenn Research Center, Cleveland, Ohio

Michael Smith
Oak Ridge National Laboratory, Oak Ridge, Tennessee

Thomas W. Packard
HX5, LLC, Brook Park, Ohio

Brandon T. Klefman
Glenn Research Center, Cleveland, Ohio

John Z. Gyekenyesi
HX5, LLC, Brook Park, Ohio

Brent F. Faller
Glenn Research Center, Cleveland, Ohio

Paul C. Schmitz
Power Computing Solutions Inc., Avon Lake, Ohio

David A. Smith
HX5, LLC, Brook Park, Ohio

Lucia Tian, Caroline R. Austin, W. Peter Simon,
Christopher R. Heldman, Onoufrios Theofylaktos, Christine L. Schmid,
Thomas J. Parkey, and Natalie J. Weckesser
Glenn Research Center, Cleveland, Ohio

Lee A. Jackson
HX5, LLC, Brook Park, Ohio

An Erratum was added to this report May 2023.

National Aeronautics and
Space Administration

Glenn Research Center
Cleveland, Ohio 44135

September 2021

Acknowledgments

The Compass Team would like to thank the following people for their technical expertise advising on portions of the design described herein: Michelle Rucker, Patrick Chai, Dave Jacobson, Michael Meyer, and Jason Hartwig. This work was done in support of the Mars Transportation Assessment Study. The team would also like to thank the Exploration Systems Mission Directorate and the Space Technology Mission Directorate for their support.

Erratum

Issued May 2023 for

NASA/TM-20210017131
Compass Final Report: Nuclear Electric Propulsion (NEP)-Chemical Vehicle 1.2
Steven R. Oleson, Laura M. Burke, Lee S. Mason, Elizabeth R. Turnbull, Steven McCarty,
Anthony J. Colozza, James E. Fittje, John T. Yim, Michael Smith, Thomas W. Packard, Brandon T. Klefman,
John Z. Gyekenyesi, Brent F. Faller, Paul C. Schmitz, David A. Smith, Lucia Tian, Caroline R. Austin,
W. Peter Simon, Christopher R. Heldman, Onoufrios Theofylaktos, Christine L. Schmid,
Thomas J. Parkey, Natalie J. Weckesser, and Lee A. Jackson

September 2021

Figure 4-35: Remove the words “upper” and “lower” in the support struts callouts.

Level of Review: This material has been technically reviewed by technical management.

Available from

NASA STI Program
Mail Stop 148
NASA Langley Research Center
Hampton, VA 23681-2199

National Technical Information Service
5285 Port Royal Road
Springfield, VA 22161
703-605-6000

This report is available in electronic form at http://www.sti.nasa.gov/ and http://ntrs.nasa.gov/

Contents

LIST OF FIGURES

LIST OF TABLES

Compass Final Report: Nuclear Electric Propulsion (NEP)-Chemical Vehicle 1.2

Steven R. Oleson, Laura M. Burke, Lee S. Mason,
Elizabeth R. Turnbull, and Steven McCarty
National Aeronautics and Space Administration
Glenn Research Center
Cleveland, Ohio 44135

Anthony J. Colozza
HX5, LLC
Brook Park, Ohio 44142

James E. Fittje
Science Applications International Corporation
Brunswick, Ohio 44212

John T. Yim
National Aeronautics and Space Administration
Glenn Research Center
Cleveland, Ohio 44135

Michael Smith
Oak Ridge National Laboratory
Oak Ridge, Tennessee 37830

Thomas W. Packard
HX5, LLC
Brook Park, Ohio 44142

Brandon T. Klefman
National Aeronautics and Space Administration
Glenn Research Center
Cleveland, Ohio 44135

John Z. Gyekenyesi
HX5, LLC
Brook Park, Ohio 44142

Brent F. Faller
National Aeronautics and Space Administration
Glenn Research Center
Cleveland, Ohio 44135

Paul C. Schmitz
Power Computing Solutions Inc.
Avon Lake, Ohio 44012

David A. Smith
HX5, LLC
Brook Park, Ohio 44142

Lucia Tian, Caroline R. Austin, W. Peter Simon,
Christopher R. Heldman, Onoufrios Theofylaktos,
Christine L. Schmid, Thomas J. Parkey, and
Natalie J. Weckesser
National Aeronautics and Space Administration
Glenn Research Center
Cleveland, Ohio 44135

Lee A. Jackson
HX5, LLC
Brook Park, Ohio 44142

1.0 Introduction

Many previous studies have examined sending crews to and from Mars. The most economical involved a 'conjunction' class whereby the crew spends around 500 days on Mars waiting for a 'cheap' return. The total mission time results in over a 1000-day mission duration (about 3 years). Given the current experience level of only one year on the International Space Station (ISS), it of interest to reduce that time to only two years, thus reducing risk and minimizing required Mars surface infrastructure. The Phase 1.1 Study goal was stated as follows, "Determine the feasibility of a two-year roundtrip class Mars mission concept of operation that enables boots on Mars no later than 2036." [1] While the Phase1 study did show feasibility for the NEP-Chemical option, the 2036 Opposition opportunity was found to stress the schedule due to proposed technology development schedules. A 2039 Opposition (which requires even more energy than the 2036 case) was chosen as representative for Phase 1.2. Phase 1.2 also sought to further refine the concept, building on the feasibility, but addressing several challenges brought by the red team and habitat team.

Given the date of 2039, nearer term technologies, primarily nuclear thermal and nuclear electric were deemed as the most viable for these missions. As will be shown, the energy required to perform such a mission in only two years (for the 2039 opportunity at least) is about three times that of the three-year conjunction mission. The rocket equation (Equation 1 below) shows that this mission would then require several times the propellant of the three-year mission unless the specific impulse (I_{SP}) of the propulsion system can be increased.

Equation 1 $\mathbf{M_{propellant} = M_{initial}\,(1-\exp(-\Delta V/(Isp*g))}$

Based on lunar needs, a limit of five Space Launch System (SLS) launchers with 8.4 m fairings was imposed for the piloted transportation portion of the mission, limiting the size of the system. When using nuclear electric propulsion, the main limiting factor was packaging the required radiator area.

The higher I_{sp} nuclear electric propulsion (NEP) system option is described herein but with a twist: in order to keep the size of radiators packageable in one SLS and use proven reactor power system technology (~1200 K reactor outlet temperature and superalloy-class Brayton) the NEP system had to be combined with a chemical propulsion system. This combination of electric propulsion and high thrust chemical was found to be useful in previous design studies combining solar electric propulsion (SEP) and chemical propulsion [2]. Such a combination allowed the low-thrust system to provide significant change in velocity (ΔV) during the interplanetary portions of the mission, thereby notably reducing the ΔV required by the high thrust system to capture and depart from the Mars gravity well. Here the high thrust 'impulsive' system is more efficient due to the Oberth Effect [3].

A plethora of trades, both at the mission and system level, as well as the subsystem level were performed to develop these vehicle concepts. The most important will be described in each appropriate section in detail. A pictorial summary showing the design evolution is shown in Figure 2-1.

An entire family of NEP-Chemical transportation vehicles is described herein. The main driver and the primary focus was the piloted vehicle, shown in Figure 1-1, but additional concepts for cargo were performed using the same 'building blocks' in order to reduce costs and provide commonality. The cargo options are described in APPENDIX B.

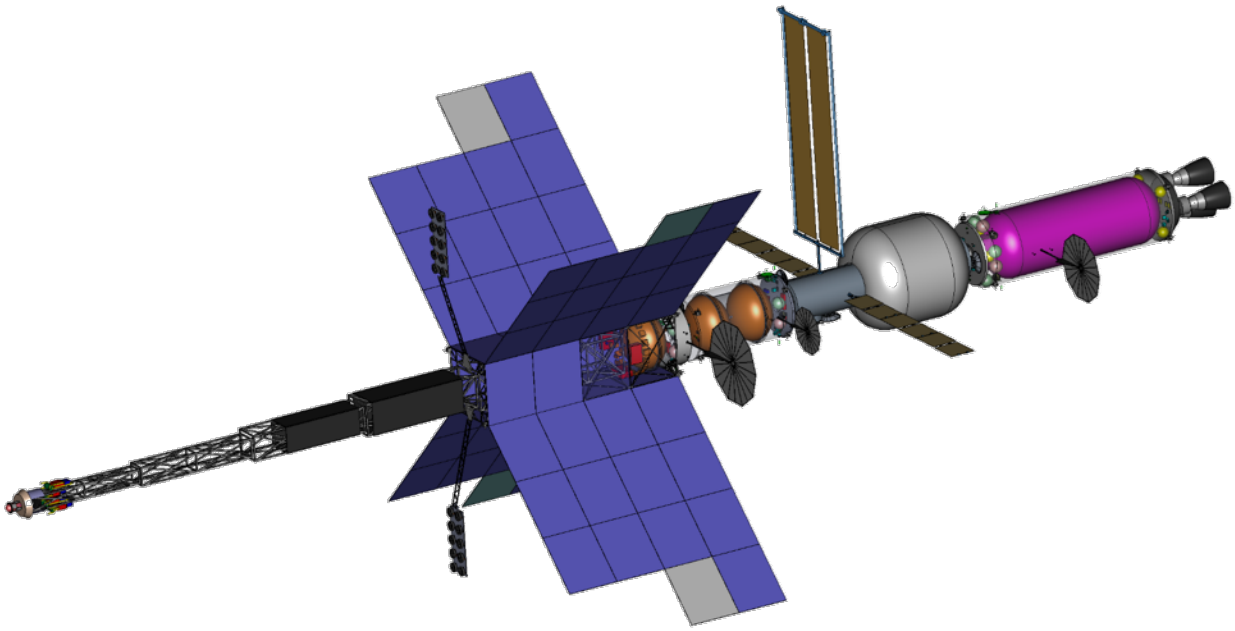

Figure 1-1 Vehicle Illustration

2.0 Study Background and Assumptions

2.1 Vehicle Concept Trade Evolution

A brief description of the design evolution of the 1.2 concept from the pre-MTAS SEP-chem concept to the MTAS NEP-Chem 1.1 concept to the final MTAS NEP-Chem concept is shown in Figure 2-1.

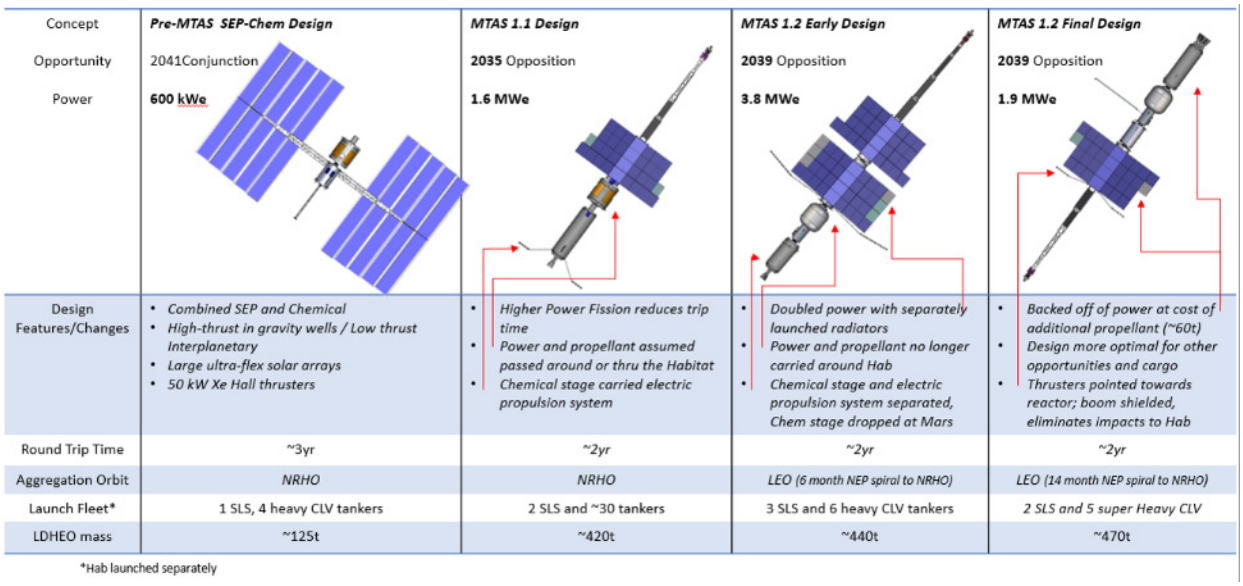

Figure 2-1 MTAS NEP-Chem Design Evolution

The 1.1 NEP-Chem concept was based on past work on the SEP-Chem concepts for three-year Mars conjunction missions. The SEP-Chem concept used solar power instead of nuclear but otherwise utilized the electric propulsion and chemical propulsion in a similar way—by using impulsive chemical for departure from and capture at the gravity wells and the SEP for reducing the required chemical burns. The SEP was so helpful for the conjunction mission that the chemical propellant could be easily combined with the SEP system using a single SLS launch. While SEP-chem was ruled out for the MTAS study, future analyses will look at just how big an SEP-chem system would need to be to perform the Mars opposition mission.

The 1.2 Mars Transportation Assembly Study (MTAS) design iteration started with the 1.1 concept. This concept was the pathfinder that showed that a combination of NEP and chemical can perform a two-year opposition crew mission for 2035. The Compass Team found two potential shortcomings in the conceptual design; a large requirement of commercial launch vehicle (CLV) propellant tankers to fuel up the vehicle at near-rectilinear halo orbit (NRHO) (~30) and the need to pass both high power [1.5 Megawatts electric (MWe)] and xenon propellant through or around the notional habitat. The electric propulsion system was also integrated into the chemical stage – thus not allowing the stage to be ‘dropped’ and provide staging benefits in reducing mass.

With the start of the 1.2 Phase of the study, the MTAS Programmatic sub-team recommended pushing the first piloted use date to 2039 to allow for sufficient time to develop and test the required technologies. This 2039 opportunity increases the required ΔV compared to the 2035 opportunity; the 2039 opportunity represents a nearly ‘worst case’ in mission energy requirements for Mars opposition missions. (See Section 2.4 Mission Description for trajectory explanations.) In order to provide the higher ΔV and still perform the mission in a roughly two year round trip the power level was more than doubled to 3.8 MWe. This was achieved by increasing the size of the reactor and doubling the number of Brayton convertors and the radiator area. In order to use the 1.1 radiator design (configured to fit in a single 8.4 m SLS fairing) an additional radiator ‘pack’ was provided to double the area when docked to the power module. Simultaneously, the electric propulsion system was moved to this element with the second radiator pack along with the xenon storage tanks. Thus, the Electric Propulsion Element was separated from the chemical stage and also carried half of the radiators. This would require passing coolant across an interface mated in space but similar (albeit at lower temperature) matings have been successfully made on the ISS. The chemical stage was now

completely separated from the NEP system and could be dropped (or staged) at Mars when the high thrust was no longer needed.

The other major change from 1.1 was assembling and commissioning the transportation system in low earth orbit. This was chosen to allow the high I_{SP} electric propulsion system to more efficiently carry itself and its propellant to NRHO to pick up the Habitat Element (previously launched and in use.) This greatly reduced the required CLV fleet by about a factor of five. However, it did come at the price of a low thrust spiral from low earth orbit (LEO) to NRHO which required about 100 metric tons (t) of Xenon propellant and seven months of thrusting. It was found that the radiation degradation from the belts was <10 kilorad [(radiation absorbed dose) krad] for the transportation system assuming 10 mm shielding on the electronics.

An additional constraint on starting the reactor in a safe orbit was added necessitating lifting the vehicle from the chosen 500 km assembly orbit to 1100 km using the chemical stage. 1100 km was chosen based on the SNAP-10A orbit. The 500 km assembly orbit (with cold reactor encapsulated in a notional 1000 kilogram (kg) reentry shield) was chosen based on a combination of maximizing launcher performance, minimizing radiation and orbital debris, as well as allowing for crew assistance in assembling the vehicle.

At this point in the study several factors diverted the Compass Team from this 3.8 MWe point. First, the power team found that using supercritical carbon dioxide (CO_2) Brayton systems and a single launched radiator pack could provide 1.9 MWe of power for the NEP system. Secondly, the study leadership allowed for decrementing I_{SP} of the propulsion systems to represent using propellant margin continuously instead of carrying propellant margin all the way back to Earth. This reduced the return mass at earth by over 20 t and allowed for lowering the NEP power required to do the mission. Subsequently it was found that a 1.9 MWe NEP-Chemical vehicle could perform the 2039 mission with an acceptable increase in chemical propellant compared to the 3.8 MWe NEP-Chemical vehicle (added about 60 t of chemical propellant). In addition, the team found that the 1.9 MWe vehicle performed the easier opposition missions (like 2035 and 2042) better than the 3.8 MWe vehicle (see Section 2.4 Mission Description.)

The 1.9 MWe NEP-Chemical Vehicle was the endpoint of the 1.2 conceptual design study. Similar to the 3.8 MWe design point it was assembled and fueled in 500 km and then boosted to 1100 km to activate its reactor and spiral to NRHO. Due to its halved NEP power, the mission would require 14 months to spiral from 1100 km to NRHO but, as before, the belt radiation was found to be acceptable (~10 krad). One final tweak provided by the study leads was allowing the use of a super heavy class of CLV. Taking the designs of Super Heavy CLV currently in development as representative allowed for ~100 t of payload launch to LEO. This allowed for the elimination of an SLS from the launch requirements and reduced the number of total launches to 2 SLS and 5 Super Heavy CLV for the piloted transportation vehicle for 2039.

The 1.9 MWe NEP-Chemical vehicle conceptual design also benefited from many subsystem trades. Each of these are described under Section 4.0 SUBSYSTEM BREAKDOWN. One in particular had a major impact on the configuration. Plume studies looking at both the erosion and deposition from the electric thrusters showed that the 3.8 MWe design with the thrusters pointed aft would cause some erosion and deposition on the surfaces of the habitat and chemical stage. While the magnitude would not cause structural concerns it could cause deposition on radiator and optical systems. While these could be mitigated, the Compass Team decided that given the preliminary design maturity of the habitat, a non-invasive placement of the electric thrusters should be considered. Three major options became apparent. First was placing the electric propulsion module aft of the habitat and once again passing high power through or around the habitat, perhaps with an arm. This option should be considered in future studies once the habitat design is finalized to evaluate its feasibility. Second was splitting up the electric propulsion and chemical propulsion systems and surrounding the habitat to allow for the power to flow around the habitat to the electric propulsion systems and the thruster plumes to point aft of all of the other elements. This option would make the configuration complex, require an arm, and block many of the habitat systems (i.e., radiators, solar arrays, docking ports, etc.). The final option considered placing the electric thrusters on short booms pointing towards the reactor end of the NEP-Chemical vehicle. While this would cause erosion and deposition of the boom and the reactor, the team found that it could be easily mitigated by a thin layer of pyrolytic graphite paper or equivalent (<500 kg) impact. With this solution even the back sputter on the main radiators was found to be minimal. Placement of the thrusters on the NEP Module eliminated the need for high power connections to other elements but would increase the radiation impact to the thrusters to over 100 krad. Preliminary analyses show this should be acceptable but further work is needed. From a design perspective, placing the electric propulsion system on the power module eliminates many integration challenges with habitats, chemical stages, and cargos; the reactor

radiation and thruster plume are all on one end of the vehicle which opens the rest of the vehicle to other systems. A full analyses of the plume impacts is shown in the propulsion section.

The final design elements of the 1.9 MWe NEP-Chem vehicle included the NEP Module (all power, electric propulsion and 50 t of xenon), the Xenon Interstages (super heavy launched, the number needed dependent upon opportunity), and a large liquid oxygen (LOX)/liquid methane (LCH4) chemical stage. The chemical stage was kept on an SLS launcher to maximize the volume to surface area ratio and minimize the mass of the stage and the zero boil off systems. It is recommended that future studies look at large, next generation, commercial chemical stage solutions as an alternative.

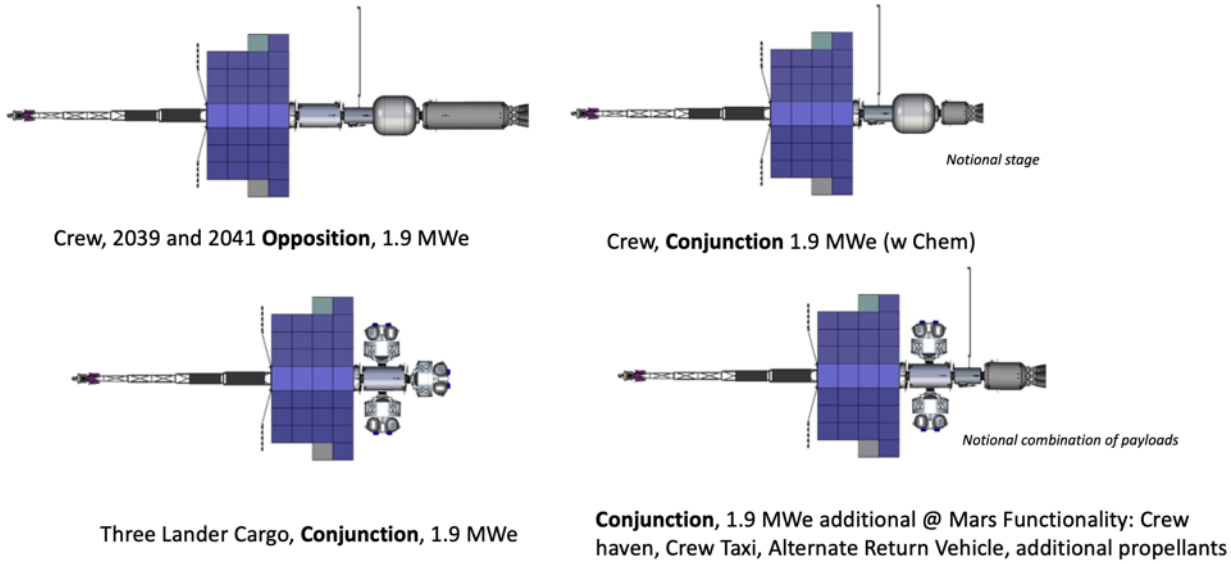

Figure 2-2 Post 2039 NEP-Chemical Family of Vehicles

By mixing these elements (NEP Module, Xenon Interstage, Chemical Stage) many different missions can be envisioned as shown in Figure 2-2. First a cargo mission carrying three large landers could be achieved using just an NEP Module and a single Xenon interstage. (See APPENDIX B for the first cargo mission's description.) NEP-Chemical can also be used for piloted conjunction missions, albeit with much less propellant. NEP cargo vehicles could also pre-position propellants and even return vehicles. Another consideration would be conjunction missions using just an NEP Module and a small chemical stage (sized dependent on opportunity difficulty). Landers with the crew habitat could be carried using the same elements from the 2039 opposition mission if a conjunction mission is considered. An NEP cargo mission could also carry a taxi (to carry crew to and from landers in a low Mars orbit and the piloted vehicle in a higher Mars orbit) to allow minimizing the size of the Mars ascent vehicle (MAV). Finally, a cargo mission could carry two landers plus a return habitat and xenon for an alternate path home. In general, the required launch fleet for these other opportunities (piloted conjunction, cargo, taxi, etc.) is reduced from the 2039 piloted opposition case. The single common element is the 1.9 MWe NEP Module. These mission options are fully described in the mission section below.

This document focuses on the 2039 Piloted Opposition mission and its spacecraft elements. The next section is the listing of ground rules and assumptions and margin/growth approaches. Next, the trajectory design is described followed by the concept of operations (CONOPS). After an explanation of the final configuration and the top-level spacecraft mass and power equipment lists, each subsystem is described in detail. Lessons Learned and Next Steps concludes the document. The Cargo option is presented in APPENDIX B.

2.2 Assumptions and Approach

Although the full list of ground rules and assumptions (GR&A) can be found in APPENDIX A, the primary driving GR&A are included below. Additional, subsystem level assumptions and approaches are detailed in each subsystem section.

2.2.1 Ground Rules and Assumptions Summary

The primary driving ground rules and assumptions are summarized below. A complete listing can be found in APPENDIX A. Cargo requirements are also summarized in APPENDIX B.

Mars Mission:

- Boots on Mars no later than 2036.
- No less than thirty days Surface Stay Time.
- Orbit insertion, departure, rendezvous maneuvers need to be included in Mars total orbit time (in addition to surface stay time), two Mars orbital periods on either side.
- Total Crew time away from Earth: ~ two years or less.
- 760 days or less from Trans-Mars Injection to Earth Orbit Capture.
- Propulsion performance and vehicle capabilities must envelope 2039 mission under the same ground rules.
- Earth Orbit:
    - Ninety-day launch window for crew prior to trans-Mars injection (TMI).
    - Thirty-day launch window for crew post-Earth-orbit insertion (EOI).
- Mars Orbit:
    - Two rendezvous opportunities after Mars orbit insertion (MOI) with crew lander.
    - Two rendezvous opportunities prior to trans-Earth injection (TEI) with ascent stage.

Launchers

- Average of one SLS cargo per year to support Mars activity, can surge to two in one year.
- Heavy and super heavy class assumed available.
- No limitation on CLV launch rate, though desire to minimize peaks in launch demand.
- CLV boost stage or service module to move elements around for aggregation must be developed.

Habitat

- Deep-Space Habitat (DSH), is deployed by CLV to NRHO, it can be self-sufficient in NRHO or near Gateway, but does not have propulsive capability to move away from NRHO.
- DSH launched on two (2) CLVs without logistics to cis-lunar.
- DSH must return to NRHO/Gateway post Mars mission.
- No power and propellant pass through the DSH.
- DSH power system sized to provide 20 kWe end of life (EOL) power at 1 astronomical unit (AU); Deep-Space Transport (DST) must provide power (at least) to make up for shortfall in power as it goes beyond 1AU.
- DSH must be able to easily dock/undock from the transportation elements.
- DSH must be able to support docking with Orion while attached to the transport.
- Operational empty mass of 26.4 t.
- Additional habitat masses: 4 Crew: 328 kg, payloads and research: 1000 kg, propulsion and reaction control system (RCS) expendables: 337 kg, trash dump: 11.1 kg/day
- Crew radiation limits: undefined (radiation impact from reactor designed to be on the same order or less than that of the space background.)

Technologies

- See 4.0 SUBSYSTEM BREAKDOWN, APPENDIX A, and APPENDIX B.

Programmatic

- Reference case is to be “minimally viable.”
- Propulsion system for the first mission will not be reused.
- Minimize crew time away from Earth.
- Identify potential assets, capabilities, systems, and subsystems, required to conduct current lunar program can be used, within stated limits, to support the Mars transportation development and CONOPS.
- Identify technology to improve performance, mitigate risk, and/or reduce cost.

Margin and Growth Strategy

- Align with Human Exploration Office (HEO) XM-M14282020A margin memorandum [4].

Redundancy

- All systems must be single fault tolerant except propellant tanks and structures.

2.2.2 Figures of Merit (FOM)

The Compass Team used largely qualitative parameters to define figures of merit (FOM) and guide the subsystem. The FOM for this design focused more on system performance than on current technology readiness level (TRL) or cost. For this design study, the Compass Team assumed the following FOM:

- Feasibility
- Number of SLS
- SLS Cadence
- Dual lunar/Mars Campaign launch requirements
- Number of CLV
- Cadence
- Simplicity
- Risk

2.2.3 Redundancy

While this mission is crewed, the customer directed the design be only single fault tolerant for this iteration. Future studies which focus on loss of mission versus loss of crew and abort options will further investigate required redundancies. Top-level redundancies include spare Hall-effect thrusters, chemical thrusters, and multiple path radiator loops. Propellant tanks and structures are not required to be fault tolerant.

2.3 Growth, Contingency, and Margin Policy

The mass growth, contingency, and mass margin policy used by the Compass Team is congruent with the standards described in AIAA S–120A-2015(2019) [5]. This methodology starts with the basic mass of the components and adds the mass growth allowance (MGA). This subtotal is defined as the predicted mass. Mass margin is then added to the predicted mass to calculate the allowable mass. The aerospace community typically refers to the mass margin as system level growth. This methodology is consistent with the HEO memorandum [4] on margin required in the ground rules and assumptions.

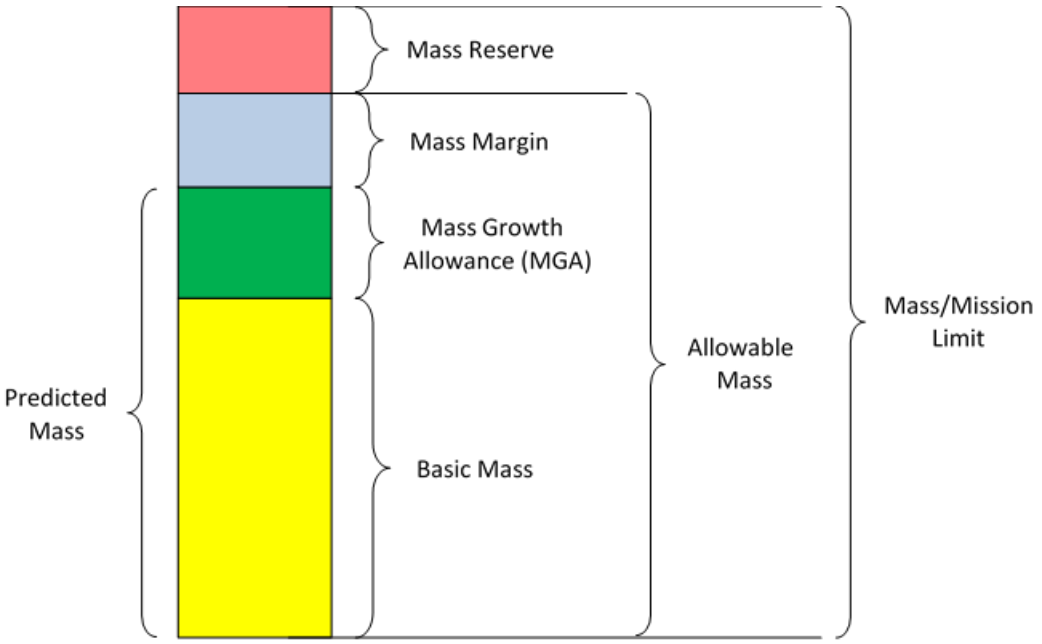

Figure 2-3 Graphic of General Mass Definitions

2.3.1 Terms and Definitions Regarding Mass

Mass	*The measure of the quantity of matter in a body.*
Basic Mass (aka CBE Mass)	*Mass data based on the most recent baseline design. This is the bottoms-up estimate of component mass, as determined by the subsystem leads.* *Note 1: This design assessment includes the estimated, calculated, or measured (actual) mass, and includes an estimate for undefined design details like cables, multi-layer insulation, and adhesives.* *Note 2: The MGAs and uncertainties are not included in the basic mass.* *Note 3: Compass has referred to this as current best estimate (CBE) in past mission designs.* *Note 4: During the course of the design study, the Compass Team carries the propellant as line items in the propulsion system in the Master Equipment List (MEL). Therefore, propellant is carried in the basic mass listing, but MGA is* ***not*** *applied to the propellant. Margins on propellant are handled differently than they are on dry masses.*
CBE Mass	*See Basic Mass.*
Dry Mass	*The dry mass is the total mass of the system or spacecraft (S/C) when no propellant or pressurants are added.*
Wet Mass	*The wet mass is the total mass of the system, including the dry mass and all of the pressurants and propellants (used, predicted boil-off, residuals, reserves, etc.*
Inert Mass	*In simplest terms, the inert mass is what the trajectory analyst plugs into the rocket equation in order to size the amount of propellant necessary to perform the mission delta-Velocities (ΔVs). Inert mass is the sum of the dry mass, along with any non-used, and therefore trapped, wet materials, such as residuals and pressurants. When the propellant being modeled has a time variation along the trajectory, such as is the case with a boil-off rate, the inert mass can be a variable function with respect to time.*

Basic Dry Mass	*This is basic mass (aka CBE mass) minus the propellant, or wet portion of the S/C mass. Mass data is based on the most recent baseline design. This is the bottoms-up estimate of component mass, as determined by the subsystem leads. This does not include the wet mass (e.g., propellant, pressurant, cryo-fluids boil-off, etc.).*
CBE Dry Mass	*See Basic Dry Mass.*
Mass Growth Allowance (MGA)	*MGA is defined as the predicted change to the basic mass of an item based on an assessment of its design maturity, fabrication status, and any in-scope design changes that may still occur.*
Predicted Mass	*This is the basic mass plus the mass growth allowance for to each line item, as defined by the subsystem engineers.* *Note: When creating the MEL, the Compass Team uses Predicted Mass as a column header, and includes the propellant mass as a line item of this section. Again, propellant is carried in the basic mass listing, but MGA is not applied to the propellant. Margins on propellant are handled differently than they are handled on dry masses. Therefore, the predicted mass as listed in the MEL is a wet mass, with no growth applied on the propellant line items.*
Predicted Dry Mass	*This is the predicted mass minus the propellant or wet portion of the mass. The predicted mass is the basic dry mass plus the mass growth allowance as the subsystem engineers apply it to each line item. This does not include the wet mass (e.g., propellant, pressurant, cryo-fluids boil-off, etc.).*
Mass Reserve (aka Margin)	*This is the difference between the allowable mass for the space system and its total mass. Compass does not set a mass reserve, it is arrived at by subtracting the total mass of the design from the design requirement established at the start of the design study, such as an allowable mass. The goal is to have a mass reserve greater than or equal to zero in order to arrive at a feasible design case. A negative mass reserve would indicate that the design has not yet been closed and cannot be considered feasible. More work would need to be completed.*
Mass Margin	*The extra allowance carried at the system level needed to reach the AIAA recommended "green" mass risk assessment level, which is currently set at >15% for the Authorization to Proceed program milestone. This value is defined as the difference between allowable mass and predicted mass, with the percentage being with respect to basic mass:* *% Mass Margin = (Allowable Mass - Predicted Mass)/Basic Mass*100* *For the current Compass design process, a mass margin of 15% is applied with respect to the basic mass and added to the predicted mass. The resulting total mass is compared to the allowable mass as the design progresses. If the total mass is < than the allowable mass, then the mass margin is > 15% and the design closes while maintaining a "green" mass risk assessment level.* *If total mass ≥ allowable mass, then the design does not close with the required 15% mass margin, and either the total mass needs to be reduced, or the mass risk posture reevaluated and the mass margin reduced. However, depending on the numerical difference, the design may not close even if the mass margin is set to 0%.*
System-Level Growth	*See Mass Margin*
Total Mass	*The summation of basic mass, applied MGA, and the mass margin (aka system-level growth).*
Allowable Mass	*The limits against which margins are calculated.* *Note: Derived from or given as a requirement early in the design, the allowable mass is intended to remain constant for its duration.*

Table 2-1 expands definitions for the MEL column titles to provide information on the way masses are tracked through the MEL used in the Compass design sessions. These definitions are consistent with those above in Figure 2-3 and in the terms and definitions. This table is an alternate way to present the same information to provide more clarity.

Table 2-1 Definition of Masses Tracked in MEL

Item	Definition
Basic Mass	Mass data based on the most recent baseline design (includes propellants and pressurants)
	Basic Dry Mass + Propellants + Pressurants + Residuals
MGA (Growth)	Predicted change to the basic dry mass of an item phrased as a percentage of basic dry mass
	MGA% * Basic Dry Mass = Growth
Predicted Mass	The basic mass plus the MGA
	Basic Dry Mass + Propellant + Growth

For the conceptual level studies conducted by the Compass Team, a mass margin of 15% based on basic dry mass is used, which is recommended in the AIAA standard [5] for a grade of "green" at the authorization to proceed milestone, as is shown in Table 2-2. It is worth noting that we assume 30% MGA + Mass Margin is suitable for a green rating, assuming that there is more allowable mass that would fit to push the percentage slightly above 30%. For all elements designed by the Compass Team for this study, a "green" rating was achieved across the board.

Table 2-2 Mass Risk Assessment

Program Milestone	Recommended MGA (%)	Recommended Mass Margin (%)	MGA + Mass Margin (%)	Grade
Authorization to Proceed	> 15	> 15	> 30	Green
	9 < MGA ≤ 15	10 < Mass Margin ≤ 15	19 < MGA + Mass Margin ≤ 30	Yellow
	≤ 9	≤ 10	≤ 19	Red

2.3.2 Mass Growth

In keeping with the in AIAA standard S–120A-2015(2019), Table 2-3 on the following page shows the percent mass growth of a piece of equipment based on both its level of design maturity and its functional subsystem. Note that for designs requiring propellant, propellant margin and residual is either carried in the propellant calculation itself or in the ΔV calculation used to determine the propellant required to fly a mission. Section 2.4.4.3 explicitly details how propellant margins were handled for each leg of the mission and each propellant type.

Table 2-3 AIAA Mass Growth Allowance Guidelines from AIAA S–120A-2015(2019) [5]

Maturity Code		Design Maturity (Basis for Mass Determination)	Percentage Mass Growth Allowance												
			Electrical/Electronic Components			Primary Structure	Secondary Structure	Mechanisms	Propulsion, Fluid Systems Hardware	Batteries	Wire Harnesses	Solar Array	ECLSS, Crew Systems	Thermal Control	Instrumentation
			0-5 kg	5-15 kg	>15 kg										
E	1	**Estimated**	20-35	15-25	10-20	18-25	20-35	18-25	15-25	20-25	50-100	20-35	20-30	30-50	25-75
	2	**Layout**	15-30	10-20	5-15	10-20	10-25	10-20	10-20	10-20	15-45	10-20	10-20	15-30	20-30
C	3	**Preliminary Design**	5-20	3-15	3-12	4-15	8-15	5-15	5-15	5-15	10-25	5-15	5-15	8-15	10-25
	4	**Released Design**	5-10	2-10	2-10	2-6	3-8	3-4	2-7	3-7	3-10	3-5	3-8	3-8	3-5
A	5	**Existing Hardware**	1-5	1-3	1-3	1-3	1-5	1-3	1-3	1-3	1-5	1-3	1-4	1-3	1-3
	6	**Actual Mass**	Measured mass of specific flight hardware; no MGA; use appropriate measurement uncertainty.												
S	7	**CFE or Specification Value**	Typically, an NTE value is provided, and no MGA is applied.												

Expanded Definitions of Maturity Categories		
E1	**Estimated**	a. An approximation based on rough sketches, parametric analysis, or incomplete requirements. b. A guess based on experience. c. A value with unknown basis or pedigree.
E2	**Layout**	a. A calculation or approximation based on conceptual designs (layout drawings or models) prior to initial sizing. b. Major modifications to existing hardware.
C3	**Preliminary Design**	a. Calculations based on new design after initial sizing but prior to final structural, thermal, or manufacturing analysis. b. Minor modification of existing hardware.
C4	**Released Design**	a. Calculations based on a design after final signoff and release for procurement or production. b. Very minor modification of existing hardware.
A5	**Existing Hardware**	a. Measured mass from another program, assuming that hardware will satisfy program requirements with no changes. b. Values substituted based on empirical production variation of same or similar hardware or qualification hardware. c. Catalog values.

Note: The MGA percentage ranges in the above table are applied to the basic mass to arrive at the predicted mass.

2.3.3 Power Growth

The Compass Team typically uses a 30% growth on the bottoms-up power requirements of the bus subsystems when modeling the amount of required power. There is an exception, however, for the electric propulsion subsystem. If present, only 5% growth is applied to the power requirements needed for the electric thrusters. No additional margin is carried on top of this power growth.

2.4 Mission Description

2.4.1 Path to 1.2

For the 2035 piloted opposition 1.1 MTAS design, a plot of Earth departure mass versus electric propulsion (EP) power level was created to compare the results of NEP-Chem [using liquid oxygen/liquid methane (LOX/LCH_4) for the chemical propulsion system] and all-NEP (Figure 2-4). Producing equivalent mission performance at a significantly lower power level led to the down selection to NEP-Chem for Phase 1.1. Due to the desire to limit the number of SLS launches required for this vehicle and radiator packaging constraints, the fairing radiator area is limited to 2500 m^2. This radiator area for a 1200 K reactor corresponds to approximately 1.5 megawatt (MW) EP power (see Table 4-1 in Section 4.1.2). Since this value was near the optimal power level for the 1200 K NEP-Chem curve, it was baselined as the power level for the Phase 1.1 design.

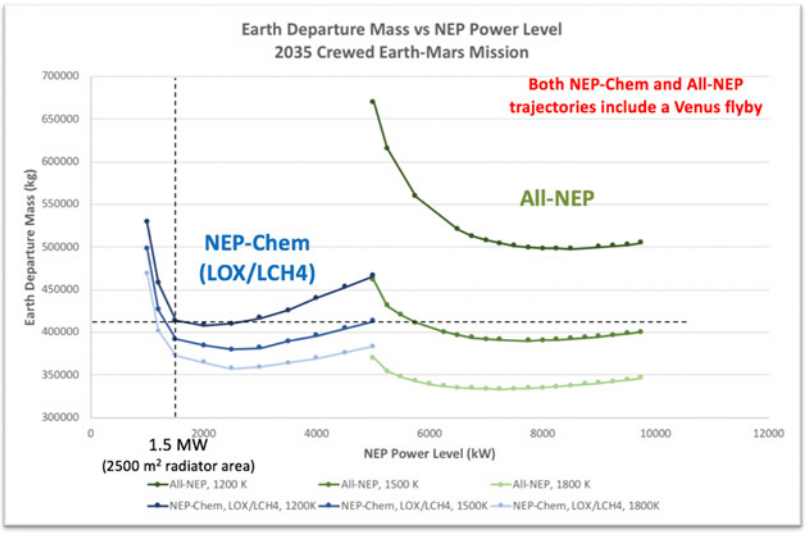

Figure 2-4 Comparison of NEP-Chem to all-NEP for the Crewed 2035 Earth-Mars Opposition Mission

For the Phase 1.2 design, a more difficult mission opportunity (2039) was selected in order to ensure the NEP-Chem vehicle would be capable of performing the piloted mission for a wider range of opportunities. The initial analysis for Phase 1.2 utilized the same assumptions as Phase 1.1: a 1.5 MW NEP-Chem vehicle that carried all elements and unused propellant margin for the entire mission. The Phase 1.2 propellant margin can be over 10 t. Maintaining these assumptions for 2039 required a considerably larger propellant load. Several assumptions were gradually altered to reduce the propellant load to near-2035 levels. Initially, the reactor was updated to 1200 K High-Assay Low Enriched Uranium (HALEU)/supercritical carbon dioxide ($scCO_2$), which increased the power level associated with a 2500 m^2 radiator to 1.8 MW (to the EP thrusters) and two SLS launches were dedicated to the radiators resulting in a 3.6 MW NEP-Chem vehicle. Other assumptions were modified following this including the decision to drop the chemical stage following the TEI burn. Eventually when the 2035 opportunity was reanalyzed with these new assumptions it was evident that the spacecraft was overpowered for these easier opportunities. Although a 1.8 MW reactor does not perform as well for the 2039 opportunity (requires about 40 t more chemical propellant), it reduced the Earth Departure Mass (EDM) for 2035 compared to the 3.6 MW design. It also reduced the required power level of the reactor. Consequently, the 1.8 MW reactor option was baselined for the 1.2 phase of the study as described in Section 2.1, Vehicle Concept Trade Evolution.

2.4.2 Opposition Design Reference Mission

The NEP-Chem trajectory uses a hybrid propulsion system to perform a crewed Opposition Earth-Mars roundtrip mission departing Earth on February 26, 2039 and arriving at Mars on December 11, 2039. Chemical engines are used at Earth and Mars to perform the major departure and capture maneuvers in the planetary gravity wells. The NEP system is used during the interplanetary transit to provide sustained acceleration which reduces the magnitude of the chemical maneuvers. This combination keeps transit times low by eliminating long spiral in and out maneuvers at Earth and Mars and reduces the overall propellant load by limiting chemical ΔV. Ballistic Opposition missions have significant ΔV requirements, between approximately 6 and 10 km/s depending on mission opportunity. Using only a chemical propulsion system results in a vehicle of unrealistic mass due to the propellant load to perform the necessary ΔV. By using the NEP system during interplanetary transits the ΔV that the chemical system needs to perform is reduced to roughly a third of the ballistic requirement. Since the NEP system is highly efficient the trade from chemical ΔV to low-thrust ΔV saves a significant amount of total propellant. Figure 2-5 NEP-Chem Earth-Mars Crewed Mission Overview and Assumptions shows the mission overview and assumption for the crewed NEP-Chem Opposition mission.

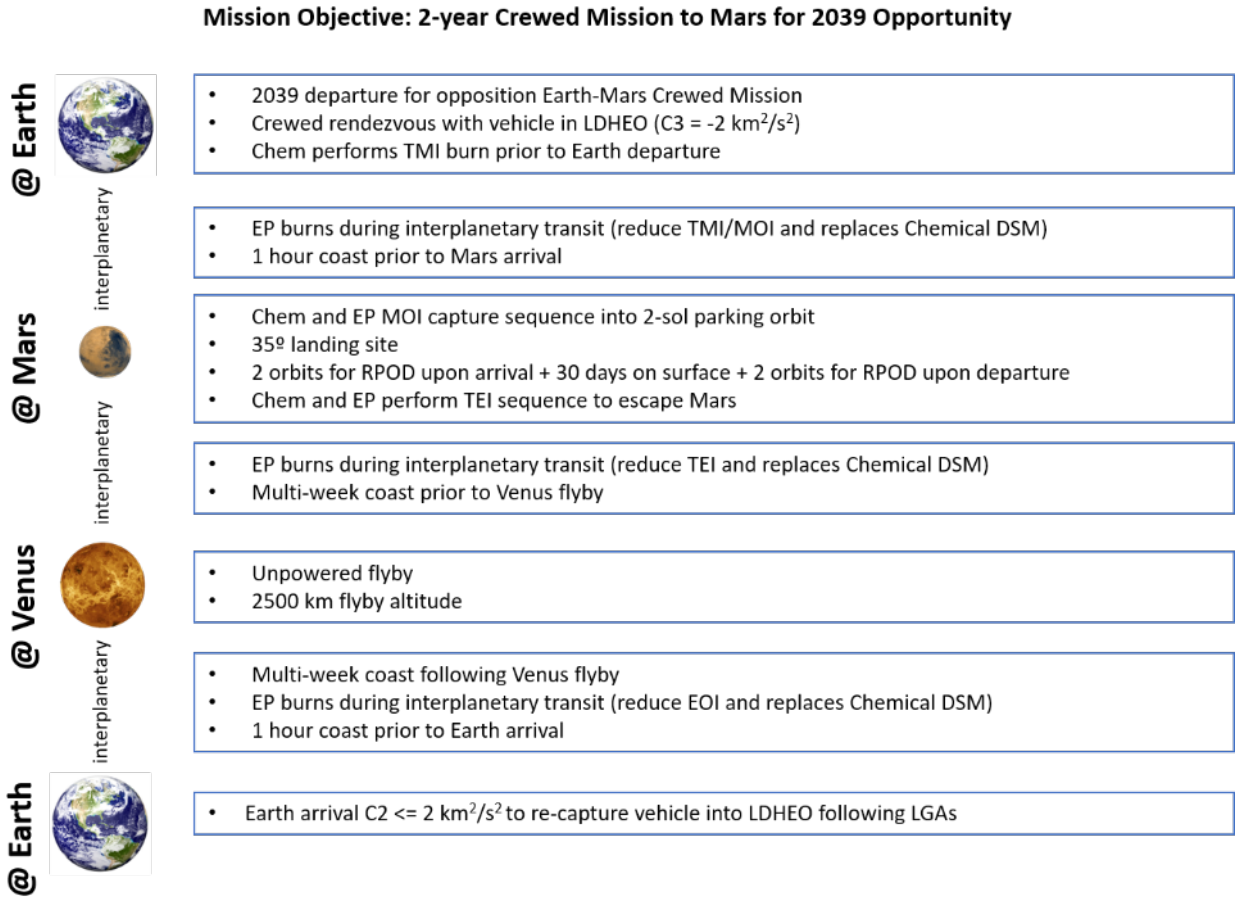

Figure 2-5 NEP-Chem Earth-Mars Crewed Mission Overview and Assumptions

The following propulsion system performance assumptions were made for the chemical and electric propulsion (EP) systems:

- Chemical (modeled impulsively)
  - LOX/LCH_4Specific Impulse: 360 s nominally but modeled as 351 s to represent margin dumping following burns
- EP
  - Xenon Specific Impulse: 2600 s
  - 90% Duty Cycle
  - 59.4% efficiency

Following a chemical TMI burn to escape Earth, the NEP system is active during the Earth to Mars transit. Prior to arrival at Mars the NEP system is shut down and the vehicle is re-oriented in order for the chemical system to perform the chemical MOI burn to capture into an elliptical Mars orbit. Following an hour long coast, an EP burn is used to refine the parking orbit further to achieve the 2-sol size and orientation to reach the 35° landing site. The actual size of the initial capture orbit following MOI is left open to the optimization process with an upper period limit of 10-sol. An upper limit of 10-sol was selected in order to reduce the capture sequence duration. Following capture into the parking orbit, the crewed vehicle spends two orbits performing RPOD activities with the lander prior to descent. After successfully rendezvous with the lander the crew descends to the surface for thirty days to complete surface operations. After the crew ascends they will spend two orbits completing RPOD operations with NEP-Chem vehicle. The crewed NEP-Chem vehicle will then perform a short EP burn to align the vehicle to perform the trans-Earth injection (TEI) burn. After TEI is completed, the chemical stage is dropped along with any remaining xenon margin that was carried for the outbound transit. For 2039, the NEP-Chem vehicle has not escaped Mars following TEI. Rather, TEI has increased the captured orbit size and the EP burn that follows it completes the Mars escape. Figure 2-6 shows the capture and departure sequence at Mars.

The NEP system is used during the Earth-Venus transit and again following the Venus flyby. The Venus flyby is unpowered with multi-week coasting periods preceding and following the flyby. For the 2039 opportunity, there was a minimum flyby altitude of 2500 km. Once at Earth, a series of lunar gravity assist (LGA) maneuvers are performed to re-capture into the LDHEO. An overview of the interplanetary trajectory is shown in Figure 2-7. Minimum solar distance for this trajectory is 0.592 AU.

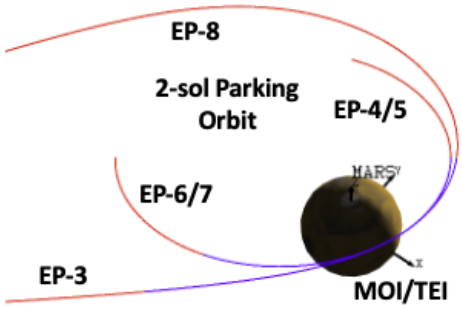

Figure 2-6 Hybrid NEP-Chem Capture and Departure Sequences

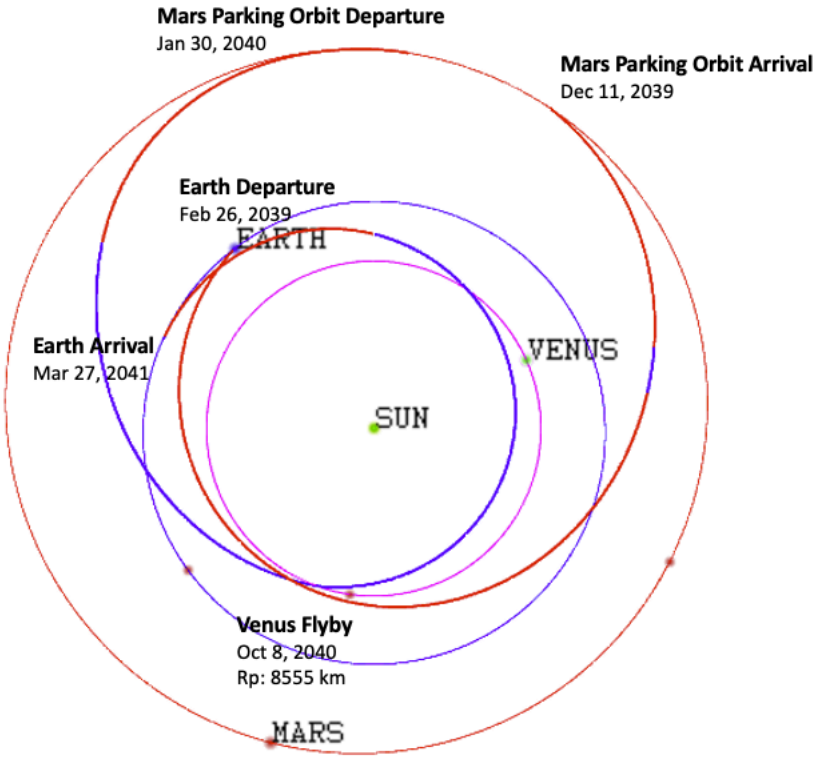

Figure 2-7 2039 Earth-Mars Crewed Opposition Mission

The ΔVs used for the 2039 crewed opposition design are provided in Table 2-4. Following further optimization later in the study a ΔV reduction was achieved (Table 2-5). These ΔV changes were not incorporated into the final vehicle design but should be used for any future updates.

Table 2-4 2039 1.9MW Original Reference Mission

Mission ΔVs	
TMI	1306.1 m/s
EP-1	1187.2 m/s
EP-2	2853.0 m/s
EP-3	2097.7 m/s
MOI	822.6 m/s
EP-4	10.8 m/s
EP-5	0.0 m/s
Mars Stay	
EP-6	0.0 m/s
EP-7	7.9 m/s
TEI	56.9 m/s
EP-8	800.0 m/s
EP-9	5178.1 m/s
EP-10	0.0 m/s
Venus Flyby	
EP-11	3337.0 m/s

Table 2-5 2039 1.9MW Updated Reference Mission

Mission ΔVs	
TMI	1180.2 m/s
EP-1	1173.2 m/s
EP-2	2998.0 m/s
EP-3	2105.5 m/s
MOI	751.1 m/s
EP-4	61.2 m/s
EP-5	0.0 m/s
Mars Stay	
EP-6	0.0 m/s
EP-7	7.2 m/s
TEI	79.7 m/s
EP-8	826.4 m/s
EP-9	5147.5 m/s
EP-10	0.0 m/s
Venus Flyby	
EP-11	3207.1 m/s

2.4.3 Low-Thrust Earth Spiral Reference Mission

The low thrust spiral phase of the mission, shown in Figure 2-8, begins in a circular orbit with an altitude of 1,100 km and inclination of 28.5 degrees. The spiral is designed to deliver 451,000 kg to an interior Ballistic Lunar Transfer (BLT) target state that will allow the spacecraft to enter into the Near Rectilinear Halo Orbit (NRHO) after approximately 30 days. Assuming a constant thrust magnitude of 83.9 N and specific impulse of 2600 s, this spiral trajectory requires 429 days of continuous thrusting to arrive at the BLT target after imparting a total ΔV of 6.107 km/s. The total flight time of this transfer, including the coast to NRHO insertion along the BLT, is 459 days. Due to the nature of this type of transfer, the total ΔV required is relatively insensitive to changes in spacecraft mass, thrust, and specific impulse. The total ΔV of 6.107 is valid as long as the initial orbit and final target remain the same.

This spiral trajectory was designed using NASA's General Mission Analysis Tool and a closed-loop optimal guidance law known as Directional Adaptive Guidance. The objective function for this transfer was minimum time, which is equivalent to minimum ΔV for a continuous thrust trajectory.

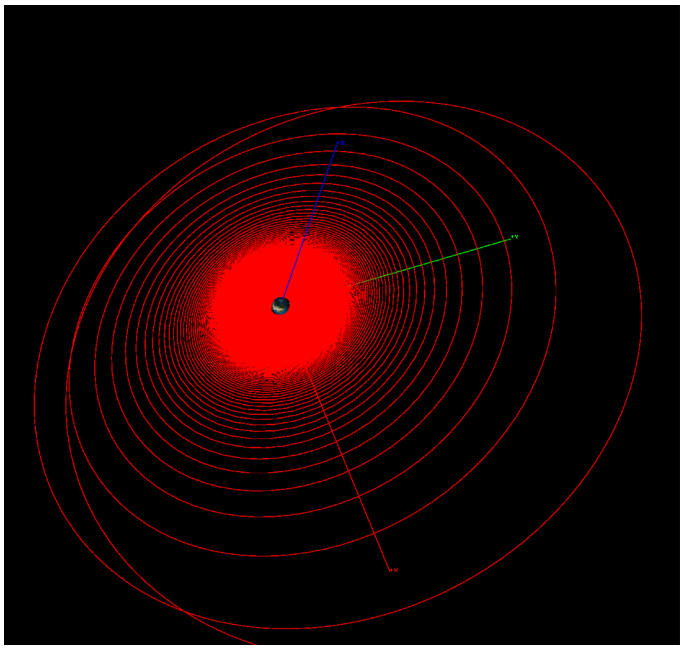

Figure 2-8 Plot of the low thrust spiral transfer shown in the Earth-centered EME2000 frame

2.4.4 NEP-Chem Family of Trajectories

Although 2039 is one of the more ΔV demanding opportunities, one of this study's objectives was ensuring that the 1.9MW spacecraft designed for the 2039 mission would also be able to perform other opposition missions, conjunction missions, and cargo missions.

2.4.4.1 Opposition Reference Cases

In addition to 2039, reference missions for 2035 were also generated. The low thrust and high thrust ΔVs for these references cases for both 1.9MW and 3.8MW reactor power levels are provided in Table 2-6 and Table 2-7, respectively. A reference case at 1.9MW for 2042 is also provided in Table 2-6.

Table 2-6 1.9MW Crewed NEP-Chem Opposition Reference Cases

2035 1.9MW

Mission ΔVs	
TMI	334.3 m/s
EP-1	2558.4 m/s
EP-2	1295.5 m/s
EP-3	3263.9 m/s
MOI	1038.7 m/s
EP-4	82.1 m/s
EP-5	0.0 m/s
Mars Stay	
EP-6	0.0 m/s
EP-7	59.6 m/s
TEI	468.5 m/s
EP-8	422.6 m/s
EP-9	4301.3 m/s
EP-10	0.0 m/s
Venus Flyby	
EP-11	2198.6 m/s

2039 1.9MW

Mission ΔVs	
TMI	1180.2 m/s
EP-1	1173.2 m/s
EP-2	2998.0 m/s
EP-3	2105.5 m/s
MOI	751.1 m/s
EP-4	61.2 m/s
EP-5	0.0 m/s
Mars Stay	
EP-6	0.0 m/s
EP-7	7.2 m/s
TEI	79.7 m/s
EP-8	826.4 m/s
EP-9	5147.5 m/s
EP-10	0.0 m/s
Venus Flyby	
EP-11	3207.1 m/s

2042 1.9MW

Mission ΔVs	
TMI	878.3 m/s
EP-1	1217.1 m/s
EP-2	345.5 m/s
Venus Flyby	
EP-3	2590.5 m/s
MOI	1010.0 m/s
EP-4	10.4 m/s
EP-5	0.0 m/s
Mars Stay	
EP-6	0.0 m/s
EP-7	28.1 m/s
TEI	5.9 m/s
EP-8	5051.4 m/s
EP-9	0.0 m/s
EP-10	6268.9 m/s
EP-11	0.0 m/s

Table 2-7 3.8MW Crewed NEP-Chem Opposition Reference Cases

2035 3.8MW

Mission ΔVs	
TMI	248.9 m/s
EP-1	1068.1 m/s
EP-2	2617.2 m/s
EP-3	4557.7 m/s
MOI	483.3 m/s
EP-4	136.4 m/s
EP-5	0.0 m/s
Mars Stay	
EP-6	0.0 m/s
EP-7	141.6 m/s
TEI	53.4 m/s
EP-8	751.1 m/s
EP-9	6833.8 m/s
EP-10	0.0 m/s
Venus Flyby	
EP-11	2048.4 m/s

2039 3.8MW

Mission ΔVs	
TMI	333.7 m/s
EP-1	445.2 m/s
EP-2	4970.9 m/s
EP-3	3259.8 m/s
MOI	374.6 m/s
EP-4	25.4 m/s
EP-5	31.0 m/s
Mars Stay	
EP-6	3.4 m/s
EP-7	0.0 m/s
TEI	0.0 m/s
EP-8	5626.6 m/s
EP-9	0.0 m/s
EP-10	0.0 m/s
Venus Flyby	
EP-11	3049.0 m/s

2.4.4.2 Conjunction Reference Cases

Table 2-8 1.8MW Crewed NEP-Chem Conjunction Reference Cases

2035 1.8MW	
Mission ΔVs	
TMI	123.7 m/s
EP-1	2498.0 m/s
EP-2	1361.6 m/s
EP-3	1078.9 m/s
MOI	219.9 m/s
EP-4	24.6 m/s
Mars Stay	
EP-5	102.3
TEI	138.1 m/s
EP-6	502.1 m/s
EP-7	897.2 m/s
EP-8	2816.4 m/s

2039 1.8MW	
Mission ΔVs	
TMI	192.6 m/s
EP-1	2205.9 m/s
EP-2	1249.2 m/s
EP-3	1162.3 m/s
MOI	369.5 m/s
EP-4	138.3 m/s
Mars Stay	
EP-5	117.2
TEI	138.1 m/s
EP-6	497.0 m/s
EP-7	2125.6 m/s
EP-8	1826.4 m/s

2.4.4.3 Mission ΔV Details: Pre-Mars Departure Phase

The sequence of events shown below in Table 2-9 represents all propulsive and mass change events considered for the LEO, cislunar, and Lunar Distant High Earth Orbit (LDHEO) phases of the mission:

Table 2-9 Pre-Mars Departure Sequence of Events

Mission DeltaV Summary Case 3_SLS_Chem NEP_Chem_Vehicle_Family CD-2020-181												
Phase #	Phase Name	Pre-Burn Mass	EP DV	Main Chem DV	RCS/ ACS DV	Main Isp	ACS Isp	EP Prop	Main Chem Prop	RCS/ ACS Prop	Post Burn Mass	Change In Mass
		(kg)	(m/s)	(m/s)	(m/s)	(s)	(s)	(kg)	(kg)	(kg)	(kg)	(kg)
1	Launch Reactor Power Module	88351	0	0	0			0	0	0	88351	0
	Null Tip off Rates	88351	0	0	1		295	0	0	31	88320	31
	Correct Insertion Errors	88320	0	0	10		295	0	0	305	88015	305
2	Launch Xe Interstage 1	97381	0	0	0			0	0	0	97381	0
	Null Tip off Rates	97381	0	0	1		295	0	0	34	97348	34
	Correct Insertion Errors	97348	0	0	10		295	0	0	336	97012	336
3	Launch Chem Stage	98439	0	0	0			0	0	0	98439	0
	Null Tip off Rates	98439	0	0	1		295	0	0	34	98405	34
	Correct Insertion Errors	98405	0	0	10		295	0	0	340	98065	340
4	Xe1 RNDZ with NEP	97012	0	0	25		295	0	0	835	96177	62268
	Null Docking Pert	159280	0	0	2		295	0	0	110	159170	110
5	Xenon Interstage 2/3 Ops											
	Xe2 Null Tip off Rates	88184	0	0	1		295	0	0	30	88154	61
	Xe3 Null Tip off Rates	88245	0	0	1		295	0	0	30	88215	30
	Xe2 Correct Insertion Errors	88154	0	0	10		295	0	0	304	87850	61
	Xe3 Correct Insertion Errors	88215	0	0	10		295	0	0	304	87910	304
	Xe2 RNDZ with NEP	87850	0	0	25		295	0	0	756	87094	61
	Xe3 RNDZ with NEP	87910	0	0	25		295	0	0	756	87154	158353
	Correct Docking Perts for Xe2	246263	0	0	2		295	0	0	170	246093	86984
	Correct Docking Perts for Xe3	333247	0	0	2		295	0	0	230	333017	230
	Chem Stage RNDZ with Stack	98065	0	0	25		295	0	0	844	97221	179333
	Correct Docking Perts	277398	0	0	2		295	0	0	192	277207	192
	Refuel Chem Stage	382736	0	0	0			0	0	0	382736	0
	6 Months of Orbital Maintenance	382736	0	0	30		295	0	0	3948	378788	3948
6	Raise orbit altitude to 1100km for Reactor Ops	531627	0	312	0	352		0	45956	0	485671	45956
	Jettison Reactor Heat Shield	484671	0	0	0			0	0	0	484671	1000
	Chem Stage Refueled	580707	0	0	0			0	0	0	580707	96036
	Total for LEO Operations		**0**	**312**	**193**			**0**	**45956**	**9590**		
7	Spiral Out	580707	6076	0	0	2444		130037	0	0	450670	130037
	Chem Stage Detaches and Loiters	230579	0	20	0	352		0	1334	0	229245	1334
	Correct Undocking Perturbations	220090	0	0	1		295	0	0	76	220014	76
	Jettison Xe2	10504	0	0	1		295	0	0	4	10500	4
	Jettison Xe3	10504	0	0	1		295	0	0	4	10500	4
	Acquire Hab	244366	0	0	1		295	0	0	84	244282	24352
	Chem Stage Rendezvous with Stack	229169	0	20	0	352		0	1326	0	227844	1326
	Correct Docking Perturbations	472125	0	0	1		295	0	0	163	471962	163
8	Transfer to LDHEO	471962	45	0	0	2444		885	0	0	471077	885
	Maintain LHDEO: 1m/s/day for 90 days	471077	90	0	0	2444		1766	0	0	469311	1766
	Orion Docks: Transfer of Crew and Supplies	469639	0	0	2		295	0	0	325	469315	653
	Total for Cislunar Operations		**6211**	**40**	**7**			**132688**	**2660**	**656**		

In addition to the primary propulsive events discussed in Section 2.3.2, Table 2-9 and Table 2-10 include ΔV allotments for orbital maintenance, orbit targeting, attitude control, rendezvous proximity operations and docking/undocking (RPODU), and separation burns. Also present are instantaneous mass changes occurring during vehicle matings/dematings, component jettisons, vehicle refueling, and waste removal. RPODU ΔV allotment was based on a preliminary analysis of the far-field approach phase for a notional rendezvous in the 500 km LEO. The analysis did not account for factors such as passive vehicle attitude holds and fail-safe active vehicle burns during the terminal phase of the rendezvous profile.

Margin for the cryogenic propellants and the Xenon are carried by decrementing the nominal specific impulse (I_{SP}) of a thruster by a set percentage. The chemical element cryogenic thrusters have an I_{SP} that is decremented by 5% whereas the Hall thrusters are decremented by 6%. This effectively leads to a situation where it is assumed the margin dedicated to a particular propulsive event is consumed during that event. The RCS propellant margin is carried as inert mass equal to 10% of the usable RCS propellant for the entire mission in the associated module RCS propellant tanks.

The two Xenon Interstages used in part to store the propellant necessary for the spiral to NRHO transfer their residual propellant to the first Xenon Interstage before undocking in the NRHO. Afterwards, they are disposed of into a heliocentric escape trajectory. Next the Habitat is acquired and the chemical stage loiters behind or in front of the nuclear power module in the NRHO.

The first sub-event under Phase 6, 'Jettison Reactor Heat Shield', relates to the jettison of a precautionary heat shield around the reactor which would allow the reactor to survive re-entry in the event the nuclear power module were to re-enter the Earth's atmosphere as a result of a failure leading to a "Loss of Mission". The reactor heat shield is jettisoned in the 1100 km Nuclear Safe orbit prior to the initiation of the spiral out to NRHO.

2.4.4.4 Mission ΔV Details: Outbound, Mars Stay, and Return Phase

The sequence of events shown below in Table 2-10 represents all propulsive and mass change events considered for the Earth-Moon system departure, Mars arrival, Mars stay, Mars departure, and Earth return phases of the mission:

Table 2-10 Outbound, Mars Stay, and Return Sequence of Events

Mission DeltaV Summary Case 3_SLS_Chem NEP_Chem_Vehicle_Family CD-2020-181												
Phase #	Phase Name	Pre-Burn Mass (kg)	EP DV (m/s)	Main Chem DV (m/s)	RCS/ ACS DV (m/s)	Main Isp (s)	ACS Isp (s)	EP Prop (kg)	Main Chem Prop (kg)	RCS/ ACS Prop (kg)	Post Burn Mass (kg)	Change In Mass (kg)
9	Trans-Mars Injection Burn	469315	0	1306	0	352		0	148017	0	321298	148017
	EP-1	321298	1187	0	0	2444		15527	0	0	305770	15527
	EP-2	305770	2853	0	0	2444		34315	0	0	271455	34315
	EP-3	271455	2098	0	0	2444		22749	0	0	248707	22749
	Drop Outbound Consumables	248707	0	0	0			0	0	0	245234	3473
10	Mars Orbit Insertion: Capture into 2 SOL_Orbit	245234	0	823	0	352		0	52064	0	193171	52064
	EP-4	193171	11	0	0	2600		82	0	0	193089	82
	EP-5	193089	0	0	0	2600		0	0	0	193089	0
	Lander RNDZ with Stack	247089	0	0	0			0	0	0	247089	54000
	Crew Transfers to Lander	247089	0	0	0			0	0	0	247089	0
	Lander Departs with Crew	192761	0	0	0			0	0	0	192761	54328
	Correct Undocking Perturbation	192761	1	0	0	2600		8	0	0	192753	8
	Orbital Maintenance for 30 day	192753	5	0	0	2600		38	0	0	192716	38
	MAV RNDZ with Stack	193044	0	0	0			0	0	0	193044	0
	Crew Transfers to Stack with Samples	193294	0	0	0			0	0	0	193294	540
	MAV Undocks	193294	0	0	0			0	0	0	193294	0
	Drop Stay Consumables	193294	0	0	0			0	0	0	192848	445
	Total for Mars Outbound and Stay Operations		**6161**	**2129**	**0**			**72724**	**200080**	**0**		
11	Mars Departure	192848									192848	
	EP-6	192848	0	0	0	2600		0	0	0	192848	0
	EP-7	192848	8	0	0	2600		60	0	0	192789	60
	TEI	192789	0	57	0	352		0	3156	0	189632	3156
	Drop Chem Stage	24119	0	0	0	352		0	0	0	24119	0
	EP-8	165513	800	0	0	2600		5113	0	0	160401	5113
	EP-9	160401	5178	0	0	2600		29480	0	0	130921	29480
	EP-10	130921	0	0	0	2600		0	0	0	130921	0
	Venus Flyby Targeting	130921	10	0	0	2600		51	0	0	130869	51
	Venus Flyby	130869									130869	
12	EP-11: Insertion into LDHEO	130869	3337	0	0	2600		16054	0	0	114815	16054
	Drop Inbound Consumables	114815	0	0	0			0	0	0	109696	5119
	Orion Docks and Crew transfers with samples	109696	0	0	2		295	0	0	76	109620	76
13	Return to NRHO	109620	45	0	0	2600		193	0	0	109427	193
	Total For Earth Return Operations		**9378**	**57**	**2**			**50951**	**3156**	**76**		
	Total For Entire Mission		**21750**	**2537**	**202**			**256363**	**251853**	**10321**		

There are several points in the trajectory where consumables are assumed to be dropped in bulk. The amount dropped at each point uses an accumulation rate of 11.13 kg/day over the duration of that specific mission leg.

Note the I_{SP} margin method for Xenon is only used until arrival at Mars. The Mars stay and return to Earth phase assumes 6% of the usable Xenon required for the Mars stay onward is stored as inert mass in the nuclear power element and remaining Xenon Interstage Xenon tanks.

The chemical stage undocks from the aft end of the stack and separates itself after the TEI maneuver. The Chemical Stage performs a 1 m/s separation burn afterwards.

The overall chemical and electric propulsion (EP) ΔV totals along with total Chemical and EP propellant usages are shown in the last row of Table 2-10. Mission phase totals are shown in rows highlighted yellow.

2.4.4.5 Case 4: Cargo Variant Mission Sequence of Events

The cargo mission variant sequence of events is shown below in Table 2-11:

Table 2-11 Cargo Mission Sequence of Events

Mission DeltaV Summary Case 4_Cargo NEP_Chem_Vehicle_Family CD-2020-181												
Phase #	Phase Name	Pre-Burn Mass	EP DV	Main Chem DV	RCS/ ACS DV	Main Isp	ACS Isp	EP Prop	Main Chem Prop	RCS/ ACS Prop	Post Burn Mass	Change In Mass
		(kg)	(m/s)	(m/s)	(m/s)	(s)	(s)	(kg)	(kg)	(kg)	(kg)	(kg)
1	Launch Reactor Power Module	88351	0	0	0			0	0	0	88351	0
	Null Tip off Rates	88351	0	0	1		295	0	0	31	88320	31
	Correct Insertion Errors	88320	0	0	10		295	0	0	305	88015	305
2	Launch Electric Propulsion Module	100551	0	0	0			0	0	0	100551	0
	Null Tip off Rates	100551	0	0	1		295	0	0	35	100516	35
	Correct Insertion Errors	100516	0	0	10		295	0	0	347	100169	347
3	Launch Chem Stage	46137	0	0	0			0	0	0	46137	0
	Null Tip off Rates	46137	0	0	1		295	0	0	16	46121	16
	Correct Insertion Errors	46121	0	0	10		295	0	0	159	45962	159
4	EP RNDZ with NEP	100169	0	0	25		295	0	0	862	99307	59145
	Null Docking Pert	159314	0	0	2		295	0	0	110	159204	110
	Refuel EP Interstage	159204	0	0	0			0	0	0	159204	0
	6 Months of Orbital Maintenance	200201	0	0	30		295	0	0	2065	198136	2065
5	Chem Stage RNDZ with Stack	45962	0	0	25		295	0	0	395	45566	197740
	Correct Docking Perts	243702	0	0	2		295	0	0	168	243534	168
6	Raise orbit altitude to 1100km for Reactor Operatio	243534	0	312	1	333	295	0	22199	84	221251	22283
	Jettison Reactor Heat Shield	221251	0	0	0			0	0	0	220251	1000
	Total for LEO Operations		**0**	**312**	**118**			**0**	**22199**	**4577**		
7	Spiral Out	198136	6076	0	0	2444		44368	0	0	153768	44368
8	Cargo Vehicle 1 Docks to RPE-EP	153768	0	0	0			0	0	0	218768	65000
	Null Tip off rates from C1 Docking	218768	0	0	2		295	0	0	151	218616	151
	Slews for OM in NRHO	218616	5	0	0	2444		46	0	0	218571	46
	OM in NRHO	218571	10	0	0	2444		91	0	0	218480	91
	Attitude Control in NRHO	218480	5	0	0	2444		46	0	0	218434	46
9	Cargo Vehicle 2 Docks to RPE-EP	218434	0	0	0			0	0	0	282434	64000
	Null Tip off rates from C2 Docking	282434	0	0	2		295	0	0	195	282239	195
	Slews for OM in NRHO	282239	5	0	0	2444		59	0	0	282180	59
	OM in NRHO	282180	10	0	0	2444		118	0	0	282062	118
	Attitude Control in NRHO	282062	5	0	0	2444		59	0	0	282004	59
10	Crew Lander Docks to RPE-EP	282004	0	0	0			0	0	0	282004	65000
	Null Tip off rates from CL Docking	347004	0	0	2		295	0	0	240	346764	240
	Slews for OM in NRHO	346764	5	0	0	2444		72	0	0	346691	72
	OM in NRHO	346691	10	0	0	2444		145	0	0	346547	145
	Attitude Control in NRHO	346547	5	0	0	2444		72	0	0	346474	72
	Total for Cislunar Ops		**6136**	**0**	**6**			**45075**	**0**	**586**		
11	Outbound Transit	346474	2000	0	0	2444		27739	0	0	318736	27739
	Spiral into 5-Sol orbit around Mars	318736	4225	0	0	2444		51513	0	0	267223	51513
12	5-Sol Parking Orbit Maintenance (7 Days)	267223	1	0	0	2444		11	0	0	267211	11
	Attitude Control	267211	3	0	0	2444		33	0	0	267178	33
13	C1 undocks from RPE-EP	267178	0	0	0			0	0	0	202178	65000
	Null rates from C1 undock	202178	0	0	2		295	0	0	140	202038	140
	Orbital Correction burn due to C1 undock	202038	2	0	0	2444		17	0	0	202021	17
	5-Sol Parking Orbit Maintenance (7 Days)	202021	1	0	0	2444		8	0	0	202013	8
	Attitude Control	202013	3	0	0	2444		25	0	0	201988	25
14	C2 undocks from RPE-EP	201988	0	0	0			0	0	0	201988	0
	Null rates from C2 undock	133515	0	0	2		295	0	0	92	133423	92
	Orbital Correction burn due to C2 undock	133423	2	0	0	2444		11	0	0	133412	11
15	Spiral Down to 2-Sol	133412	265	0	0	2444		1467	0	0	131943	1469
	2-Sol Parking Orbit Maintenance (540 Days)	131945	20	0	0	2444		110	0	0	131835	110
	Attitude Control	131835	3	0	0	2444		17	0	0	131818	17
16	Deploy Crew Lander	70291	0	0	0			0	0	0	70291	0
	Null rates from CL undock	70291	0	0	2		295	0	0	49	70242	49
	Orbital Correction burn due to CL undock	70242	2	0	0	2444		6	0	0	70236	6
	Total For Outbound and Mars Ops		**6527**	**21**	**6**			**80958**	**21**	**281**		
	Total For Entire Mission		**12663**	**333**	**130**			**126033**	**22220**	**5444**		

For this variant, only one Xenon Interstage is required. A generic cryogenic Upper Stage boosts the Nuclear Power Element and the refueled Xenon Interstage to the 1100 km Nuclear Safe orbit. After which, the Upper Stage undocks and the stack spirals out to NRHO. The stack is the passive vehicle for all three lander rendezvous. Note that a last minute ground rule change required the first lander to go to Mars earlier, using a chemical stage. Consequently, one of the cargo vehicles above could be a spare lander, or additional Xe propellant and a spare habitat.

Each cargo lander is deployed into a 5-Sol orbit about Mars. The stack performs orbital maintenance after spiraling down to a 2-Sol orbit where the crew lander is deployed 540 days later.

The Xenon margin is managed by decrementing the I_{SP} by 6% as was done with the crewed variant.

2.4.5 Concept of Operations (CONOPS) – Case 1

Due to the multiple launch and staging nature of the NEP-Chemical Concepts it is important to layout the concept of operations to ensure all subsystems are sufficiently designed for all mission phases. The Crewed vehicle CONOPS is described below to support a piloted 2039 mission. From this driving mission the main in-space transportation elements were designed. Other mission options (other year opposition and conjunction as described in the mission section) are similar but may have fewer launches/elements and less propellant needs. The All NEP Cargo CONOPS is described in APPENDIX B.

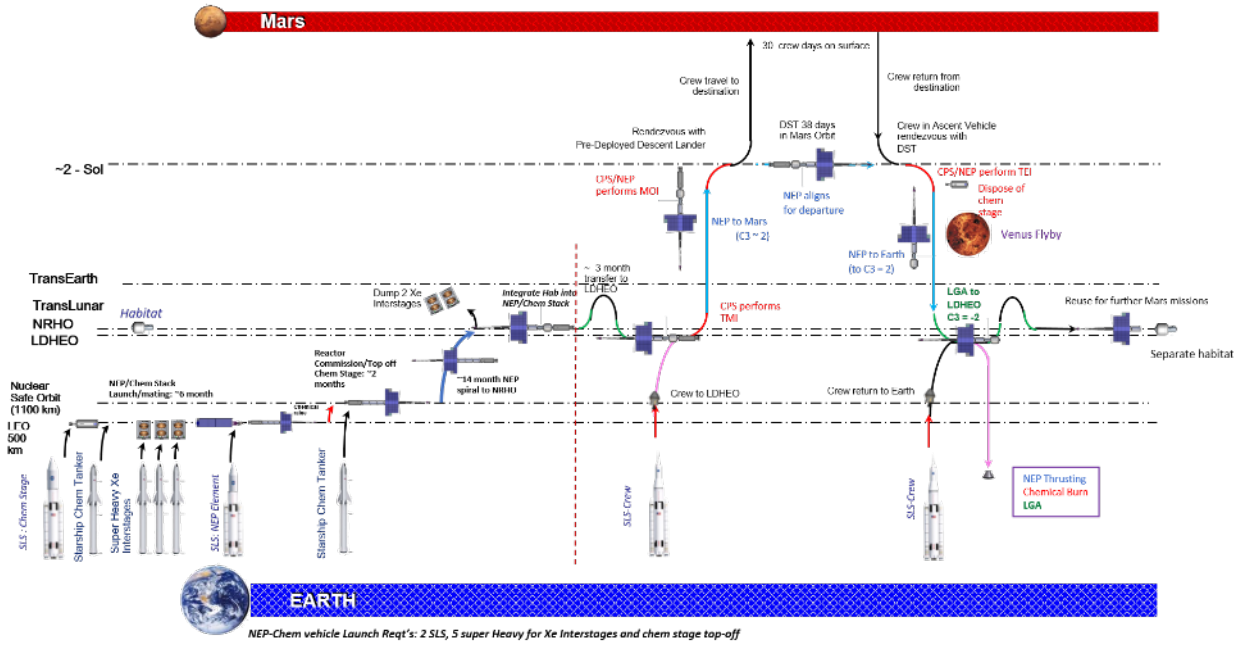

Figure 2-9 Crew NEP-Chem Concept of Operations (2039)

Figure 2-9 above shows the top-level CONOPS for the 2039 Opposition NEP-Chem Crewed mission. CONOPS phases are further defined below for each specific element (Nuclear Electric Propulsion Module, Xenon Interstages, Chemical Stage and habitat). Overall, the NEP-Chemical solution requires only two SLS launches and five super heavy CLVs: three to carry the Xenon Interstages and two to tank up the chemical stage with liquid oxygen (LOX), and liquid methane (LCH4) propellants.

The CONOPS figure illustrates that the assembly and fueling of the elements could occur in less than a year. The spiral out of the transportation system to NRHO (where it meets up with the habitat) will take about 14 months exclusively using the NEP system. This spiral will be a 'shakedown' cruise for the NEP-Chemical transportation system. Table 2-12 on the next page shows a more specific event list

Table 2-12 NEP-Chem Crew Vehicle CONOPS Activity Approximate Dates

Crew Vehicle CONOPS Activity	Approximate Date
Launch campaign for NEP-Chem stack begins	Oct 2036
SLS Chem stage launched	Oct 2036
NEP Module launched SLS	Feb 2037
NEP vehicle commissioning	April 2037
NEP vehicle departs 1100km	May 2037
NEP vehicle arrives in NRHO and mates with Habitat	July 2038
NEP vehicle departs NRHO	Aug 2038
NEP vehicle arrives at LDHEO	Dec 2038
90 day wait for crew in LDHEO	
Crew departs LDHEO	Feb 2039
Crew arrives at Mars	Dec 2039
Crew Departs Mars	Jan 2040
Crew Arrives in Earth LDHEO	March 2041

Launch and Assembly Phase (~ 6 months): A 500 km, 28.5° orbit was chosen for commissioning and fueling due to the benign qualities of few orbital debris and no Van Allen Belt radiation. In addition, 500 km is a sufficiently low orbit to allow commercially launched crew to assist in assembly of the NEP-Chemical vehicle if needed. Only two SLS launches will be required: the Nuclear Electric Propulsion Module and the Chemical propulsion stage. The Chemical propulsion stage would be launched first, partially fueled, then the Nuclear Electric Propulsion Module. A super heavy CLV will top off the chemical stage. Simultaneously three super heavy CLVs will launch three Xenon Interstages (carrying all the xenon required for the mission). Each element will have sufficient propulsion, power, and docking equipment to loiter at 500 km LEO and dock to the other elements. At some point the NEP Module will deploy its reactor boom, and electric thruster booms but will not start its reactor.

Boost to Nuclear Safe Orbit (1-2 days): Once the NEP-Chemical, three Xenon Interstages and the Chemical Stage Elements are docked, the chemical element will perform two burns to lift the transportation stack to an 1100 km nuclear safe orbit. This phase should only take a day or so to complete.

Reactor Commissioning Phase in Nuclear Safe Orbit (1-2 weeks): Once at 1100 km two important activities take place. First the chemical stage is undocked and refueled by another super heavy CLV. At the same time the reactor will be started using the commissioning solar arrays for power. For startup, the reactor control system will actuate the control rods to achieve criticality (~1 kW for 1 hour) while powering the primary loop pumps to circulate the reactor heat. When a suitable temperature is achieved, the Brayton units will be individually motored to establish a self-sustaining condition (~10 kWhr of energy over 4 hours). In parallel, the radiator loops will be charged and the radiator pumps started to circulate the coolant before the radiator panels are deployed. As reactor power is increased and more Brayton waste heat is generated, the panels will be gradually deployed to match the desired radiator temperature. Once the reactor and the electric propulsion system has been checked out and the chemical stage refueled they will be remated and begin their spiral to NRHO.

Spiral to NRHO (14 months): The spiral to NRHO will exclusively use the NEP system for thrust along with ~100 t of xenon. The integrated transportation system includes all the xenon and chemical propellants for the subsequent Mars mission, eliminating any fueling at NRHO. Analyses of the Van Allen radiation belt impacts showed that only ~10 krad of radiation impacts the electronics, mainly from the proton belts, is expected assuming proper shielding (~10 mm). (See Section 4.3, Thermal Control System for further analyses.)

Integration of the Habitat at NHRO (1-2 weeks): Once in the NRHO the chemical element will again be undocked and two of the nearly empty Xenon Interstages will be undocked after transferring their margin and residuals to the NEP Module's single Xenon tank. The habitat will dock in place of the two Xenon Interstages and the chemical stage will reattach. The habitat is assumed to be a free flyer already at NRHO and is outfitted for the Mars mission while the rest of the transportation system is spiraling to NRHO. Operational empty mass of the reusable habitat is 26.4 t with 20 kW of power required and a trash dump of 11.1 kg / day assumed during the transit to/from Mars.

Mars Mission (~2 years) Phase: Once assembled, outfitted and fueled the NEP-Chem vehicle will be sent to the LDHEO using electric propulsion and a weak stability bound (WSB) transfer. Once there an SLS will launch the crew of 4 to dock with the NEP-Chem vehicle using Orion. After the unmanned Orion separates, the NEP Stack leaves from LDHEO with crew using a small chemical burn. Once in interplanetary space the vehicle uses NEP to accelerate and then decelerate at Mars (to reduce the chemical capture ΔV). The vehicle captures chemically in a two solar day (SOL) elliptical orbit where it meets up with the lander previously delivered by a cargo vehicle. Two of the crew descend to Mars surface for a 30 day stay and then return to the NEP-Chem Vehicle using the MAV. After the MAV separates the NEP-Chem vehicle performs a chemical burn to escape Mars, dumps the chemical stage element and uses NEP to return to Earth, also utilizing a Venus flyby. Once recaptured into the LDHEO an unmanned Orion is launched to retrieve the crew. The NEP-Chem vehicle then returns to NRHO using NEP and a WSB transfer to return the habitat for refit and potentially reuse of the NEP Module.

3.0 Baseline Design

The NEP-Chem Vehicle consists of multiple elements; the NEP Module, the Xenon Interstages, the Habitat, and the Chemical Stage. The Compass team did not design the Habitat, instead using a provided mass and representative configuration. This section discusses the design of the vehicle as a whole, while subsequent sections explore each subsystem design in detail.

3.1 System-Level Summary

Figure 3-1 below shows the system block diagram that capture the subsystems of the NEP-Chem Vehicle concept.

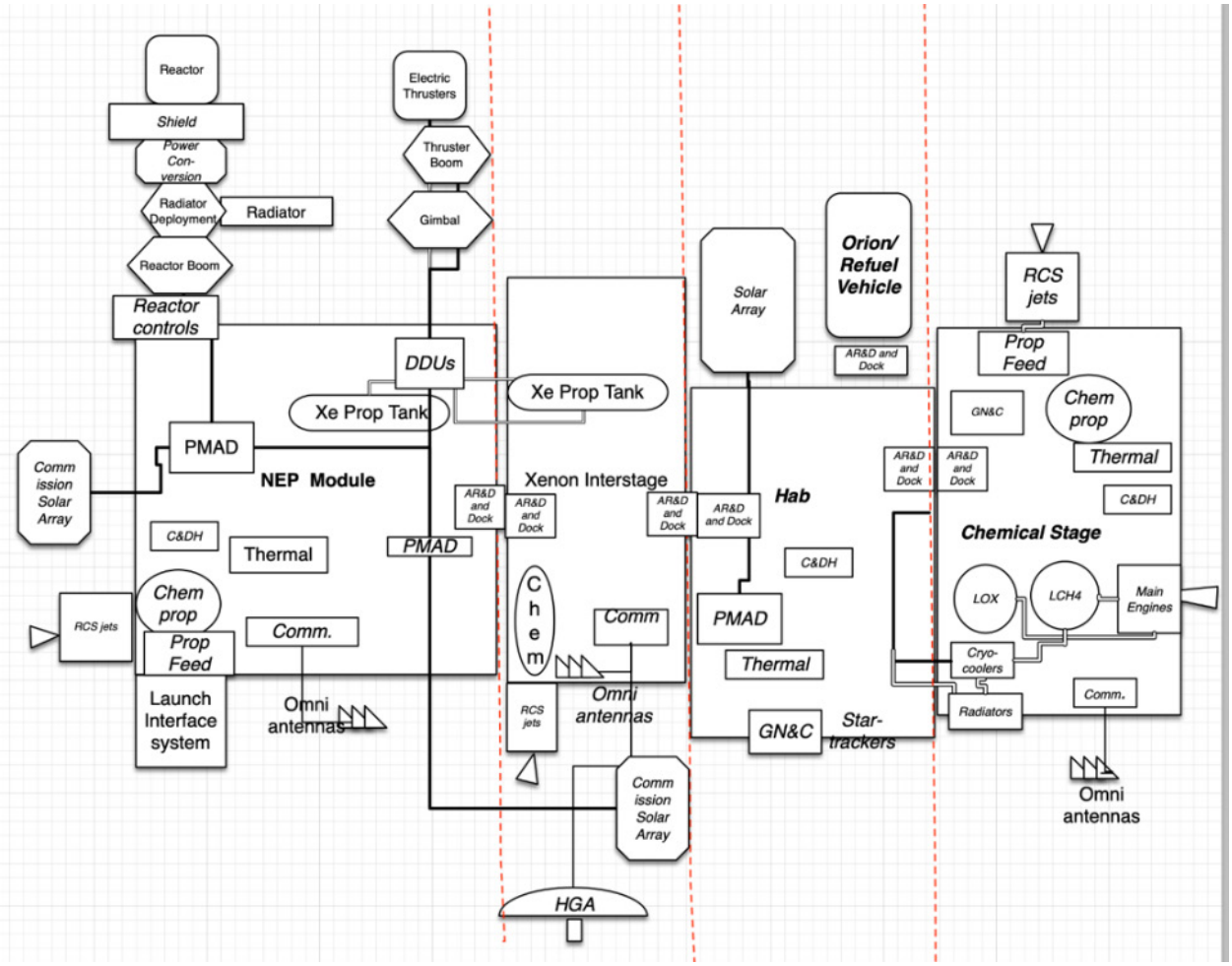

Figure 3-1 Schematic Diagram of the NEP-Chem Vehicle with the NEP Module, Xenon Interstage, Habitat, and Chemical Stage

3.2 Top-Level Design Details

A top-level look at the masses of each element in the architecture is included below. The description of each subsystem can be found in each corresponding subsystem subsection.

3.2.1 Master Equipment List (MEL)

Table 3-1, Table 3-2, and Table 3-3 below provide the NEP-Chem Vehicle MELs for the NEP Module, Xenon Interstage, and Chemical Stage elements, respectively. The top line sum reported for the NEP-Chem Vehicle includes the totals for all three elements in each table. The basic mass reported in the MEL are also captured in Section 4.0, SUBSYSTEM BREAKDOWN, where bottoms-up mass estimation is captured at the spacecraft level.

The MELs reported below are top-level summaries of all subsystem masses. Each subsystem section provides details for these top-level summaries. The masses include basic mass and subsystem margin as applied by each subsystem lead, but do not show the additional 15% mass margin added at the spacecraft level. It is also worth noting that these masses reflect the launch mass of each module, not their post refueling mass on orbit. Also these MELs reflect only a single Xenon Interstage.

Table 3-1 NEP Module MEL

Description Case 3_SLS_Chem NEP_Chem_Vehicle_Family CD-2020-181	Basic Mass	Growth	Growth	Total Mass
	(kg)	(%)	(kg)	(kg)
NEP Chem Vehicle	259944	4%	11346	271290
NEP Module	72875	11%	7678	80553
Nuclear Power System	25684.0	15%	3852.6	29536.6
Attitude Determination and Control	71.6	13%	9.2	80.8
Command & Data Handling	79.4	68%	53.9	133.3
Communications and Tracking	42.0	10%	4.2	46.2
Electrical Power Subsystem	462.3	40%	183.7	646.0
Thermal Control (Non-Propellant)	1192.4	18%	214.6	1407.0
Propulsion (Chemical Hardware)	427.6	8%	35.6	463.1
Propellant (Chemical)	3085.9	0%	0.0	3085.9
Propulsion (EP Hardware)	9294.4	24%	2192.1	11486.5
Propellant (EP)	26028.7	0%	0.0	26028.7
Structures and Mechanisms	6506.9	17%	1131.7	7638.6

Table 3-2 Xenon Interstage MEL

Description Case 3_SLS_Chem NEP_Chem_Vehicle_Family CD-2020-181	Basic Mass	Growth	Growth	Total Mass
	(kg)	(%)	(kg)	(kg)
NEP Chem Vehicle	259944	4%	11346	271290
Xenon Interstage	93641	1%	1227	94867
Attitude Determination and Control	101.6	14%	14.6	116.2
Command & Data Handling	48.1	62%	30.0	78.1
Communications and Tracking	54.8	10%	5.5	60.3
Electrical Power Subsystem	235.6	38%	90.0	325.6
Thermal Control (Non-Propellant)	705.4	18%	127.0	832.4
Propulsion (Chemical Hardware)	399.0	11%	42.4	441.4
Propellant (Chemical)	1510.7	0%	0.0	1510.7
Propulsion (EP Hardware)	3714.8	15%	557.2	4272.1
Propellant (EP)	84343.5	0%	0.0	84343.5
Structures and Mechanisms	2527.2	14%	359.7	2886.9

Table 3-3 Chemical Stage MEL

Description Case 3_SLS_Chem NEP_Chem_Vehicle_Family CD-2020-181	Basic Mass	Growth	Growth	Total Mass
	(kg)	(%)	(kg)	(kg)
NEP Chem Vehicle	259944	4%	11346	271290
Chemical Propulsion Module	93428	3%	2442	95870
Attitude Determination and Control	73.6	18%	13.2	86.8
Command & Data Handling	49.3	65%	32.2	81.5
Communications and Tracking	42.0	10%	4.2	46.2
Electrical Power Subsystem	360.9	39%	141.5	502.4
Thermal Control (Non-Propellant)	869.4	18%	156.5	1025.9
Propulsion (Chemical Hardware)	10152.5	14%	1427.7	11580.2
Propellant (Chemical)	77865.6	0%	0.0	77865.6
Structures and Mechanisms	4015.0	17%	666.7	4681.7

3.2.2 Architecture Details – Launch Vehicle Payload Assumptions

Launch Vehicle performance is assumed for this study and provided in the ground rules and assumptions. Each element is designed to not exceed the payload limits of either a super-heavy class launch vehicle or the SLS Block 2 performance dictated in the Ground Rules and Assumptions (GR&A), as applicable. The assumed rough payload capabilities are further decremented by a launch vehicle (LV) margin and the mass of a payload adapter. The NEP Module's LV performance is additionally decremented by a 10 t strongback placeholder. This strongback is further discussed in Section 4.4.6, Structures and Mechanisms System Design. It is assumed that the NEP Module and Chemical Stage will each be launched on an SLS Block 2 to a 500 km circular orbit. After decrementing the performance and allowing for a payload adapter, this leaves a performance of ~98.4 t. A representative super-heavy launch vehicle is assumed to launch the Xenon Interstages. The performance to a 500 km circular orbit is assumed to be ~100 t after decrementing performance and allowing for a payload adapter.

3.2.3 Spacecraft Total Mass Summary

The MEL in Table 3-4 below captures the bottoms-up CBE and growth percentage of the NEP-Chem Vehicle elements that were calculated for each line subsystem by individual subsystem team leads. Mass details per subsystem are provided in Section 4.0, Subsystem Breakdown, of this document.

In order to meet the American Institute for Aeronautics and Astronautics (AIAA) MGA and margin recommendations, an allocation is necessary for margin on basic dry mass at the system-level, in addition to the growth calculated on each individual subsystem. This additional system-level mass is counted as part of the inert mass to be flown along the required trajectory. Therefore, the additional system-level growth mass impacts the total propellant required for the mission design. Total masses in the MEL below only include masses launched for assembly in LEO and do not include additional propellant required for the full mission. As such, wet masses, with growth in the chart below do not exceed the launch vehicle limitations that were assumed. It should be noted that the habitat is not included below, as its mass was assumed for the study.

The "Additional Dry Mass- Dropped during mission (no growth)" line in Table 3-4 below is meant to capture a representative re-entry shield for the nuclear reactor. This 1000 kgs is carried from launch until the spacecraft reaches a nuclear-safe orbit. At that point, the placeholder mass is dropped.

Table 3-4 Summary of System Level Mass by Design Element

MEL Summary: Case 3_SLS_Chem NEP_Chem_Vehicle_Family CD-2020-181	NEP Module	Xenon Interstage	Chemical Propulsion
Main Subsystems	**Basic Mass (kg)**	**Basic Mass (kg)**	**Basic Mass (kg)**
Nuclear Power System	25684	0	0
Attitude Determination and Control	72	102	74
Command & Data Handling	79	48	49
Communications and Tracking	42	55	42
Electrical Power Subsystem	462	236	361
Thermal Control (Non-Propellant)	1192	705	869
Propulsion (Chemical Hardware)	428	399	10152
Propellant (Chemical) at Launch	3086	1511	77866
Propulsion (EP Hardware)	9294	3715	0
Propellant (EP) at Launch	26029	84343	0
Structures and Mechanisms	6507	2527	4015
ECLSS and Crew Systems			
Element Total	***72875***	***93641***	***93428***
Element Dry Mass (no prop,consum)	43761	7786	15563
Element Propellant at Launch	29115	85854	77866
Element Other Consumables, Sparing and Crew			
Element Mass Growth Allowance (Aggregate)	7678	1227	2442
MGA %'age	17.5%	15.8%	15.7%
Predicted Mass (Basic + MGA)	51438	9013	18005
Recommended Mass Margin (Additional System Level Growth)	6564	1168	2334
Margin %'age	15.0%	15.0%	15.0%
Additional Dry Mass- Dropped during mission (no growth)	1000	0	0
Element Dry Mass (Basic+MGA+Margin)	59002	10181	20339
Element Inert Mass (Basic+MGA+Margin)	63103	10500	24112
Total Launched Wet Mass (Allowable Mass)	***88117***	***96035***	***98205***

3.2.4 Power Equipment List (PEL)

Table 3-5 below provides assumptions to model the power systems power modes.

Table 3-5 Power Mode Titles and Description

Mode	Title	Description & Assumptions
Power mode 1	*Assembly in LEO*	6 months
Power mode 2	*Burn to Nuclear Safe Orbit*	2 burns totaling 30 mins from 500 km to 1100 km
Power mode 3	*Start Up*	5 hr. nuclear system start up sequence
Power mode 4	*NRHO to LDHEO and Crew Embark*	90 days of spiral out. NEP thrusters run for a small percentage of this time, captured in Power mode 5.
Power mode 5	*NEP Thrusting*	Approximately 814 days, including spiral out
Power mode 6	*Deep Space Coasting*	Approximately 297 days of total deep space coasting time (out and back)
Power mode 7	*Burn in Mars Orbit*	2 burns, the first is approximately 6.5 hours and the second is approximately 5 hours
Power mode 8	*Venus Flyby*	
Power mode 9	*Capture in LDHEO*	Approximately 56 days of EP thruster burns

The power equipment list (PEL) top-level and element level summary from the bottoms-up analysis on the NEP-Chem are listed in Table 4-1 in the Electrical Power System (EPS) subsection.

3.3 Concept Drawing and Description

There are four main elements of which the Piloted Mars 1.9 MWe NEP Vehicle is comprised: The NEP Module, the Xenon Interstage, the Habitat, and the Chemical Propulsion Module. All four of these elements will be launched separately on their own launch vehicle and assembled in space through an automated rendezvous and docking process. The habitat will not be covered in this section as it was provided to the team for this study and treated as a 'black box' to which minor design changes were made as it related to the design of the full Piloted Mars NEP Vehicle. The NEP Module, Xenon Interstage, and Chemical Propulsion Module will all be covered here, as they were the primary elements designed within this particular Compass Team study. Figure 3-2 below shows these four main elements in the full vehicle configuration during its transit to Mars. Note that during the spiral from LEO to the NRHO the full vehicle configuration will have three Xenon Interstages and will not contain the habitat. Once in NHRO, the chemical propulsion stage will be separated, then two of the Xenon Interstages used for the spiral out will be jettisoned, and the habitat will dock with the vehicle, with the chemical propulsion stage then docking to the habitat. This is the configuration utilized for the Mars transfer. Finally, prior to departing Mars, the chemical stage will then be jettisoned.

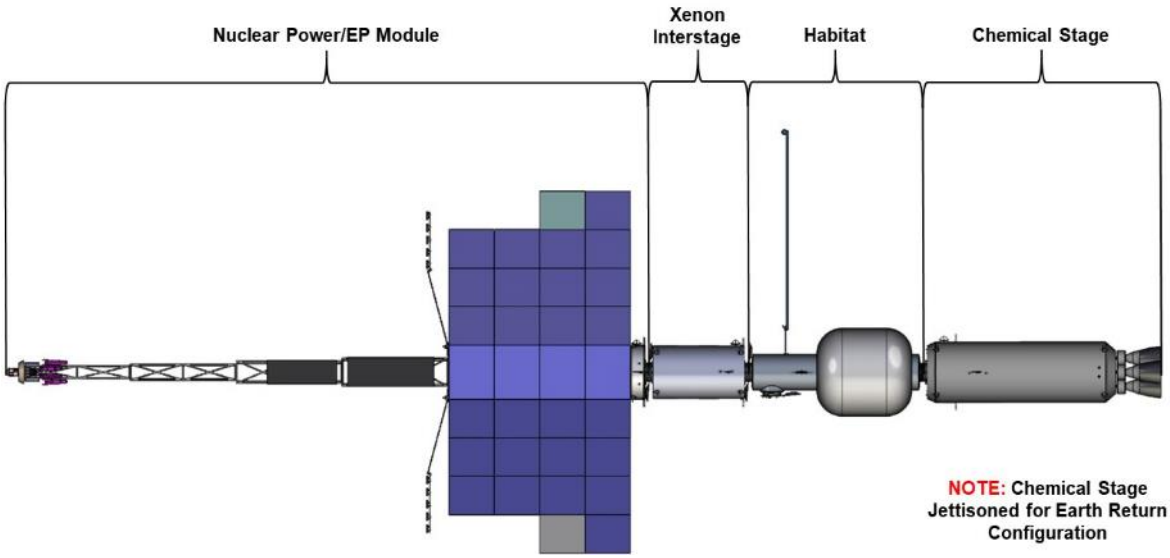

Figure 3-2 The Four Major Elements of the Piloted Mars 1.9 MWe NEP Vehicle

Both the NEP and Chemical Propulsion Modules are to be launched separately on an SLS utilizing the 8.4-meter diameter long payload fairing. While a payload specific payload attach fitting (PAF) is required for launch, both the bus of the NEP Module and the bottom of the bus on the chemical propulsion module were designed to have the same diameter to allow the same PAF to be used for both launches. Figure 3-3 below shows the NEP Module stowed within this payload fairing, while Figure 3-4 below shows the Chemical Propulsion Module inside the fairing.

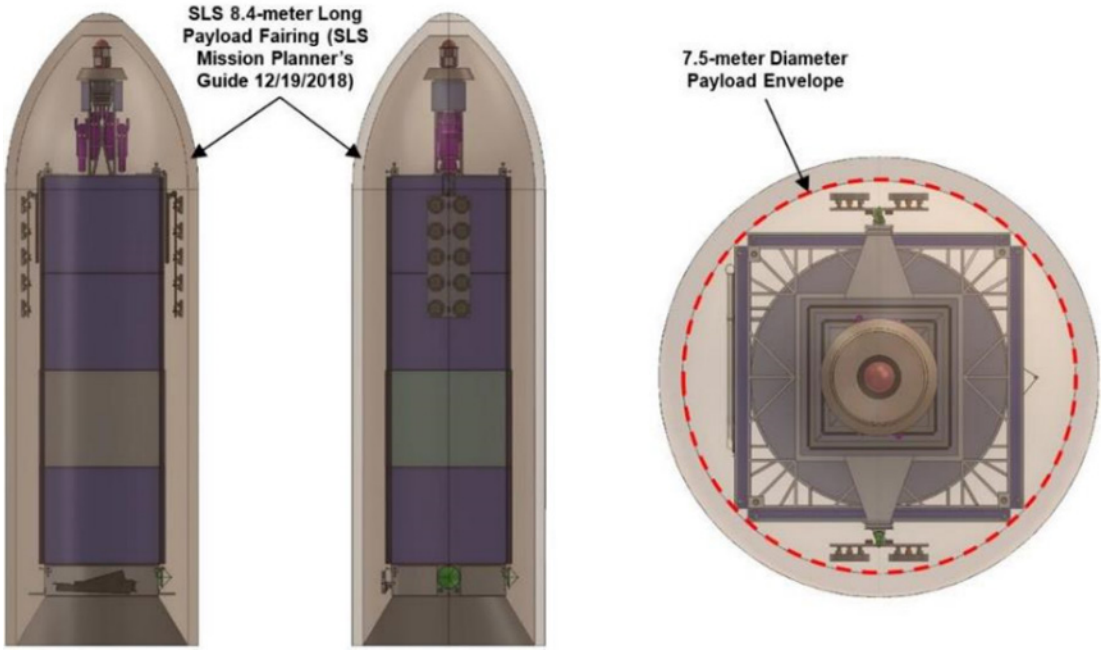

Figure 3-3 NEP Module Stowed Within the SLS 8.4 Meter Long Payload Fairing

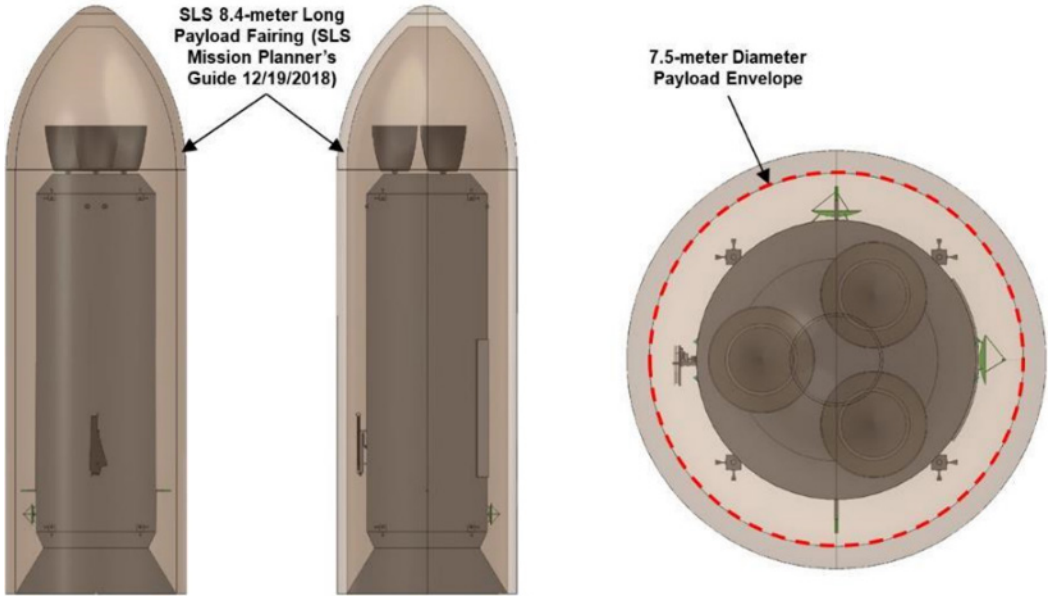

Figure 3-4 Chemical Propulsion Module Stowed Within the SLS 8.4 Meter Long Payload Fairing

Unlike the NEP and Chemical Propulsion Modules, the Xenon Interstage is designed and sized to be launched on a Super Heavy class CLV. This not only reduces the need for additional SLS launches but allows the two xenon tanks contained in the Xenon Interstage to be launched full without the need for topping off the xenon tanks. Little definition is available for the super heavy Launch Vehicle Adaptor (LVA) and Payload Adaptor (PLA) at this time, thus the bus size for the Xenon Interstage was kept at the same diameter as the bus for the NEP Module. This allows for identical xenon tanks to be used on both the Xenon Interstage and NEP Module, thus providing the same interface diameter between the stage and PLA. This will most likely require a payload specific PLA for launch of the Xenon Interstage, but there is sufficient height within the super heavy CLV fairing to accommodate the PLA, regardless of the size of the final design. Further work is needed to understand the PLA design requirements for super heavy CLVs and determine the necessary interface diameters to both the LVA and the Xenon Interstage. Figure 3-5 below shows the Xenon Interstage stowed within the super heavy CLV payload fairing with a notional PLA.

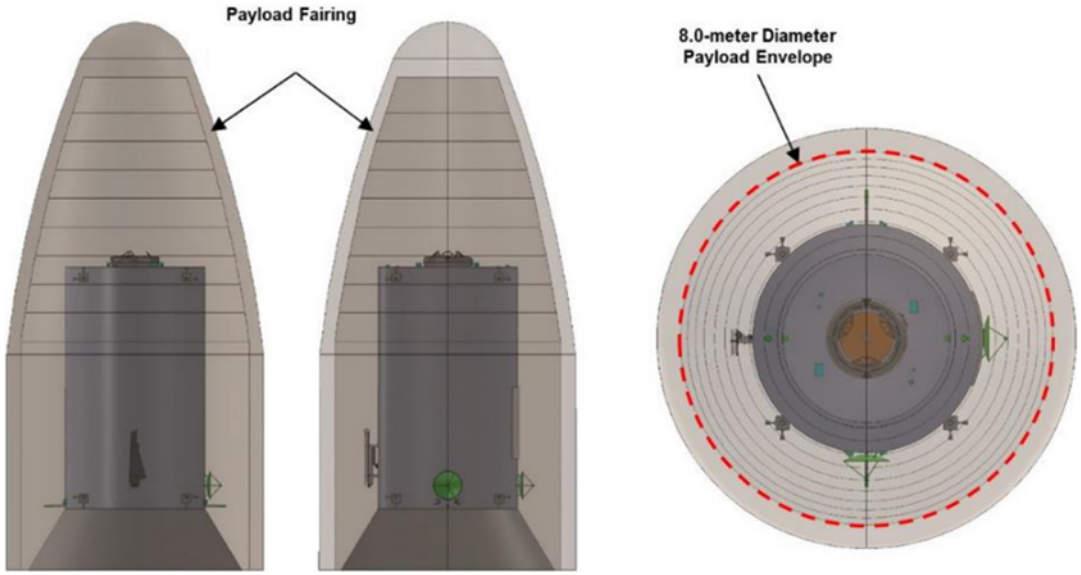

Figure 3-5 Xenon Interstage Stowed within the Super Heavy Payload Fairing

While the NEP Module is launched with the reactor end up, and the Electric Propulsion (EP) thrusters relatively high in the fairing, the mass of the bus at the bottom of the fairing which contains a large xenon tank, the reactor Power Management and Distribution (PMAD) system, and the 20 Direct Drive Units (DDUs) for the EP thrusters should counteract the reactor, shield, power conversion, and EP thruster mass, to keep the center of gravity as low as possible at launch. This will require further analysis along with the potential impacts to the design if it is desired to launch with the reactor located near the bottom at launch. Launching with the reactor on top was selected for this study to maximize the amount of reactor radiator area that could be stowed within the fairing and allowing the reactor, shield, and power conversion components to reside within the conical section of the fairing. Figure 3-6 below shows the stowed dimensions of the NEP Module.

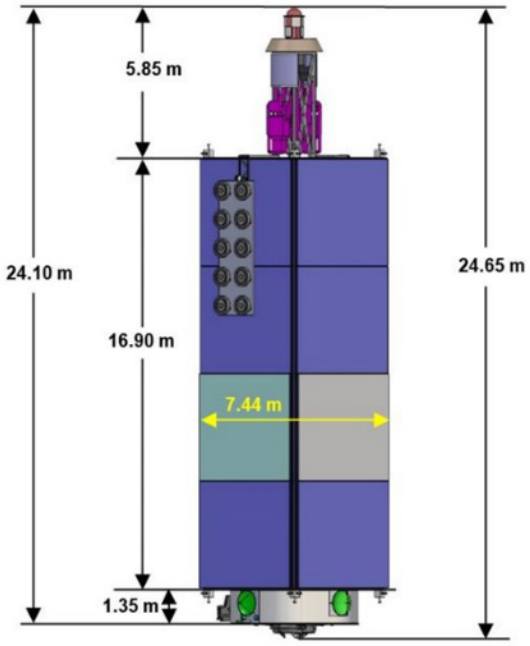

Figure 3-6 Stowed Dimensions of the NEP Module

For the NEP Module to fit within the fairing, several components must be stowed for launch and deployed once delivered to the appropriate orbit. These components include the nuclear power system (reactor, shield, and power conversion), the parasitic load radiators, the 52 double-sided reactor radiator panels, the two double sided reactor PMAD radiator panels, the two double sided direct drive unit (DDU) radiator panels, the two EP thruster booms, and the Ultraflex® solar array used for commissioning power.

The Ultraflex® array is deployed prior to any other deployments so it can provide the commissioning power for deployment of all the other components as well as provide power for startup of the reactor. Deployment of the nuclear power components is performed by a telescoping boom that extends these components out and away from the bus. This not only allows the module to fit within the fairing when stowed, but also, when deployed, provides at least a 50 m distance between the base of the reactor shield and the reactor PMAD electronics located inside the aft end of the module (minimizing radiation exposure to the reactor PMAD electronics), and allows the deployed radiators to fit within the radiation shield cone provided by the reactor shield. Prior to the deployment of the double sided reactor, reactor PMAD, and DDU radiator panels, the two EP thruster booms need to be deployed as they are stowed on the outside of the stowed radiator panels. Figure 3-7 below shows both the stowed and deployed reactor and EP thruster booms, while Figure 3-8 shows the distance between the power conversion units and the reactor PMAD electronics (the minimum length of high power cabling that is required).

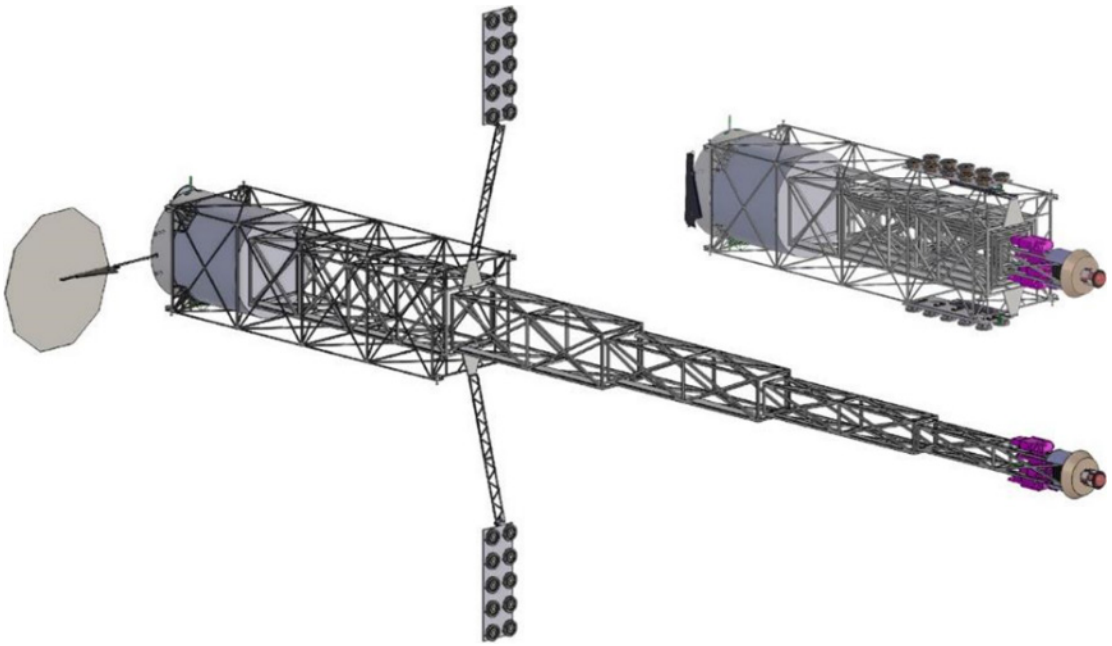

Figure 3-7 Images of Both the Stowed and Deployed Telescoping Reactor Boom and EP Thruster Booms

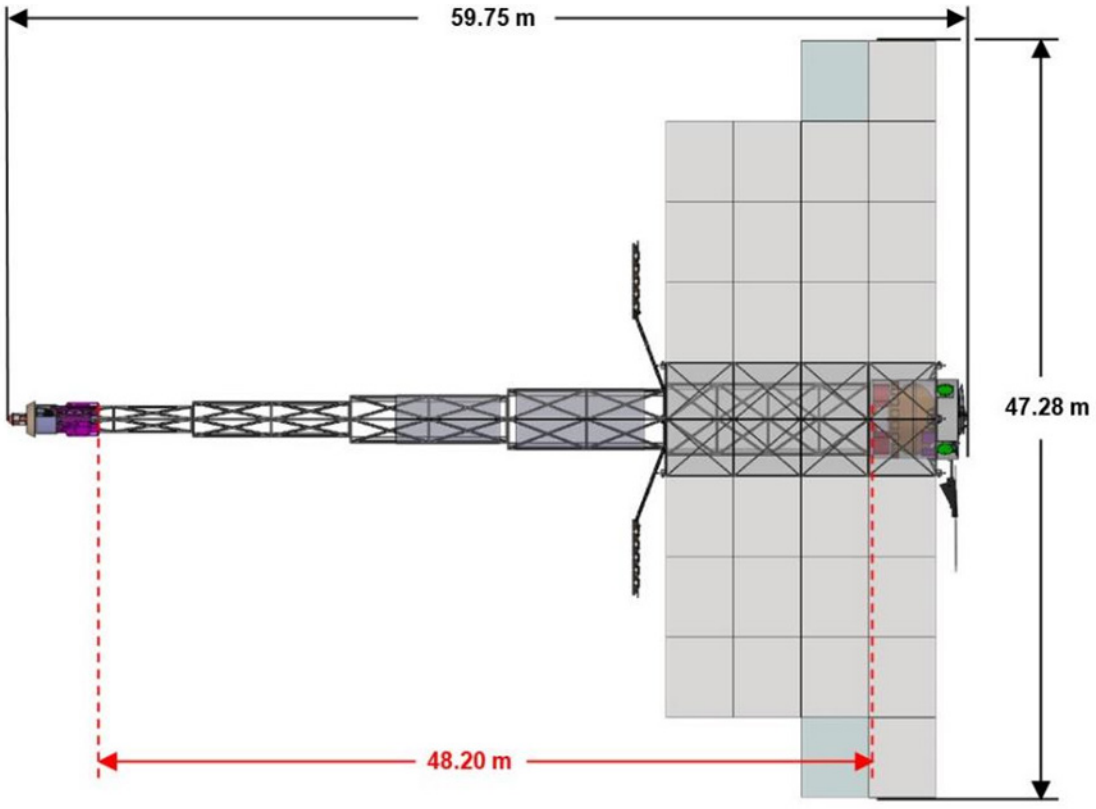

Figure 3-8 Key Dimensions of the Deployed NEP Module

The telescoping boom also provides the required area for the parasitic load radiators. This radiator is split into two separate radiators that wrap around and are fixed to the two largest deployable sections of the telescoping truss (the largest section of the truss is fixed to the bus structure and is located underneath the fixed single sided radiator panels). Figure 3-9 below shows these parasitic load radiators, along with the other major nuclear power and thermal control components of the NEP Module.

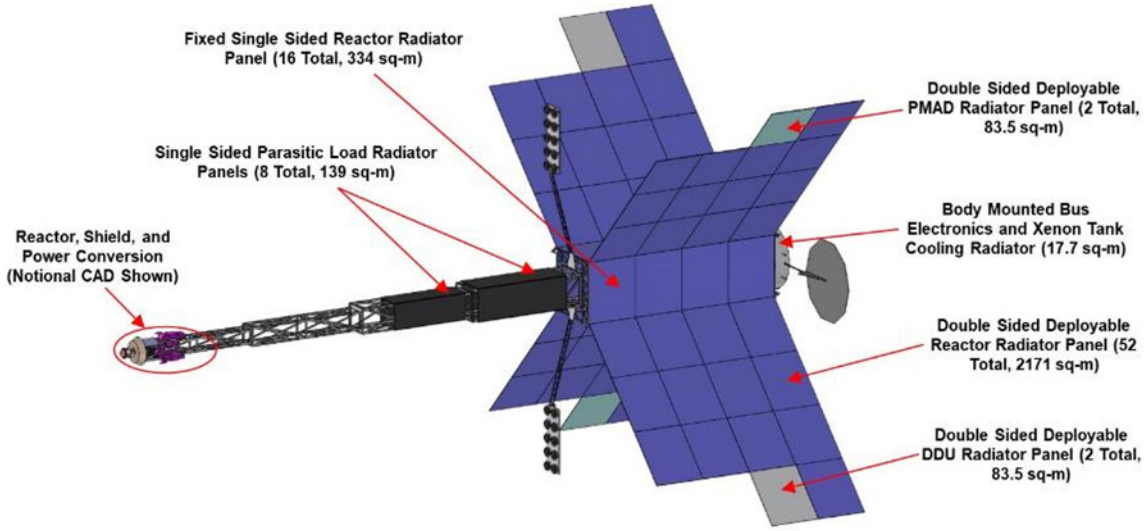

Figure 3-9 Major Nuclear Power and Thermal Control Components of the NEP Module

The reactor, reactor PMAD, and DDU radiator panels are mounted to a box truss that surrounds and ties into the bus structure and the outer most (fixed) truss section of the telescoping boom. Mounted directly to this radiator box truss are 16 single-sided radiator panels (four per side of the box truss) each with an effective area of 20.88 sq. meters, providing a total fixed effective radiator area of 334.08 sq. meters. The 52 double-sided radiators (13 per side of the box truss) are stacked on top of the fixed radiator panels. Each radiator panel has an area of 20.88 sq. meters, but since they are double sided, they have an effective radiator of 41.76 sq. meters. With all 52 double-sided panels, their effective radiator is 2171.52 sq. meters. When combined with the 16 fixed, single sided radiators, there is a total effective radiator area of 2505.60 sq. meters for the reactor heat rejection. The double sided radiator panels are stacked three deep on twelve of the fixed radiator panels, and stacked four deep on the remaining four fixed radiator panels that are furthest from the radiator. This stacking allows the radiators to remain within the 26-degree radiation shield cone when deployed as shown in Figure 3-10 below. The double-sided radiator panels will deploy out 135 degrees from the face the fixed radiator to which they are stacked upon when stowed by way of hinges at the edges of the panels. The two double sided reactor PMAD and two double sided DDU radiator panels are located on the end of the deployed radiator panel wings that are the second furthest from the reactor, allowing them to remain within the 26-degree radiation shield cone when deployed.

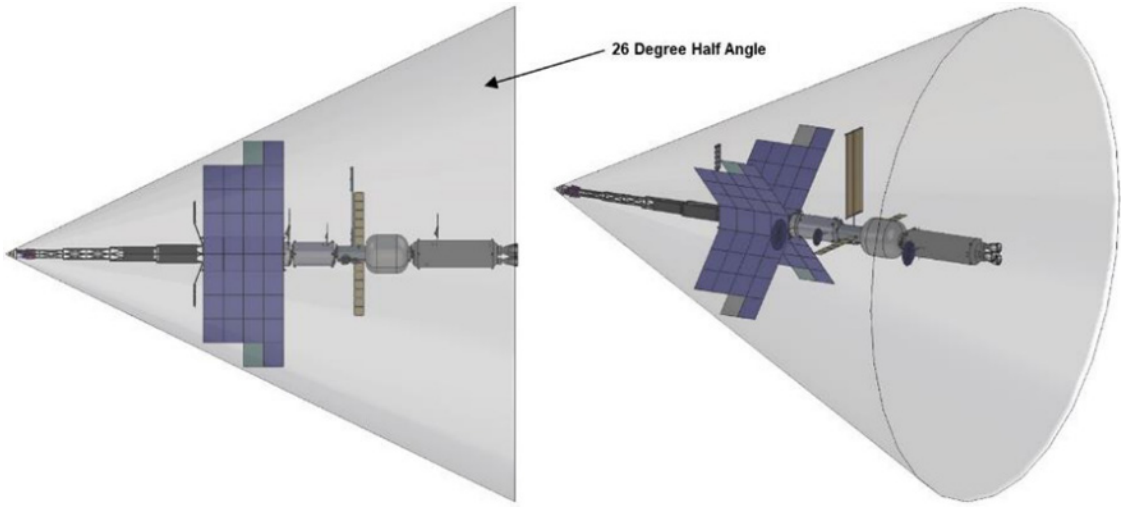

Figure 3-10 Radiation Shield Cone Provided by the Reactor Shield

Each of the two EP thruster booms consists of two boom sections that provide a total boom length of 6.88-m. At the end of each of the thruster booms is a two-axis gimbal that will gimbal a thruster platform that contains ten 100 kWe Hall thrusters and ten low pressure xenon flow controllers (one per Hall thruster). Those components contained on the thruster booms can be seen in Figure 3-11 below.

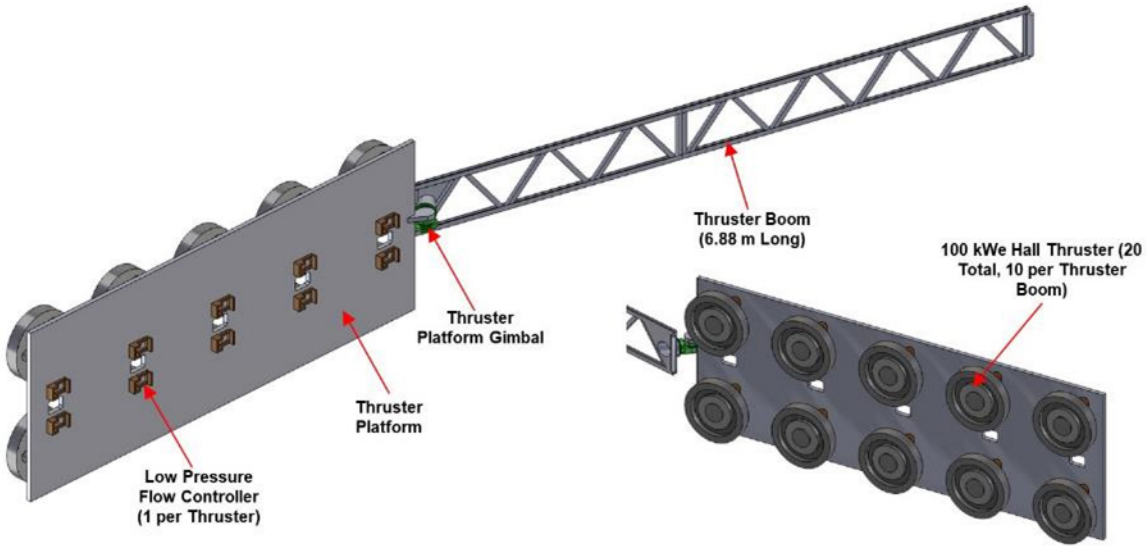

Figure 3-11 EP Thruster Booms and Components

The bus for the NEP Module is located inside the radiator box truss opposite the reactor. Structurally, the bus is composed of a cylinder with two panels closing off the ends and provides the structure to mount the fixed truss portion of the telescoping boom, and mount the box truss containing the reactor radiators, as well as providing the interface to the PLA at launch. A small section of the cylindrical bus structure extends out from the end of the radiator truss, providing area for the bus electronics radiator, commissioning array, four star trackers, two Tracking and Data Relay Satellite (TDRS) S-band antennas, and the two X-band antennas. Located on the end panel of the bus that extends outward from the radiator truss are the docking adaptor, and the two S-band patch and two S-band omni antennas utilized for proximity operations during automated rendezvous and docking with the Xenon Interstage. The NEP Module is the passive docking element, while the Xenon Interstage will be the active element. Finally, the eight RCS pods, each containing three thrusters, are located at the four corners of the radiator truss at the bus end, as well as the four corners of the radiator truss at the reactor end. Figure 3-12 below shows these components and their location.

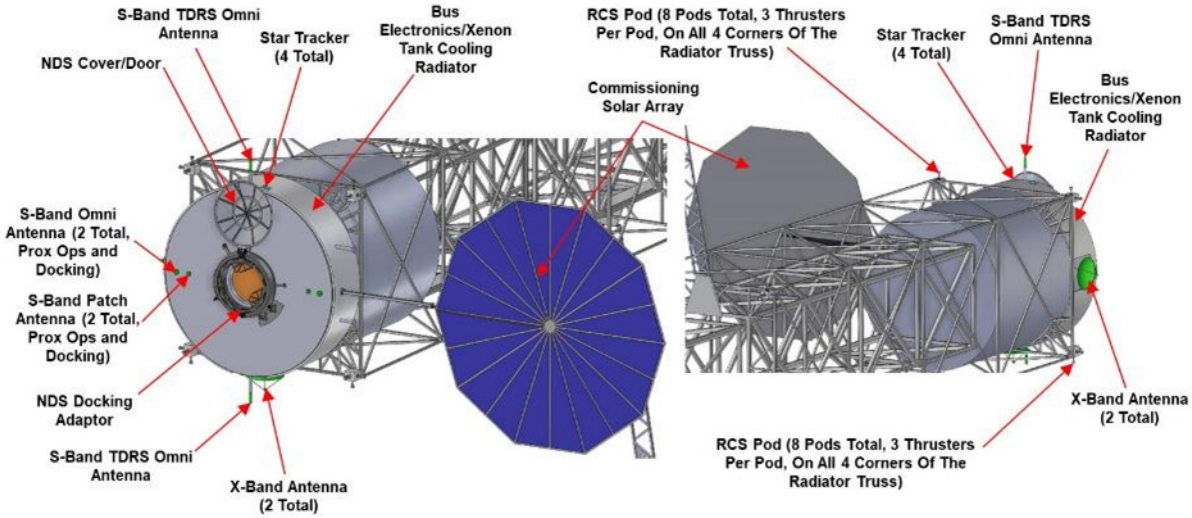

(

Figure 3-12 External Components on the NEP Module Bus

Those components located inside the bus structure of the NEP Module include: the xenon tank, four high pressure flow controllers, the Digital Control and Interface Unit (DCIU), four flow controllers and 20 DDUs of the EP system; the four reactor PMAD units and other electronics for the Electrical Power System (EPS); all the electronics associated with the communications system; the star trackers optical heads, the star tracker electronics, and the Inertial Measurement Units (IMU) of the Attitude Determination and Control (AD&C) system; the avionics enclosure of the Command and Data Handling (C&DH) system; the xenon tank cooling system; and the helium pressurant, Monomethyl Hydrazine (MMH), and Nitrogen Tetroxide (NTO) tanks for the RCS system. Figure 3-13 below shows all these components and their location within the bus. A more detailed discussion on all the components on the Nuclear Power Module can be found in their respective system section found later in this document.

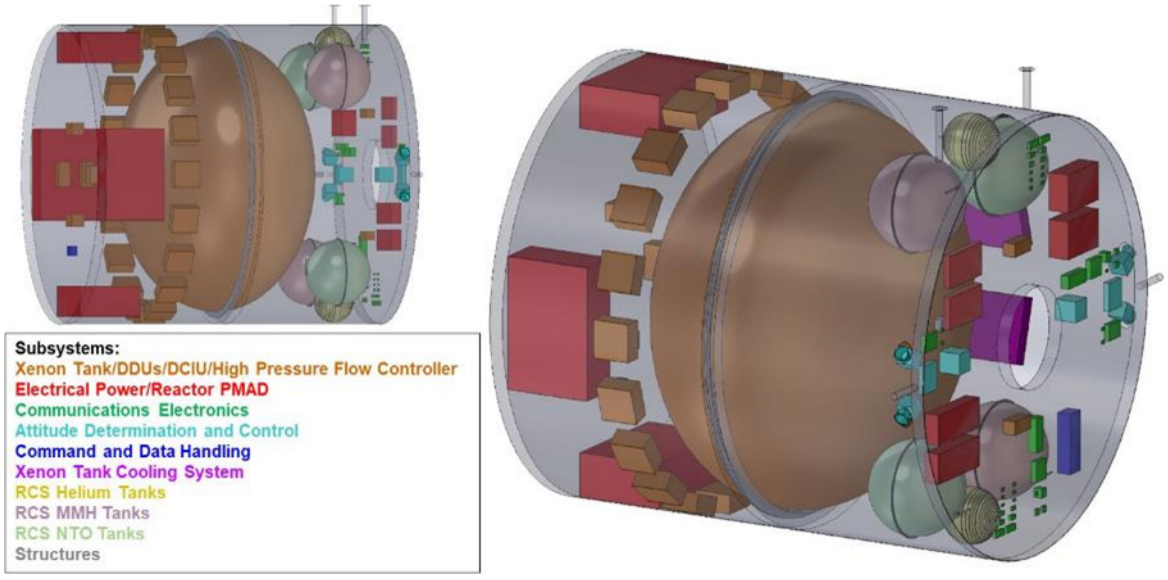

Figure 3-13 Internal Components of the NEP Module Bus

Figure 3-14 shows a transparent view of the entire deployed NEP Module, while Figure 3-15 shows a close-up transparent view of the NEP Module bus.

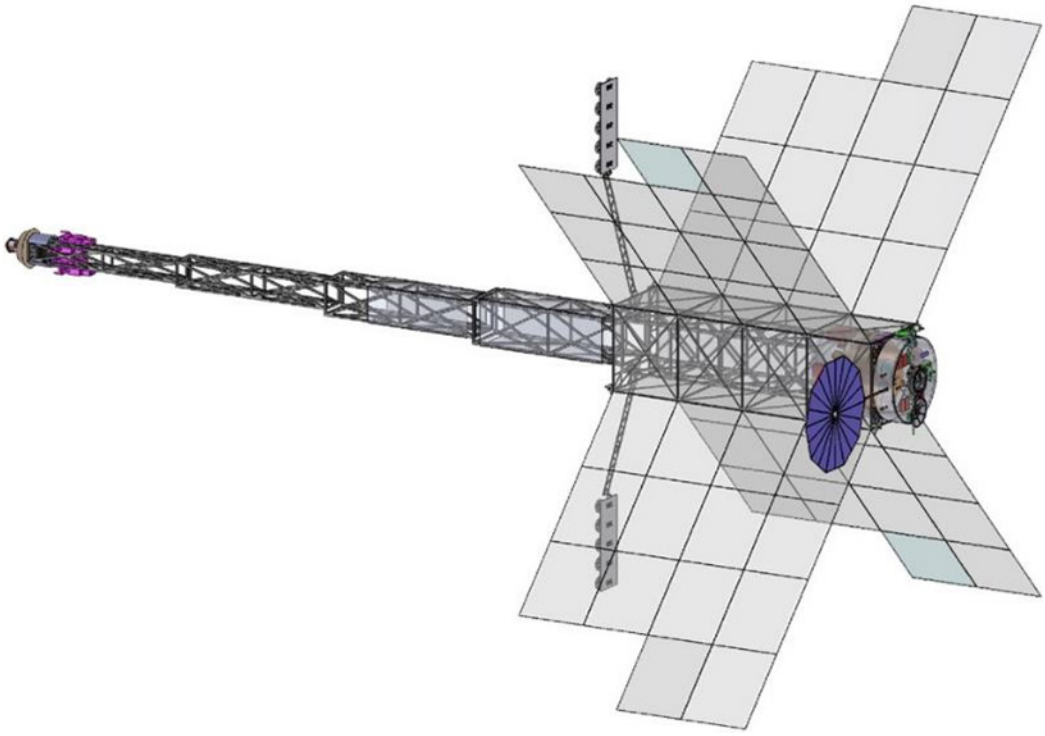

Figure 3-14 Transparent View of the Deployed NEP Module

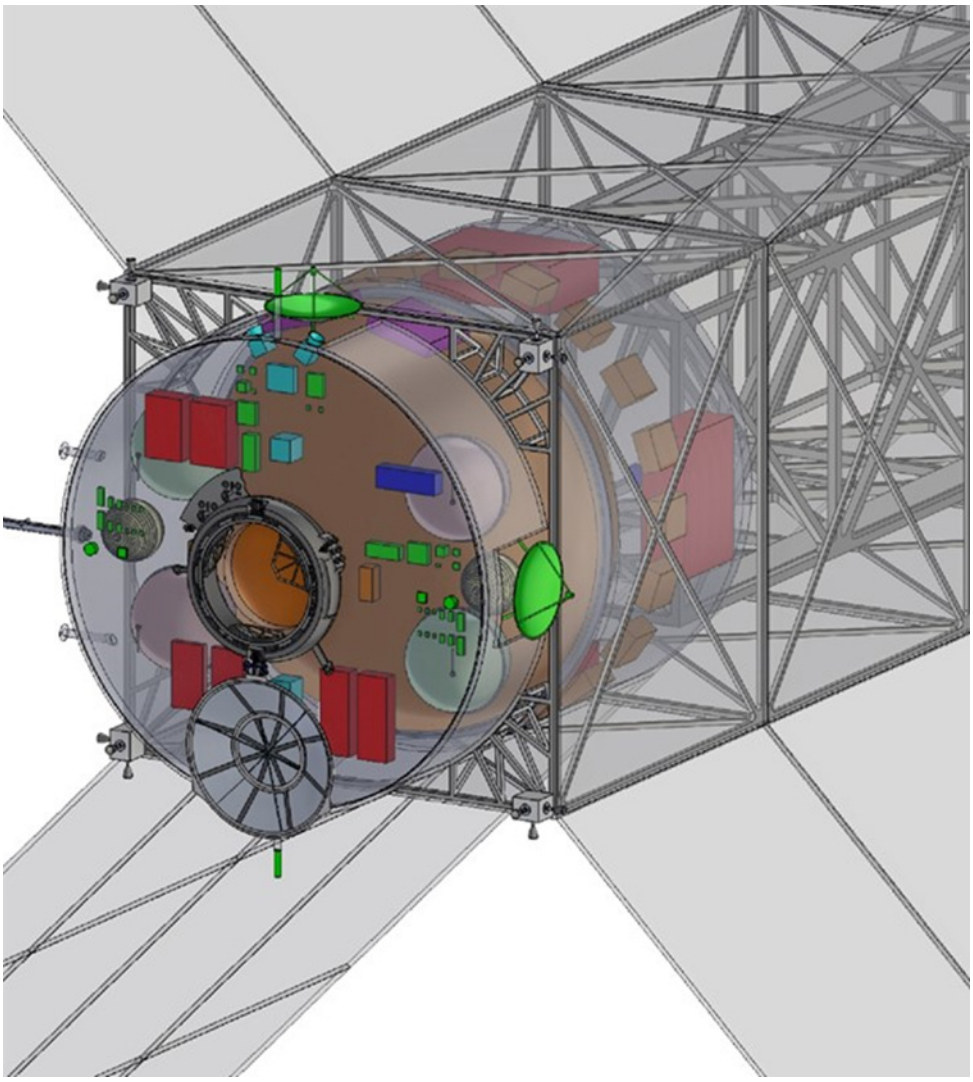

Figure 3-15 Transparent Close-up View of the NEP Module Bus

For the Chemical Propulsion Module, several components must be stowed at launch and deployed once delivered to the desired orbit so that it can fit within the payload fairing at launch. These elements include the commissioning Ultraflex® solar array and the extendable nozzle of the three main chemical thrusters. Figure 3-16 below shows the stowed configuration of the Chemical Propulsion Module with the overall stowed dimensions shown in Figure 3-17 below.

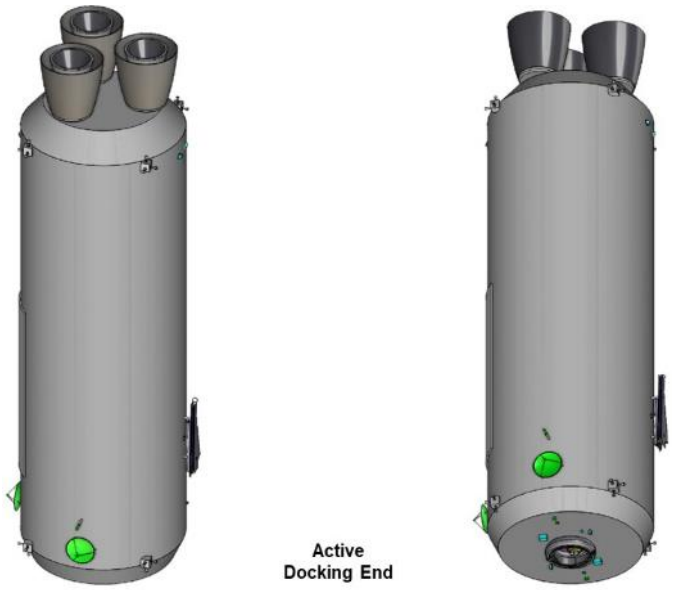

Figure 3-16 Stowed Configuration of the Chemical Propulsion Module

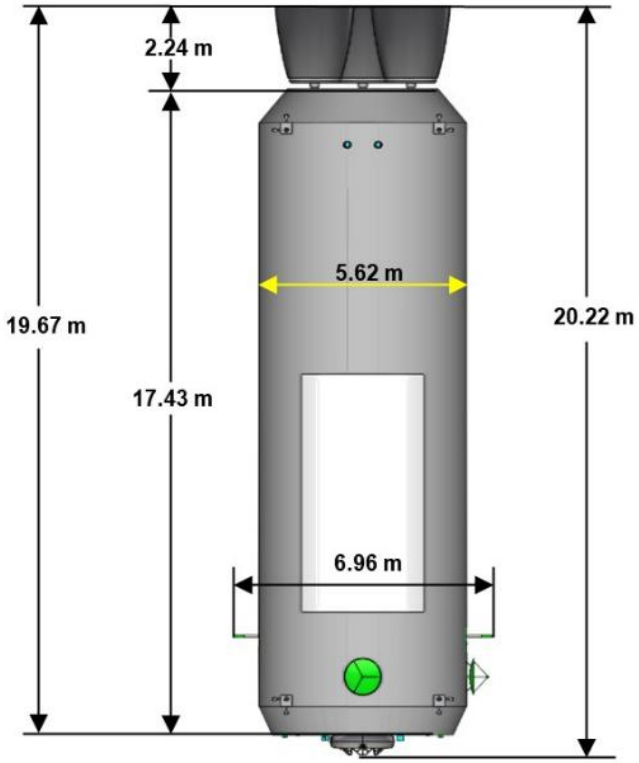

Figure 3-17 Overall Dimensions of the Stowed Propulsion Module

The commissioning Ultraflex® array is stowed on and tied down to the side of the bus structure and is deployed out on a two-section boom with a 2-axis gimbal at the end integrated to the bus structure. Due to the overall length of the chemical propulsion stage, the extendable nozzles on the three main chemical thrusters must be retracted at launch to allow it to fit within the fairing and are extended after separation from the launch vehicle. Extension of the nozzles adds an additional 1.96-m to the overall length of the Chemical Propulsion Module. Deployment of the commissioning Ultraflex® array, along with the extension of the three main thruster nozzles is shown in Figure 3-18 below.

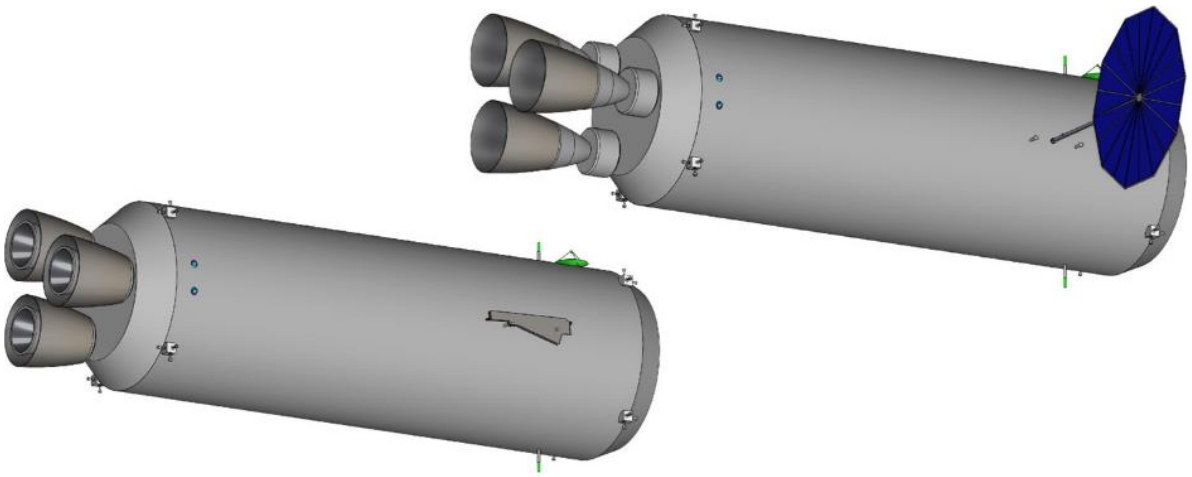

Figure 3-18 Deployment of the Chemical Propulsion Module

The bus structure for the propulsion module bus is comprised of a long cylindrical tube with a conical section and endcap at one end that reduces the diameter down to the interface dimeter of the payload launch adapter (PLA), and another conical section and endcap at the other end that acts as the thruster structure for the main chemical thrusters. The diameter of the bus structure was driven by the 5-m diameter of the chemical propellant tanks contained inside. Length of the bus structure was driven by the length of the chemical propellant tanks needed to carry the required propellant loading for the mission. A common bulkhead tank design was utilized to ensure the tanks could carry the required propellant loading while allowing the chemical stage to fit within the payload fairing. The common bulkhead is concave in the LOX tank, and convex in the Liquid Methane tank as can be seen in Figure 3-19 below. More details on the tank design can be found in Section 4.2.6, System Design.

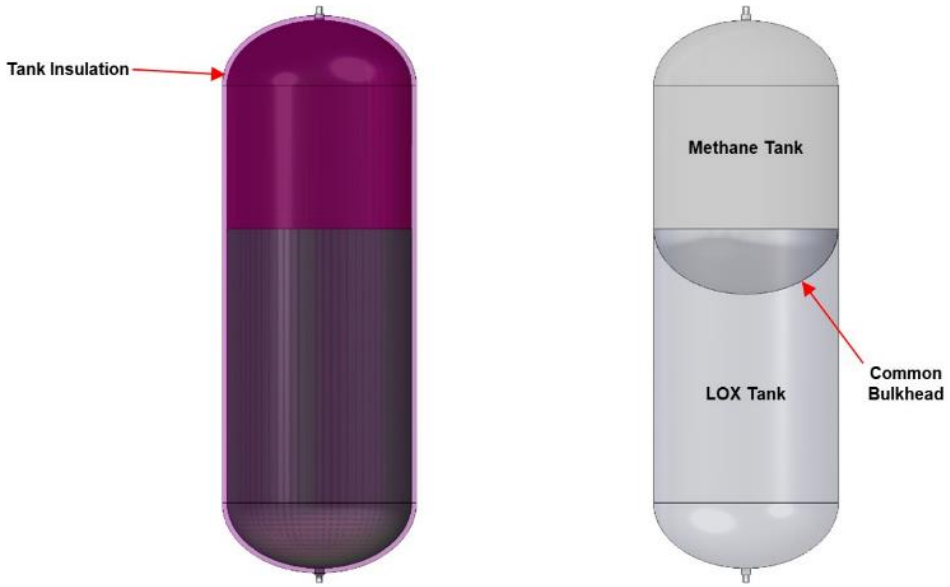

Figure 3-19 Common Bulkhead Tanks for LOX and Liquid Methane

Those components located external to the Chemical Propulsion Module bus structure include: four star tracker optical heads, two Light Detecting and Ranging (LIDAR) units, two docking cameras, and two docking lights of the AD&C system; two X-band antennas and two S-band TDRS antennas for mission communications; two S-band omni and two S-band patch antennas for communication during proximity operations and docking; the docking adaptor; the commissioning Ultraflex® solar array; the body mounted cryocooler and electronics radiator; four RCS thruster pods containing three thrusters each; and the three main chemical thrusters. Note that the LIDAR units, cameras, and lights are required as the propulsion module is always the active vehicle when docking to the full NEP vehicle assembly Figure 3-20 below shows the location of all these components.

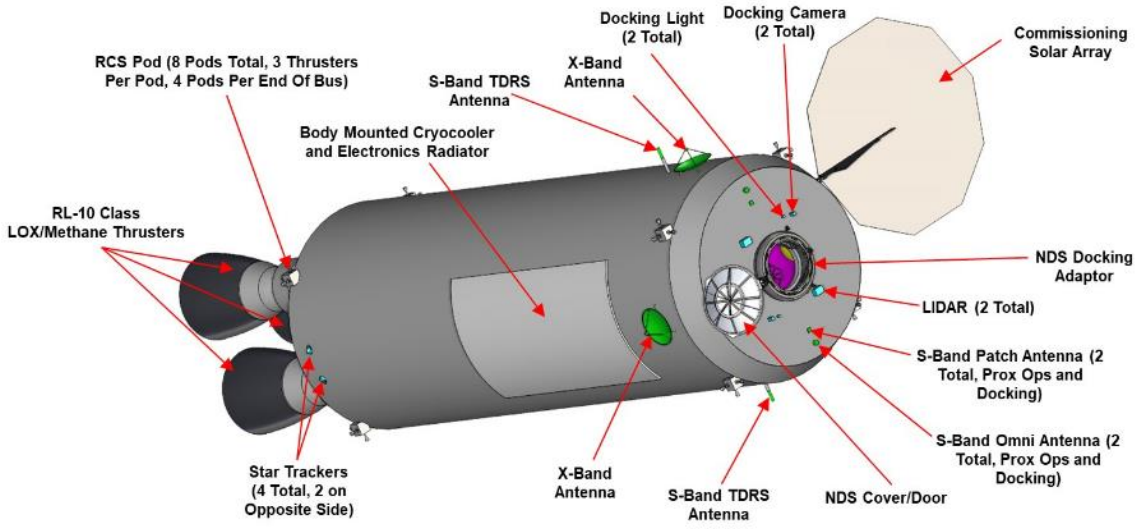

Figure 3-20 External Components on the Chemical Propulsion Module

Those components located inside the bus structure include: two star tracker electronics units and two IMUs of the AD&C system; eight helium pressurant tanks, six thrust vector controllers (TVC), and the main chemical propellant tanks for the chemical propulsion system; the electronics and batteries for the electrical power system; all of the electronics for the communications system; the avionics enclosure for the C&DH system; and the propellant tank insulation and cryocoolers for cooling the chemical propellant. Figure 3-21 below shows the locations for all these components.

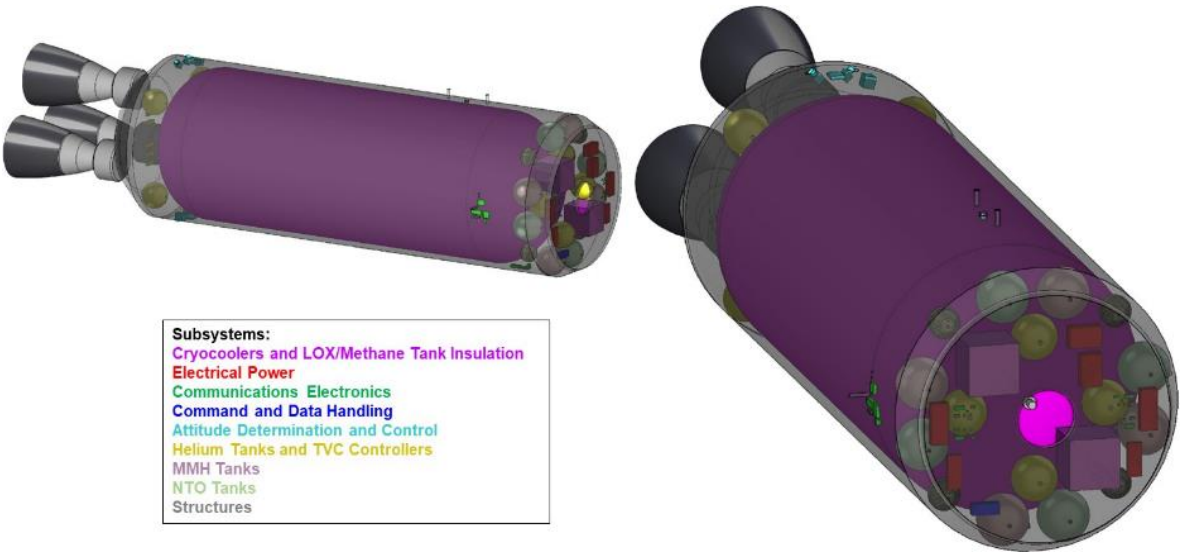

Figure 3-21 Internal Components of the Chemical Propulsion Module

More details on all the components contained on the propulsion module can be found in their respective subsystem sections found later in this document.

For the Xenon Interstage, the only component that needs to be stowed for launch is the commissioning Ultraflex® solar array. As with the commissioning array on the chemical propulsion stage, the array is stowed along the outside of the bus structure where it is tied down for launch. It is deployed out on a two-section boom with a two-axis gimbal at the end integrated to the bus structure. Figure 3-22 below shows images of the stowed Xenon Interstage, while Figure 3-23 below shows the stowed dimensions. Deployment of the commissioning array is shown in Figure 3-24 below.

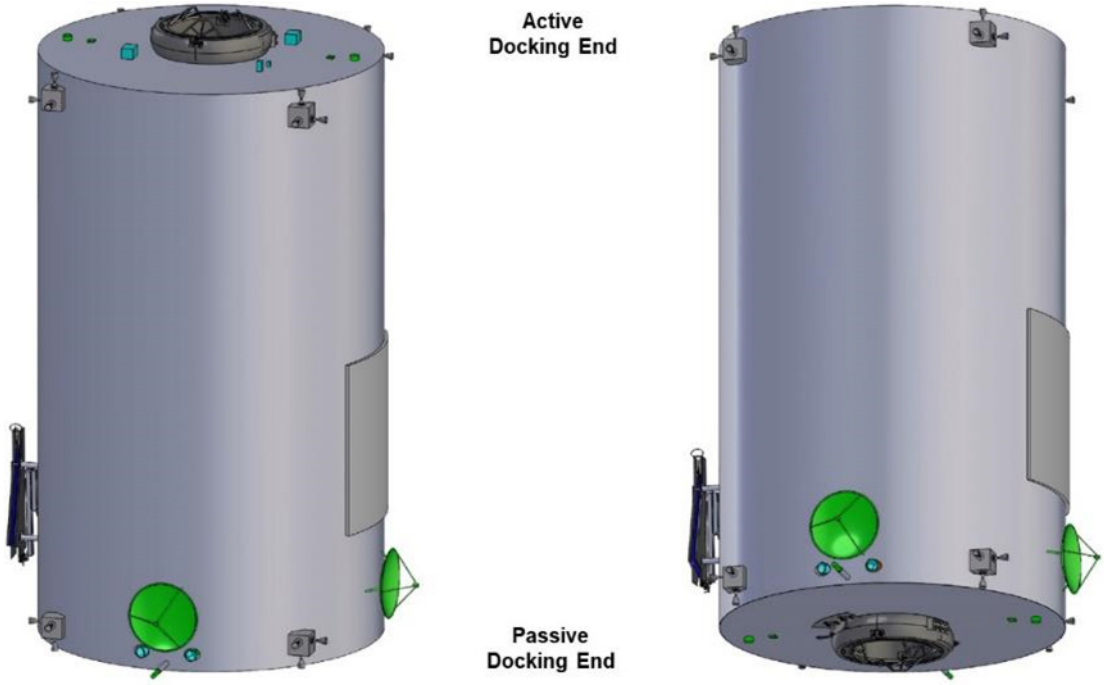

Figure 3-22 Xenon Interstage in its Stowed Configuration

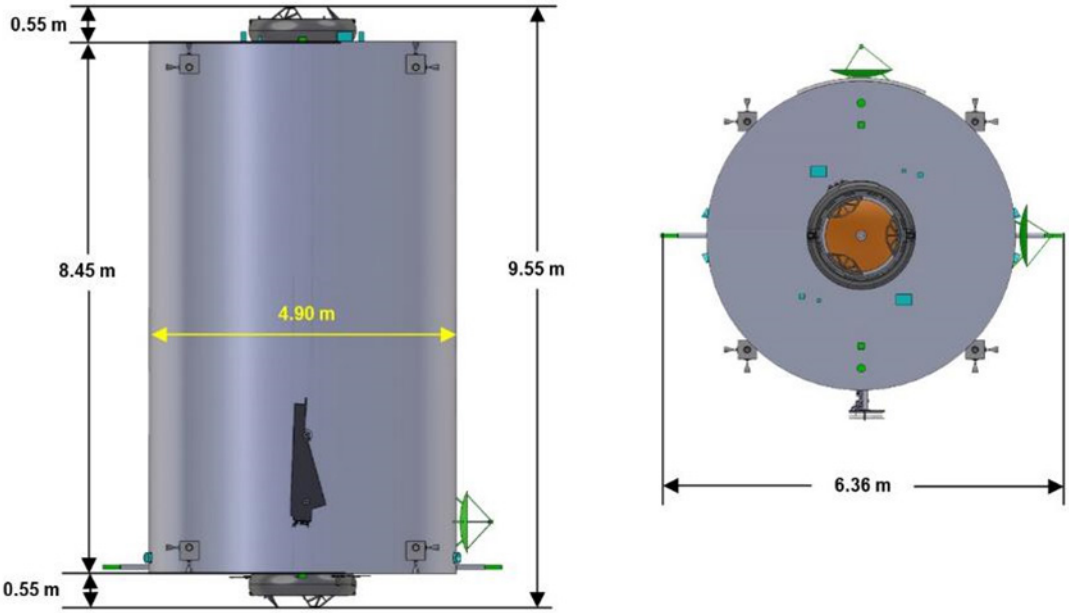

Figure 3-23 Stowed Dimensions of the Xenon Interstage

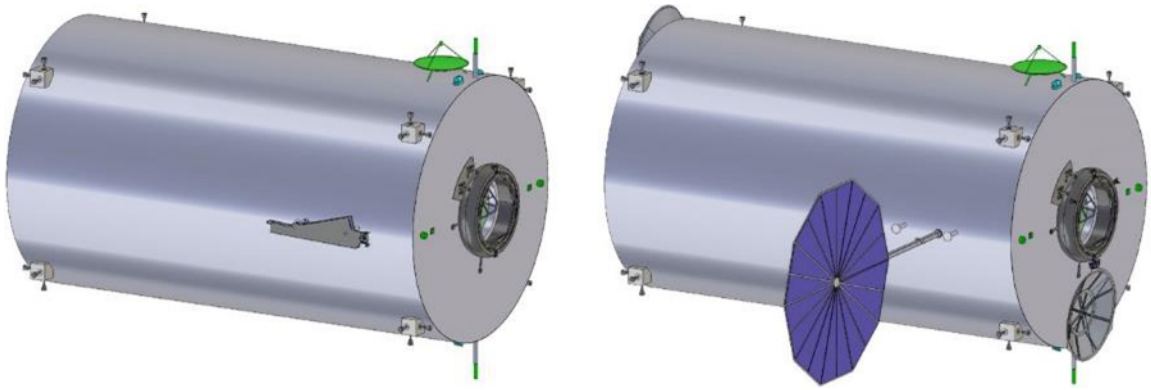

Figure 3-24 Deployment of the Commissioning Array on the Xenon Interstage

Those components located external to the Xenon Interstage bus structure include: four star tracker optical heads, two LIDAR units, two docking cameras, and two docking lights of the AD&C system; two X-band antennas and two S-band TDRS antennas for mission communications; four S-band omni and four S-band patch antennas for communication during proximity operations and docking; two docking adaptors; the commissioning Ultraflex® solar array; the body mounted electronics radiator; and four RCS thruster pods containing three thrusters each. All of the external components can be seen in Figure 3-25 below. Note that there is a docking adaptor and S-band proximity operations antennas on each end of the Xenon Interstage, while the LIDAR, docking cameras, and docking lights are only on one end. The end containing the LIDAR, docking cameras, and docking lights is the active end of the Xenon Interstage and has an active docking adaptor, while the other end is the passive end containing a passive docking adaptor. The Xenon Interstage will be the active docking element when docking with the NEP Module or when docking to other Xenon Interstages already integrated with the NEP Module (as would be the case for the configuration used to spiral out to NRHO from LEO). Once the Xenon Interstage is docked with the NEP Module, it will then be on the passive side when other Xenon Interstages, the habitat, or the chemical propulsion stage are docking to the Xenon Interstage contained on the full vehicle assembly.

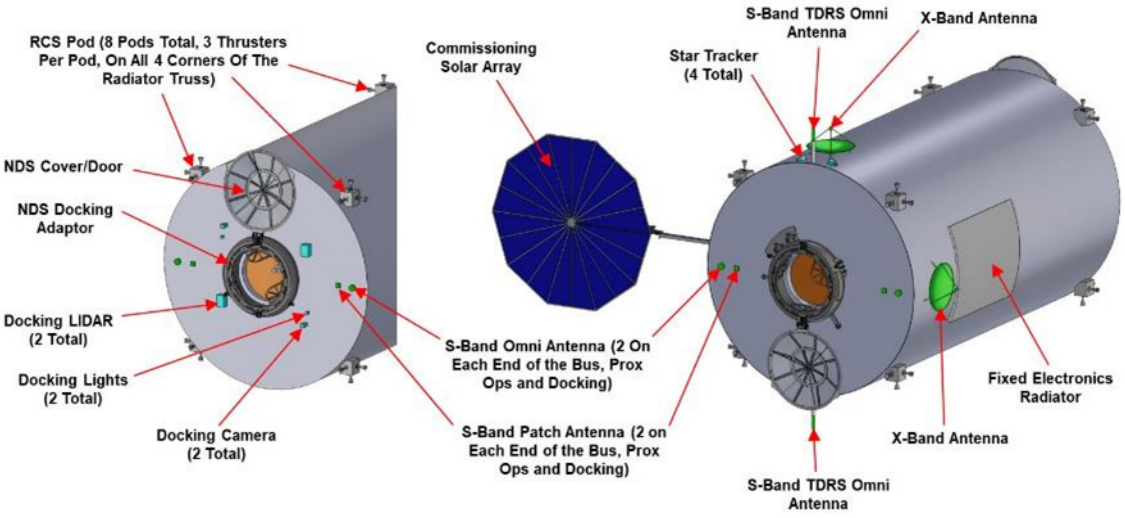

Figure 3-25 External Components on the Xenon Interstage

Those components located inside the cylindrical bus structure of the Xenon Interstage include: two xenon tanks (identical to the xenon tank inside the NEP Module bus); the batteries and electronics of the EPS; all the communications electronics; the star tracker optical heads, star tracker electronics, and IMUs of the AD&C system; the avionics enclosure for the C&DH system; and the helium pressurant and fuels tanks for the RCS system. These components along with their location within the bus is shown in Figure 3-26 below.

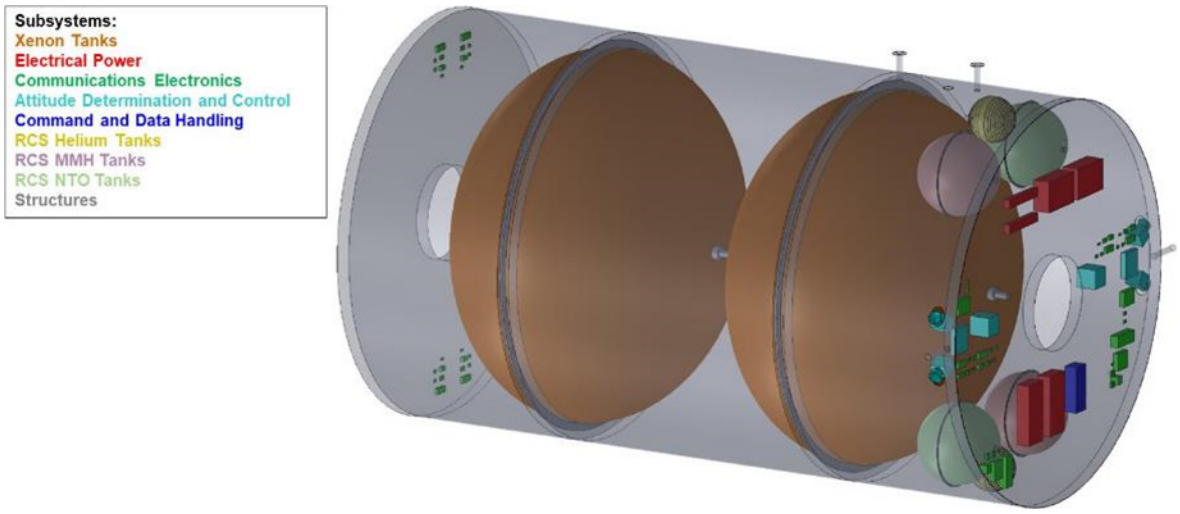

Figure 3-26 Internal Components on the Xenon Interstage

More details on all the components contained on the NEP Module, Chemical Propulsion Stage, and Xenon Interstage can be found in their respective system sections later in this document.

As stated upfront in this section, there are three main configurations for the full NEP vehicle dependent upon the stage of the mission. They include the spiral from LEO to NRHO configuration, the Mars transit configuration, and the Earth return configuration. These three vehicle configurations are shown in Figure 3-27 below.

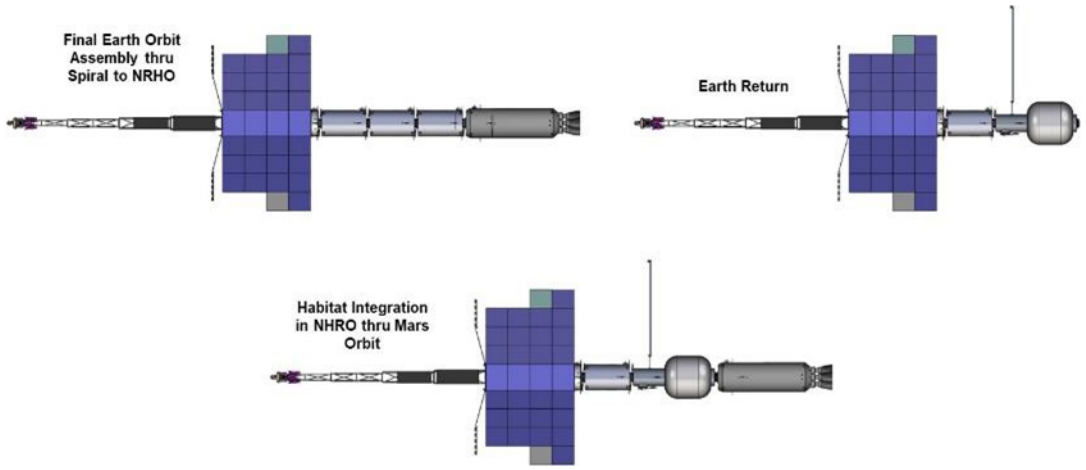

Figure 3-27 Various Configuration of the Full NEP Vehicle

Figure 3-28 and Figure 3-29 below show transparent views of the full NEP vehicle in the spiral out to NRHO configuration. An isometric view of the Mars transit configuration is shown in Figure 3-30 below.

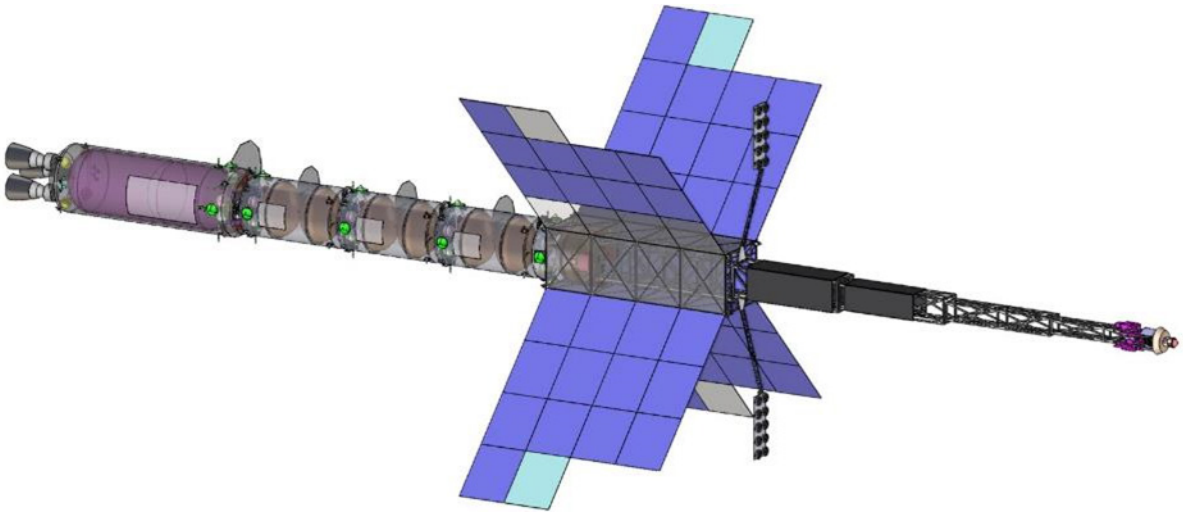

Figure 3-28 Transparent View of the Spiral out to NRHO Vehicle Configuration

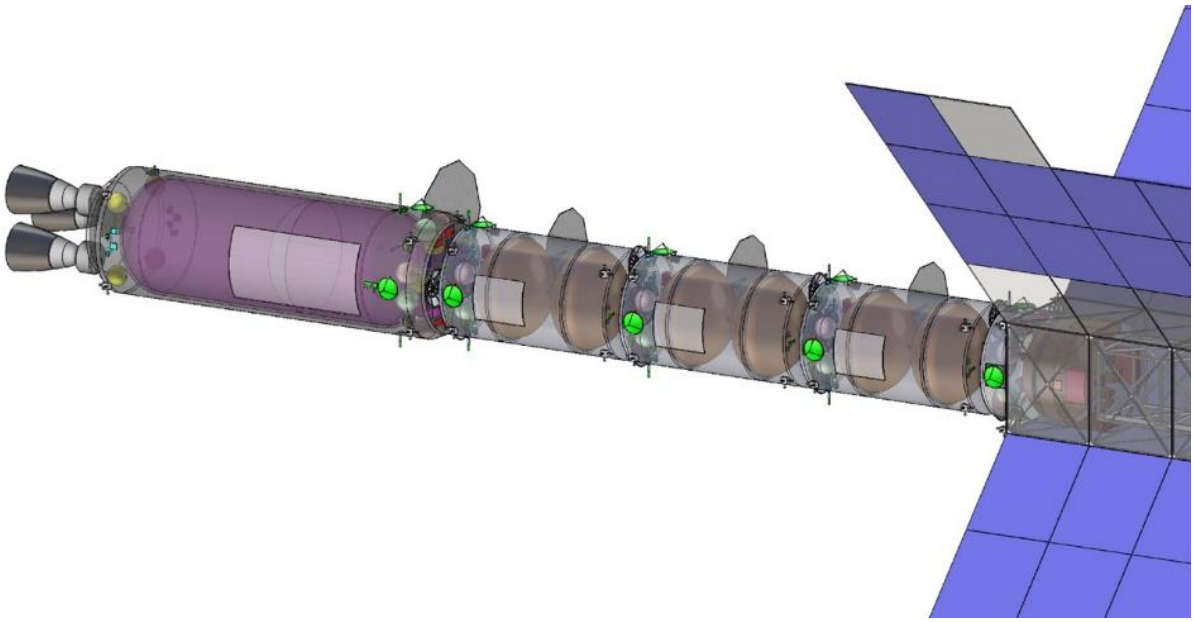

Figure 3-29 Additional Transparent View of the Spiral out to NRHO Vehicle Configuration

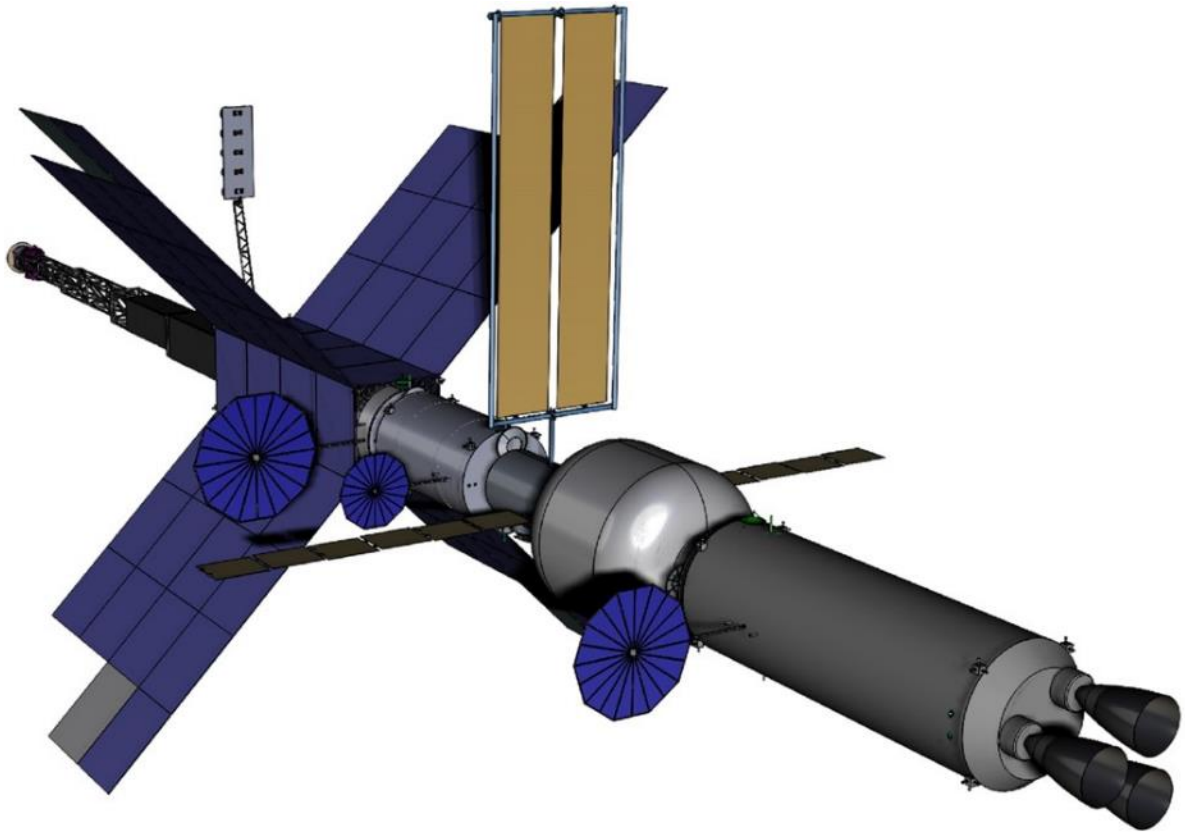

Figure 3-30 Isometric View of the Mars Transit Configuration of the NEP Vehicle

4.0 Subsystem Breakdown

This section provides a detailed description of each major vehicle subsystem. In addition to the descriptions and diagrams, each subsection includes a subsystem MEL, which rolls up into the overall system level MEL and mass summary for each case.

4.1 Electrical Power System (EPS)

The EPS provides electrical power to the loads on the spacecraft from launch through operation. During commissioning, all vehicle stages use their own commissioning solar arrays and rechargeable batteries for power needs, with some of the commissioning power used for startup of the nuclear reactor. Once the reactor is started up and the vehicle fully assembled, the solar arrays and batteries are no longer used because the reactor can fulfill all subsequent electrical power needs (including the large EP thrusting loads). The rest of this section focuses on the NEP Module, Xenon Interstage, and Chemical Propulsion Modules; the Habitat Stage has its own power generation capability for free flying.

4.1.1 Fission Reactor Power System

The fission power system is the major element of the EPS. NASA has pursued nuclear fission power many times in its history due to the attractive features of the technology, namely its high power density and capability to operate independently of sunlight. Nuclear electric propulsion systems have been studied over a wide range of power levels and use cases. The most recent concept study, performed in 2012 [6], targeted 2.5 MWe using a reactor core based on highly enriched uranium nitride (UN) fuel studied under the SP-100 program. This reactor power system used a pumped liquid metal loop to transfer heat to a helium xenon (HeXe) Brayton power conversion system. Since this study, significant progress in the field of space nuclear fission technology was achieved through the NASA Kilopower Project [7]. This small reactor design with a 1-10 kilowatt electric (kWe) power range used a uranium molybdenum (UMo) refractory alloy core with passive sodium heat pipes providing the heat transfer to a Stirling cycle power conversion system. The simplified, lower power design of Kilopower allowed for a successful ground nuclear prototype test in 2018 that increased the agency's interest in space fission systems. This technology is a step toward the multi-MWe systems needed for this mission.

The major design considerations for sizing the power of a nuclear electric system are the reactor core design, the heat transfer method, the power conversion system, and the heat rejection system. Core design, while complex from a nuclear engineering standpoint, can be viewed simply as determining the temperature provided by the heat source. The UMo Kilopower fuel was designed to operate at 1100 K, while the 2012 concept was designed for 1500 K operation. As with any thermodynamic cycle, the heat source temperature plays an important role in system efficiency and specific mass. Higher temperature reactors are desirable from a mass perspective but are less mature and more difficult to test and therefore lower on the TRL scale. The success in testing the relatively lower temperature Kilopower design over the higher temperature SP-100 and Prometheus designs demonstrates this fact. For higher power systems, however, the high temperature reactor becomes desirable to minimize the system mass and radiator area required to achieve a viable mission design.

Secondly, heat transfer plays a major role in system design and reliability. The three major primary heat transfer methods for cooling space reactors are heat pipes, pumped liquid metal, and pumped gas. Though all of these methods involve some sort of fluid motion, the mechanisms differ significantly. Heat pipes work on a passive two-phase evaporation/condensation cycle that requires no external power, while liquid metal or gas cooling requires drive pumps or compressors to actively circulate the fluid. The benefit of active cooling over passive heat pipes is flexibility in design and higher thermal throughput. Typical liquid metals used in pumped loops are lithium, sodium, potassium, or a mixture of sodium and potassium (NaK). Gas-cooled systems have the option of directly coupling to a Brayton engine, increasing the efficiency of the heat transfer subsystem. However, this leads to a single shared gas space for the reactor and power conversion system, which may have impacts on the system reliability.

The final major design decision is the power conversion system. The typical options include the Stirling, Brayton, and Rankine thermodynamic cycles, as well as thermoelectric and thermionic devices. Each option presents different characteristics on thermal efficiency and power throughput, and therefore on the system mass. On the low end of the efficiency scale, thermoelectric conversion has a long history of use in radioisotope power systems. However, the lower efficiency is a challenge for high power fission systems due to the larger reactor, radiation shield, and waste heat radiator. The Stirling cycle has high efficiency but does not scale well to higher power. HeXe Brayton systems fair better at higher power but the lower heat rejection temperature results in a larger radiator. A supercritical CO_2

(or perhaps other supercritical working fluid) Brayton system may perform better than the HeXe system, but that technology has been mainly focused on terrestrial applications. A potassium Rankine cycle has the potential for high efficiency and heat rejection temperature, but the two-phase system design is a challenge and the TRL is low. Figure 4-1 presents examples of the design space for reactor heat transfer and power conversion in nuclear fission systems.

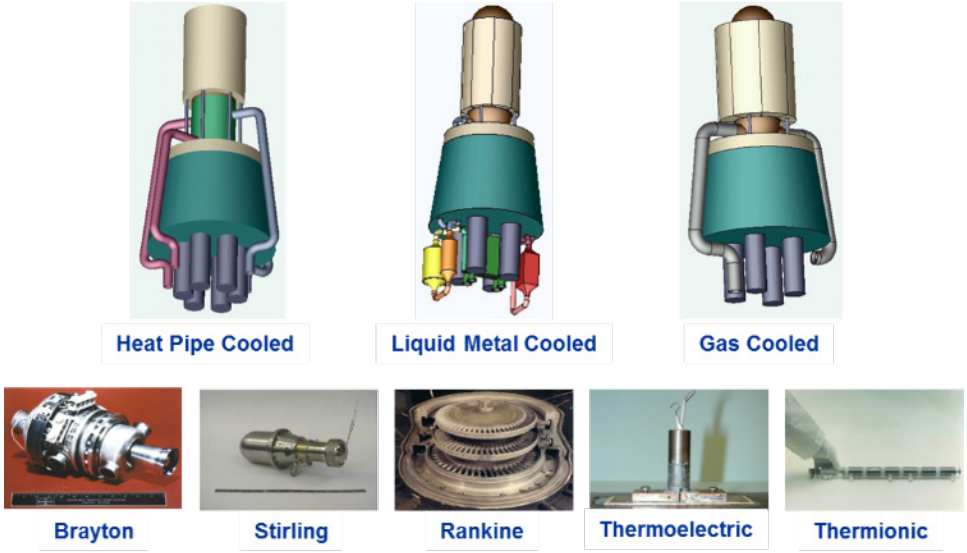

Figure 4-1 Heat Transfer and Power Conversion Options

The power conversion trades comparing HeXe and supercritical carbon dioxide ($scCO_2$) Brayton favored the $scCO_2$ option for MTAS 1.2. The $scCO_2$ option yielded a ~20% increase in power output for the same total radiator area. The reference 1.9 MWe power system concept assumes four $scCO_2$ Brayton converters each producing 25% of the total system power, shown in Figure 4-2 coupled to the Li-cooled reactor through four liquid-to-gas heat exchangers. Each Brayton unit includes a turbo alternator-compressor, recuperator, and gas cooler. The development of a ~500 kWe-class Brayton unit represents a significant scale-up over the state-of-art for HeXe Brayton technology, represented by the 10-15 kWe Brayton Rotating Unit (BRU), the 2 kWe mini-BRU, the 36 kWe converter for the Space Station Freedom Solar Dynamic Power Module, and the 100 kWe converter for the Prometheus/Jupiter Icy Moons Orbiter mission. Legacy HeXe Brayton technology, with superalloy hot-side materials that permit turbine inlet temperatures up to 1150 K, has undergone considerable NASA testing to demonstrate performance in relevant environments and for extended operating times (e.g., ~50,000 hours of BRU testing). Conversely, $scCO_2$ Brayton development has focused on MWe-class power levels but has been mostly limited to terrestrial applications with systems that are not designed for space use. If $scCO_2$ Brayton is pursued for Mars NEP, the emphasis will be on adapting high power terrestrial technology and demonstrating performance in relevant environments. If HeXe Brayton is pursued, the emphasis will be on scaling the legacy technology to higher power levels.

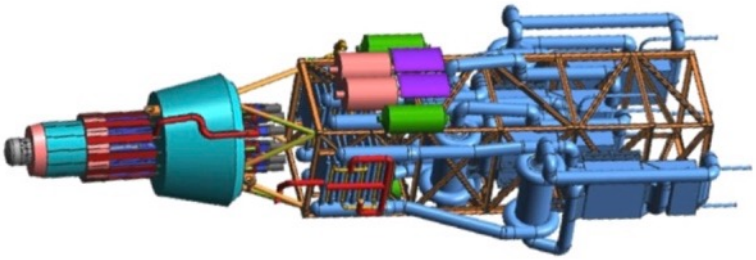

Figure 4-2 NEP Reactor-Brayton Configuration

Another challenge for space fission power systems is rejecting the waste heat. The vacuum of space requires radiative heat rejection, which is dependent on large, bulky radiators. In fact, the limiting design factor for the fission system in this study was the stowed radiator volume that could be accommodated in a single launch vehicle. Preliminary radiator stowage concepts have indicated a maximum radiator area of approximately 2500 m^2 for the 8.4 m SLS fairing. The benefits of the high temperature reactor studied in 2012 were increased efficiency and higher heat rejection temperature, both of which contribute to decrease the radiator area required for a given power level. The heat rejection subsystem for the current reactor concept assumes that each Brayton converter has a dedicated pumped-NaK cooling loop and a one-fourth segment radiator assembly. The NEP radiators would operate at temperatures between 375 and 550 K. This temperature regime was studied extensively during the NASA Prometheus Project [8] and follow-on Fission Surface Power Project [9]. Technology development was completed on high temperature Titanium in water (Ti/H_2O) heat pipes (both life testing and microgravity research), polymer-matrix composite (PMC) radiator panels (both sub-scale and full-scale thermal vacuum tests), and pumped NaK fluid loops (at operating temperatures up to 875 K). Leveraging those developments, the NEP radiators use PMC panels with embedded Ti/H_2O heat pipes. The 2500 m^2 total NEP radiator surface is comprised of four radiator segments each having 17 individual radiator panels (approx. 4 m x 5 m) that are coupled to the NaK coolant manifold, as shown in Figure 4-3.

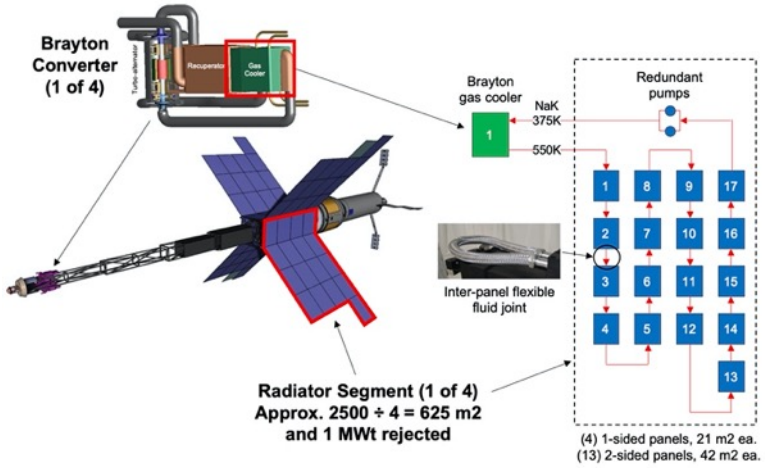

Figure 4-3 NEP Radiator Configuration

Figure 4-4 below shows a parametric analysis of radiator area and system mass across a range of relevant power levels for three different reactor-Brayton combinations. System mass includes the reactor, shield, power conversion, heat rejection and PMAD. Given the 2500 m^2 SLS radiator limit, the 1200 K HeXe case (A) permits 1.6 MWe maximum power output, the 1200 K $scCO_2$ case (B) permits 1.9 MWe, and the 1500 K HeXe case (C) permits 2.9 MWe. While the 1500 K case may appear attractive from a performance standpoint, it introduces considerable development risk relative to the other two cases. The 1500 K reactor would require a new fuel form and refractory alloy cladding/structural material beyond what was demonstrated during the SP-100 Program. It would also require new higher-temperature materials for the Brayton converters and radiators beyond the current experience base for those technologies.

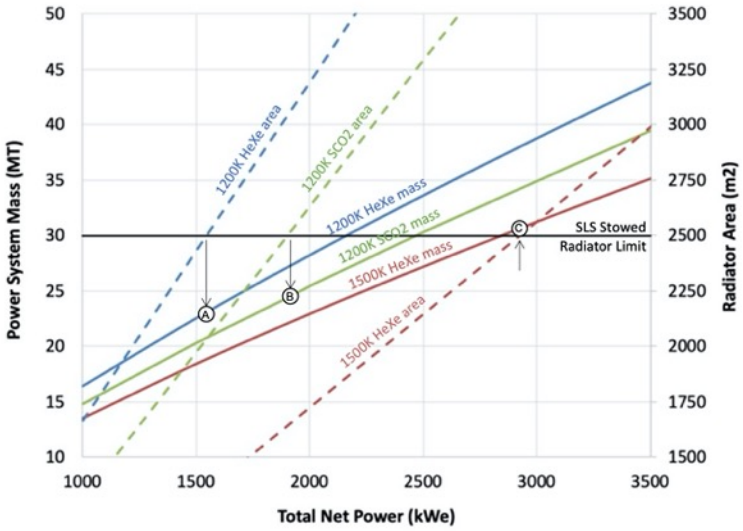

Figure 4-4 System Mass and Radiator Area Parametric Study

The reactor concept in the parametric analysis above assumed a fast-neutron spectrum core with pin-type refractory-clad fuel using Highly Enriched Uranium (HEU). The Department of Energy (DOE) was added to the team to evaluate different reactor design options and fuel enrichment levels. The Oak Ridge National Laboratory (ORNL) led the reactor trade studies (principally Lou Qualls, Brian Ade, and Jorge Navarro). They evaluated two reactor concepts: a) a fast-spectrum SP-100 derived system using UN pin fuel with pumped Li primary heat transport, and b) a derivative of the Transformational Challenge Reactor (TCR) using UN particle fuel in a solid moderator block. The TCR derivative could use either direct Brayton gas cooling or the primary Li loop, although the Li option was the preferred configuration for this study based on overall system reliability (a gas-cooled reactor with multiple Brayton units sharing a common gas circuit is vulnerable to single-point system failure, whereas the intermediate loop with separate Brayton heat exchangers offers partial power functionality in the event of individual Brayton failures). Both the SP-100 and TCR reactor approaches were evaluated with HEU (93% enrichment) and High-Assay Low Enriched Uranium (HALEU, 19.75% enrichment).

The ORNL study assumed a reactor thermal power of 10 MWt, coolant outlet temperature of 1200 K, and operational life of two years at full power. The results showed the SP-100 HEU option to be the lightest mass reactor at approximately 2400 kg including fuel, vessel, reflector, instrumentation and control, and Li primary loop. The LEU version of the fast-spectrum SP-100 reactor was found to be prohibitively heavy at over 10 t. The moderated HEU TCR option with Yttrium Hydride (YH) moderator had a similar reactor mass as the fast-spectrum HEU SP-100, but the larger reactor diameter resulted a 70% increase in shield mass. The mass of the LEU TCR reactor with YH moderator was about twice the HEU version at 4800 kg and required the heaviest shield because of the large reactor diameter. However, the total 3500 kg mass increase (including the shield) for the LEU TCR option relative to the HEU SP-100 option did not significantly impact the mission design. The LEU TCR reactor shown in Figure 4-5 was selected as the reference approach for the MTAS 1.2 mission study, with the HEU SP-100 as the study alternative. The 10 MWt power rating was based on the initial 3.8 MWe need and provides up approximately 40% power margin for the 1.9 MWe case.

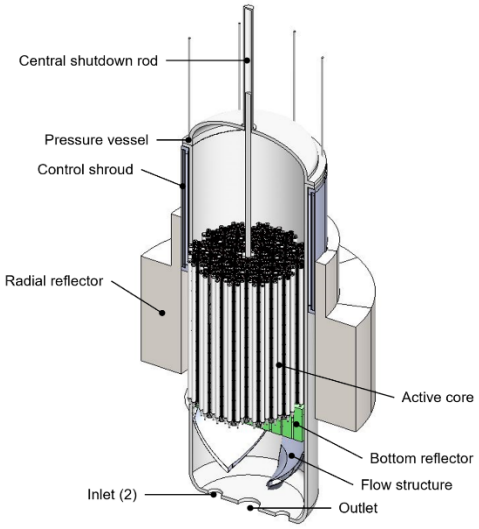

Figure 4-5 TCR-Derivative Reactor Concept for NEP

Another challenge for fission power systems is the need to shield the mixed neutron and gamma radiation field produced by the fission reactor. The amount of radiation is directly correlated to the thermal power and operating life of the reactor, which adds an additional motivation to increase the thermal efficiency of the nuclear system. The need for shielding is driven by both electronic and materials tolerance as well as human dose limits for crewed missions. Shielding design is relatively straightforward with little change between the various fission power systems studies performed in the past. Low-atomic-number materials like hydrogen, beryllium, lithium, boron, etc. provide efficient shielding for the neutron flux, while high-atomic-number materials like tungsten or depleted uranium provide efficient shielding for the gamma dose.

For this study, ORNL (principally Michael Smith) performed a shielding analysis to compare several design variants for their effectiveness in attenuating radiation at three key locations: a) the Brayton units, b) the PMAD electronics, and c) the crew habitat. The starting point was a conical lithium hydride (LiH) and Tungsten (W) shield with a 26 deg half angle that limited radiation at the PMAD electronics located 50 m from the reactor to 25 krad and $1x10^{11}$ neutrons/cm^2 after two years of reactor operation. Further analysis revealed that this shield design would not be sufficient for the crew habitat. Figure 4-6 presents the four shield configurations that were considered by ORNL in the radiation analysis. The LiH/W starting point assumed a constant shield thickness for the entire 26 deg half angle. The two compound shields assumed a thicker central section, or "plug" to provide increased protection for the vehicle centerline elements and crew habitat (within a 3 deg half angle). One of the compound shields assumed a combination of Be/B4C/LiH/W, while the other assumed only LiH/W. The fourth shield option used LiH/W and retained the central plug but reduced mass via cutouts in the perimeter shield to form a cruciform with four 26 deg extensions corresponding with the location of the radiator wings. The desire to limit radiation at the crew habitat to 50 rem/yr became the driving requirement for shield mass. 50 rem/yr was chosen in the absence of an actual requirement; 50 rem/yr is about the same as the radiation from the GCR background. Once a target rem limit is determined the shields can be designed appropriately. The ORNL analysis considered the benefits provided by the in-line Brayton engines, reactor boom, PMAD equipment, Xe propellant and tanks in attenuating crew radiation. The mass comparison among the four configurations revealed that the full-thickness LiH/W shield was the heaviest at 13,800 kg, followed by the hybrid compound at 4,750 kg, the LiH/W compound at 3500 kg and the LiH/W compound cruciform at 2,770 kg. The compound cruciform was selected as the design reference, and the corresponding radiation maps are presented in Figure 4-7. This shield results in a total absorbed gamma dose at the Brayton converters and PMAD electronics after two years of operation of 100 Mrad and 25 krad, respectively; the Brayton dose is somewhat high and may require further analysis and testing. The effective human dose at the forward external face of the crew habitat is 3 millirem (mrem)/hr, corresponding to 100 rem in two years.

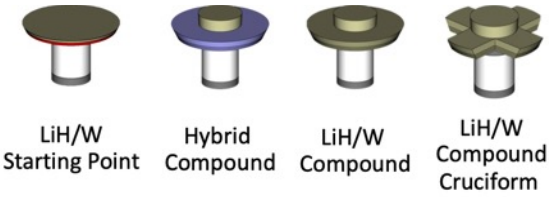

Figure 4-6 Shield Options Considered in ORNL Radiation Study

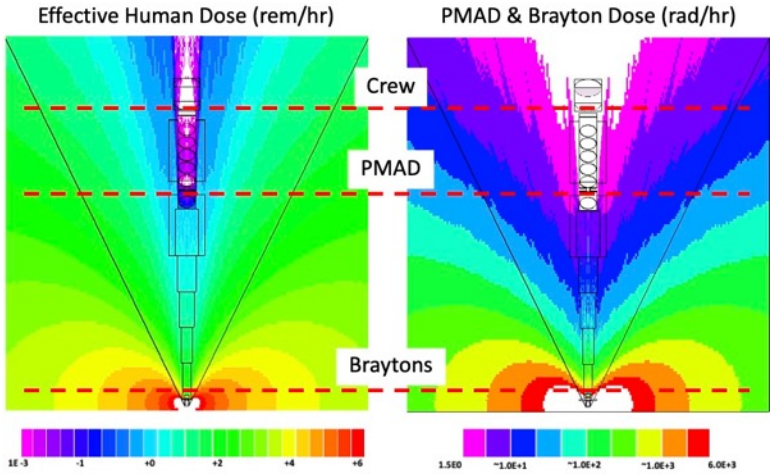

Figure 4-7 Radiation Map for Reference Compound Cruciform Shield

The NEP PMAD electrical schematic is shown in Figure 4-8. The four Brayton units produce high frequency (~2.5 kHz) 3-phase power at 960 VAC that is transmitted through cables to the PMAD electronics bank located approximately 50 m away. Each Brayton has a dedicated PMAD channel with a high voltage AC bus that feeds the 650 voltage direct current (VDC) Hall thruster DDU and 120 VDC spacecraft bus using the appropriate conversion stages. Brayton rotor speed control is accomplished via a pulse-width modulated DC parasitic load radiator (PLR) that maintains a constant load on the alternator. The PLR is sized to reject the entire 500 kWe Brayton output (at 550 deg C) allowing the Brayton units to operate at full power even if there are no external spacecraft loads. The four PLRs (~30 m^2 each) are located on the perimeter of the truss sections that comprise the reactor boom. The spacecraft receives power from the Brayton units, but also supplies power for startup and control. Startup power is delivered to a start inverter that allows the Brayton units to be electrically motored. The spacecraft also feeds power to the PMAD controller/processor that manages the PMAD operations and distributes DC power to the power system auxiliary loads. Each of the four PMAD channels includes a cold plate with a dedicated thermal radiator (~19 m^2 each) that rejects up to 15 kWt (~3%) at 100 °C.

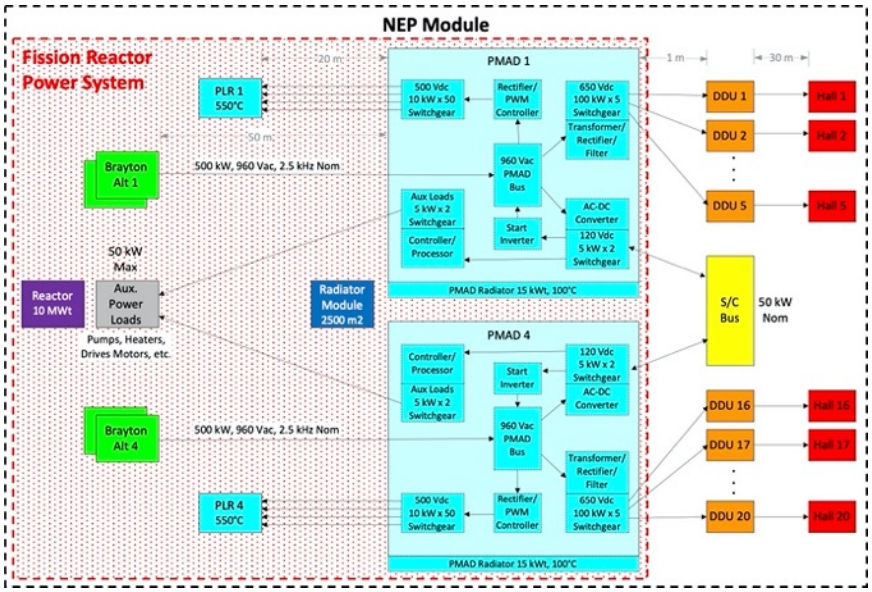

Figure 4-8 NEP PMAD Schematic

4.1.2 System Requirements

To encompass the various operational modes of the spacecraft and the associated load demand in each phase, different operational power modes were defined for the spacecraft throughout the mission. Table 4-1 illustrates these power modes as well as their durations and electrical load demands for the NEP, xenon, and chemical propulsion stages in this study. The load demands in the table include a 30% growth margin for all estimated loads except the EP, which only has a 5% growth margin. All EPS losses and parasitic power required for the EPS components are included in these power levels.

Table 4-1 NEP-Chem Mission Power Modes and Total Electrical Load Demands

	Power Mode 1	Power Mode 2	Power Mode 3	Power Mode 4	Power Mode 5	Power Mode 6	Power Mode 7	Power Mode 8	Power Mode 9
Description	Assembly in LEO	Burn to Nuclear Safe Orbit	Nuclear Startup	NRHO to LDHEO and Crew Embark	NEP Thrusting	Deep Space Coast	Burn in Mars Orbit	Venus Flyby	Capture in LDHEO
Duration	≤ 2 yrs.	30 min	5 hrs.	90 days	~862 days	~220 days	1 hr. each	~1 day	~1 hr.
NEP	1664 W	2132 W	2080 W	2979 W	1.82 MW	2775 W	2775 W	2775 W	1.82 MW
Xenon	1696 W	1078 W	1078 W	1550 W	1176 W	1166 W	1166 W	1166 W	1166 W
Chem	1996 W	2883 W	1592 W	2017 W	1634 W	1634 W	2868 W	1504 W	1165 W
Total	**5356 W**	**6093 W**	**4749 W**	**6546 W**	**1.82 MW**	**5575 W**	**6809 W**	**5445 W**	**1.82 MW**

All the NEP-Chem spacecraft stages must have commissioning solar arrays and batteries through Power Mode 3, Nuclear Startup, after which the nuclear reactor takes over as the source of electrical power. The commissioning solar arrays are designed to account for two years of LEO degradation effects including radiation and thermal cycling.

In Power Mode 4, the chemical stage detaches from the rest of the spacecraft to allow the habitat to dock in its place. The chemical stage then reattaches at the other end of the habitat. Because it will not be able to receive electrical power via the nuclear reactor during this event, the chemical stage must have commissioning arrays and batteries able to support Power Mode 4 in addition to Power Modes 1 through 3, as outlined in red in Table 4-1. As such, the commissioning array on the chemical stage must *also* account for radiation degradation due to the spiral-out trajectory from LEO to a NRHO through the Earth's Van Allen radiation belts during Power Mode 4.

4.1.3 System Ground Rules & Assumptions

The mission assumes the following for all cases and vehicle stages where applicable:

- Commissioning orbits in LEO are 1.5 hours long, with a maximum eclipse duration of 45 min.
- The nuclear startup power required (including growth and PMAD losses) does not exceed 2500 W for a maximum duration of 1 hr.
- The habitat stage nominally consumes 20 kW of electrical power.
- Fission reactor power system:
    - System operational life is two years at full power, allowing for at least one round-trip mission with residual life for contingencies.
    - The reference reactor includes a pumped lithium heat transport, a 19.75% enriched UN fuel, a refractory cladding/structure, and a 1200 K reactor outlet temperature.
    - The lithium heat transport loop includes 4 separate Li-to-HeXe heat exchangers that service individual Brayton power converters.
    - Reactor thermal power is based on required Brayton thermal input power to achieve desired system electric power output.
    - Reactor control utilizes negative-temperature reactivity feedback to permit automatic thermal load following and control rod position adjustment to permit reactor outlet temperature management.
    - Reference shield is a LiH/W truncated cone with 50 m payload separation, 26 deg cone half angle, reactor radiation less than 1E11 n/cm^2 and 25 krad at payload after 2 years at full power.
    - Reference power conversion is a closed cycle, recuperated Brayton with 4 independent converters providing 25% power per converter.
    - Total Brayton output power is based on summation of EP thruster loads, spacecraft housekeeping loads, and NEP power system parasitic loads (PMAD, pumps, drive motors, etc.).
    - Reference design assumes supercritical CO_2 Brayton with 1150 K turbine inlet.
    - Reference heat rejection includes pumped NaK heat transport and deployable, composite radiator panels with embedded H_2O heat pipes.
    - Each Brayton converter has a dedicated NaK cooling loop and radiator segment. Reference design assumes 4 independent NaK cooling loops providing 25% heat rejection per loop.
    - Overall radiator sizing is based on producing maximum system power with 4 K thermal sink and 10% radiator area margin. System power will vary based on thermal sink.
    - Radiator is integrated with deployable boom that extends reactor to specified separation distance to achieve shield radiation limits. The reference boom includes nested, telescoping trusses that accommodate radiator fluid lines and power transmission cabling.
    - Reference PMAD includes power cabling, power conditioning, power control, and switchgear to supply electric power to twenty 650 VDC Electric Propulsion (EP) direct drive units and one 120 VDC spacecraft bus.
    - Each Brayton converter has a dedicated power transmission channel that terminates at the switchgear. Reference design assumes four independent 960 Vac transmission channels providing 25% power per channel.
    - PMAD power controls include channelized parasitic load radiator to regulate Brayton unit operating speed and power output.
    - PMAD power controls include NEP power system health monitoring and control with functionality for system startup, full power operation, part power operation, power standby, and shutdown.

    - NEP power system parasitic loads, including reactor pumps, reactor control drives, radiator pumps, and health monitoring, are fed by the 120 VDC spacecraft bus.

- Solar arrays:
    - Solar arrays have continuous, near-perfect pointing for at least 50% of the orbit period (≥ 45 minutes).
    - Solar array gimbals provide fore-aft movement and 360° rotation about the boom axes, and are scaled from Orion's solar array gimbals (120 W/kg).
    - All solar arrays use Northrop Grumman's UltraFlex® [10] array technology and are assumed to support up to 0.1 g deployed strength; 150 W/kg specific power at beginning of life (BOL), 28 °C, and 1 AU; and 80% solar cell wing packing factor.
    - All solar arrays use state-of-the-art SolAero IMM-α [11] solar cells, which have a 32% efficiency (BOL, 28 °C, 1 AU).
    - Unused solar array strings are shunted by the solar array regulator.
    - Bus regulation is maintained at 120 VDC.
- Rechargeable lithium-ion batteries:
    - The batteries are sized to provide 120 VDC nominally to the bus.
    - The batteries will operate with a maximum depth of discharge (DoD) of 60% to accommodate the expected ~12,000 charge/discharge cycles in LEO.
    - Each battery includes one spare string for redundancy.
    - All batteries use commercial off-the-shelf (COTS) Panasonic NCR 18650B [12] battery cells.
    - The total battery cell mass includes a mass factor of 1.5 to account for any additional battery components (circuit protection devices, battery enclosure, wiring, etc.). The resulting battery specific energy is ~160 Wh/kg.
    - The total battery cell volume includes a packing factor of 1.2.
- Power management and distribution (PMAD):
    - The nominal EPS bus voltage is 120 VDC.
    - The PMAD boxes are based on NASA GRC's Advanced Modular Power Systems (AMPS) [13] technology, which consists of card-based electronic modules that can be combined to provide various PMAD functions.
    - Each vehicle stage has a two-channel power architecture, similar to the NASA Gateway reference architecture [13], where each channel can independently support all spacecraft loads in the event of a failure. *Each* channel includes array regulation, a battery with battery regulation, and a complete set of PMAD components.
    - Both power channels are operating in the nominal configuration.
    - The mass of wire harnessing, excluding the EP power cables, is assumed to be 25% of the base EPS mass.
- 30% growth is applied to the estimated electrical load demand on the spacecraft except for the EP power, which instead uses 5% growth.

4.1.4 System Trades

Body-mounted solar arrays were briefly considered for earlier iterations of the NEP vehicle design but required excessive body area. Deployable arrays allow for smaller stowed area and better pointing; combined with the high deployed-strength requirement of 0.1 g during vehicle burns, this led to the selection of the flexible UltraFlex® solar array technology.

Many lithium-ion battery technologies other than the COTS Panasonic 18650B cells are available in the market today, but no formal trades were performed for this study.

4.1.5 Analytical Methods

The different EPS components were sized as follows:

- The solar arrays and batteries were sized using Compass EPS array and battery spreadsheets.
- The array gimbals were scaled from the Orion multi-purpose crew vehicle (MPCV) gimbals.
- The sequential shunt units (SSU) used for solar array regulation were sized using the Metcalf Model [14], which is based on the ISS PMAD components.
- The AMPS PMAD cards and boxes were designed based on information provided by NASA Glenn Research Center (GRC) AMPS engineers.

4.1.6 Risk Inputs

The primary EPS risk is that the solar arrays may overheat, requiring exotic or high-temperature materials in the array blanket and structure to prevent failure. Since the solar arrays are located near the high-temperature reactor radiators, high-temperature materials may be required to prevent structural failure of the solar arrays during the mission. In addition, the solar array strings are shunted after the nuclear reactor startup such that the solar cells and solar array structure further increase in temperature. Therefore, a detailed thermal analysis of the solar array and radiator interaction is required to mitigate this risk.

4.1.7 System Design

4.1.7.1 NEP Module

The NEP Module of the vehicle contains both the nuclear reactor and EP thrusters; Figure 4-9 illustrates how the reactor, thrusters, and spacecraft bus are connected within this stage.

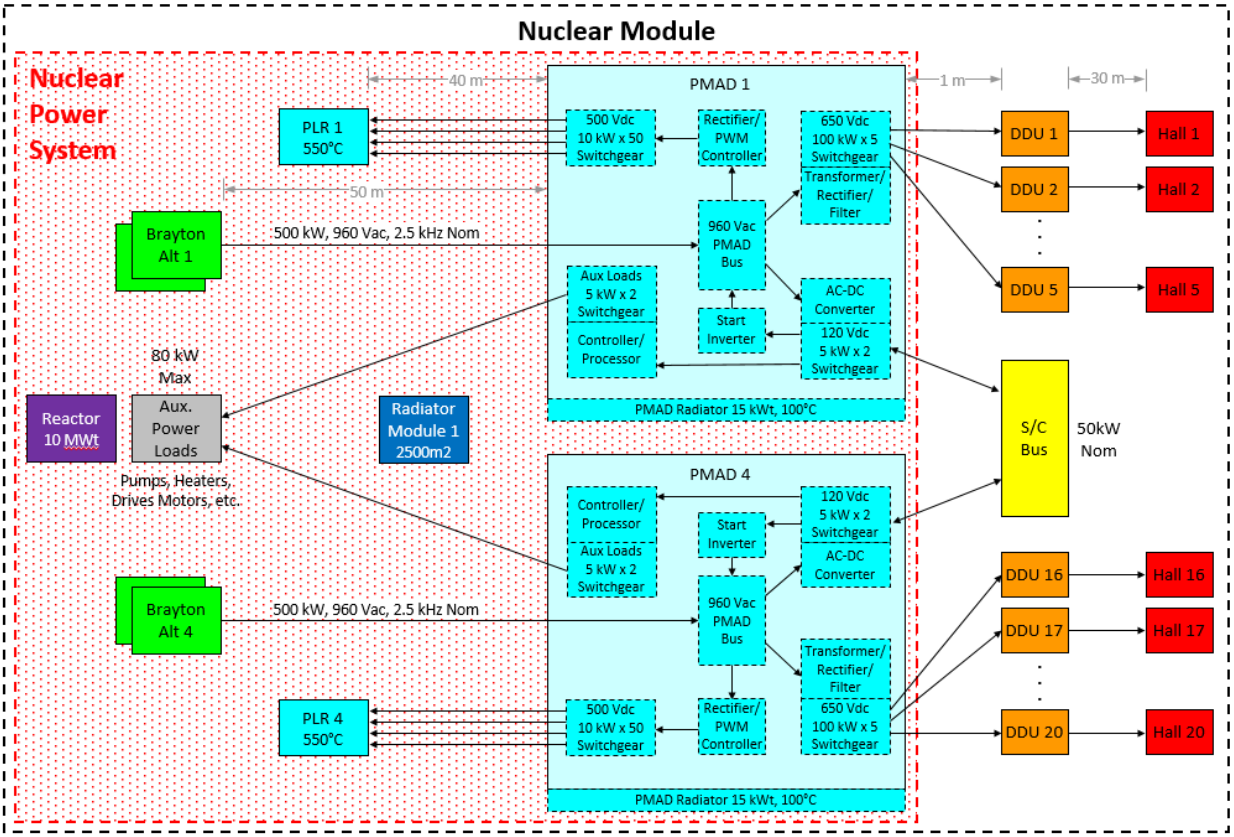

Figure 4-9 NEP Module Nuclear Power System Schematic

The nuclear reactor PMAD on the NEP Module must provide power regulation and conversion from the 960 VAC output of the nuclear reactor to 120 VDC for the non-EP spacecraft loads. Most of the PMAD for the nuclear power system, shown within the dotted red box, and for the EP system (DDUs and Hall thrusters) are detailed in their own respective subsystems and considered out of scope for this section. The vehicle's EPS design starts at the spacecraft bus, given in yellow ("S/C Bus").

Figure 4-10 shows the NEP Module's electrical power system starting with the yellow spacecraft bus from the previous figure, which outputs 50 kW nominally at 120 VDC from the nuclear reactor. Part of this power is used to support a DC-DC converter unit (DDCU), which allows for a secondary 120 VDC spacecraft bus that supports the solar array and array regulator unit (ARU), lithium (Li)-ion battery and battery charge/discharge unit (BCDU), and power distribution unit (PDU) responsible for providing power to the NEP Module's internal loads. The remainder of the reactor power is passed along a 120 VDC pass-through cable to the rest of the spacecraft via the Xenon Interstage.

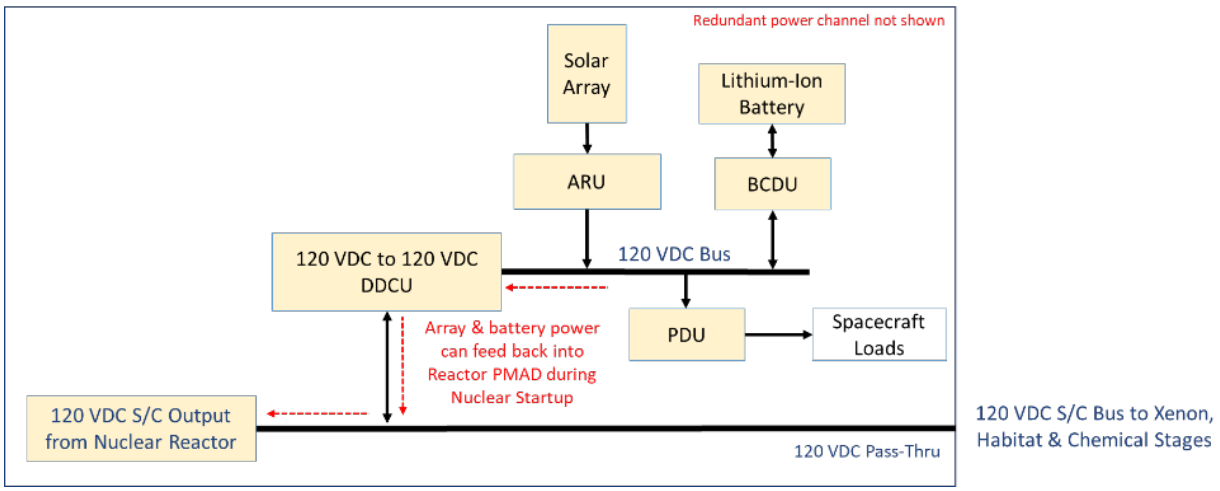

Figure 4-10 NEP Module EPS Schematic

The power architecture breakdown for the secondary power bus is the same for all three vehicle stages and illustrated in Figure 4-11. Each Main Bus Switching Unit (MBSU) provides switching to transfer power from the primary 650 VDC bus to each power channel on the 120 VDC bus. The DC-DC Converter Unit (DDCU) converts the 650 VDC input voltage to the 120 VDC of the secondary buses and provides isolation. The Array Regulator Unit (ARU) shunts solar array strings as needed to meet the power needs of the spacecraft bus. The Battery Charge-Discharge Unit (BCDU) regulates the charge and discharge of the lithium-ion batteries on each channel. The Power Distribution Unit (PDU) provides load switching and fault protection for the power system components and is switchable between either of the two secondary 120 VDC buses, ensuring all spacecraft loads are powered even if one of the two power channels fails. Each functional unit (MBSU, DDCU, BCDU, or PDU) is composed of one or more AMPS PMAD cards: high current switchgear modules (HCSMs), bus switchgear modules (BSGMs), load switchgear modules (LSGMs), bi-directional converter modules (BDCMs), housekeeping power modules (HKPMs), and/or controller modules (CTLMs). The diagram illustrates the AMPS card composition for each functional unit but does not show the CTLM and HKPMs included in the overall box. In addition, the DDCUs are bi-directional, which allows power to flow both directions such that the solar arrays and Li-ion batteries can be used to power the start-up electronics and control mechanisms required for the nuclear reactor startup. Unless specifically stated, all subsequent numbers refer to components within a single channel.

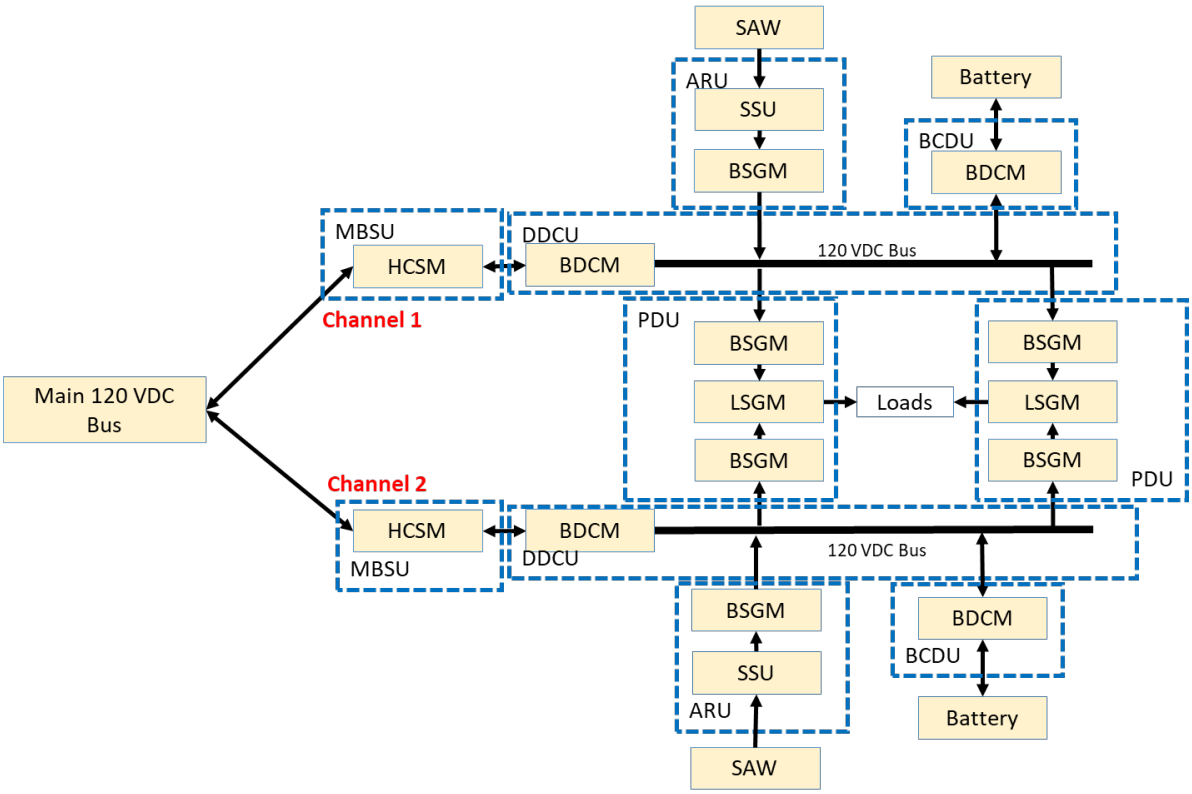

Figure 4-11 Secondary Two-Channel PMAD Architecture

(Note each stage has two ARUs but only one solar array)

Each PDU is sized to account for the NEP Module's maximum internal load through all power modes. After the reactor is started, electrical power flows into the NEP Module from the main bus through the DDCU and to the PDU/loads. However, the architecture of this stage must be able to flow power back to the reactor for initial startup (Power Mode 3), as illustrated by the dotted red arrows in Figure 4-10. Each DDCU is sized for the maximum of three numbers: Power Modes 1-2 (only DDCU parasitic power is needed to keep it alive), Power Mode 3 (2500 W output to the main bus), and Power Modes 4-9 (PDU input power plus ARU and BCDU parasitic power). In this case, Power Mode 3 was the limiting case (maximum power requirement) for DDCU sizing. Note that the power reaching the reactor will be less than 2500 W due to various losses as the power flows through the nuclear reactor PMAD, and that the ARU and BCDU are kept alive via a parasitic power supply even after reactor startup, in case of array or battery emergency use. Also note that unlike for the other two stages, the MBSU for the NEP Module (input to the DDCU) is assumed to be part of the nuclear subsystem PMAD and not thus bookkept within the electrical power subsystem.

Similarly, each ARU is sized to provide solar array power to the PDU in Power Mode 3 while also charging the battery during periods of insolation, and each BCDU is sized for the maximum charge/discharge needs of the bus. PMAD parasitic and efficiency losses are accounted for in component sizing. All PMAD components except for the sequential shunt unit (SSU) used in array regulation are based on the TRL-5 AMPS components developed at NASA GRC. All cards for each channel are distributed within a 120 VDC PMAD box, where each function is provided by one or more cards in parallel; because there are two channels, no spare cards were included within each box. To support the two-channel architecture, there are two ARUs for the single solar array and wire harnessing connects the various EPS components together.

The NEP solar array uses an UltraFlex® design that attaches to a boom and gimbal to extend away from the spacecraft body; *only one solar panel* is used for both power channels due to the relatively low commissioning power requirements. The array consists of 122 strings of 36 solar cells per string for a total EOL power generation of 9.09 kW at 65 °C and 1.02 AU. This results in a total wing area of 35.8 m^2 and a diameter of 6.8 m.

Each rechargeable lithium-ion battery has a total capacity of 45.9 ampere hours (Ah), a voltage range of 99.2-130.2 V, and a 31S-17P configuration totaling 527 battery cells.

The 650 VDC nuclear bus must also feed the electric thrusters in the propulsion stage. Twenty total power transfer cables with an average length of 30 m are provided in the NEP Module, each capable of transferring 100 kW at 650 VDC to a thruster DDU. Each DDU cable consists of three parallel 2-AWG lines with ETFE insulation and has a mass of 48.1 kg. To simplify the layout, the DDU cables are separated into two bundles of 30 lines each for the two thruster booms. Wire current derating was determined using the same specifications as the Orion MPCV.

4.1.7.2 Xenon Interstage

The Xenon Interstage's EPS schematic is shown in Figure 4-12. After commissioning, feed-through power from the NEP Module is supplied to the Xenon Interstage, which uses some power for its internal components and passes the rest to the habitat and chemical stages. Only the NEP Module is responsible for reactor startup, so the xenon and chemical stages do not have to account for power flow back through the DDCU to the MBSU.

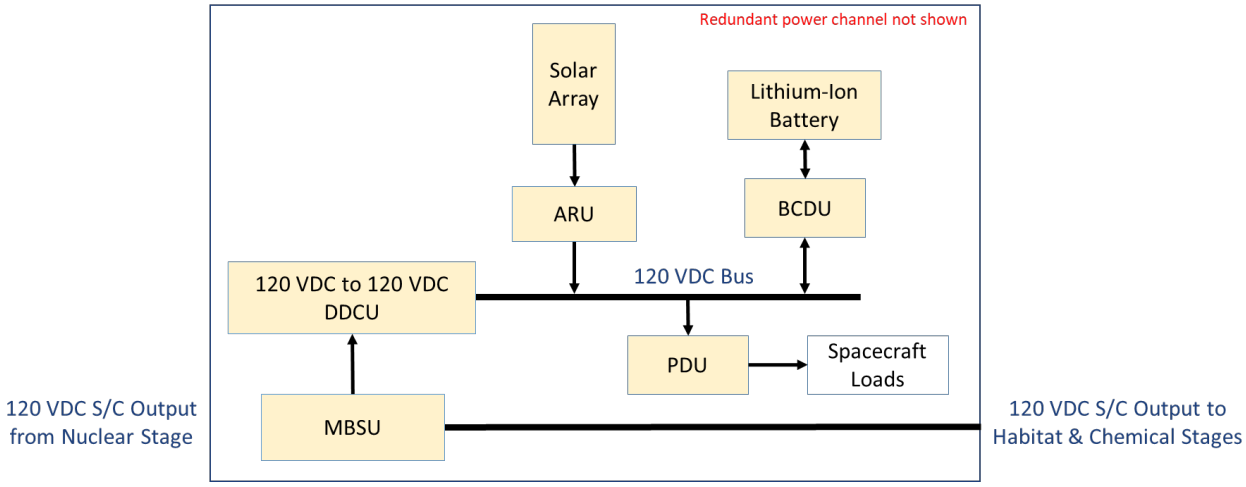

Figure 4-12 Xenon Interstage EPS Schematic

Each PDU is sized to account for the Xenon Interstage's maximum internal load through all power modes. Each ARU is sized for the maximum array output- enough to provide commissioning power to the PDU input, charge the battery, and keep the DDCU and MBSU alive via parasitic power. Likewise, each BCDU is sized for the worst-case commissioning PDU input plus ARU, DDCU, and MBSU parasitic power. The DDCU and MBSU are sized for the maximum post-commissioning power fed in from the NEP Module. PMAD parasitic and efficiency losses are factored into all component sizing. Each channel's cards are distributed within a 120 VDC PMAD box.

The single solar array uses an UltraFlex® design and consists of 36 strings of 38 solar cells per string for a total EOL power generation of 2.80 kW (65 °C, 1.02 AU). This results in a total wing area of 11.2 m^2 and a diameter of 3.8 m.

Each rechargeable lithium-ion battery has a total capacity of 13.5 Ah, a voltage range of 99.2 to 130.2 V and a 31S-5P configuration totaling 155 battery cells.

4.1.7.3 Chemical Stage

The chemical propulsion stage's EPS schematic is shown in Figure 4-13. After commissioning, power generated by the nuclear reactor is passed from the Habitat to the Chemical Stage.

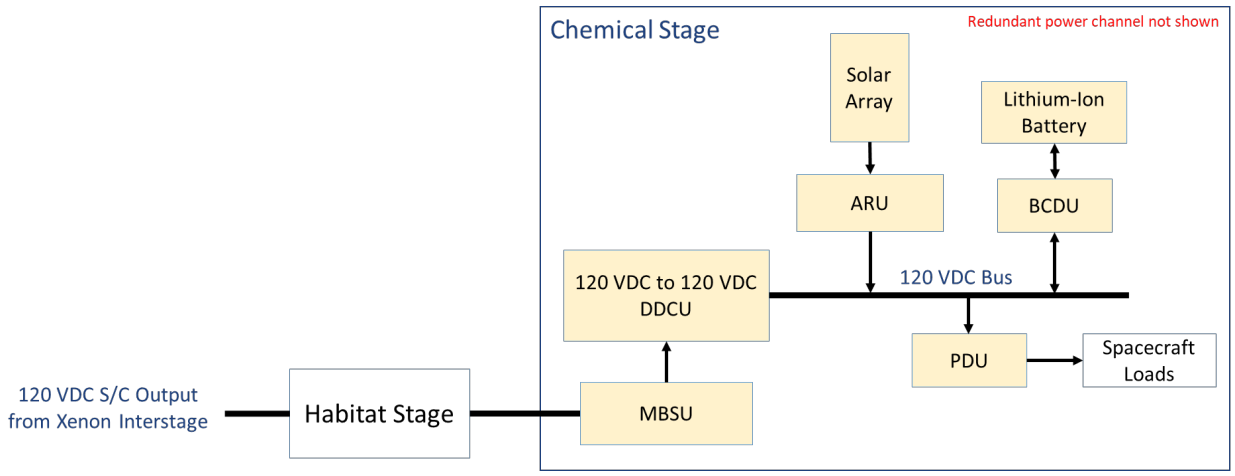

Figure 4-13 Chemical Stage EPS Schematic

Each PDU is sized to account for the chemical stage's maximum internal load through all power modes. Each ARU is sized for the maximum array output, enough to provide commissioning power to the PDU input, charge the battery, and keep the DDCU and MBSU alive via parasitic power. Likewise, each BCDU is sized for the worst-case commissioning PDU input plus ARU, DDCU, and MBSU parasitic power. The DDCU and MBSU are sized for the maximum post-commissioning power fed in from the habitat stage. PMAD parasitic and efficiency losses are factored into all component sizing. Each channel's cards are distributed within a 120 VDC.

The single solar array uses an UltraFlex® design and consists of 88 strings of 34 solar cells per string for a total EOL power generation of 6.40 kW (65 °C, 1.02 AU). This results in a total area of 24.3 m^2 and a diameter of 5.6 m.

Each rechargeable Li-ion battery has a total capacity of 35.1 Ah, a voltage range of 99.2 to 130.2 V, a 31S-13P configuration totaling 403 battery cells.

4.1.7.4 Design Summary

The total EPS mass for each of the stages on the NEP-Chem vehicle is provided in Table 2-1. These masses include mass growth allowance as this is an early phase design. Note that the total EPS mass in the NEP Module does not include the EP power transfer cables as they are included in the propulsion subsystem.

Table 4-2 Total EPS Mass for Each Stage

	NEP Module	Xenon Interstage	Chemical Stage
Total EPS Mass	646 kg	326 kg	502 kg

The TRLs of EPS components used in the spacecraft design are as follows:

- Solar arrays: TRL 8 because the UltraFlex® design has flown many times, including on multiple Mars surface missions with Phoenix and InSight.
- Li-ion batteries: TRL 6 for custom designs using off-the-shelf cells.
- Array gimbals: TRL 6 because they are scaled from Orion MPCV gimbals.
- ARUs/SSUs: TRL 8 because they are based on flight-proven ISS SSUs.
- Non-ARU PMAD components: TRL 5 as they are based on existing NASA AMPS hardware.
- Wire harnessing: TRL 6 for standard spacecraft harnessing that must be configured to this specific design.
- NEP power transfer cables: TRL 3 because of their novel high-voltage aspect.

4.1.8 Master Equipment List

The tables below show the EPS MELs for the three separate stages of the NEP spacecraft.

Table 4-3 NEP Module Nuclear Power System MEL

Description Case 3_SLS_Chem NEP_Chem_Vehicle_Family CD-2020-181	QTY	Unit Mass	Basic Mass	Growth	Growth	Total Mass
Nuclear Power System			25684.0	15%	3852.6	29536.6
Science Package Group One			25684.0	15%	3852.6	29536.6
Reactor	1	4850.0	4850.0	15%	727.5	5577.5
Shield	1	3500.0	3500.0	15%	525.0	4025.0
Power Conversion	4	512.0	2048.0	15%	307.2	2355.2
Heat Rejection	1	9500.0	9500.0	15%	1425.0	10925.0
PMAD	1	5786.0	5786.0	15%	867.9	6653.9

Table 4-4 NEP Module EPS MEL

Description Case 3_SLS_Chem NEP_Chem_Vehicle_Family CD-2020-181	QTY	Unit Mass	Basic Mass	Growth	Growth	Total Mass
Electrical Power Subsystem			462.3	40%	183.7	646.0
Power Generation			134.5	30%	40.3	174.8
Commissioning Array	1	60.6	60.6	30%	18.2	78.7
Solar Array Gimbal	1	73.9	73.9	30%	22.2	96.0
Power Management & Distribution			252.0	49%	124.4	376.3
Solar Array Regulator	2	27.3	54.5	20%	10.9	65.4
120VDC AMPS PMAD Box	2	52.5	105.0	20%	21.0	126.0
Harnessing	1	92.5	92.5	100%	92.5	184.9
Energy Storage			75.9	25%	19.0	94.9
Li-Ion Battery	2	37.9	75.9	25%	19.0	94.9

Table 4-5 Xenon Interstage EPS MEL

Description Case 3_SLS_Chem NEP_Chem_Vehicle_Family CD-2020-181	QTY	Unit Mass	Basic Mass	Growth	Growth	Total Mass
Electrical Power Subsystem			**235.6**	**38%**	**90.0**	**325.6**
Power Generation			**41.4**	**30%**	**12.4**	**53.8**
Commissioning Array	1	18.7	18.7	30%	5.6	24.3
Solar Array Gimbal	1	22.8	22.8	30%	6.8	29.6
Power Management & Distribution			**172.5**	**42%**	**72.2**	**244.7**
Solar Array Regulator	2	19.2	38.4	20%	7.7	46.1
120VDC AMPS PMAD Box	2	43.5	87.0	20%	17.4	104.4
Harnessing	1	47.1	47.1	100%	47.1	94.2
Energy Storage			**21.6**	**25%**	**5.4**	**27.0**
Li-Ion Battery	2	10.8	21.6	25%	5.4	27.0

Table 4-6 Chemical Stage EPS MEL

Description Case 3_SLS_Chem NEP_Chem_Vehicle_Family CD-2020-181	QTY	Unit Mass	Basic Mass	Growth	Growth	Total Mass
Electrical Power Subsystem			**360.9**	**39%**	**141.5**	**502.4**
Power Generation			**89.0**	**30%**	**26.7**	**115.7**
Commissioning Array	1	40.1	40.1	30%	12.0	52.1
Solar Array Gimbal	1	48.9	48.9	30%	14.7	63.6
Power Management & Distribution			**215.7**	**47%**	**100.7**	**316.4**
Solar Array Regulator	2	23.9	47.7	20%	9.5	57.3
120VDC PMAD Box	2	48.0	96.0	20%	19.2	115.2
Harnessing	1	72.0	72.0	100%	72.0	143.9
Energy Storage			**56.2**	**25%**	**14.1**	**70.3**
Li-Ion Battery	2	28.1	56.2	25%	14.1	70.3

4.2 Propulsion

The propulsion system for this design consists of three independent systems that work together to provide the S/C with its required ΔV capability and controllability, with two of those systems being interconnected across multiple S/C modules. The main propulsion system is based on 100 kWe class Hall thrusters utilizing xenon propellant. The other two systems are a high thrust system based on LOX/LCH_4 being used for departure and capture maneuvers, and an MMH and NTO based RCS used for S/C attitude control.

4.2.1 System Requirements

The propulsion systems are required to provide adequate propulsive performance to assemble the S/C in Earth orbit, deliver the S/C to the desired Martian orbit, and return the S/C to Earth. It is required that 100 kWe class Hall thrusters be used for primary propulsion in an 18 +2 configuration with no cross strapping among thruster strings. A cryogenic based high thrust propulsion system is required for certain S/C maneuvers, and those cryogenic tanks are required to be metallic with internal components such as a propellant management device (PMD), slosh baffles, mixers, thermal vent system (TVS), etc. The cryogenic tanks are also required to have an active thermal

management system. All S/C modules are required to have active RCS for docking and S/C stack assembly. The propulsion systems on the NEP Module include provisions for refueling both the xenon and RCS propellants for potential additional missions. The xenon and RCS feed systems are required to be designed so that both propellants can be cross-fed between modules, and the RCS feed system is required to have no trapped volumes. All three systems are required to be human rated.

4.2.2 System Assumptions

There are several assumptions made regarding the design of the various propulsion systems. For the EP system, xenon is assumed to be the propellant and the thrusters are assumed to be powered via DDUs and not from individual power processing units (PPUs). It is also assumed that the xenon would be stored in multiple large tanks, some of which would be dropped during the mission. Due to the large anticipated mass of the xenon residuals, it is assumed that a compressor system is used to extract as much of the xenon residuals from a spent tank as possible prior to jettisoning it. The high thrust chemical propulsion is assumed to be a LOX/LCH_4 system with multiple engines each with individual TVC, an extendible nozzle, and fuel side autogenous pressurization. It is also assumed that both COTS components and reusable identical components would be used as much as possible to reduce both cost and risk.

4.2.3 System Trades

Various xenon tank configurations are traded to determine a viable tank layout with a minimal number of tanks, some of which will be jettisoned as xenon is consumed, while also minimizing the number of launches. Numerous configurations are evaluated including cylindrical drop tanks along the cryogenic stage, numerous small door-knob shaped tanks, a couple large cylindrical tanks, and various combinations. A small number of larger tanks are shown to be advantageous from both a mass and launch perspective, as did combining tanks into a stage. This led to a design where two large door-knob tanks (identical to the one that's already on the power module) are combined to form a Xenon Interstage Module. This design led to a tank mean operating pressure (MOP) of 7.6 MPa (1,100 psi) which is lower than the ~13.8 MPa (~2,000 psi) typically used for xenon, but due to the non-linearity of supercritical xenon, five tanks at the lower pressure actually had a lower total mass than four at a higher pressure. This led to the design of a single xenon tank on the NEP Module with modular Xenon Interstage Modules, each containing two additional identical tanks, which are added as necessary.

A cryogenic tank design trade between discrete tanks and a common bulkhead design is conducted. The discrete two tank solution allows for each propellant to be individually conditioned and is considered a more traditional design. Due to the amount of cryogenic propellant required, this design quickly became limited by launcher fairing volume, and not necessarily by launcher performance. Since liquid oxygen and liquid methane store at similar temperatures and have similar thermal conditioning requirements, they are good candidates for a common bulkhead design. The trade showed a very modest mass savings in dry tank mass, but a fair reduction in overall tank assembly length for a given tank diameter and propellant load. This savings in overall length allowed the cryogenic tank to fit on a single launch as part of an entire S/C module, and thus is selected for use in this design

There is also a RCS propellant trade among bipropellant MMH/NTO, monopropellant hydrazine, and gaseous methane and oxygen (Chemical Propulsion Module only). Both the hydrazine and MMH/NTO options have extensive heritage and numerous COTS thrusters are available. Due to the current RCS propellant load requirement and higher I_{SP}, the bipropellant MMH/NTO system resulted in a lower overall system mass. This system can also leverage thrusters and other components utilized by Orion Service Module, and is thus chosen for use in this design. For the Chemical Propulsion Module, a gaseous methane oxygen (CH_4/O_2) system results in lower propellant mass due to its higher I_{SP}, and saves some propellant storage tank mass by storing the main and RCS propellant together. However, to make the system functional, pumps, evaporators, high pressure storage tanks, and valves are all required. The collective mass of these components, in conjunction with its greatly increased complexity, higher risk, and lack of COTS hardware outweigh the slightly higher I_{SP} and propellant mass savings. In addition, the MMH/NTO system is compatible with the systems on the other two S/C modules, allowing for component reuse and propellant sharing between modules, thus it is chosen for this design.

Another trade is performed on the location and orientation of the Hall thrusters to find options where plume impingement would not present a significant issue. At a high level, three main choices are assessed with the thruster firing primary aft (away from the reactor and the same direction as the Chemical Propulsion Module), forwards (towards the reactor), and sideways perpendicular to the main axis of the spacecraft. The primary areas of both plume impingement erosion and redeposition contamination concern are the likely sensitive surfaces of the habitat

element or of the primary radiators. In general, redeposition contamination is found to be the more limiting effect, where a crude rule of thumb criterion of 100 Angstroms (Å) of deposited thickness is applied. Contamination amounts on that order or greater have been observed to impact solar absorptivity and potentially degrade passive thermal control surfaces.

For the aft-pointing options, acceptable solutions are found where the EP thrusters are downstream of the habitat and most of the chemical stage to ensure minimal impacts to the habitat surfaces. Other implementations where the thrusters are mounted to long booms upstream of the habitat were found to have deleterious impacts to the Habitat. The sideways-pointing options had the added complications of all of the thrusters on one side of the spacecraft and significant gimbaling required as the center of mass (CM) of the spacecraft shifts significantly off the thrust axis as various modules are docked and undocked. For a closed solution to handle the shifting CM and avoiding impacts to both the radiators and habitat required a lengthy boom on the order of 20 m.

Finally, the forward-pointing options are evaluated, which required placing the thrusters between the radiators and the reactor, and adding flat panel carbon-based shielding along the truss sections to minimize erosion redeposition contamination on the radiators. The thrusters are also canted 10° out away from the center axis. This configuration impacts only two quadrants of radiator surfaces (assuming two EP pallets) and provided flexibility for maintaining spacecraft orientations to minimize solar exposure to affected surfaces as the plume impingement has a more drastic effect on absorptivity and less so on emissivity. By moving the thrusters away from the S/C axis and toward the reactor by just a few meters, the effects of erosion and deposition can be greatly reduced even further, thus this configuration is selected. The solutions for the forward-pointing configuration are shown below in Figure 4-14.

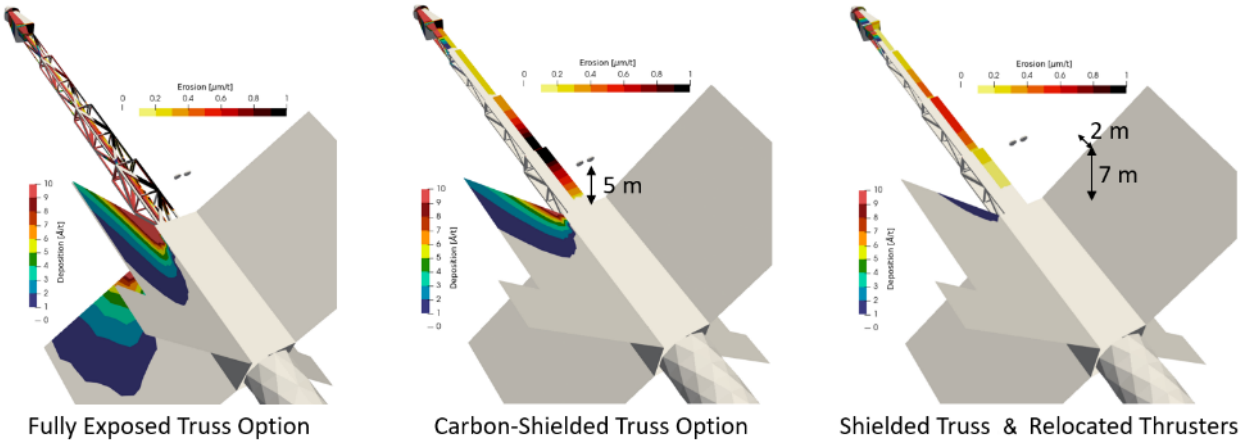

Figure 4-14 EP Plume Impingement Results for Forward Pointing Configuration

4.2.4 Analytical Methods

The methods used to design the propulsion system involved using a mix of published values, empirical data, and analytical tools. Published values for COTS components and empirical data are used wherever possible, with analytical tools being employed as necessary. Empirical data is used to aid in the mass and size estimation of similar components when published values are not available. Numerous analytical tools are used in this analysis, including National Institute of Standards and Technology (NIST) [15] tables, fluid and gas property codes, as well as custom tools developed from basic physical relationships and conservation equations with empirical based inclusions for real life hardware requirements (mounting bosses, flanges, etc.).

The EP plume analysis uses the NASA Hall effect rocket with magnetic shielding (HERMeS) Hall thruster plume maps as a first-order estimate of the plume profiles. The current densities are scaled to provide rates based on total throughput, assumed to be 13 t of propellant per thruster. These plume maps are input into the Coliseum EP plume code to assess impacts of spacecraft surface sputter erosion and subsequent redeposition. The material sputter yields are obtained from available literature values [16]. Since certain materials are unknown or do not have available data, a conservative estimate based on yields for glass is used.

4.2.5 Risk Inputs

Electric Hall Thruster System Risks:

This design utilizes a carbon overwrapped pressure vessel (COPV) tank for xenon storage that is larger than others that have been developed and flown to date. Although similar to other tanks of its type, it does have unique operational requirements and size, and thus its development may pose a cost and/or schedule risk.

Although PPUs have flight heritage, DDUs have no known flight experience. The DDU is simpler than a PPU because there is no voltage conversion needed for the discharge, thus the DC-DC converters that power the primary plasma discharge are eliminated. However, the DDU must be mated to a transformer to ensure the Hall thruster operation is isolated from the Brayton operation. The electronics technology and implantation requirements for DDUs are well understood, but there are potential unknown developmental risks that could pose a risk to both cost and schedule.

The Hall thrusters used in this design will require performance and lifetime testing. Currently, there is a lack of adequate test facilities to perform these tests at the power levels required in their current state. This risk can be mitigated via capital improvements to facilities such as VF6 at the NASA Glenn Research Center.

The Hall thrusters used in this design will also be exposed to both the ambient interplanetary radiation, as well as additional radiation from the reactor, which may cumulatively exceed 250 krad during the mission. The cumulative effect of this radiative dose may adversely affect the Hall thruster component materials, and thus potentially its operational characteristics.

LOX/CH4 Cryogenic Propulsion System Risks:

The fluid behavior, handling, and long term storage of cryogenic fluids in a microgravity environment is currently unproven. This induces potential unknown issues that cannot be determined or easily evaluated on the ground, but could prove critical to future mission success.

Although common bulkhead tank designs have been used, a LOX/LCH4 tank of this type and size that is used for many months and can be refueled is unique. This induces potential unknown issues that cannot be determined or easily evaluated on the ground, thus analytical modeling, prototype testing, and proper design are needed to minimize risk.

There are risks surrounding the large scale active cooling, storage, and transfer of cryogenic fluids in a microgravity environment, which is currently unproven. This induces potential unknown issues that cannot be determined or easily evaluated on the ground and could also prove critical to future mission success.

The RL-10 family of expander cycle engines have a long and very successful flight history. Many studies of a LOX/LCH4 based variant have been conducted, an only the SpaceX Raptor engine has been flown suborbitally to date. The Japanese space agency over the last few years has successfully conducted component testing for a 30 kN thrust class LOX/LCH4 based expander cycle [17]. Although the engine design is well understood, and smaller engines are in development, there are cost and schedule overrun risks with any new engine development program which could impact its mission readiness.

All the LOX/LCH4 risks are common to those of the Mars landers which will use the same components and have the same life requirements. Thus it is assumed that those developments will occur in the lander program and can be used by the NEP/Chemical transportation system.

4.2.6 System Design

4.2.6.1 NEP Module

The NEP Module propulsion system consists of two independent systems, a Hall thruster based EP system and a bipropellant RCS. This module houses a single large COPV for storing xenon propellant, twenty DDUs, twenty Hall thrusters mounted on gimbaled pallets located on the end of deployable booms, as well as the xenon feed and compressor systems. It also has 24 RCS thrusters, two COTS COPV helium tanks, and four COTS propellant tanks, two for MMH and two for NTO. The configuration of this module is shown in Figure 4-15.

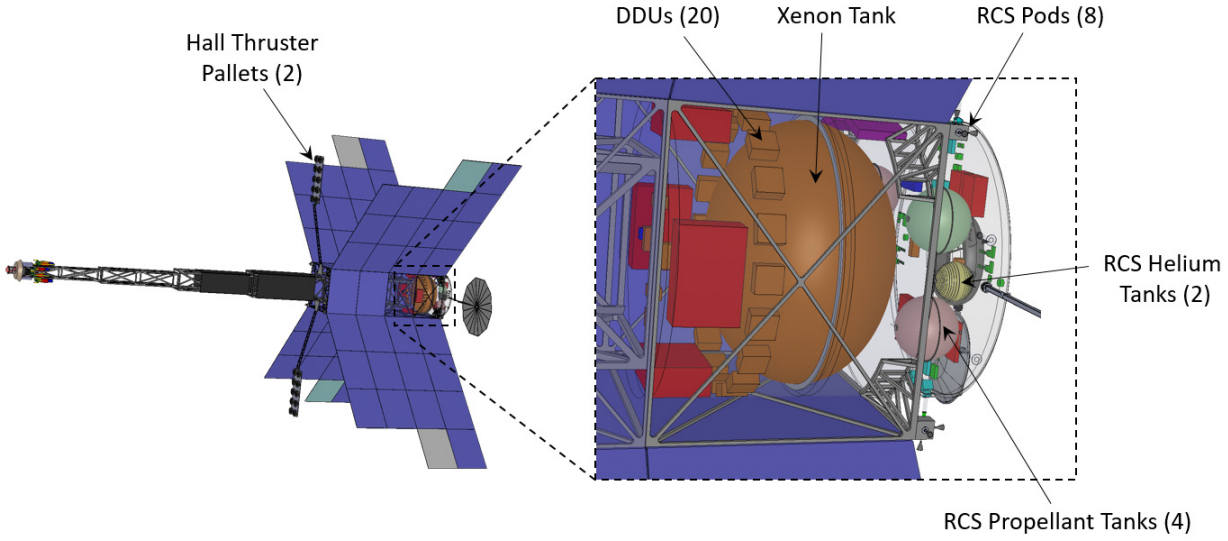

Figure 4-15 NEP Module Propulsion System Configuration

4.2.6.1.1 Electric Propulsion System

The EP system is designed around 100 kWe Hall thrusters which are mounted on gimballed pallets located at the end of deployable booms. These pallets are orientated so that the Hall thruster plumes are projected toward the reactor and away from the rest of the S/C. There are twenty Hall thrusters in total, ten on each pallet, that are in an 18 +2 configuration. These thrusters are magnetically shielded, have a nominal I_{SP} of 2,600 s at 600 V with xenon propellant, and are a single channel design with a center mounted cathode. The thrusters have an estimated propellant throughput capacity of 13.5 t, which equates to approximately 22,000 hrs of operation. These thrusters are based on previous high power designs that have already been developed, such as the NASA 457 Hall thruster shown in Figure 4-16.

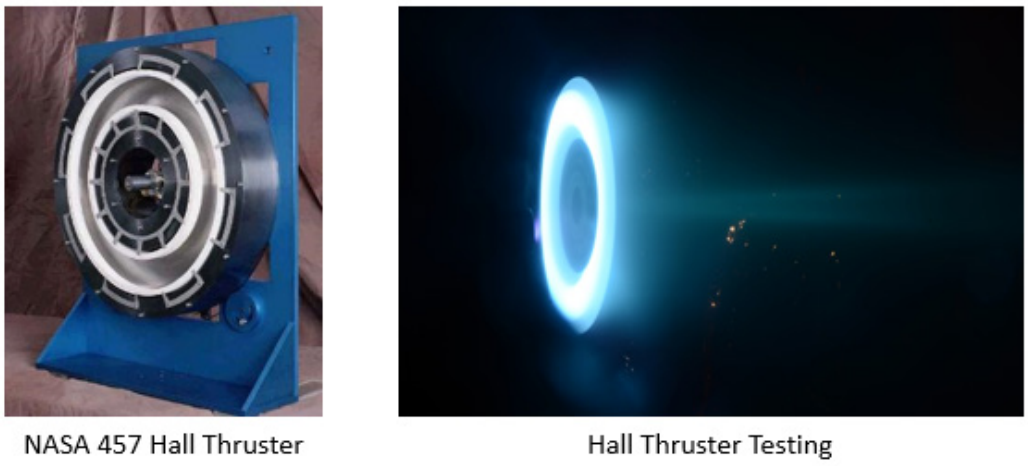

NASA 457 Hall Thruster Hall Thruster Testing

Figure 4-16 NASA High Power Hall Thruster and Hall Thruster Testing

The thrusters are powered by individual DDUs that receive 600 VDC power directly from the S/C PMAD system via a dedicated transformer/rectifier. The DDUs filter the power for the thrusters, control the low pressure feed system, and send data to the S/C for the entire thruster string. Each thruster string is zero fault tolerant and there is no cross strapping across strings, but there are two entire redundant thruster strings (one on each pallet.) The nominal thruster string efficiency is 59.4% which includes the DDU. A schematic of the EP system is shown in Figure 4-17.

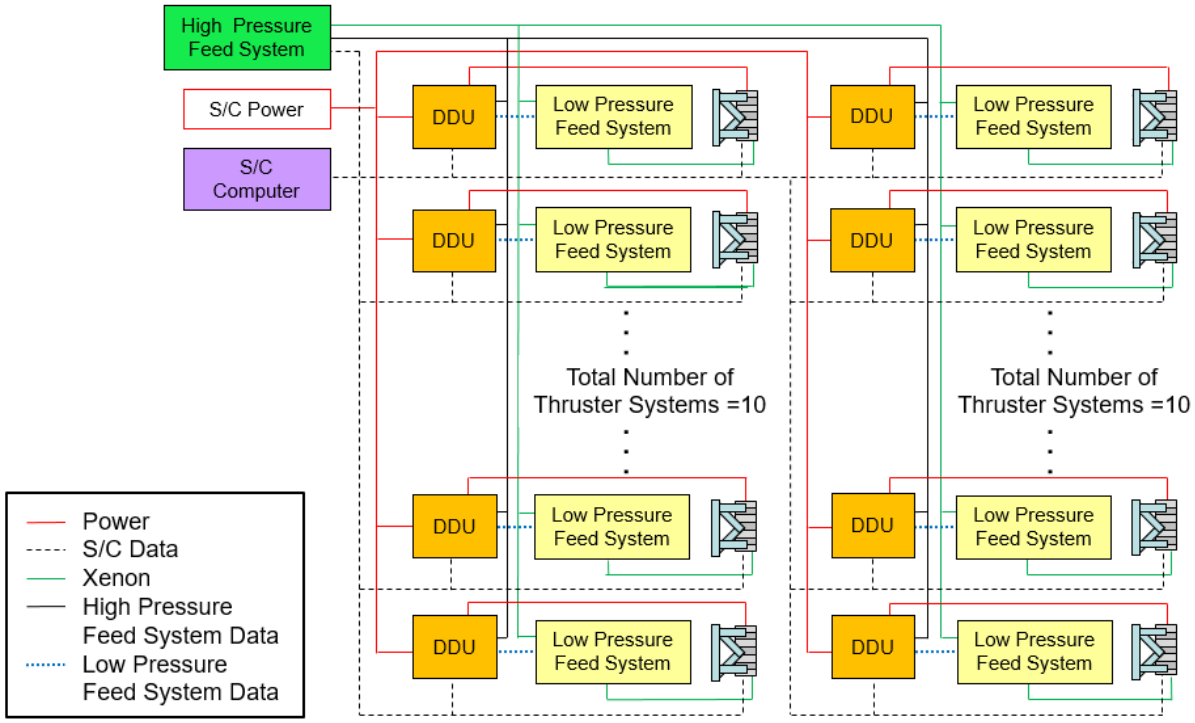

Figure 4-17 Electric Propulsion Schematic

The xenon propellant for the Hall thrusters is stored in five identical door-knob shaped tanks, one on the NEP Module and two on each of the Xenon Interstage Modules. The tanks are COPVs with a titanium alloy liner, T-1000 overwrap, and a mounting flange at the equator. They are sized to hold the largest quantity of xenon required on the NEP Module during the mission, which is estimated to be 44.2 t (97.4 klb_m) which exerts 7.6 MPa (1,100 psi) on the tank walls at 300 K. This design point could be considered overly conservative for the other xenon tanks on the S/C, but in making all the xenon tanks the same, it allows reuse of a single tank design (which lowers development cost) and provides for some extra propellant capacity in the future if needed.

The xenon feed system processes and conditions the xenon propellant and distributes it to the Hall thrusters via pressure management assemblies and low pressure flow controllers. Xenon is first conditioned via a set of four pressure management assemblies, with one processing xenon for the thrusters on each boom and one spare unit per boom. The xenon then flows down the lines to the thruster pallets where it is processed by an individual low pressure xenon flow controller for each thruster. Both units are based on the existing Moog pressure management assembly [18] and xenon flow controller [19], but scaled appropriately to handle the required increase in propellant mass flow rate. There are redundant valves and lines on the booms.

The design also allows for xenon to be cross feed between tanks so that xenon can be consumed from any tank, and the compressor system allows for xenon to be moved between tanks and residuals to be extracted from the Xenon Interstage Modules prior to jettisoning. This capability allows for ~600 kg (1,320 lb_m) of xenon to be extracted from each tank, turning that propellant back into useable propellant that is then stored in the other tanks. The valve arrangement currently allows for xenon to flow to the high pressure flow controllers from either the xenon tank on the NEP Module or from tanks on the Xenon Interstage Modules. By selectively opening certain valves, the Xenon Interstage Module lines can act as redundant flow paths, or a path to allow xenon to flow from one tank to another. A preliminary plumbing and instrumentation diagram (P&ID) of this system is shown in Figure 4-18.

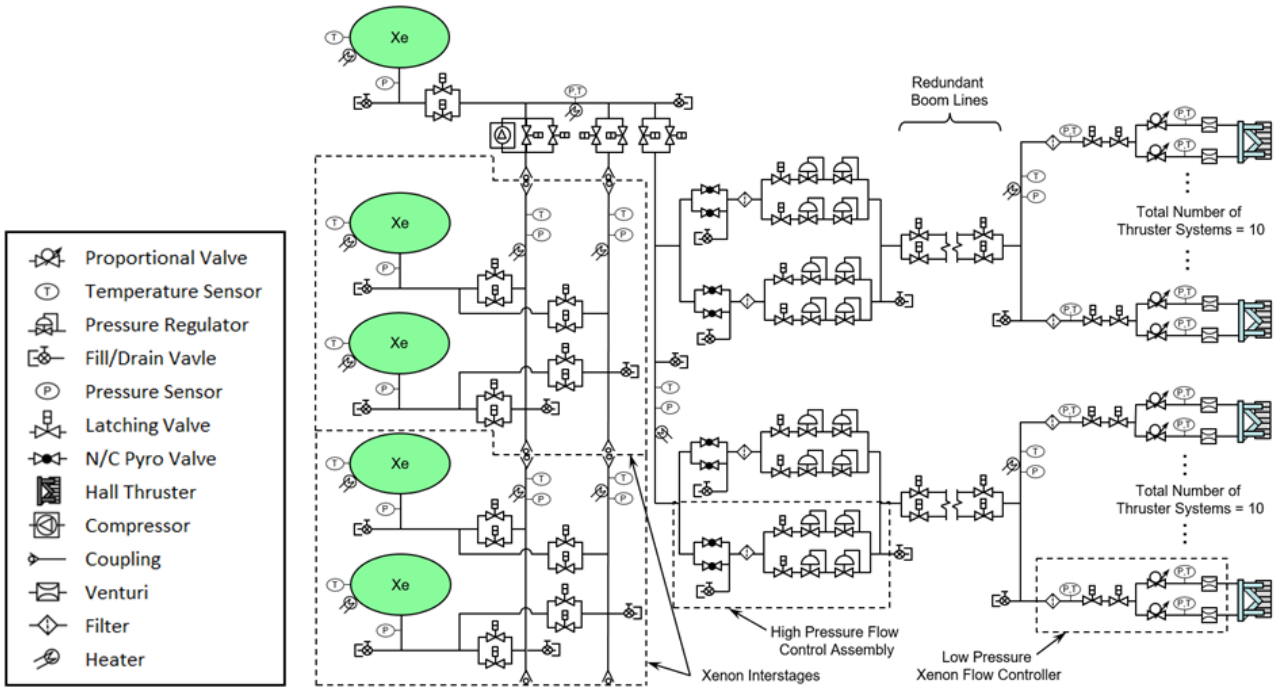

Figure 4-18 Xenon System Preliminary P&ID

4.2.6.1.2 Reaction Control System

The RCS on the NEP Module consists of 24 thrusters located in eight pods containing three thrusters each. These thrusters are bipropellant (MMH/NTO) thrusters with Orion Service Module and autonomous transfer vehicle (ATV) heritage. They have a nominal thrust of 220 N (50 lb_f) a nominal Oxidizer to Fuel Mass Ratio (O/F) ratio of 1.65, a minimum impulse bit less than 8 Ns, a pulse frequency of 1 to 5 Hz, a nozzle area ratio of 50:1, a niobium C-103 chamber and nozzle, and integrated temperature and chamber pressure sensors [20].

The MMH and NTO propellants are stored in four Northrop Grumman (NG) model 80352-1 spherical titanium alloy tanks, two for MMH and two for NTO. These tanks are 1.07 m (42.1 in.) diameter and have an integral PMD [21]. The tanks are pressurized via a discrete pressurization system with helium stored in two COTS Arde D4657 helium tanks. The helium tanks are 63.5 cm (25.0 in.) diameter COPV spheres with a MOP of 31.0 MPa (4,500 psi) [22]. Both the pressurization system and propellant feed systems have interconnects to allow refilling of the helium tanks, the removal of the propellant tank ullage, and refueling of the propellant tanks. The propellant interconnects also allow for both propellants to be fed to the thrusters from propellant tanks on the on the other S/C modules. A preliminary P&ID of the NEP Module RCS system is shown in Figure 4-19.

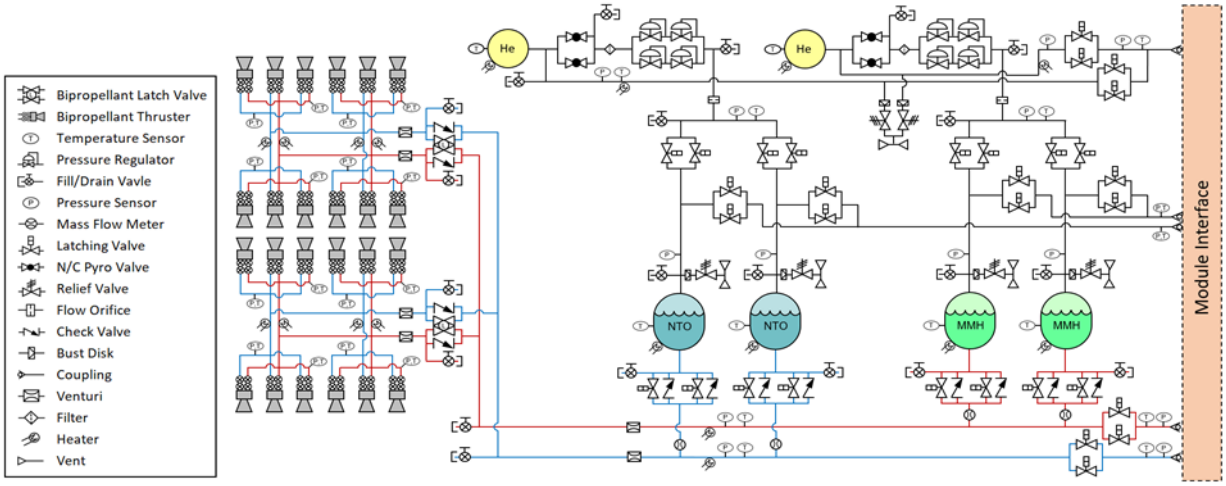

Figure 4-19 NEP Module Preliminary RCS P&ID

4.2.6.1.3 Xenon Compressor System

A compressor system is used in this design to move xenon from tank to tank and to extract xenon residuals from tanks prior to jettisoning, thus moving ~600 kg of xenon residuals per tank to useable propellant in another tank. For this design, a four stage centrifugal compressor with intercooling is used. The reason for intercooling between stages is twofold. First, xenon has a high specific heats ratio (24% higher that air [15]), meaning that adiabatic compression results in a very high discharge temperature. In this design the compression ratio will be ~100:1 near the end of residuals extraction, which would result in temperatures high enough to damage seals, valve seats, wiring insulation, and possibly other components in the xenon feed system. By removing excess heat via the intercoolers during compression, the xenon temperature can be reduced to a more manageable level. Second, intercooling reduces the amount of work the compressor motor must perform. By cooling the flow between stages, its density increases, and the initial temperature for the next compressor stage is reduced. This allows the overall compression cycle to more closely follow a less work intensive isothermal curve versus an isentropic curve. This reduces the amount of work the motor has to provide for a given mass flow rate and pressure ratio [23]. This effect is shown on a pressure and volume diagram in Figure 4-20.

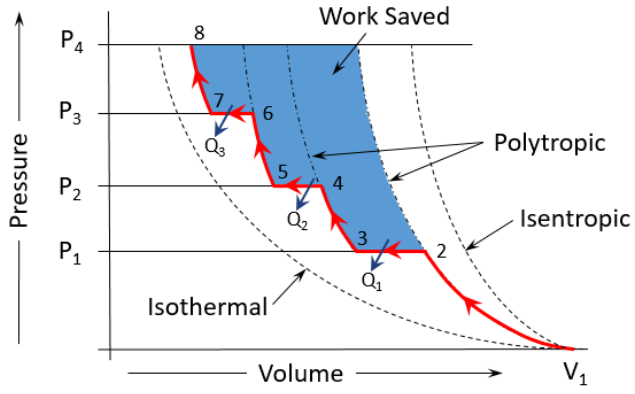

Figure 4-20 Effect of Intercooling on Compression Work

The compressor system is envisioned to have its own internal valves, instrumentation, filters, controllers, and either an MIL-STD-1553B or RS-422 interface to communicate with the S/C computer. It is driven by a brushless direct current (DC) motor powered directly off the low voltage S/C bus. The heat extracted via intercooling and xenon thermal conditioning is accounted for in the S/C thermal management system design, but detailed design of the compressor system and its components are beyond the scope of this vehicle level design study.

4.2.6.2 Xenon Interstage Module

A Xenon Interstage Module carries two large door knob shaped COPV tanks and a bipropellant RCS. The xenon tanks occupy the majority of the modules interior, while the RCS propellant and helium tanks are located at its aft end. The eight RCS thruster pods are located at the ends of the module, with four pods equally spaced circumferentially at each end. The Xenon Interstage Module propulsion system configuration is shown in Figure 4-21.

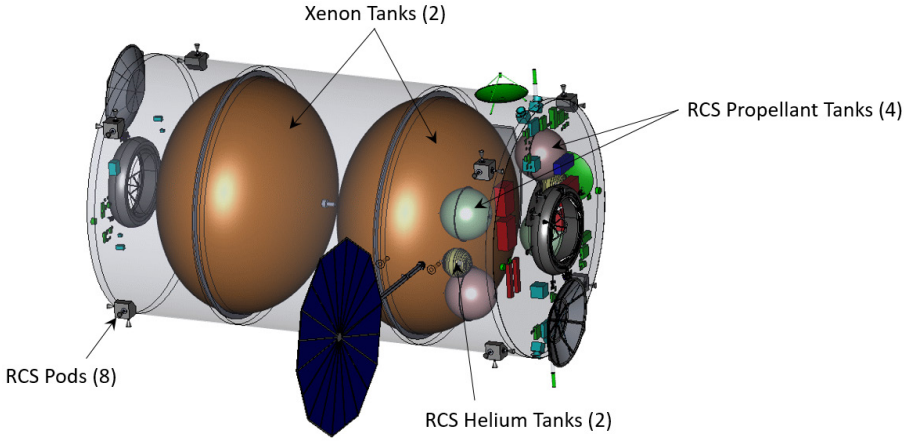

Figure 4-21 Xenon Interstage Propulsions System Configuration

The xenon tanks are identical to the one on the NEP Module described above, and are plumbed individually to two manifold lines that have interconnects at both ends of the module. This is shown in the xenon system preliminary P&ID. These two sets of interconnects enable these modules to be connected together in a modular fashion, while still permitting xenon to flow in both directions along the manifolds to either other tanks, the compressor system, or to the Hall thruster feed systems, regardless of the number of modules utilized.

The RCS system is a bimodal (MMH/NTO) based system with discrete helium pressurization. There are a total of 24 220 N (50 lb_f) thrusters mounted in eight pods containing three thrusters each. These thrusters are the same model as those used on the Nuclear Power Module and are described above [20]. The propellants are stored in four NG model 80340-1 titanium alloy tanks that are 99.0 cm (38.9 in.) in diameter and have an integral PMD [21], two for MMH and two for NTO. Helium for the system is stored in two Arde model E4256 spherical COPV tanks that are 55.9 cm (22.0 in.) in diameter and have a MOP of 27.6 MPa (4,000 psi) [22].

The Xenon Interstage Module RCS is not designed to be refueled on orbit, but has couplings on both ends of the module for both MMH and NTO, thus allowing its propellant to be shared with other modules in the S/C stack, or to just serve as a pass-through for other modules to share their RCS propellant. A preliminary RCS P&ID is shown in Figure 4-22.

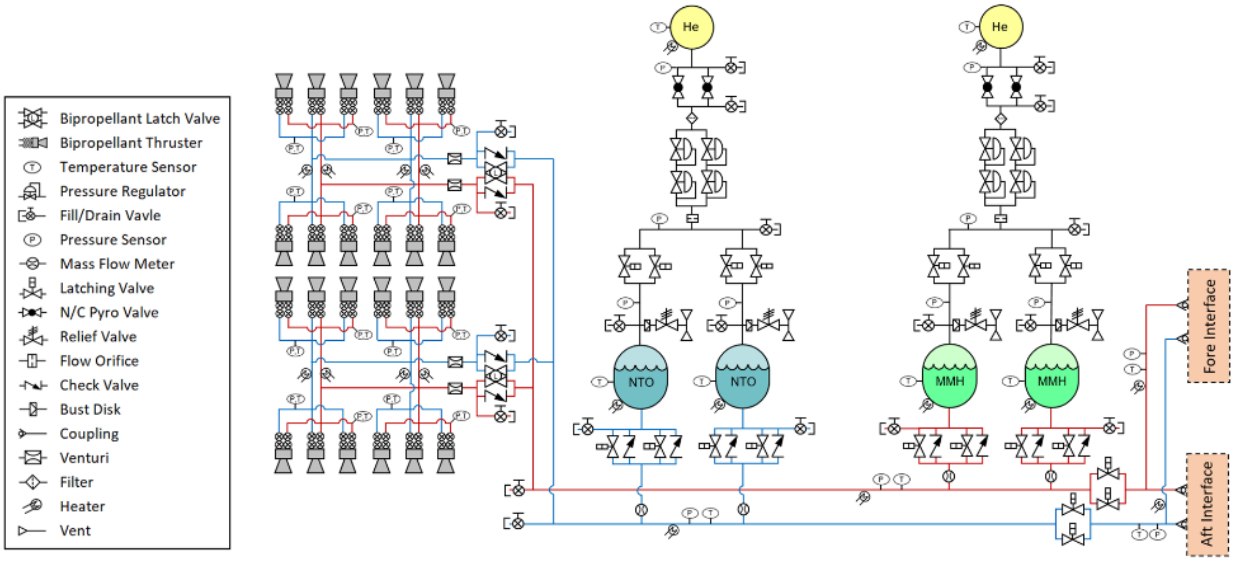

Figure 4-22 Xenon Interstage Module Preliminary RCS P&ID

4.2.6.3 Chemical Propulsion Module

The Chemical Propulsion Module is used for large ΔV maneuvers that must be completed within a narrow time window, and thus require a much higher thrust level than delivered by the EP system. The high thrust comes from LOX/LCH_4 based engines, with the cryogenic propellant being stored in a single common bulkhead tank. Since the module does have to dock with the S/C stack, it also has a full RCS that is compatible with the other S/C modules. The chemical propulsion module propulsion system configuration is shown in Figure 4-23.

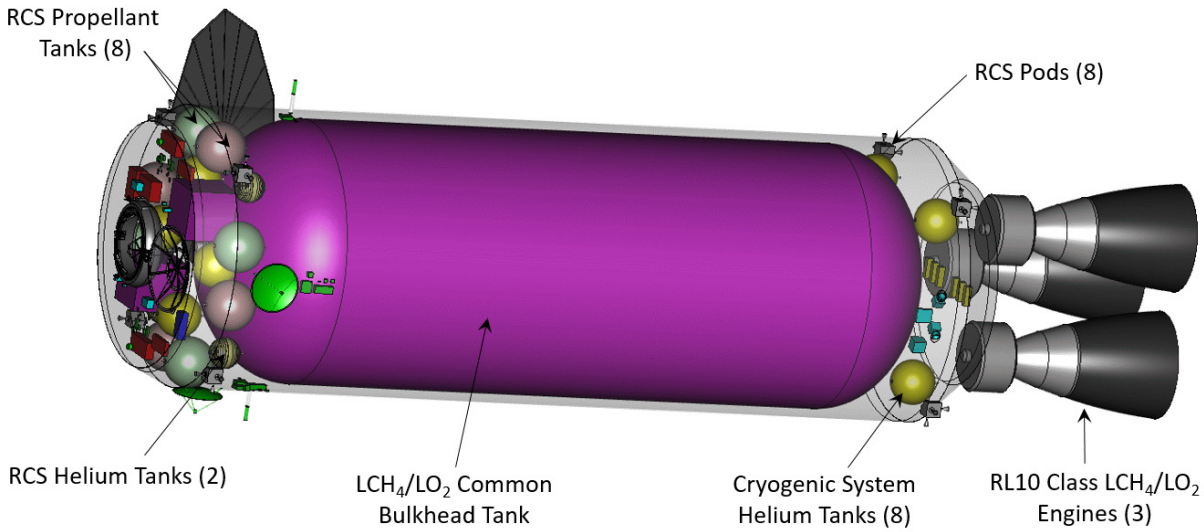

Figure 4-23 Chemical Propulsion Module Propulsion System Configuration

4.2.6.3.1 Cryogenic Propellant Storage

The cryogenic propulsion system is comprised of single common bulkhead tank that stores the LOX/LCH_4 propellants, three 110 kN [25 kilopounds force (klbf)] class engines, and both a helium and autogenous pressurization system. The mission can be completed using only two 110 kN engines. The system is designed to allow propellant refueling on orbit and provide active thermal management of the propellants during the mission.

The common bulkhead tank design has the fuel and oxidizer share a common bulkhead inside the tank structure. The tank is made of 2090-T83 aluminum alloy, mounted via low thermal conductivity struts, has a nominal MOP of 14.8 kPa (50 psi), houses internal propellant level gauging hardware for both propellants, and has integral PMDs and slosh baffles. The thermal management system consists of cryo-coolers, mixers, multi-layer insulation (MLI), and a TVS.

The cryogenic feed system is a nominal multi-engine feed system with helium actuated pre-valves, helium engine purge lines, redundant valves, refueling couplings, and a methane side autogenous pressurization system. Both the oxygen and methane are initially pressurized with helium, which is stored in eight Ariane COPV tanks. These tanks are 90 cm (35.4 in.) in diameter, have a MOP of 40.0 MPa (5,800 psi) [24], and are currently being used on the Orion program European Service Module. For this design, oxygen is pressurized exclusively with helium. Although human rated oxygen autogenous pressurizations systems have been flown on vehicles such as the Space Shuttle, there are concerns regarding potential particle ignition in the gaseous oxygen flow path [25]. Therefore, for this design, a conservative route is taken by using helium for the oxygen pressurization. A preliminary P&ID of the cryogenic system is shown in Figure 4-24.

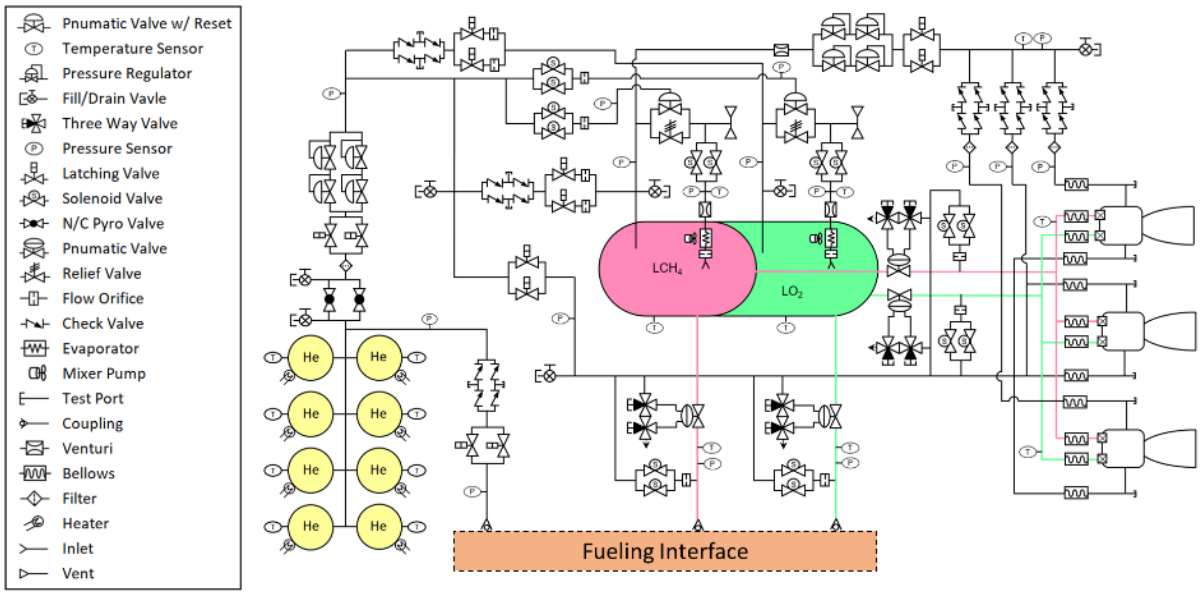

Figure 4-24 Preliminary Cryogenic Propulsion System P&ID

4.2.6.3.2 Cryogenic Engines

There are three 110 kN (25 klbf) class LOX/LCH_4 engines on the Chemical Propulsion Module in a 2 +1 configuration. They are based on the RL-10C-2 architecture, are expander cycle based with autogenous pressurization tap (methane side only), and have an assumed O/F of 3.2. It is assumed that these engines have the same overall dimensions as RL-10C-2, pneumatic main valves, a regenerative cooling jacket to a nozzle area ratio of 61, and an overall nozzle area ratio of 280. The high nozzle area ratio is obtained via a deployable radiatively cooled carbon composite nozzle extension that retracts around the engine powerhead for launch [26].

These engines do require cryogenic propellant for chill down and thermal conditioning prior to start-up. This is modeled by assuming 100 kg (220 lb_m) of propellant is used per engine per engine start sequence.

The engines are directed via a two-axis TVC system with dual motors per actuator and a redundant controller per actuator pair. The TVC electronics are redundant (closed loop) modular units that communicate with the main S/C

computer, filter electrical power for the actuators, and are MIL-STD-1553B [27] and RS-422 [28] compatible. They are based on existing Moog TVC units and provide a nominal +/- 10 deg in both axes [29].

4.2.6.3.3 Reaction Control System

The RCS is a bimodal (MMH/NTO) based system with discrete helium pressurization. There are a total of twenty-four 220 N (50 lb_f) thrusters mounted in eight pods containing three thrusters each. These thrusters are the same model as those used on both the NEP and Xenon Interstage Modules and are described above. The propellants are stored in eight NG model 80430-1 spherical titanium alloy tanks that are 1.03 cm (40.6 in.) in diameter and have an integral PMD [21], four for MMH and four for NTO. Helium for the pressurization system is stored in four Arde model 4866 spherical COPV tanks that are 65.0 cm (25.6 in.) in diameter and have a MOP of 28.0 MPa (4,060 psi) [22]. Similar to the Xenon Interstage Module RCS, the chemical propulsion stage RCS is not designed to be refueled, but does allow for thrusters on other stages to utilize its propellants via a coupling interface. A preliminary P&ID of this system is shown in Figure 4-25.

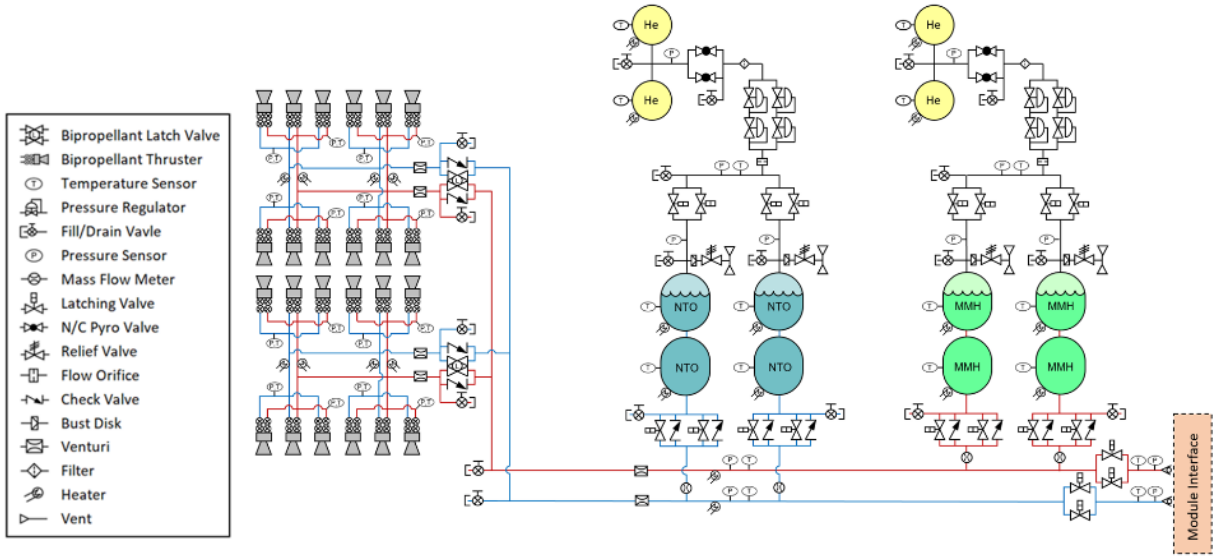

Figure 4-25 Chemical Propulsion Module Preliminary RCS P&ID

4.2.7 Recommendation(s)

There are several propulsion related recommendations from this study. The first recommendation is for further analysis and refinement of the xenon compressor system. This system could be utilized by both S/C designs that utilize xenon, and those that act as tankers to refuel other S/C that do. It is envisioned at a single compressor system could be developed and deployed across a range of S/C platforms, thus reducing cost and risk.

Second, there is a recommendation to evaluate the effects of a high radiation dose on both Hall thruster materials and performance. As Hall thrusters will be potentially used for both longer missions, and those with nuclear power onboard, the cumulative effects of radiation on the thruster need to be better understood.

Finally, there is a recommendation to better determine the high thrust chemical engine type and required thrust level. It is envisioned that the cryogenic engine used in this design would also be used on other S/C such as Mars landers, ascent vehicles, or even commercial upper stages. Currently, these engines are in development, so their performance, thrust level, dimensions, and mass are ill defined at this time. Although the engines used in this design are based on an existing system and its proposed derivatives, the assumed values used in this design will differ to some degree from the actual developed engines.

4.2.8 Master Equipment List

The MEL containing the propulsion system hardware components for the NEP, Xenon Interstage, and Chemical Propellant Modules are shown in the tables below. Note that the propellant loads are those at launch and do not include the propellants added on-orbit by tankers.

Table 4-7 NEP Module Propulsion – Primary EP System Hardware & Power Processing Unit MEL

Description Case 3_SLS_Chem NEP_Chem_Vehicle_Family CD-2020-181	QTY	Unit Mass	Basic Mass	Growth	Growth	Total Mass
Propulsion (EP Hardware)			**9294.4**	**24%**	**2192.1**	**11486.5**
Primary EP System Hardware			**7080.4**	**22%**	**1563.9**	**8644.3**
EP System Hardware			7080.4	22%	1563.9	8644.3
NASA 100 kWe Hall Thrusters	20	250.0	5000.0	25%	1250.0	6250.0
Xenon Tank	1	1829.4	1829.4	15%	274.4	2103.8
Xenon Feed System	1	85.0	85.0	15%	12.8	97.8
Propellant Transfer Hardware	1	10.0	10.0	25%	2.5	12.5
High Pressure Flow Controller	4	12.0	48.0	15%	7.2	55.2
Low Pressure Flow Controller	20	1.5	30.0	15%	4.5	34.5
Line Heaters	1	8.0	8.0	25%	2.0	10.0
Xe Pump System	2	35.0	70.0	15%	10.5	80.5
Power Processing Unit (PPU)			**2214.0**	**28%**	**628.2**	**2842.2**
DDU	20	35.0	700.0	25%	175.0	875.0
DCIU and Flow Controller	1	20.0	20.0	25%	5.0	25.0
Cabling	20	74.7	1494.0	30%	448.2	1942.2

Table 4-8 NEP Module Main Propellant (EP) MEL

Description Case 3_SLS_Chem NEP_Chem_Vehicle_Family CD-2020-181	QTY	Unit Mass	Basic Mass	Growth	Growth	Total Mass
Propellant (EP)			**26028.7**	**0%**	**0.0**	**26028.7**
Main Propellant (EP)			**26028.7**	**0%**	**0.0**	**26028.7**
Primary EP Propellant Used	1	22339.0	22339.0	0%	0.0	22339.0
Primary EP Propellant Residulals (Unused)	1	625.0	625.0	0%	0.0	625.0
Primary EP Propellant Performance Margin (Unus	1	3064.7	3064.7	0%	0.0	3064.7

Table 4-9 NEP Module Propulsion – Primary Chemical System Hardware MEL

Description Case 3_SLS_Chem NEP_Chem_Vehicle_Family CD-2020-181	QTY	Unit Mass	Basic Mass	Growth	Growth	Total Mass
Propulsion (Chemical Hardware)			**427.6**	**8%**	**35.6**	**463.1**
Primary Chemical System Hardware			**427.6**	**8%**	**35.6**	**463.1**
Reaction Control System Hardware			427.6	8%	35.6	463.1
200N Biprop RCS Thrusters	24	1.9	45.6	3%	1.4	47.0
RCS Thruster Subassembly	8	3.0	24.0	15%	3.6	27.6
RCS Feed System	1	111.5	111.5	15%	16.7	128.2
Helium Tanks	2	49.5	99.0	3%	3.0	102.0
Pressurization System	1	54.0	54.0	15%	8.1	62.1
RCS NTO Tanks	2	23.4	46.7	3%	1.4	48.1
RCS MMH Tanks	2	23.4	46.7	3%	1.4	48.1

Table 4-10 Xenon Interstage Module Propulsion System MEL

Description Case 3_SLS_Chem NEP_Chem_Vehicle_Family CD-2020-181	QTY	Unit Mass	Basic Mass	Growth	Growth	Total Mass
Propellant (Chemical)			**1510.7**	**0%**	**0.0**	**1510.7**
RCS Propellant			**1510.7**	**0%**	**0.0**	**1510.7**
Fuel			567.8	0%	0.0	567.8
Fuel Usable	1	498.7	498.7	0%	0.0	498.7
Fuel Margin	1	49.9	49.9	0%	0.0	49.9
Fuel Residulals (Unused)	1	19.2	19.2	0%	0.0	19.2
Oxidizer			936.9	0%	0.0	936.9
Oxidizer Usable	1	822.9	822.9	0%	0.0	822.9
Oxidizer Margin	1	82.3	82.3	0%	0.0	82.3
Oxidizer Residuals (Unused)	1	31.7	31.7	0%	0.0	31.7
RCS Pressurant			6.0	0%	0.0	6.0
Helium Pressurant	1	6.0	6.0	0%	0.0	6.0

Table 4-11 Xenon Interstage Propulsion – Primary EP System Hardware MEL

Description Case 3_SLS_Chem NEP_Chem_Vehicle_Family CD-2020-181	QTY	Unit Mass	Basic Mass	Growth	Growth	Total Mass
Propulsion (EP Hardware)			**3714.8**	**15%**	**557.2**	**4272.1**
Primary EP System Hardware			**3714.8**	**15%**	**557.2**	**4272.1**
EP System Hardware			3714.8	15%	557.2	4272.1
Xenon Tanks	2	1829.4	3658.8	15%	548.8	4207.7
Feed system	1	36.0	36.0	15%	5.4	41.4
Propellant Transfer Hardware	2	10.0	20.0	15%	3.0	23.0

Table 4-12 Xenon Interstage Main Propellant (EP) MEL

Description Case 3_SLS_Chem NEP_Chem_Vehicle_Family CD-2020-181	QTY	Unit Mass	Basic Mass	Growth	Growth	Total Mass
Propellant (EP)			**84343.5**	**0%**	**0.0**	**84343.5**
Main Propellant (EP)			**84343.5**	**0%**	**0.0**	**84343.5**
Primary EP Propellant Used	1	84213.5	84213.5	0%	0.0	84213.5
Primary EP Propellant Residulals (Unused)	1	130.0	130.0	0%	0.0	130.0

Table 4-13 Xenon Interstage RCS Propellant (Chemical) MEL

Description Case 3_SLS_Chem NEP_Chem_Vehicle_Family CD-2020-181	QTY	Unit Mass	Basic Mass	Growth	Growth	Total Mass
Propellant (Chemical)			**3085.9**	**0%**	**0.0**	**3085.9**
RCS Propellant			**3085.9**	**0%**	**0.0**	**3085.9**
Fuel			1158.5	0%	0.0	1158.5
Fuel Usable	1	1009.5	1009.5	0%	0.0	1009.5
Fuel Margin	1	109.8	109.8	0%	0.0	109.8
Fuel Residulals (Unused)	1	39.2	39.2	0%	0.0	39.2
Oxidizer			1911.5	0%	0.0	1911.5
Oxidizer Usable	1	1665.7	1665.7	0%	0.0	1665.7
Oxidizer Margin	1	181.1	181.1	0%	0.0	181.1
Oxidizer Residuals (Unused)	1	64.6	64.6	0%	0.0	64.6
RCS Pressurant			16.0	0%	0.0	16.0
Helium Pressurant	1	16.0	16.0	0%	0.0	16.0

Table 4-14 Xenon Interstage Propulsion – Primary Chemical System Hardware MEL

Description Case 3_SLS_Chem NEP_Chem_Vehicle_Family CD-2020-181	QTY	Unit Mass	Basic Mass	Growth	Growth	Total Mass
Propulsion (Chemical Hardware)			**399.0**	**11%**	**42.4**	**441.4**
Primary Chemical System Hardware			**399.0**	**11%**	**42.4**	**441.4**
Reaction Control System Hardware			399.0	11%	42.4	441.4
ATV/Service Module Thrusters	24	1.9	45.6	3%	1.4	47.0
RCS Thruster Subassembly	8	7.5	60.0	25%	15.0	75.0
RCS Feed System	1	60.0	60.0	15%	9.0	69.0
Helium Tanks	2	40.4	80.8	3%	2.4	83.3
Pressurization System	2	42.0	84.0	15%	12.6	96.6
RCS NTO Tanks	2	17.1	34.3	3%	1.0	35.3
RCS MMH Tanks	2	17.1	34.3	3%	1.0	35.3

Table 4-15 Chemical Stage Main Engine Propellant (Chemical) MEL

Description Case 3_SLS_Chem NEP_Chem_Vehicle_Family CD-2020-181	QTY	Unit Mass	Basic Mass	Growth	Growth	Total Mass
Propellant (Chemical)			**77865.6**	**0%**	**0.0**	**77865.6**
Main Engine Propellant			**73552.2**	**0%**	**0.0**	**73552.2**
Fuel			17483.9	0%	0.0	17483.9
Fuel Usable	1	16748.5	16748.5	0%	0.0	16748.5
Fuel Residulals (Unused)	1	735.4	735.4	0%	0.0	735.4
Oxidizer			55948.3	0%	0.0	55948.3
Oxidizer Usable	1	53595.2	53595.2	0%	0.0	53595.2
Oxidizer Residuals (Unused)	1	2353.2	2353.2	0%	0.0	2353.2
Main Engine Pressurant			120.0	0%	0.0	120.0
Helium Pressurant	1	120.0	120.0	0%	0.0	120.0
RCS Propellant			**4313.4**	**0%**	**0.0**	**4313.4**
Fuel			1619.8	0%	0.0	1619.8
Fuel Usable	1	1414.7	1414.7	0%	0.0	1414.7
Fuel Margin	1	150.3	150.3	0%	0.0	150.3
Fuel Residulals (Unused)	1	54.8	54.8	0%	0.0	54.8
Oxidizer			2672.6	0%	0.0	2672.6
Oxidizer Usable	1	2334.3	2334.3	0%	0.0	2334.3
Oxidizer Margin	1	248.0	248.0	0%	0.0	248.0
Oxidizer Residuals (Unused)	1	90.4	90.4	0%	0.0	90.4
RCS Pressurant			21.0	0%	0.0	21.0
Helium Pressurant	1	21.0	21.0	0%	0.0	21.0

Table 4-16 Chemical Stage Propulsion – Primary Chemical System Hardware MEL

Description Case 3_SLS_Chem NEP_Chem_Vehicle_Family CD-2020-181	QTY	Unit Mass	Basic Mass	Growth	Growth	Total Mass
Propulsion (Chemical Hardware)			**10152.5**	**14%**	**1427.7**	**11580.2**
Primary Chemical System Hardware			**1493.2**	**14%**	**212.3**	**1705.6**
Main Engine Hardware			1053.0	15%	158.0	1211.0
Main Engine	3	230.0	690.0	15%	103.5	793.5
Main Engine Gimbal	3	10.0	30.0	15%	4.5	34.5
TVC	3	65.0	195.0	15%	29.3	224.3
TVC Controller	6	23.0	138.0	15%	20.7	158.7
Reaction Control System Hardware			440.2	12%	54.4	494.6
ATV/Service Module Thrusters	24	1.9	45.6	3%	1.4	47.0
RCS Thruster Subassembly	8	7.5	60.0	25%	15.0	75.0
RCS Feed System	1	125.0	125.0	15%	18.8	143.8
Helium Tanks	4	25.4	101.6	3%	3.0	104.7
Pressurization System	2	54.0	108.0	15%	16.2	124.2
Propellant Management (Chemical)			**8659.3**	**14%**	**1215.4**	**9874.7**
Main Engine Propellant Management			8485.0	14%	**1210.2**	**9695.2**
LCH4 Tank	1	2581.0	2581.0	15%	387.2	2968.2
LOX tank	1	4769.0	4769.0	15%	715.4	5484.4
Cryo Feed System	1	265.4	265.4	15%	39.8	305.2
Refueling Hardware	1	80.0	80.0	25%	20.0	100.0
Pressurization System	1	110.0	110.0	15%	16.5	126.5
Helium Tanks	8	78.7	629.6	3%	18.9	648.5
Prop Mass Gauging System	2	25.0	50.0	25%	12.5	62.5
RCS Propellant Management			174.2	3%	**5.2**	**179.5**
MMH Tanks	4	21.8	87.1	3%	2.6	89.7
NTO Tanks	4	21.8	87.1	3%	2.6	89.7

4.3 Thermal Control System

The Mars NEP spacecraft utilizes a combination of a nuclear reactor powered electric propulsion system and a chemical stage to transit to Mars from Earth orbit. The thermal system has to maintain the temperature of the liquid oxygen and methane tanks below the boiling point to eliminate any boiloff of the propellant in order to ensure that the propellant can last throughout the mission. The radiator systems for the reactor power conversion system are included in the power system description.

4.3.1 System Requirements and Assumptions

The thermal system accomplishes its task by using a zero-boiloff system consisting of a number of cryocoolers, multi-layer insulation, and the associated system for rejecting the waste heat from the cryocoolers. The thermal system also has to reject the waste heat from the electric propulsion direct drive power units as well as the waste heat from the other support electrical systems.

The spacecraft operation will take place from Earth (1 AU) to Venus (0.74 AU) to Mars (1.54 AU). The thermal system will be sized to operate within this environment. Solar Intensity and view angle as well as the view to warm bodies such as the spacecraft solar arrays and radiators, and operation during shadow are used to determine the worst-case hot and cold conditions. The worst-case warm conditions will occur in sunlight conditions near Venus

with all equipment operating. Whereas the worst-case cold will be at Mars in shadow. The aspects of the thermal control and environment as well as the system components that were addressed or sized in the design and analysis are listed below.

- Radiator Panels
- Thermal Control Cryogenic Tanks and Propellant Lines, cryocoolers and zero boiloff system.
- Cryocoolers for eliminating propellant boil-off
- Spacecraft & Propellant tank Insulation
- Pump loop cooling system for moving the waste heat from the cryocoolers to the radiators.
- Heaters for controlling the spacecraft components temperature
- Temperature Sensors, Controllers, Switches, Data Acquisition
- Heat leak through the insulation & insulation pass-through
- Radiation exposure

Table 4-17 below lists the requirements and assumptions utilized in sizing the thermal system components.

Table 4-17 Vehicle Specification, Requirements and Assumptions for the Thermal System Sizing

Variable/Component	Value/Description
Nested LOX/L-Methane Tank	5.0 m Diameter, 14.8 m Total Length (Oblate Spheroid Ends, 11.3 m Barrel Length)
Xenon Tank Module	5.0 m Diameter, 14.9 m Length
Nuclear Power Module	Electronics Section: 4.5 m Length, 3.2 m Diameter Xenon Tank Section: 5.0 m Length, 5.0 m Diameter
Waste Heat Load to be Rejected:	Nuclear Module Electronics: 2,193 W at 300 K Nuclear Module DDU: 18,184 W at 303 K Chemical Stage Cryocooler: 338 W at 300 K Chemical Stage Electronics: 2,500 W at 300 K Xenon Interstage Electronics: 1,100 W at 300 K Xenon Tanks (1 in Nuclear section): 1,212 W at 300 K
Operating Temperature	Electronics & Cryocooler: 300 K Rejection Temperature DDU: 303 K Rejection Temperature Tank: 90.4 K LOX tank (L-Methane tank will be operated at slightly above to avoid freezing the methane) Reactor: 450 K Rejection Temperature
Insulation (multi-layer insulation MLI was used for the electronics)	Electronics Section Outer frame is wrapped in 25 layers of MLI, Cryogenic Propellant tank 35 layers of MLI
Environment	Operational Environment: Venus 10,000 km Altitude 0.72 AU (worst case hot), Mars 1.54 AU (worst case cold)
Radiator & View Factors	Max 70° Angle to the Sun View Factor to the Spacecraft & Solar Arrays 0.20 View Factor to Venus: 0.064 (at closest approach), Cryocoolers & Electronics: Deployable Reactor: Foldout Deployable
Heat Pipes/Pump Loop Coolant System	Xenon Tank (Nuclear Section) Cryocoolers & Electronics: Heat Pipe based coolant system DDU: Pump Loop Coolant System

4.3.2 Operating Environments

Since the mission takes the spacecraft from Earth to Mars and returns with a Venus flyby, the thermal environment at each of these locations has to be evaluated. The first step in sizing the thermal components is to determine an effective sink temperature at each location. This is accomplished by performing an energy balance on an object with no internal heat generation at each of the locations to determine its equilibrium temperature. This equilibrium temperature is the sink temperature at each location. For this analysis a 6-sided cube was used for the object shape. Each side of the object has a different view to the heat sources and sinks in the environment around the object. The net power into or emitted from side "i" (Pi) of the object is given by Equation 2 and the total energy balance power (Peb) is given by Equation 3.

Equation 2 $$P_i = \left(\varepsilon_i \sigma T_c^4 - \alpha_{si} I_s \cos(\beta_i + f_{pi} A_p\right) - \alpha_{IRi} I_p f_{pi}) A_{si}$$

Where the Stefan-Boltzman Constant) $\sigma = 5.67 \times 10^{-8}$ $(\frac{W}{m^2 K^4})$.

Equation 3 $$P_{eb} = \sum_{i=1}^{i=6} P_i$$

Table 4-18 provides the variables used and their corresponding values for each side and planet.

Table 4-18 Sink Temperature Properties

	Side 1 (i=1)	*Side 2 (i=2)*	*Side 3 (i=3)*	*Side 4 (i=4)*	*Side 5 (i=5)*	*Side 6 (i=6)*
Length	1 m	1 m	1 m	1m	1 m	1 m
Width	1 m	1 m	1 m	1m	1 m	1 m
Area (A_{si})	1 m^2	1 m^2	1 m^2	1 m^2	1 m^2	1 m^2
Emissivity(ε_i)	0.85	0.85	0.85	0.85	0.85	0.85
Solar Absorptivity(α_{si})	0.14	0.14	0.14	0.14	0.14	0.14
Solar Angle (β□)	45	45	45	0	0	0
View to Planet (f_{pi})	0	0	0	0.06	0.06	0.06
IR Absorptivity (α_{IRi})	0.3	0.3	0.3	0.3	0.3	0.3
Location	Earth		Venus		Mars	
Solar Intensity (I_s)	1353 W/m^2		2613 W/m^2		617 W/m^2	
Albedo (A_p)	0.3		0.75		0.16	
IR Emission (I_p)	240 W/m^2		148 W/m^2		140 W/m^2	
Sink Temperature	220.7 K		255.2 K		187.7 K	

The sink temperature at the three locations is determined by iterating on the cube temperature (Tc) in Equation 2 so that Equation 3 is equal to 0. The cube temperature at which Equation 2 equals 0 is the sink temperature (Ts) for that location and input conditions. Table 4-18 gives the calculated sink temperature for each location and Figure 4-26 shows the mission illustration.

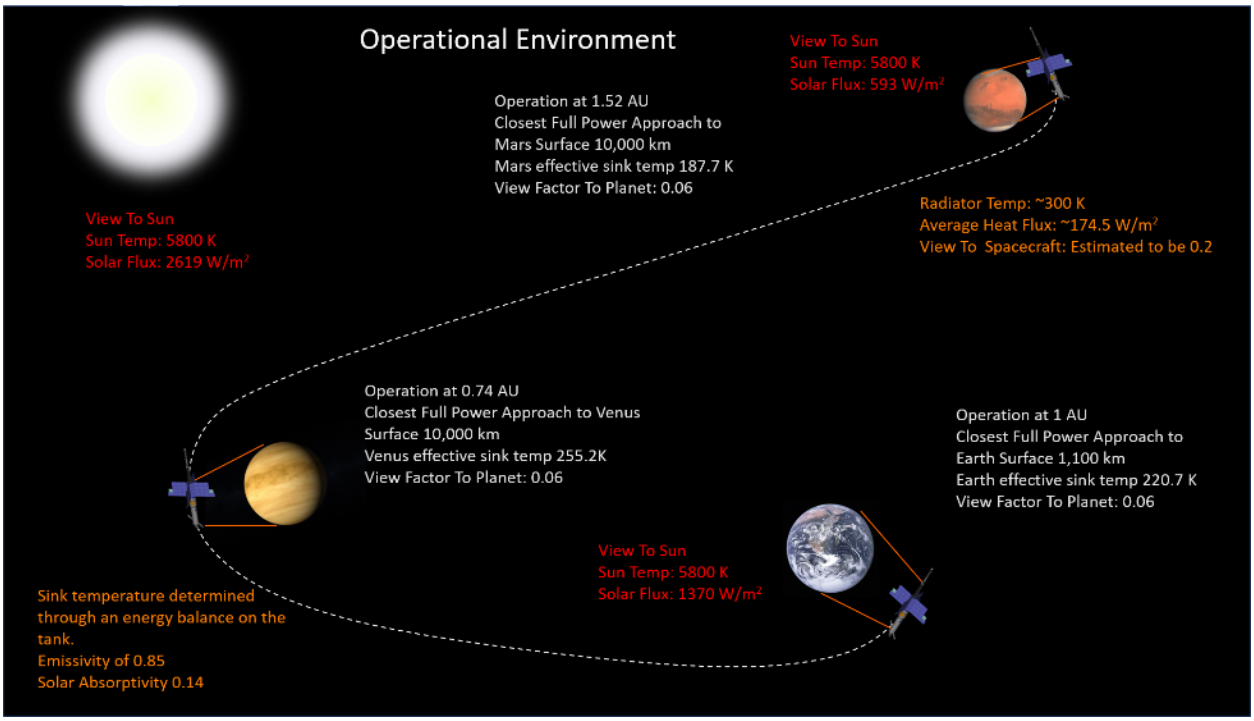

Figure 4-26 Environmental Thermal Properties Throughout the Mission

4.3.3 System Design

The thermal system for the mission involved a number of aspects of the spacecraft and their operation. The thermal system consisted of three main categories. The electric propulsion system thermal control which includes the DDUs and Xe tanks, the chemical propulsion system thermal control which includes the cryogenic tank control and management, and the various spacecraft electronics thermal control. Figure 4-27 shows these main components.

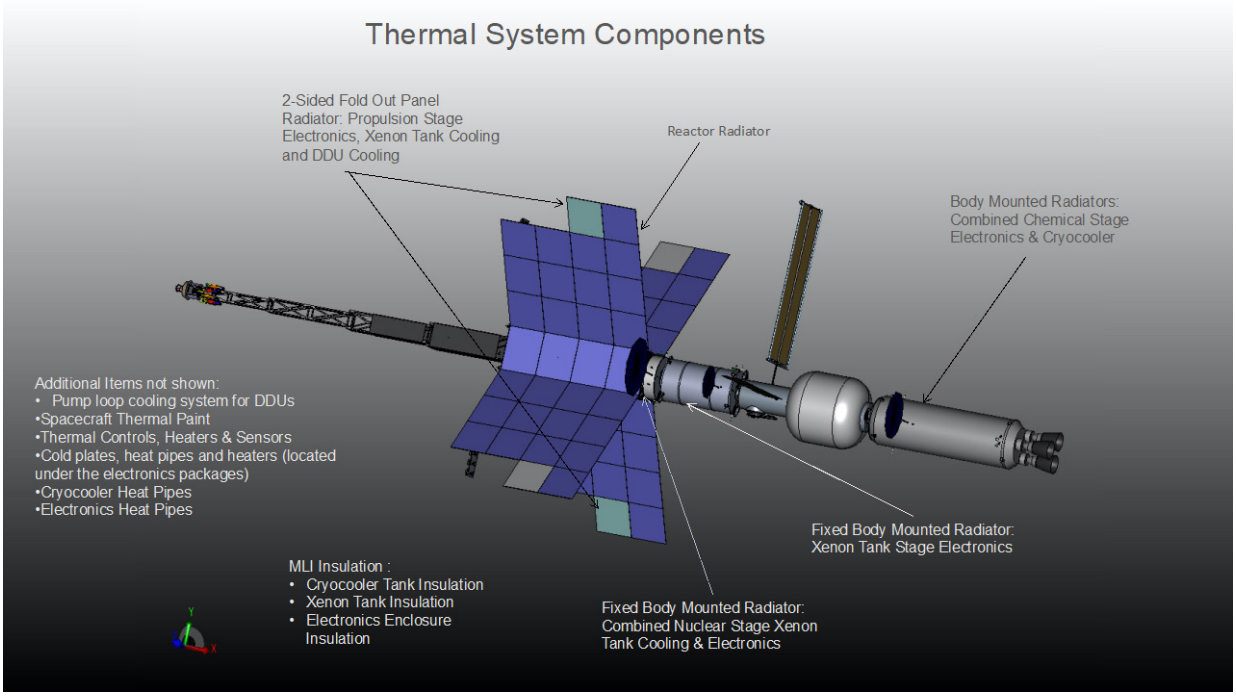

Figure 4-27 Main Thermal Control Areas

4.3.4 Radiators

Radiators are used to reject the excess heat from each of the main systems to space. The radiator design and required area is specific for each system, its specific function, and operational conditions. The radiators are sized based on energy balance approach for rejecting excess heat to the surroundings. Heat inputs and view factors to surrounding components of an environmental body such as the sun and planets are taken into account in this energy balance approach.

The required radiator area (Ar) is determined by the thermal power that needs to be rejected (Pr) as given by Equation 4. The radiator is sized based on the worst-case operating conditions as given by the variables used in its sizing and described in Table 4-19.

Equation 4

$$A_r = \frac{P_r}{\sigma(\varepsilon_r T_r^4) - \alpha_{IR} f_p I_p - \alpha_r I_s (Cos(\theta_{rs}) + f_p A_p) - f_{sc} \alpha_{IR} I_{sc}}$$

Table 4-19 Radiator Sizing Variables and Results

Variable	Value
Radiator Solar Absorptivity (α_r)	0.14
Radiator IR Absorptivity (α_{IR})	0.30
Radiator Emissivity (ε_r)	0.84
Max Radiator Sun Angle	30°
View Factor Planetary Body (f_p)	0.06
View Factor to Solar Array & Spacecraft (f_{sc})	0.2
Power System Radiator IR Emission (I_{sc})	1800 W/m^2
Radiator Operating Temperature	Nominal 300 K
Waste Heat Source	Waste Heat (P_r), Operating Temperature (T_r) & Radiator Area
NEP Module Electronics:	2,193 W at 300 K, Area 10.5 m^2
NEP Module Xenon Tank:	1,212 W at 300 K, Area 7.2 m^2
NEP Module DDUs:	18,184 W at 300 K, Area 80.6 m^2
Xenon Interstage Electronics:	1,100 W at 300 K, Area 5.2 m^2
Chemical Propulsion Module Electronics:	2,500 W at 300 K, Area 11.9 m^2
Chemical Propulsion Module Cryocooler:	339 W at 300 K, Area 1.6 m^2

An estimate of the mass of the radiator panel (Mr) can be made based on its required area. The radiator structure can be separated into a number of components with a scaling coefficient for each component to linearly scale the mass based on the required radiator area. These coefficients were derived from satellite and spacecraft radiator mass data and are listed in Table 4-20. The total radiator mass is given by Equation 5.

Table 4-20 Radiator Mass Scaling Coefficients

Radiator Component Coefficient	Value (kg/m^2)
Panels (C_p)	3.3
Coating (C_c)	0.42
Tubing (C_t)	1.31
Header (C_h)	0.23
Adhesives (C_a)	0.29
Stingers (C_s)	1.50
Attachment (C_{at})	0.75
Deployment Mechanism (C_d)	3.4

Equation 5

$$M_r = C_p A_r + C_c A_r + C_t A_r + C_h A_r + C_a A_r + C_s A_r + C_{at} A_r + C_d A_r$$

Typically, louvers are used on the radiator to insulate it when it is not in use during shadowed operation or when the waste heat levels are low. The louvers are required to reduce the heat loss to the environment during these times. Utilizing louvers on the radiator however will increase the required radiator area needed by approximately 30%. This is due to the louvers reducing the view factor of the radiator to deep space or other cold surfaces to reject heat. For this application since the power system and loads such as the cryocooler and electronics will be operated continuously louvers were not utilized.

The main power source for the spacecraft is the fission reactor. This reactor generates a significant amount of waste heat that needed to be dissipated during the mission. The reactor radiator was by far the largest of the radiator systems on the spacecraft. The radiator design for the reactor is included in Section 4.1.1, Fission Reactor Power System.

4.3.5 DDU Radiators & Coolant System

The DDUs which are used to provide power to the electric propulsion engines require a radiator to reject their waste heat. They provide the largest waste heat load of the items that are handled by the thermal control system. Due to the large heat load from the DDUs, just over 18 kW, the radiator panels for the DDUs were incorporated onto the large main radiator for the reactor. However, since these panels operated at a lower temperature then the main reactor radiator, 300 K for the DDUs compared to 450 K for the reactor, a separate pump loop cooling system was utilized to move heat from the DDUs to the radiator panels. A pump loop system was utilized instead of heat pipes due to the high heat load and the distance that the panels were from the DDU heat sources. The placement of the DDU radiators is illustrated in Figure 4-28.

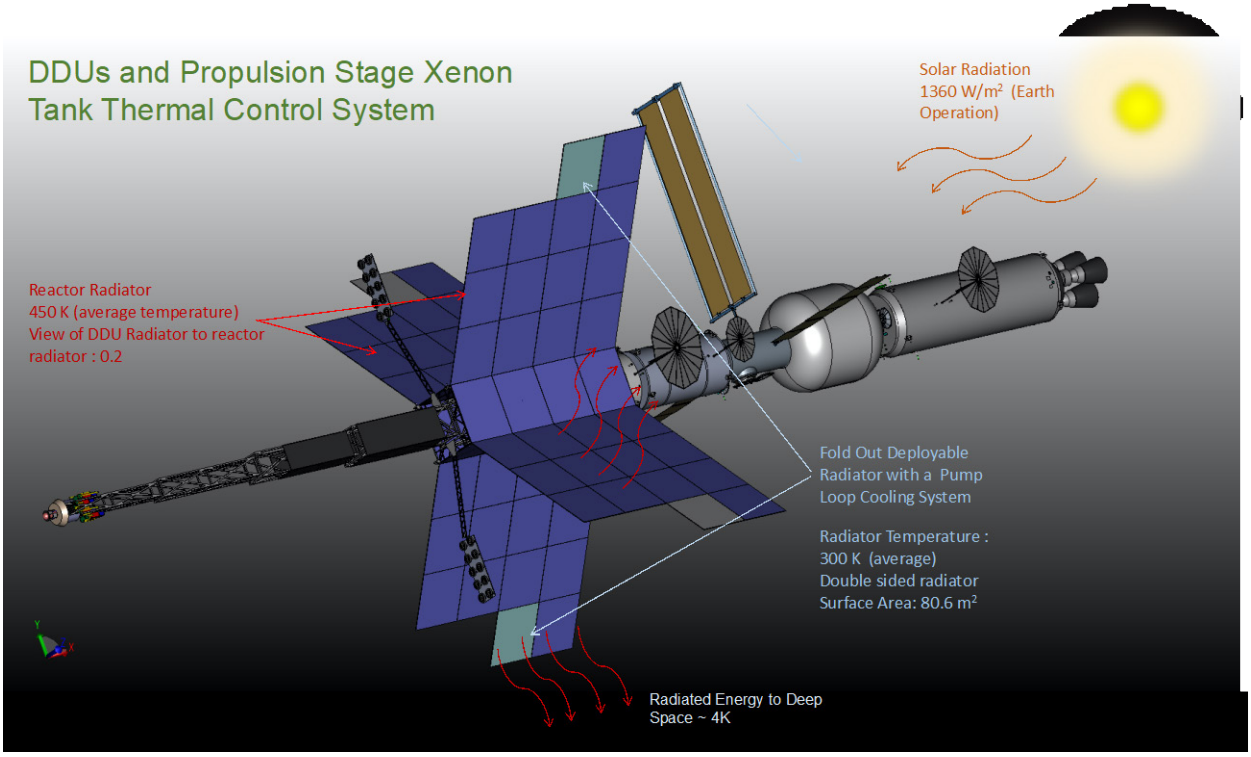

Figure 4-28 Illustration of the Power System Radiator Thermal Balance

This radiator utilized a fold out design that enabled the radiator panels to reject heat from both sides of the panels. Utilizing a 2-sided radiator panel provides significant benefits in reducing mass and required deployed area. This is particularly beneficial for the large radiator required by the reactor system. Since the radiator is double sided half the required area is used in Equation 4 to determine its mass.

A pump loop coolant system is utilized with the radiator to move the heat from the DDUs to the radiator. The pump loop system is broken into two segments, each feeding one of the two DDU radiator panels. Each segment has a redundant pump and associated components to keep it operational in case of a failure. The segments are also cross

tied together so that a single pump loop system can transfer fluid through the two radiator segments if needed. The system is controlled by a series of valves and sensors. Heat is collected from the DDUs through a cold plate and moved to the radiator. The average radiator operating temperature is 300 K. An example showing the components and connection of a 2 segments pump loop system is given in Figure 4-29.

The DDU radiators were sized for operation at the 1 AU thermal environment. This was used instead of the hotter near Venus operating conditions because the electric propulsion system was not used during the flyby.

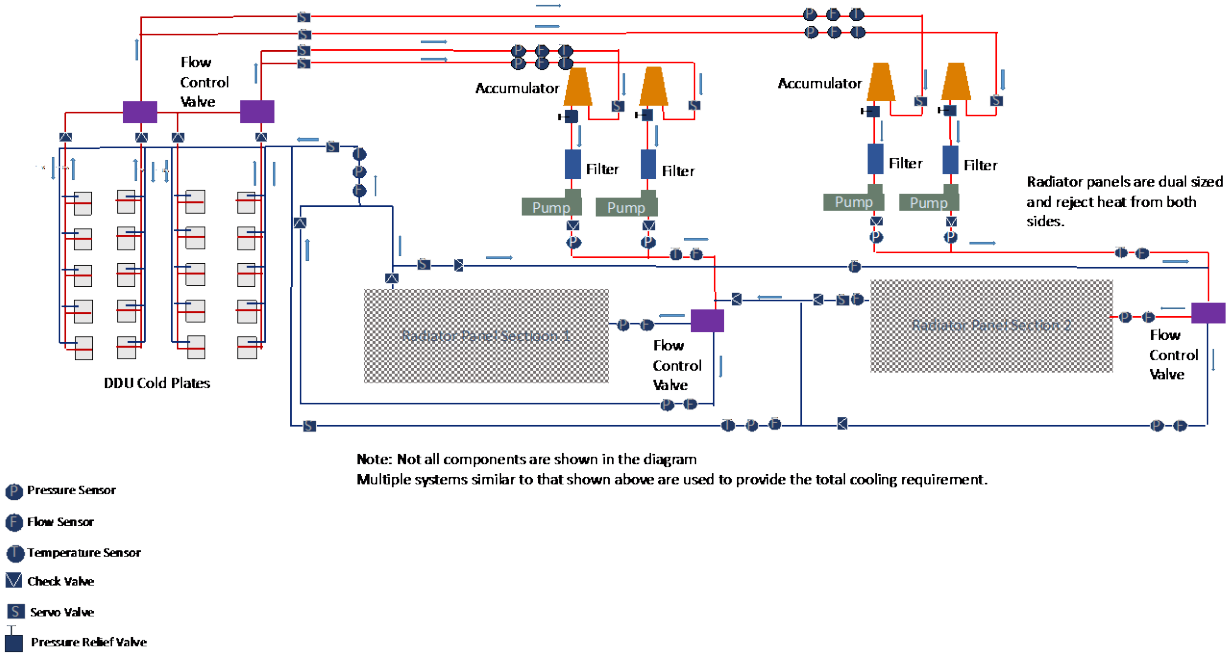

Figure 4-29 Illustration of the DDU Pump Loop Cooling System

4.3.6 Xenon Tank & Electronics Radiators

The radiator for the Xenon tank and electronics within the nuclear section and the Xenon tank section as well as the cryocooler and electronics within the chemical section are sized in a similar fashion to that of the DDUs. However, for these systems the radiators are single sided body mounted radiators and the heat transport system from the heat sources to the radiators utilize heat pipes instead of a pump loop system. For all of these systems the waste heat needs to be rejected to the surroundings in order for these components to operate at their desired temperature. As with the DDU radiator, the radiator sizing is based on an energy balance analysis of the area needed to reject the identified heat load to space.

The electronics, Xenon, and cryocooler propellant management thermal control utilized body mounted radiators. This was due to the proximity of the radiators to the heat loads and the available surface area to accommodate them. Utilizing body mounted radiators near the heat sources enabled heat pipes to be used to move the heat from the source to the radiators. The electronics are mounted to the cold plates where the heat generated is collected. The heat pipes move the heat from the cold plates to the radiator. The number of heat pipe runs are dependent on the amount of heat to be moved, their capacity, and the amount of redundancy needed in the system. The heat pipe condenser sections are distributed throughout the back side of the radiator which allows for uniform heating and heat rejection. The radiator is coated to reflect most of the incoming visible solar radiation. This significantly reduces the heat load on the radiator.

Since the radiators were mounted over the curved surface of the spacecraft sections the average worst-case sun angle on the radiator surface was estimated to be 30°. This is because, due to the curved surface if a portion off the radiator was normal to the sun other portions off the radiator would experience lower sun angles to no direct sun view. Since the radiator is thermally connected and acts as a single heat rejection surface it will equalize the heat load over its surface to accommodate the uneven solar heat load. The mass of the radiator is given by Equation 4

without the need for the deployment mechanism term. The radiators were sized to remove the waste heat from the Xenon tanks, cryocoolers and electronics during the worst case hot operational conditions which occur while sunlit at Venus.

4.3.7 Heat Pipe Cooling Systems

The heat pipes which are utilized with the body mounted radiators are passive, self-contained, sealed heat transport systems. Heat pipes in general operate by boiling a liquid fluid when the heat pipe is subjected to heat at a design operating temperature. The fluid vapor then moves to the opposite end of the heat pipe (radiator) where heat is rejected, and the fluid condenses back to a liquid. A wick structure in conjunction with gravity is used to help move the fluid back to the heating section through capillary forces. Once back to the heat input section the fluid will boil again repeating the process.

The working fluid for the heat pipe is dependent on the desired operating temperature for the system. The operating temperature sets the boiling point for the working fluid. The Merit number is used to gauge the heat transfer capability of different working fluids as a function of operating temperature. The Merit number (N_f), given by Equation 6 is based on the properties of the working fluid, density (r_f), latent heat (s_f), surface tension (g_f) and dynamic viscosity (m_f).

Equation 6 $$N_f = \frac{\rho_f \sigma_f \gamma_f}{\mu_f}$$

The physical properties used to calculate the Merit number all vary as a function of temperature. The Merit number plotted for a number of different working fluids as a function of operating temperature is given in Figure 4-30. From this figure it can be seen that for the 300 K operating point water provides the best heat transfer capability for the heat pipe and therefore was selected as the working fluid for the heat pipes. It should be noted that Ammonia has a slightly lower Merit number and can also be considered for use as the working fluid in the heat pipes if freezing concerns with water are an issue.

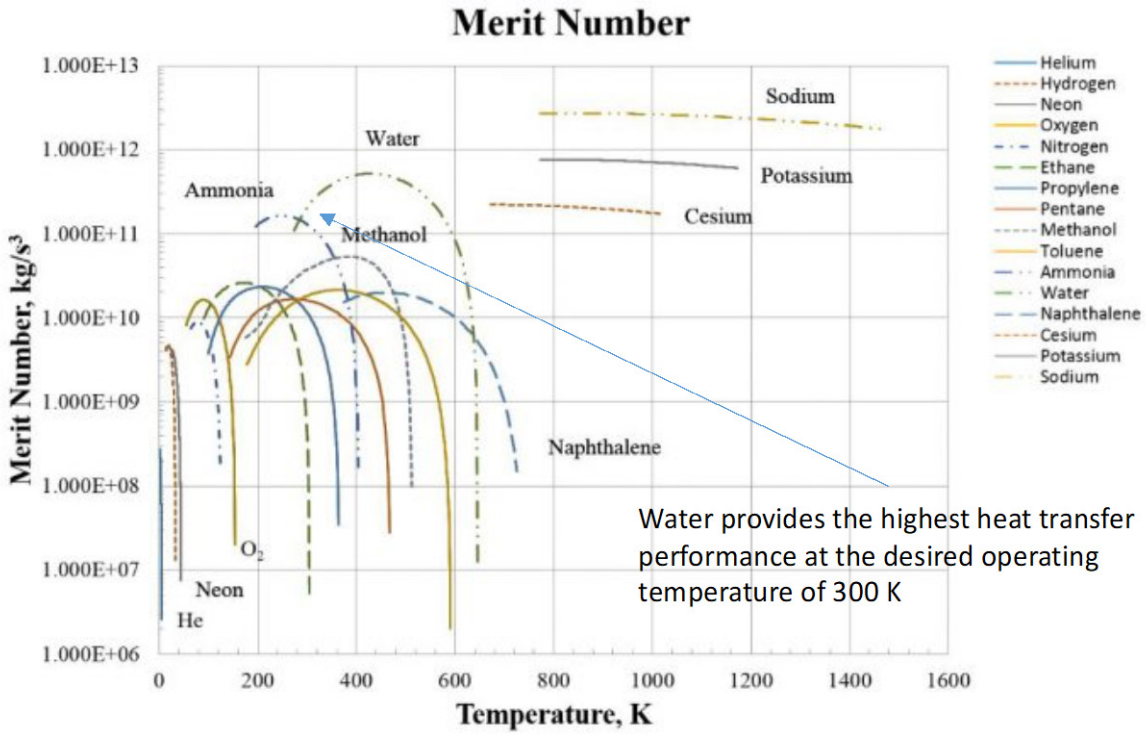

Figure 4-30 Merit Number for Commonly Used Heat Pipe Working Fluids [30]

Variable conductance heat pipes operate in a similar fashion but use a varying volume, non-condensable gas to adjust the amount of heat that the heat pipe is capable of moving while maintain a fixed operating temperature.

At high heat loads the temperature dependent saturation pressure of the working fluid increases. This increase in pressure compresses the non-condensable gas into a reservoir at the end of the heat pipe providing a larger active condenser area, thereby enabling more heat to be moved to the radiator by the heat pipe. As the heat load decreases the pressure decreases and the non-condensable gas fills up a greater volume of the heat pipe reducing the condenser area and thereby reducing the heat flow. A variable conductance heat pipe is a passive device that adjusts automatically to varying heat load inputs maintaining a constant operating temperature.

The heat pipes were sized for the heat produced by each of the loads. Table 4-21 below provides the required heat pipe size and specific mass.

Table 4-21 Heat Pipe Sizing Specifications for Each Load Type in the Propulsion Section

Heat Pipe	Radius	Effective Length	Heat Transfer Capability	Heat Pipe Specific Mass
NEP Module Xenon Tank	1.0 cm	4 m	54 W/Heat Pipe	0.31 kg/m
NEP Module Electronics	2.0 cm	3 m	286 W/Heat Pipe	0.66 kg/m
Chemical Stage Cryocooler	1.0 cm	5 m	50 W/Heat Pipe	0.31 kg/m
Chemical Stage Electronics	1.5 cm	4 m	161 W/Heat Pipe	0.48 kg/m
Xenon Interstage Electronics	1.35 cm	4 m	141 W/Heat Pipe	0.43 kg/m

4.3.8 Cold Plates and Heat Transport

Cold plates are used to interface the heat pipes to the loads. These plates come in a number of shapes and sizes depending on the heat source configuration. They are used to provide a good thermal connection between the heat source and the heat pipe evaporator section. The heat source is mounted to the cold plate which in turn has the heat pipe either mounted to it or incorporated into it. This provides a good thermal contact between the cold plate and the heat pipe.

Heaters are also utilized in conjunction with the cold plates to ensure that the electronics or other components are maintained at their desired temperature. The heaters are only utilized if the component temperature drops to where it may go below its designed temperature range. Due to the mission and type of operation it is not expected that any of the components will need active heating throughout the mission. However, heaters are still included to accommodate unforeseen events or times during the mission when items will not be operational such as during buildup.

4.3.9 Heaters

The heaters utilized consist of flexible flat plate and strip heaters. Waste heat from the internal components as well as electric heaters are used to provide heat to the spacecraft electronic bus interior if needed. Flat plate heaters are used on the cold plates to provide heat to the electronics if necessary. Heaters are located on each cold plate.

Thermal control is accomplished through the use of a network of thermocouples whose output is used to control the power to the various heaters. A data acquisition and control computer are used to operate the thermal system. Under normal operation there is no expected heater power requirement.

4.3.10 Heat Collection Layout

The number of cold plates and heat pipe runs is dependent on the distribution of the loads and the desired redundancy for the thermal system. The cold plate layout and corresponding number of heat pipes is summarized below and illustrated in Figure 4-31, Figure 4-32, and Figure 4-33 for the three body mounted radiators utilized.

Figure 4-31 below illustrates the cold plates and heat pipes utilized with the NEP Module. The NEP Module consists of cold plates for the electronics and the Xenon tank housed in that section. The electronics have two heat pipe runs from each cold plate to the radiator. The heat pipes share the load from each cold plate. Each heat pipe is sized to be capable of moving the total heat generated from the source to the radiator. This provides a redundant heat transfer path for each engine. The radiators are connected with heat pipes to balance the thermal load between them as well as provide a redundant thermal path in case of a failure.

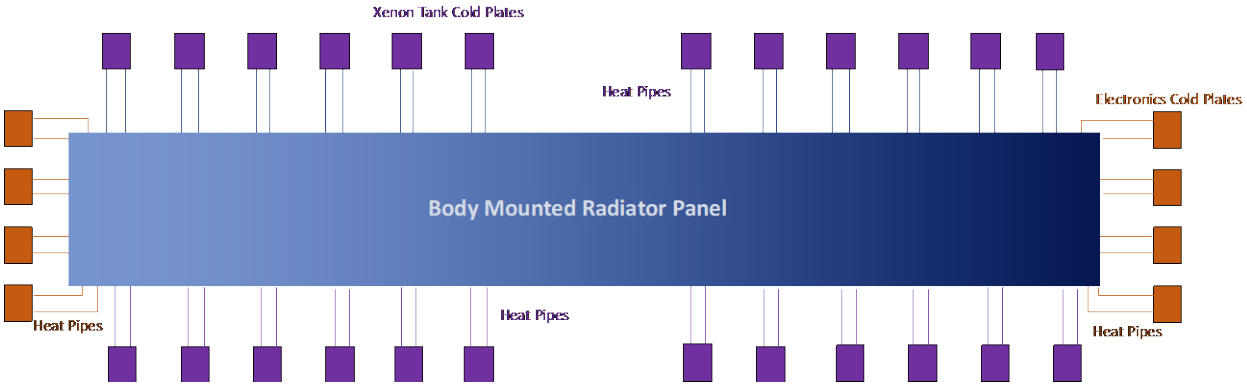

Figure 4-31 NEP Module Body Mounted Radiator Cold Plate and Heat Pipe Layout

Figure 4-32 illustrates the cold plates and heat pipes utilized in the Xenon Interstage for the electronics utilized within that stage. The electronics have two heat pipes runs from each cold plate to the radiator. The heat pipes share the load from each cold plate. Each heat pipe is sized to be capable of moving the total heat generated from the source to the radiator. This provides a redundant heat transfer path for each engine. The radiators are connected with heat pipes to balance the thermal load between them as well as provide a redundant thermal path in case of a failure.

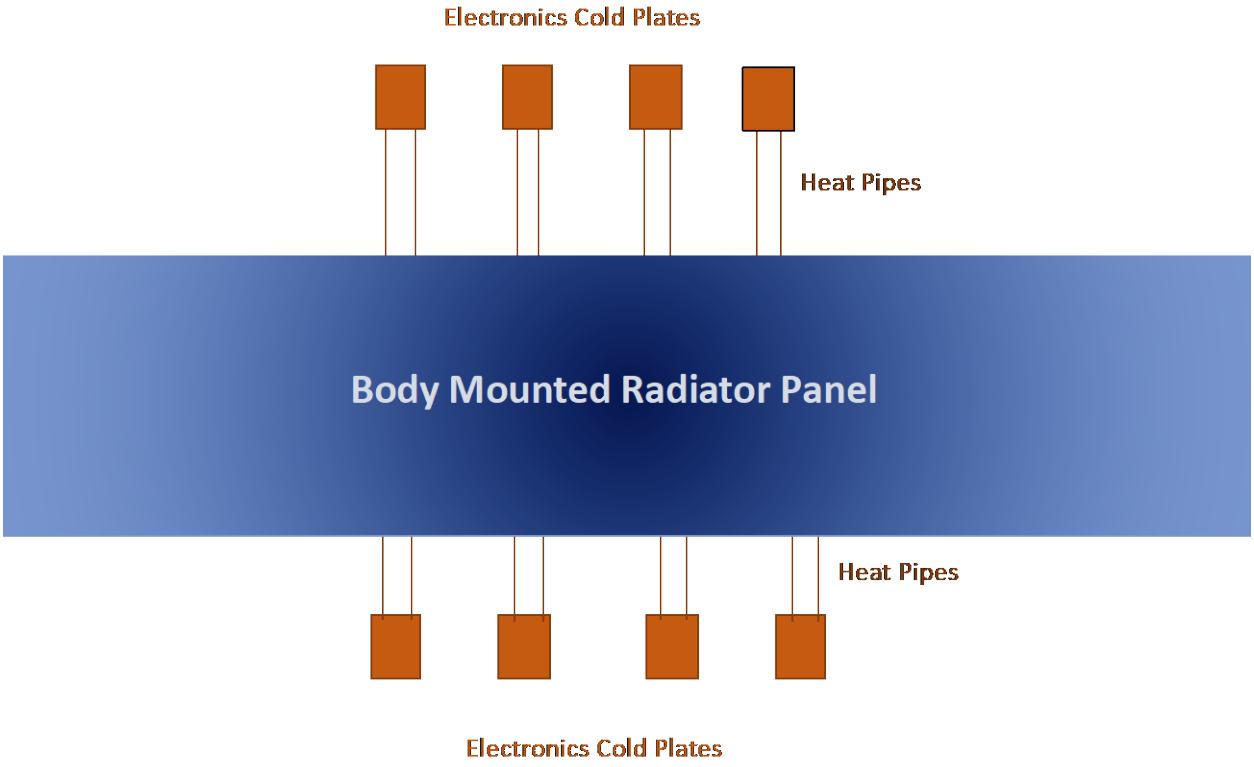

Figure 4-32 Xenon Interstage Body Mounted Radiator Cold Plate and Heat Pipe Layout

The last section is the chemical propulsion section which houses the cryogenic propellant tanks. Figure 4-33 shows the cold plate and heat pipe layout for this section. The electronics have three heat pipe runs from each cold plate to the radiator. The cryocooler has two heat pipe runs from each cold plate to the radiator. The heat pipes share the load from each cold plate. Each heat pipe from the cryocooler is sized to be capable of moving the total heat generated from the source to the radiator. Two of the three heat pipes for the electronics can handle the complete heat load on the cold plate. This provides a redundant heat transfer path for each engine.

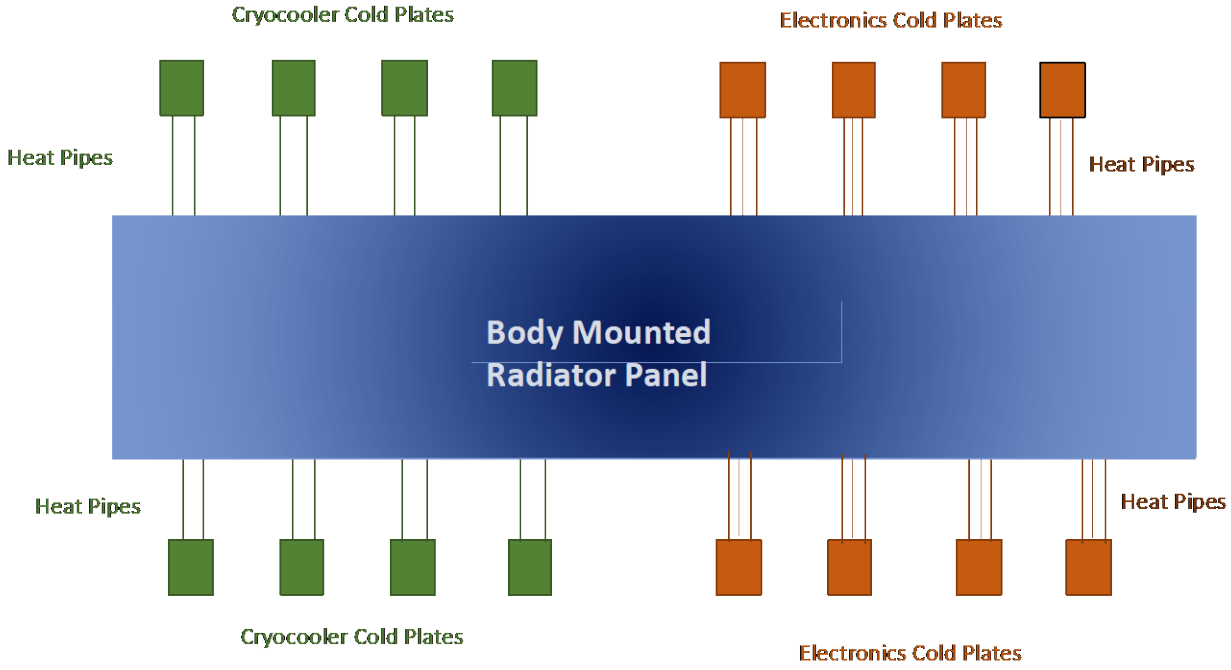

Figure 4-33 Chemical Stage Body Mounted Radiator Cold Plate and Heat Pipe Layout

Table 4-22 provides the cold plate details and size breakdown for each of the stages shown Figure 4-31 and Figure 4-32.

Table 4-22 Cold Plate Specifications

Variable	Value
Cooling Plate and Line Material	Aluminum
Cooling Plate and Line Material Density	2,770 kg/m^3
Number and size of the Cold Plates	NEP Module Electronics: 8 at 0.2 m X 0.2 m NEP Module Xenon Tank: 24 at 0.2 X 0.2 m NEP Module DDUs: 20 at 0.43 m X 0.43 m Xenon Interstage Electronics: 8 at 0.1 m X 0.1 m Chemical Stage Cryocoolers: 24 at 0.2 m X 0.2 m Chemical Stage Electronics: 8 at 0.2 m X 0.2 m
Cooling Plate Thickness	5 mm

4.3.11 Cryogenic Storage Thermal Control

The thermal control for the cryogenic system is a major aspect of the overall thermal design for the spacecraft. In order for the spacecraft to perform the mission of transit to Mars and then back to Earth, the cryogenic propellants must be stored and maintained at cryogenic temperatures. In-space cryogenic propellant storage is a fairly new technology that is still being developed. Although cryogenic fuels are commonly used with launch vehicles their use in space has been limited and long-term storage of cryogenics in space has not been previously accomplished. For launch vehicle applications the propellant is utilized quickly upon launch with no need for long term storage. The

propellant tanks are filled right before launch and a thin layer of foam insulation is used to help reduce the heat leak into the tank and minimize boil-off of the cryogenic propellant prior to launch.

4.3.12 Multi-Layer Insulation

In the vacuum of space radiation heat transfer is the main mechanism for heat leak into the tank from the surroundings. For long term use in space the propellant tanks must be more resistant to this heat leak and therefore utilized MLI as the main barrier to heat leak. MLI is constructed of a number of layers of metalized material with a nonconductive spacer between the layers. The metalized material has a low absorptivity which resists radiative heat transfer between the layers. MLI can be conformed to fit over various shapes. It can be held in place with Velcro or glue. Its construction is illustrated in Figure 4-34. For long duration space use the cryogenic tanks will need to be wrapped in MLI to minimize their heat flow from the surroundings. To insulate the propellant tanks MLI is used to cover the exterior of the propulsion section and the electronics bus enclosure.

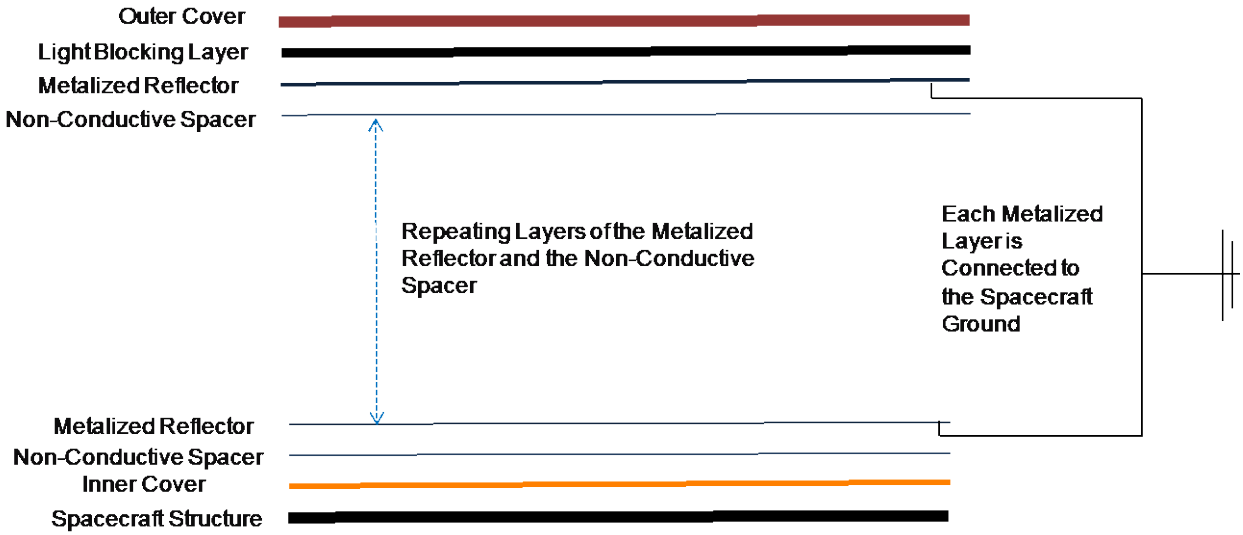

Figure 4-34 Illustration of MLI Construction Layout and Component Layers

The heat transfer through the MLI was analyzed to determine the required number of layers, their corresponding mass and the heat leak into the tanks. The insulation model was based on radiation heat transfer analysis of the heat transfer from the spacecraft through the insulation to space. Table 4-23 provides the MLI specifications.

Table 4-23 MLI Specifications

Variable	Value
Spacecraft MLI Material	Aluminum
Spacecraft MLI Material Aerial Density Outer Covering Inner Covering Spacer Reflective Layer Attachment & Seals Percentage	 0.11 kg/m^2 0.05 kg/m^2 0.0063 kg/m^2 0.055 kg/m^2 10%
MLI Thickness	2 cm Propellant Tanks 1 cm Spacecraft Bus
Number of Insulation Layers	25 Spacecraft Electronics Bus & Xenon Tanks 35 Cryogenic Propellant Tanks
MLI Layer Spacing	0.2 mm

The type of MLI utilized to insulate the tanks is based on a new design approach that limits seam and joint losses and also allows for the integration of Micrometeoroid and Orbital Debris (MMOD) with the MLI insulation layers. This insulation is termed integrated MLI or IMLI.

Integrated MLI utilizes discrete spacers to improve the thermal performance over traditional MLI layer structures. IMLI had initially been under development through a small business innovative research (SBIR) program by the Quest thermal group [31] [32] [33]. Projected advantages of IMLI over traditional MLI Include:

- Better performance over traditional MLI by up to 27%.
- Fewer layers required for the same heat leak compared to traditional MLI.
- More consistent and predictable performance from installation to installation.
- Ability to be installed onto a large cryogenic tank in panels.
- Effective of the thermal conductivity of the IMLI is 0.069 mW/m-K
- Thickest IMLI blanket tested to date was 20 layers thick.

IMLI can be integrated with micro-meteor protection. The structural capabilities of IMLI are utilized to support the layers of ballistic material (Kevlar® and Nextel®) used in MMOD shielding. This reduces the mass of the MMOD shielding. Effective thermal conductivity of the MMOD-IMLI is estimated to be 0.117 mW/m-K.

Another benefit of the IMLI is that it can be designed to bare external loads without compromising the insulation performance. This load-bearing (LB)-MLI eliminates the need for structural supports that pass through the MLI to hold the barrier shield. IMLI is currently under development and has been tested to a TRL of 5. The advantages of LB-MLI include:

- The support of the broad area cooling shield without the need for structural standoffs that would need to pass through the insulation.
- Reduces the heat flux by up to 56% over traditional MLI
- Low mass of 0.07 kg/m^2/layer
- Recent LB-MLI calorimeter testing indicated heat fluxes ~ 0.1 W/m^2 between 20 and 90 K at similar layer numbers.

The cryogenic propellants, liquid oxygen and liquid methane, are held in conformal nested tanks. The nested cryogenic propellant tank is broken into two segments the liquid oxygen section held at 90 K and the liquid methane section which was maintained at an average temperature of ~100 K. Figure 4-35 illustrates this arrangement.

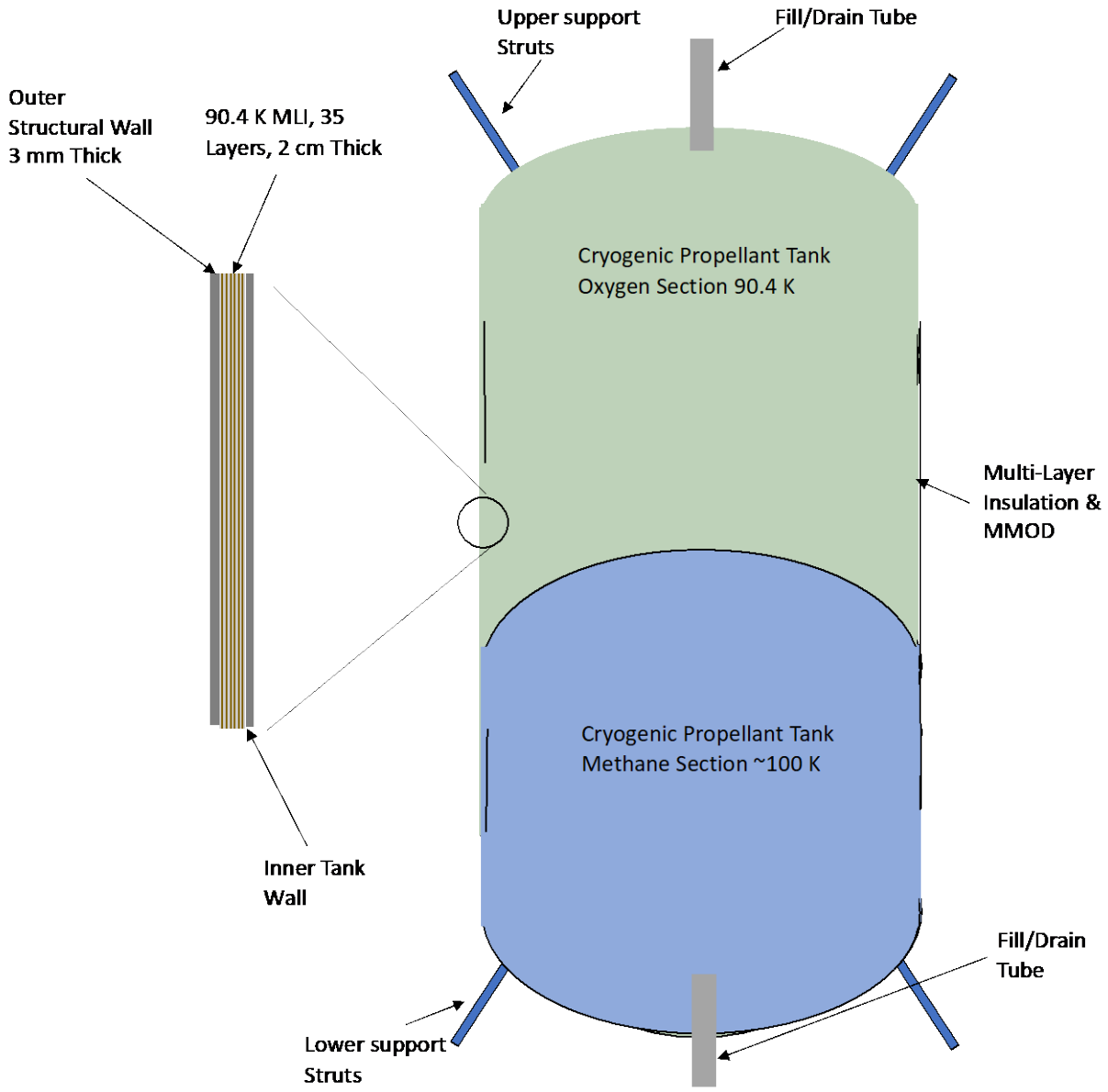

Figure 4-35 Nested Cryogenic Tank Layout

4.3.13 Cryocooler

The heat leak into the tanks must be removed to maintain the propellant in its cryogenic state. This heat removal is accomplished through the broad area cooling system. The broad area cooling system consists of a cryocoolers and a coolant loop that surrounds the tanks. The cryocoolers cool down helium gas to the desired operating temperature of the tank. A pump is used to pump this coolant through tubes that surround the tank. Figure 4-36 illustrates this system.

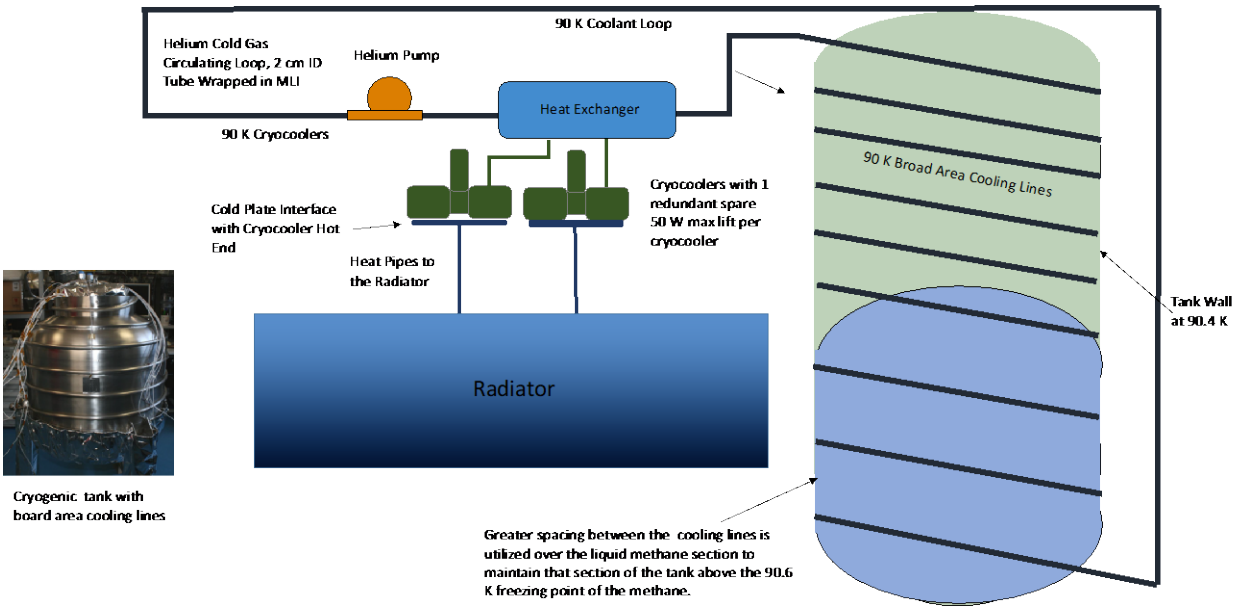

Figure 4-36 Illustration of the Cryogenic Tank Broad Area Cooling System

The amount of heat that the cryocoolers need to extract from the tank is based on the heat leak into the tank from the surroundings. The heat leak into the tank is in turn based on the average sink temperature that the tank will operate in and the heat paths into the tank. In addition to heat leak through the insulation itself and its installation there are some physical connections to the tank that are necessary for both the operation of the tank and structurally to hold the tank under the various loads experienced during the mission. These components provide a direct heat path from the outside environment which is nominally at the sink temperature to the tank itself which is at the cryogenic temperatures. Table 4-24 lists these items. To minimize the heat leak through these components a number of approaches can be taken. Utilizing low thermal conductivity materials is the first step in minimizing heat leak. Also insulating the pass-through component and utilizing as long a path length as possible will also help minimize the heat leak.

Table 4-24 Heat Leak Paths for the Cryogenic Tank and Their Specifications

Component	Specification
Fill Tubes: Titanium Alloy (Ti-6Al-4V), thermal conductivity 6.7 W/m K	2 at 10 cm OD 2 mm wall thickness, 1.0 m insulated length
Structural Supports: Material S-Glass Composite, thermal conductivity 0.75 W/mK	11 at 20.3 cm OD, 19.2 mm wall thickness, 1.0 m insulated length
MLI Layers	35 on the Tank
Internal Temperature:	LOX, 90.4 K
Tank Dimensions	Tank: 5.0 m Diameter, 10.4 m Length 6.15 m Barrel Section Length
Emissivity per inner layer: Effective emissivity including passthrough joint heat losses:	0.035 0.046

The heat leak paths given in Table 4-24 are also shown in Figure 4-36.

The heat leak through fill tubes and the structural supports is based on standard conduction along the length of those components. The MLI heat leak is broken into two separate components, the direct heat leak through the insulation, and the heat leak through the seams, joints and around the passthroughs that penetrate the insulation. The heat leak in the vicinity of the seams where the insulation panels are joined together can be significant. Data from Cassini spacecraft, shown in Figure 4-37, shows a significant increase in heat loss near the seams of the MLI used to

insulate the spacecraft. This data showed a heat loss increase 15 times greater near the seams then through the bulk insulation. This data was for a temperature difference of 206 K. This temperature difference is on the order of what would be expected for the liquid oxygen tanks in this mission.

However, the newly developed IMLI has a much lower heat loss due to seams due to its method of manufacturing and installation. Therefore, the heat conduction losses through the insulation utilized the values provided by the IMLI and LB-MLI which included seam losses.

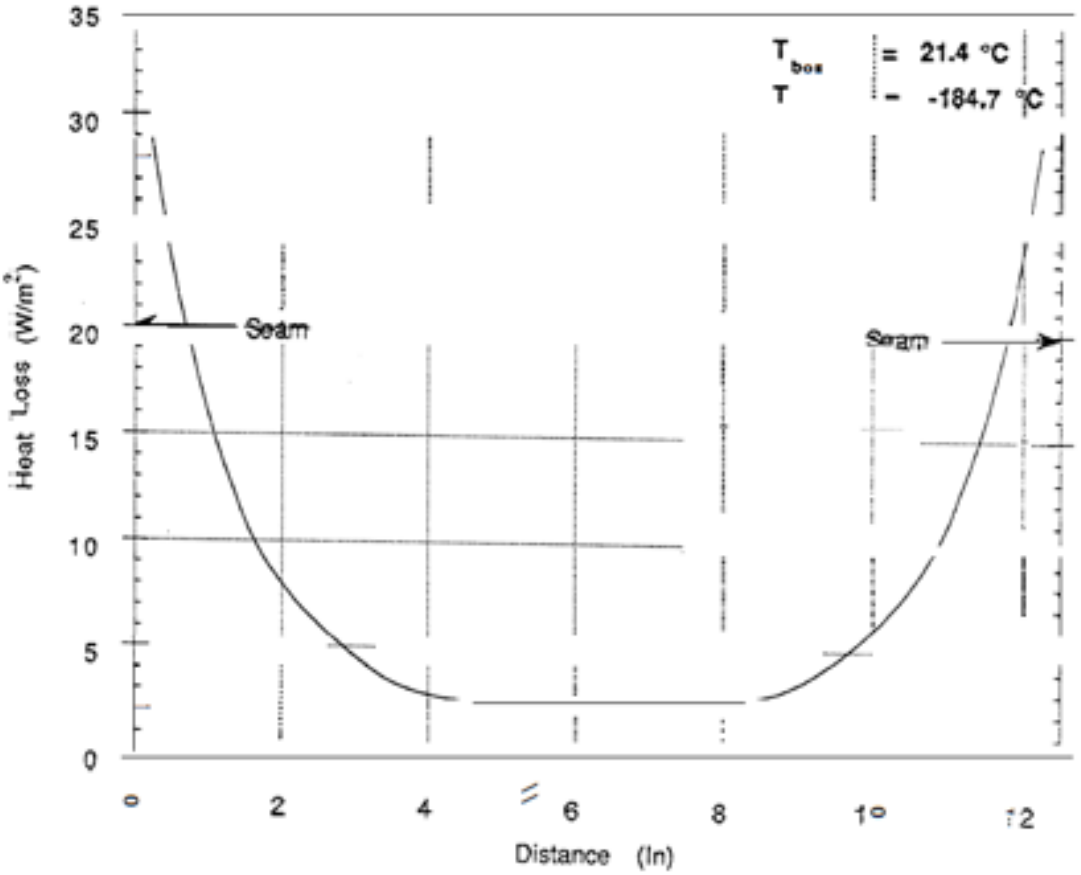

Figure 4-37 Example of MLI Seam Heat Leak from the Cassini Spacecraft

The heat leak into the tank using the estimates for the IMLI and from each source is listed in Table 4-25 for operation near Venus with a sink temperature of 255.8 K. This is the worst-case operating location for the mission. Therefore, this is used to determine the heat leak into the propellant tank that the broad area cooling system has to be capable of removing.

Table 4-25 Propellant Tank Heat Leak Summary for Operation Near Venus

Heat Leak Path	90 K Section
Fill Tubes	1.4 W
Structural Supports	15.1 W
MLI (Note: includes passthrough joints, no seam losses)	24.8 W
Total (heat to be removed by cryocoolers)	41.3 W

Cryocoolers are used to remove the waste heat given in Table 4-25 as illustrated in Figure 4-36. The number of cryocoolers required is based on the lift or heat removal capability achievable per cryocooler system. The cryocooler specifications are listed in Table 4-26 to meet the total heat removal requirements listed in Table 4-25.

Table 4-26 Cryocooler Specifications

Cryocooler Specifications	90 K
Electrical to Cooling Power Ratio	8.2 We/Wc
Specific Mass	0.81 kg/Wc
Cooling Lift per Cryocooler	50 W
Cryocooler Mass	40.5 kg
Required Heat Removal (worst case)	41.31 W
Number of Cryocoolers required	2 (1 + 1 Redundant)
Total Cryocooler Power Required	338.8 W

The cryocooler power will vary throughout the mission with the operation near Venus being the highest. Since operation near Venus is the worst-case operating conditions the cryocooler system was designed to operate at this location.

4.3.14 Master Equipment List

Table 4-27 Thermal Control (Non-Propellant) NEP Module MEL

Description Case 3_SLS_Chem NEP_Chem_Vehicle_Family CD-2020-181	QTY	Unit Mass	Basic Mass	Growth	Growth	Total Mass
Thermal Control (Non-Propellant)			**1192.4**	**18%**	**214.6**	**1407.0**
Active Thermal Control			**2.2**	**18%**	**0.4**	**2.6**
Heaters	8	0.1	0.4	18%	0.1	0.5
Thermal Control	2	0.2	0.4	18%	0.1	0.5
Thermocouples	8	0.0	0.1	18%	0.0	0.1
Data Acquisition	2	0.3	0.5	18%	0.1	0.6
Switches	8	0.1	0.8	18%	0.1	0.9
Passive Thermal Control			**812.0**	**18%**	**146.2**	**958.1**
Electronics Radiator	1	43.9	43.9	18%	7.9	51.9
DDU & Electronics Cold Plate	28	0.6	16.8	18%	3.0	19.8
DDU & Electronics Heat Pipe	56	2.7	149.5	18%	26.9	176.4
MLI	1	114.2	114.2	18%	20.6	134.7
DDU Radiator	1	339.1	339.1	18%	61.0	400.1
thermal paint	1	1.2	1.2	18%	0.2	1.5
Xenon Tank Cold Plates	24	0.6	13.2	18%	2.4	15.6
Filter	2	0.4	0.8	18%	0.1	0.9
Accumulator	2	4.0	8.0	18%	1.4	9.4
Flow Sensor	6	0.3	1.8	18%	0.3	2.1
Temperature Sensor	8	0.0	0.1	18%	0.0	0.1
Pressure Sensor	7	0.1	0.7	18%	0.1	0.8
Coolant Lines	1	21.1	21.1	18%	3.8	24.8
Coolant	1	101.6	101.6	18%	18.3	119.9
Semi-Passive Thermal Control			**378.2**	**18%**	**68.1**	**446.3**
Diverter Valve	2	1.0	2.0	18%	0.4	2.4
Check Valve	7	0.3	2.1	18%	0.4	2.5
Coolant Pump	4	5.0	20.0	18%	3.6	23.6
Vent Valve	2	0.1	0.2	18%	0.0	0.2
Liquid to Heat Pipe Manifold	40	2.6	102.4	18%	18.4	120.9
Xenon Tanks Insulation	1	221.1	221.1	18%	39.8	260.9
Xenon Tanks Radiator	1	30.4	30.4	18%	5.5	35.9

Table 4-28 Thermal Control (Non-Propellant) Xenon Interstage MEL

Description Case 3_SLS_Chem NEP_Chem_Vehicle_Family CD-2020-181	QTY	Unit Mass	Basic Mass	Growth	Growth	Total Mass
Thermal Control (Non-Propellant)			**705.4**	**18%**	**127.0**	**832.4**
Active Thermal Control			**14.2**	**18%**	**2.6**	**16.7**
Heaters	8	0.1	0.4	18%	0.1	0.5
Thermal Control	2	0.2	0.4	18%	0.1	0.5
Thermocouples	8	0.0	0.1	18%	0.0	0.1
Data Acquisition	2	0.3	0.5	18%	0.1	0.6
Switches	8	0.1	0.8	18%	0.1	0.9
Servo Valves	24	0.5	12.0	18%	2.2	14.2
Passive Thermal Control			**178.9**	**18%**	**32.2**	**211.1**
Stage MLI	1	84.2	84.2	18%	15.2	99.4
Electronics Radiator	1	22.0	22.0	18%	4.0	26.0
Electronics Cold Plate	8	0.1	1.1	18%	0.2	1.3
Electronics Heat Pipe	16	2.6	41.6	18%	7.5	49.1
Bulkehead MLI	2	15.0	29.9	18%	5.4	35.3
Semi-Passive Thermal Control (cruise deck and internal)			**512.3**	**18%**	**92.2**	**604.6**
Xenon Tanks Insulation	1	512.3	512.3	18%	92.2	604.6

Table 4-29 Thermal Control (Non-Propellant) Chemical Stage MEL

Description Case 3_SLS_Chem NEP_Chem_Vehicle_Family CD-2020-181	QTY	Unit Mass	Basic Mass	Growth	Growth	Total Mass
Thermal Control (Non-Propellant)			**869.4**	**18%**	**156.5**	**1025.9**
Active Thermal Control			**2.2**	**18%**	**0.4**	**2.6**
Heaters	8	0.1	0.4	18%	0.1	0.5
Thermal Controller	2	0.2	0.4	18%	0.1	0.5
Data Acquisition	2	0.3	0.5	18%	0.1	0.6
Thermocouples	8	0.0	0.1	18%	0.0	0.1
Switches	8	0.1	0.8	18%	0.1	0.9
Passive Thermal Control			**867.2**	**18%**	**156.1**	**1023.3**
L-Methane MLI	1	170.4	170.4	18%	30.7	201.0
LOX MLI	1	444.7	444.7	18%	80.0	524.7
Electronics Radiator	1	50.0	50.0	18%	9.0	59.0
Electronics Cold Plate	8	0.6	4.4	18%	0.8	5.2
Electronics Heat Pipe	16	1.9	30.6	18%	5.5	36.1
Propellant Line MLI	4	0.7	2.7	18%	0.5	3.2
Cryocooler Radiator	1	43.9	43.9	18%	7.9	51.9
LOX Cryocooler	2	44.4	88.8	18%	16.0	104.8
cryocooler Heat Pipes	16	1.6	25.0	18%	4.5	29.5
Cryocooler Cold Plates	8	0.6	4.4	18%	0.8	5.2
electronics MLI	1	2.4	2.4	18%	0.4	2.8

4.4 Structures and Mechanisms

The NEP-Chem 1.2 design structures must contain the necessary hardware for avionics, command and data handling, thermal systems, propulsion, and electrical power. The structural components must be able to withstand applied mechanical and thermal loads. In addition, the structures must provide minimum mass and deflections, sufficient stiffness, and vibration damping. The operational loads include an approximate maximum axial acceleration of -5.5 g along with a 2.0 g lateral acceleration from the launch vehicle. One potential launch vehicle, NASA's SLS (2018), also needs the payload cantilevered fundamental mode frequency to have a minimum of 8 Hz lateral and 15 Hz axial.

Mechanisms are used to setup up the various systems into an operational condition. Mechanisms are used to separate from hardware that is no longer necessary for the mission and to deploy other hardware to initiate parts of other systems.

Figure 4-38 illustrates the overall spacecraft with deployed power system boom, deployed radiators, and thruster booms. This study focused on the Transportation Vehicle Stack.

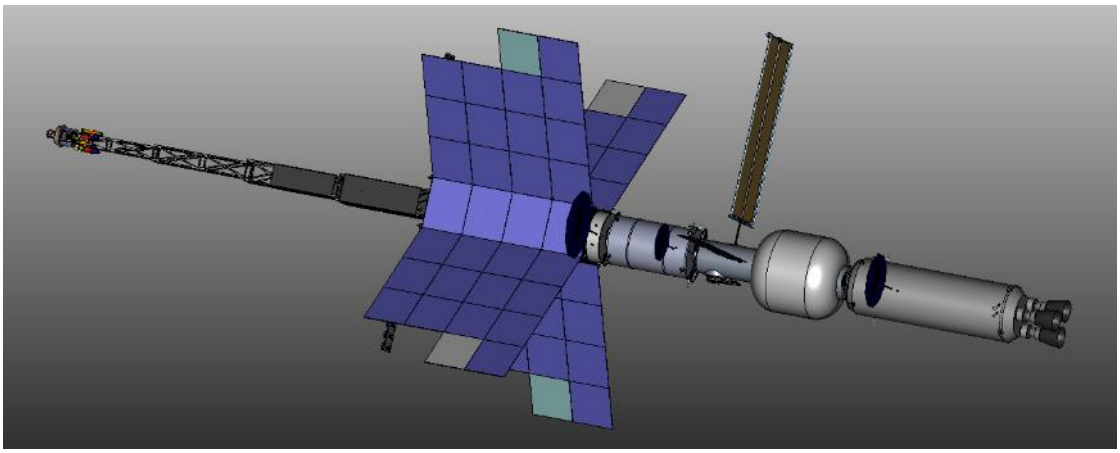

Figure 4-38 NEP Spacecraft with the NEP Module, Xenon Interstage, Habitat and Chemical Stage

4.4.1 System Requirements

The bus is to support the mounted hardware bearing launch and operational mechanical and thermal loads without failure. The structures shall not degrade for the extent of the mission in the Earth, Mars, and deep space environments.

4.4.2 System Assumptions

The bus provides the backbone for the mounted hardware. The primary materials for the bus are carbon/cyanate ester composite, aluminum, and glass/epoxy composite. The carbon/cyanate ester composite, M55J 6k/954-3 as described by Department of Defense MIL-HDBK-17F (2002), is used in a composite sandwich structure with aluminum honeycomb. The aluminum alloy is 7075 T73 as described in the Federal Aviation Administration's Metallic Materials Properties Development and Standardization (MMPDS-14) (2019). The glass/epoxy composite, S2-449 43.5k/SP 381 as described by Department of Defense MIL-HDBK-17 (2002), is used in wound tubes of struts. The materials are at a Technology Readiness Level of 6 (TRL6) as presented by Mankins (1995). Components are of shells and tubular members. Joining of components is by threaded fasteners, riveting, or bonding.

Secondary structures include decks to support internal hardware and decks to support thrusters. Other secondary structures are the components for installation hardware.

Mechanisms include the passive and active sides of International Docking System Standard (IDSS) docking mechanisms. The deployable boom of the NEP Module has a screw drive deployment mechanism. There is a hinge for each solar array boom. Each EP thruster boom has a locking spring loaded hinge and a gimbal. There is a gimbal for each EP thruster deck.

4.4.3 System Trades

The Transportation Vehicle Stack design was derived from an earlier Compass design for a NEP Kuiper Belt Object Orbiter (KBOO). The NEP-KBOO bus used an aluminum cylinder. The bus material was changed to a composite sandwich structure using carbon/cyanate ester face sheets and an aluminum honeycomb core. The composite architecture is thought to provide greater resistance to buckling without a significant mass penalty with the anticipated increased mass for the spacecraft.

4.4.4 Analytical Methods

Analytical methods were by hand calculations and spreadsheet to conduct preliminary stress analysis. In addition, a quick finite element analysis (FEA) was conducted on a simple model of the main structural components with smaller components being represented by concentrated masses. The FEA model utilized the study's computer aided design (CAD) model.

4.4.5 Risk Inputs

A potential risk for the structural system may be excessive g loads or impact from operational loads or a foreign object which may cause too much deformation, vibrations, or fracture of sections of the support structure. Consequences include lower performance from mounted hardware to loss of mission.

The likelihood is a medium ranking of three. Consequences may be relatively high with a ranking of four for cost, schedule, and performance. Safety may also be at ranking of four.

For risk mitigation the structure is to be designed to NASA standards to withstand expected g loads, a given impact, and to have sufficient stiffness and damping to minimize issues with vibrations. Trajectories and operations are to be planned to minimize the probability of impact with foreign objects and to minimize excessive loads.

4.4.6 System Design

The main bus material is a carbon fiber reinforced cyanate ester, M55J 6k/954-3, used in a composite sandwich structure with an aluminum honeycomb core. Lamina properties are from the Department of Defense MIL-HDBK-17F (2002) [34]. Ply thickness is 61 μm (0.0024 in.). The ultimate strength is 2.23 giga Pascal (GPa) (324 kips per square inch [ksi]) and the Young's modulus is 329 GPa (47.7 x 10^6 psi) from the Department of Defense handbook [34]. The final laminated composite uses a quasi-isotropic layup of $[-45/0/45/90]_S$ with resulting properties of 116 GPa (16.8 x 10^6 psi) for the Young's modulus in the axial and lateral directions and a failure stress of 330 mega Pascal (MPa) (47.8 ksi) with the Tsai-Hill failure theory, as described by Agarwal and Broutman [35]. Collier Research Corporation's HyperSizer® [36] was utilized for determining the laminated composite properties. A safety factor of 2.0 is applied to the failure stress, per NASA-STD-5001B [37], for a resulting allowable stress of 165 MPa (23.9 ksi). The M55J 6k/954-3 composite density is 1.65 g/cm³ (0.060 lb/in.³).

The deployable boom material is aluminum 7075-T6. Per the Metallic Materials Properties Development and Standardization (MMPDS) [38] the ultimate strength is 510 MPa (74 ksi) and the yield strength is 462 MPa (67 ksi). Applying safety factors of 1.4 on the ultimate strength and 1.25 on the yield strength and selecting the lower value, as per NASA Standard 5001b (2016), results in an allowable stress of 370 MPa (54 ksi) at room temperature. The Young's modulus is 71.7 GPa (10.4 x 10^6 psi) and the density is 2.80 g/cm^3 (0.101 lb/in.^{3}).

The tank supports within the Chemical Propulsion Element consist of struts with tubes of a glass fiber reinforced epoxy, S2-449 43.5k/SP 381. Lamina properties are from the Department of Defense MIL-HDBK-17F [34] Ply thickness is 89 μm (0.0035 in). The ultimate strength is 1.70 GPa (246 ksi) and the Young's modulus is 47.6 GPa (6.91 x 10^6 psi) from the Department of Defense MIL-HDBK-17F [34]. The final laminated composite uses a layup of $[0/60/30/-30/-60/0]_{2S}$ with resulting properties of 29.2 GPa (4.24 x 10^6 psi) for the Young's modulus in the axial direction and 18.8 GPa (2.72 x 10^6 psi) in the lateral direction and a failure stress of 193 MPa (28.0 ksi) with the Tsai-Hill failure theory, as described by Agarwal and Broutman [35]. Collier Research Corporation's HyperSizer® [36] was utilized for determining the laminated composite properties. A safety factor of 2.0 is applied to the failure stress, per NASA-STD-5001B [37], for a resulting allowable stress of 96.5 MPa (14.0 ksi).

A preliminary stress calculation was performed on the various elements of the assembly. The components include bus cylinders, frustum, and deployable boom. The stress in the tank support struts of the Chem Stage Module was determined also.

The NEP Module bus cylinder has the mass of the top deck, deployable boom, Nuclear Power Module, and radiators to support during launch. It is assumed that the launching of the spacecraft provides the highest acceleration of the bus. The launch vehicle's assumed maximum axial acceleration is 5.5 g which results in a 2590 kilonewton (kN) (582000 lb) load on the bus cylinder. Assuming an equally distributed load on the bus circumference the stress is approximately 43 MPa (6.3 ksi). This provides a positive margin of 2.8. Due to the limited duration of the study and the limited information on the bus configuration initially the stress due to the small lateral acceleration was not determined with hand calculations.

The deployable boom in a stowed configuration on the NEP Module was evaluated with FEA using NASTRAN. As noted above, the launch phase of the mission provides the highest body load. As a result, the spacecraft in a stowed configuration was evaluated for this study. The FEA model was constructed of beam and concentrated mass elements to approximate its modal responses and approximate stress state during launch. Rigid, RBE2, elements were used to tie components together. Concentrated mass elements were used to represent xenon tanks and associated hardware, helium tanks and associated hardware, top deck, bottom deck, tank deck, IDSS, marman clamp

ring, thermal hardware, and the nuclear reactor assembly. Figure 4-39 illustrates the analysis model with key components and their materials identified. It is assumed that the load is shared among the boom sections while stowed. With an axial acceleration of 5.5 g and a lateral acceleration of 2.0 g the peak stress is 145 MPa (21.0 ksi). That provides a positive margin of 1.5 relative to the allowable stress of 364 MPa (52.9 ksi). The loaded NEP Module in a stowed configuration with its stress contour is shown in Figure 4-40.

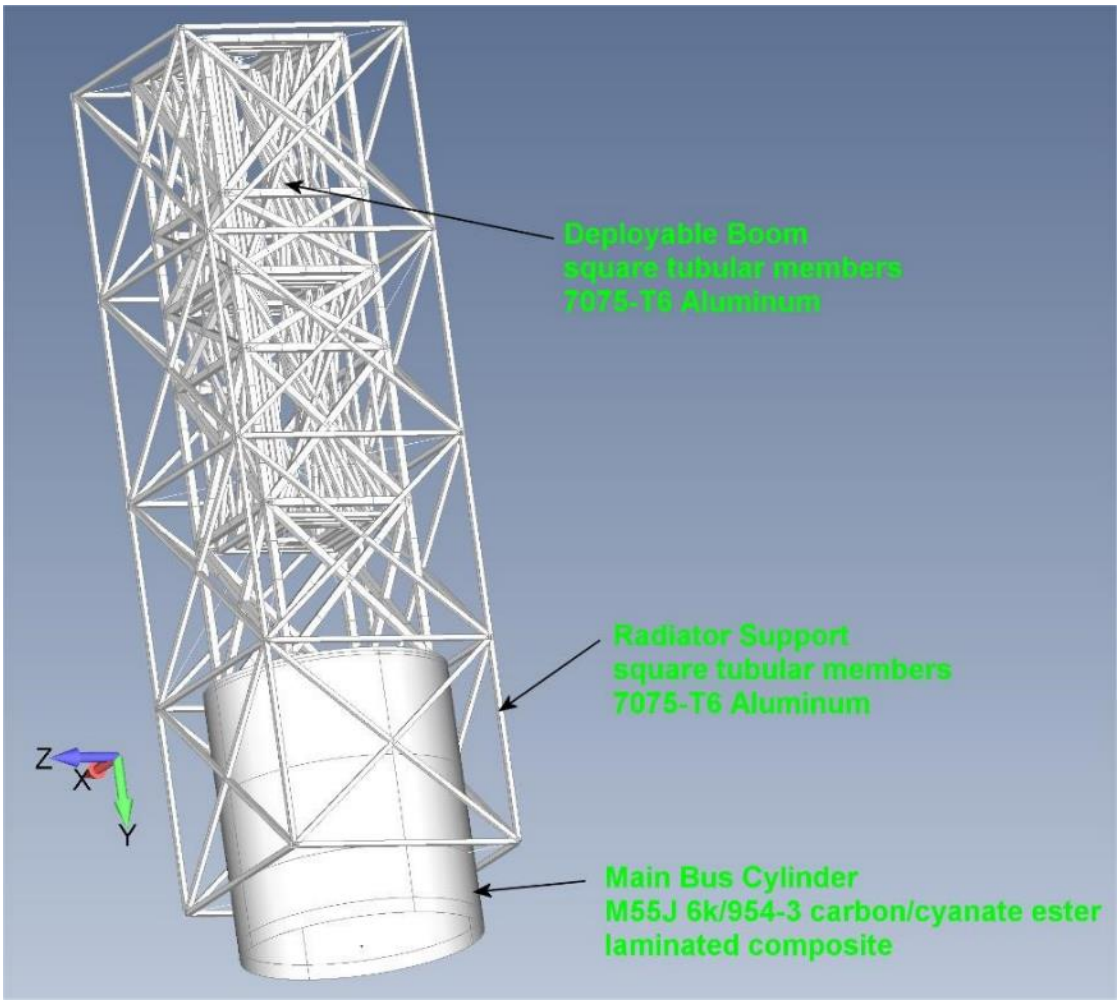

Figure 4-39 Meshed FEA Model with Key Components Identified Along with Their Materials

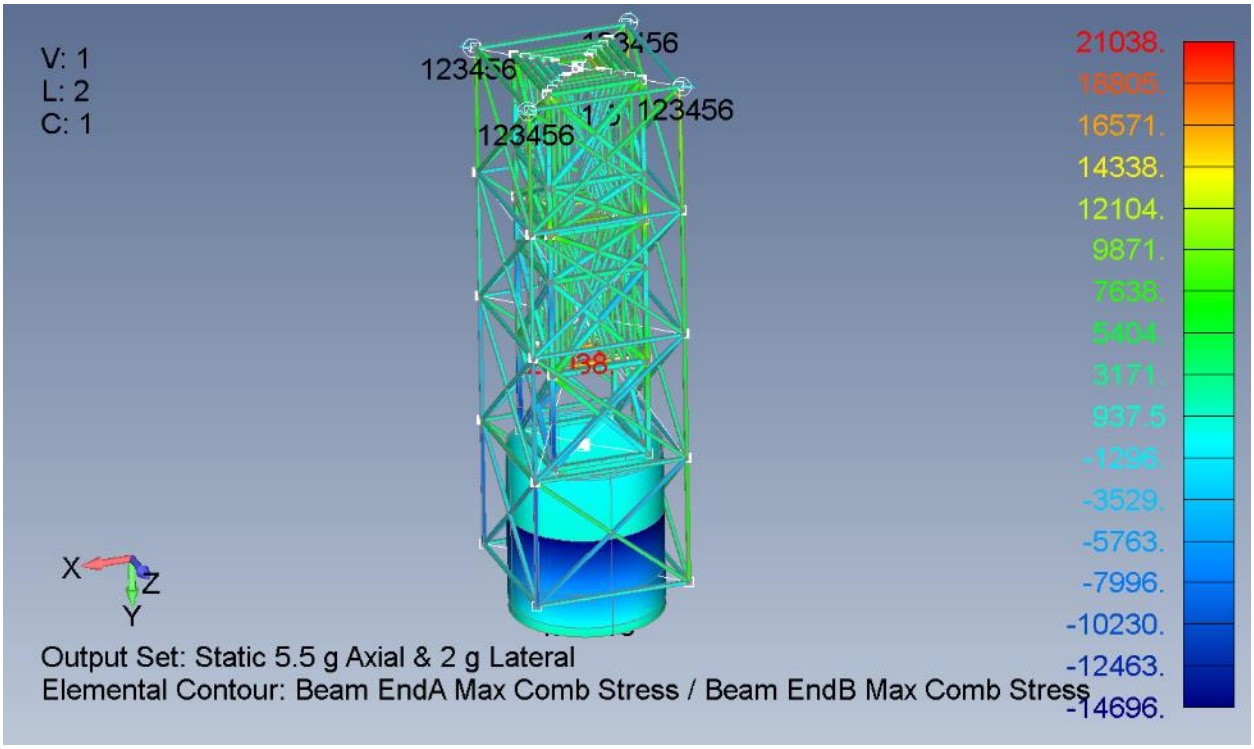

Figure 4-40 Stress Contour for the Stowed Deployable Boom of the NEP Module. A 5.5 g Axial and 2.0 g Lateral Acceleration is Applied to the Body. Stresses are in psi

The Chem Stage Module bus cylinder supports the upper deck, top frustum, and tanks with propellant. The resultant load is approximately 4400 kN (990000 lb) under launch conditions. The resulting stress in the bus cylinder is 64 MPa (9.3 ksi) with the assumption of an equally distributed load around the circumference. The margin is positive at 1.6.

The approximate stress state in the Chem Stage Module tank mounting struts was evaluated. Assuming an equal load distribution among the struts the axial load on each strut is 776 kN (174 kips) for the LOX tank. The resulting stress in the strut tube is 69.9 MPa (10.1 ksi). The margin is positive at 4.2.

The bus cylinder and the thruster booms were evaluated for the Electric Propulsion Element. The bus cylinder is subject to a load of 70000 kg (154000 lb) under a 5.5 g axial acceleration. The resulting stress is 55 MPa (7.9 ksi) which has a positive margin of 2.0.

The thruster boom was evaluated under two separate load cases. One case is during a chemical rocket operation and another case is with electric propulsion. The booms are evaluated in a deployed state. Chemical rocket operation accelerates the spacecraft with a maximum of 0.1 g in the axial direction. With a 5000 kg (2300 lb) thruster pallet at the end of each boom the resulting stress in the boom is 5.6 GPa (805 ksi) with a margin of -0.93. Electric propulsion places a force of 0.043 N (0.010 lb) at the end of the thruster boom. The resulting boom stress is 0.1 MPa (14 psi) with a large margin of 3800.

Modal results from FEA and the NEP Module deployable boom model were generated. The boom is in a stowed configuration. The first bending mode is at 2.5 Hz and it is illustrated Figure 4-41. In an attempt to emulate additional support from a strongback or a launch vehicle fairing spring elements were attached to the top of the stowed power boom model. Spring stiffness was set to 1750 N/mm (10000 lb/in.). The additional beam support raised the first bending modal frequency to 8.3 Hz. The supported stowed boom first bending modal frequency is illustrated in Figure 4-43.

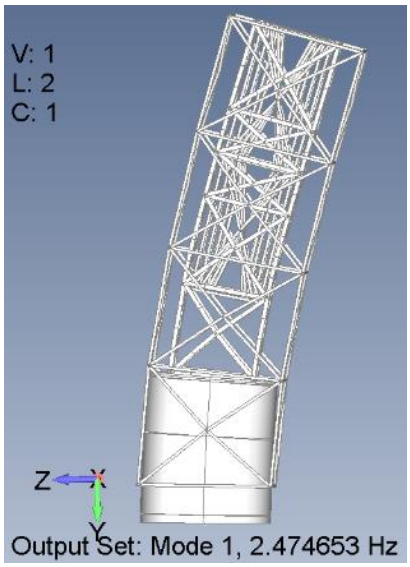

Figure 4-41 First Bending Modal Frequency of 2.47 Hz for the NEP Module in a Stowed Configuration with the Deployable Boom

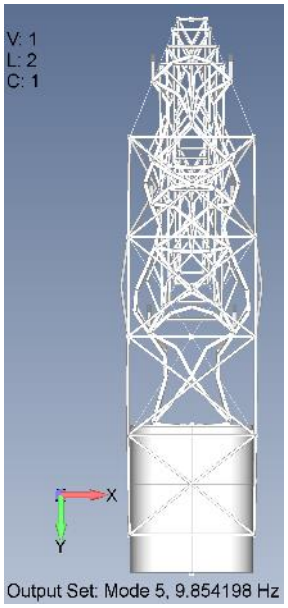

Figure 4-42 First Axial Modal Frequency at 9.85 Hz for the NEP Module in a Stowed Configuration

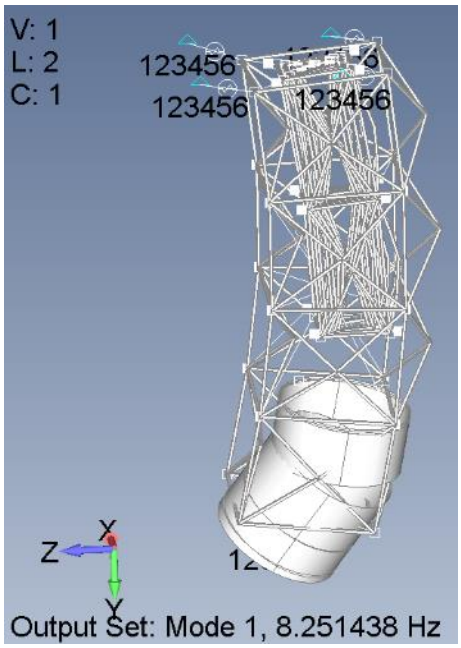

Figure 4-43 First Bending Modal Frequency of 8.3 Hz for the NEP Module in a Stowed Configuration with the Deployable Boom. Support Provided at Top of Boom to Simulate Effects of an External Support Structure, i.e., Strongback or Fairing

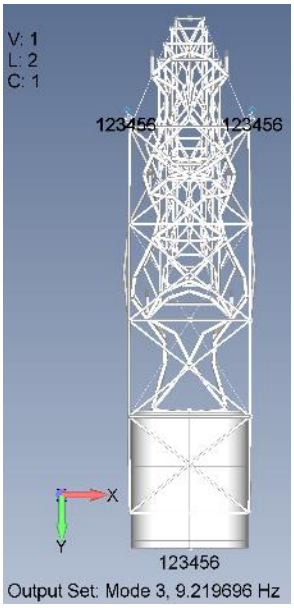

Figure 4-44 First Axial Modal Frequency of 9.2 Hz for the NEP Module in a Stowed Configuration with the Deployable Boom. Support Provided at Top of Boom to Simulate Effects of an External Support Structure, i.e., Strongback or Fairing

Due to the limited duration of the study and the limited information on the mechanical characteristics of some of the major components, i.e., solar arrays and other hardware, the deployed configuration of elements and the assembled stack were not evaluated. As noted earlier, the launch phase provides some of the highest loads with required minimum modal frequencies and as a result, the study's limited time for analysis was allocated to that phase.

Installation hardware is calculated as 4% of the installed hardware mass. Heineman [39] has shown that past space craft have shown that the 4% is a good approximation for the mass. The 4% installation hardware mass was applied to the command and data handling; communication and tracking; guidance, navigation, and control; electrical power; thermal control; and propulsion systems.

Mechanisms are used for the spacecraft. All the elements have solar array boom hinges and IDSS docking mechanisms. The NEP Module has a boom deployment mechanism utilizing motors and a screw drive, along with thruster boom gimbals and thruster pallet gimbals.

4.4.7 Recommendation(s)

The NEP Module boom needs to be supported while in a stowed position on the launch vehicle to achieve a desirable first bending modal frequency greater than 8 Hz. A stiffer boom and bus assembly for the NEP module may be needed to enhance the first axial modal frequency.

The Xenon Interstage thruster boom needs to be in a stowed position during operation of the chemical rockets. Alternately, the thruster boom may use bracing by cables.

4.4.8 Master Equipment List

Table 4-30 Structures and Mechanisms NEP Module MEL

Description Case 3_SLS_Chem NEP_Chem_Vehicle_Family CD-2020-181	QTY	Unit Mass	Basic Mass	Growth	Growth	Total Mass
Structures and Mechanisms			**6506.9**	**17%**	**1131.7**	**7638.6**
Structures			**5670.6**	**18%**	**1020.7**	**6691.3**
Primary Structures			4723.2	18%	850.2	5573.3
bus cylinder w/decks	1	1153.4	1153.4	18%	207.6	1361.0
radiator truss	1	305.5	305.5	18%	55.0	360.5
extendable boom	1	3264.3	3264.3	18%	587.6	3851.8
Secondary Structures			947.4	18%	170.5	1118.0
solar array boom	1	5.0	5.0	18%	0.9	5.9
solar array boom tie down	1	2.4	2.4	18%	0.4	2.8
graphite sheet covering	1	168.0	168.0	18%	30.2	198.3
thruster boom assy.	2	151.2	302.3	18%	54.4	356.7
thruster deck	2	213.8	427.7	18%	77.0	504.7
Thruster Support/Standoff	48	0.1	3.8	18%	0.7	4.5
Thruster Boom Cable	2	19.1	38.3	18%	6.9	45.1
Mechanisms			**836.3**	**13%**	**111.0**	**947.3**
Power System Mechanisms			55.8	18%	10.0	65.8
extendable boom deploy motor	2	27.2	54.4	18%	9.8	64.2
solar array boom hinge	2	0.7	1.4	18%	0.2	1.6
Adaptors and Separation			327.9	6%	19.5	347.4
Intermodule Support	1	55.6	55.6	18%	10.0	65.6
IDSS Docking Mechanism Passive	1	245.0	245.0	2%	4.9	249.9
Thruster Boom Gimbal	2	2.7	5.5	18%	1.0	6.4
Thruster Deck Gimbal	2	10.0	20.0	18%	3.6	23.6
Thruster Boom Spring/Lock Hinge	2	0.9	1.8	0%	0.0	1.8
Installations			452.6	18%	81.5	534.1
C&DH Installation	1	3.2	3.2	18%	0.6	3.7
Electrical Power Installation	1	10.0	10.0	18%	1.8	11.8
Thermal Control Installation	1	47.7	47.7	18%	8.6	56.3
GN&C Installation	1	2.9	2.9	18%	0.5	3.4
EP Propulsion Installation	1	371.8	371.8	18%	66.9	438.7
Chemical Propulsion Installation	1	17.1	17.1	18%	3.1	20.2

Table 4-31 Structures and Mechanisms Interstage MEL

Description Case 3_SLS_Chem NEP_Chem_Vehicle_Family CD-2020-181	QTY	Unit Mass	Basic Mass	Growth	Growth	Total Mass
Structures and Mechanisms			**2527.2**	**14%**	**359.7**	**2886.9**
Structures			**1580.0**	**18%**	**284.4**	**1864.4**
Primary Structures			1042.0	18%	187.6	1229.5
Main Cylinder	1	1042.0	1042.0	18%	187.6	1229.5
Secondary Structures			538.0	18%	96.8	634.9
Xenon Tank Deck	2	123.5	246.9	18%	44.4	291.4
Bottom Deck	1	283.5	283.5	18%	51.0	334.6
Solar Array Boom	1	3.6	3.6	18%	0.7	4.3
Solar Array Boom Base	1	2.4	2.4	18%	0.4	2.8
Solar Array Boom Tie Down	1	1.5	1.5	18%	0.3	1.8
Mechanisms			**947.2**	**8%**	**75.3**	**1022.5**
Power System Mechanisms			1.4	18%	0.2	1.6
solar array boom hinge	2	0.7	1.4	18%	0.2	1.6
Adaptors and Separation			658.0	4%	23.2	681.3
IDSS Docking Mechanism Active	1	350.0	350.0	2%	7.0	357.0
IDSS Docking Mechanism Passive	1	245.0	245.0	2%	4.9	249.9
Intermodule Support	1	63.0	63.0	18%	11.3	74.4
Installations			287.8	18%	51.8	339.6
C&DH installation	1	1.9	1.9	18%	0.3	2.3
GN&C installation	1	4.1	4.1	18%	0.7	4.8
Electrical Power installation	1	9.4	9.4	18%	1.7	11.1
Thermal Control installation	1	28.2	28.2	18%	5.1	33.3
Propulsion (Chem) installation	1	16.0	16.0	18%	2.9	18.8
Therrmal Control Installation	1	28.2	28.2	18%	5.1	33.3
EP Propulsion Installation	1	200.0	200.0	18%	36.0	236.0

Table 4-32 Structures and Mechanisms Chemical Stage MEL

Description Case 3_SLS_Chem NEP_Chem_Vehicle_Family CD-2020-181	QTY	Unit Mass	Basic Mass	Growth	Growth	Total Mass
Structures and Mechanisms			**4015.0**	**17%**	**666.7**	**4681.7**
Structures			**3204.1**	**18%**	**576.7**	**3780.9**
Primary Structures			2144.5	18%	**386.0**	**2530.5**
Bus, Cylinder	1	1917.8	1917.8	18%	345.2	2263.0
Top Frustum	1	108.2	108.2	18%	19.5	127.7
Bottom Frustum	1	118.5	118.5	18%	21.3	139.8
Secondary Structures			1059.6	18%	**190.7**	**1250.4**
Top Deck	1	265.9	265.9	18%	47.9	313.8
Bottom Deck	1	251.4	251.4	18%	45.2	296.6
Solar Array Boom	1	4.7	4.7	18%	0.9	5.6
LOX Tank Support Struts	6	54.8	329.0	18%	59.2	388.2
LCH4 Tank Support Struts	6	34.5	207.1	18%	37.3	244.4
Solar Array Boom Tie Down	1	1.6	1.6	18%	0.3	1.8
Mechanisms			**810.9**	**11%**	**90.0**	**900.9**
Power System Mechanisms			0.7	18%	**0.1**	**0.8**
Solar Array Boom Hinge	1	0.7	0.7	18%	0.1	0.8
Adaptors and Separation			350.0	2%	**7.0**	**357.0**
IDSS Docking Mechanism Active	1	350.0	350.0	2%	7.0	357.0
Installations			460.2	18%	**82.8**	**543.1**
GN&C Installation	1	2.9	2.9	18%	0.5	3.5
Command and Data Handling Installation	1	2.0	2.0	18%	0.4	2.3
Electrical Power Installation	1	14.4	14.4	18%	2.6	17.0
Therrmal Control Installation	1	34.8	34.8	18%	6.3	41.0
Chemical Propulsion Installation	1	406.1	406.1	18%	73.1	479.2

4.5 Attitude Determination & Control

The AD&C subsystem is responsible for assessing the performance of selected attitude effectors for the individual elements as well as for the stack. Additionally, the AD&C subsystem specifies the navigation sensors and hardware required for each element to perform all relevant aspects of the mission.

4.5.1 System Requirements

The AD&C subsystem has the following system requirements:

- Single Fault Tolerance for all hardware components. The strategy employed is to have multiple independent instances of the same navigation hardware.
- Maintain pointing knowledge at “optical bench” to within 0.5 deg/axis (ISS derived)
- Maintain rate knowledge at “optical bench” to within 0.01 deg/s/axis (ISS derived)
- Control rates to within 0.02 deg/s/axis of commanded rates (ISS derived)
- Provide capability to offset internal/external attitude perturbations
- Complete 90° slew maneuver about highest MOI axis within 30 min (Typical ISS delta time)

4.5.2 System Assumptions

The AD&C subsystem has the following assumptions and limitations:

- NEP Module is passive for all stages of the mission
- Habitat is the active vehicle during RPODU in NRHO
- Chemical Element and Xenon Interstages are the active vehicles during RPODU phases
- Orion Vehicle is active vehicle when docking/undocking with Stack
- Vehicles waiting to dock with Stack are in Leader/Follower orientation in same orbit, separated by some phase angle
- Stack is passive vehicle in Mars orbit
    - Lander is active and performs RPODU maneuvers
    - Ascent stage is active when bringing the crew back up to Stack from the Martian surface
- Attitude control performed during EP thrusting arcs is performed by EP thrusters
- Simple shapes and mass distribution for calculations of moments of inertia

4.5.3 Analytical Methods

Standard analytical methods are used to verify attitude control system (ACS) hardware meets system and subsystem level requirements. The sections below detail the mathematical models and methods used to analyze aspects of the system which correspond to attitude control.

4.5.3.1 Vehicle Mass Properties

The mass properties for various configurations of the stack relies on determining the Principal Moments of Inertia (MOI) of a composite object through the use of the Parallel Axis Theorem. Constraining cases are considered when verifying the system level requirements are met. The elements of the stack contributing most to the overall MOIs are modelled as common geometric shapes. Aspects such as propellant levels and the presence of an element are configurable within the set of analysis tools used. Table 4-33 provides insight into the evolution of key mass properties over the course of the mission:

Table 4-33 Principal Moment of Inertias for Different Configurations

Stage Configuration	Mission Phase	**Approximate MOI** I_{XX} | I_{YY} | I_{ZZ} **(kg*m^2)**	CG from Reactor (m)
NPM|XT1|XT2|XT3|CHEM	LEO: 500km	1.8E6|1.8E8|1.8E8	70.1
NPM|XT1|XT2|XT3|CHEM	LEO: 1100km	1.9E6|1.9E8|1.9E8	71.5
NPM|XT1|HAB|CHEM	NRHO	1.9E6|1.9E8|1.9E8	72.3
NPM|XT1|HAB|CHEM	Post TMI	1.5E6|1.5E8|1.5E8	66
NPM|XT1|HAB|CHEM	Post Mars Capture	1.2E6|1.2E8|1.2E8	62.4
NPM|XT1|HAB	Post Chem Jettison	9.6E5|9.6E7|9.6E7	58
NPM|XT1|HAB	End of Mission (EOM)	9.1E5|9.1E7|9.1E7	56

NPM = Nuclear Power Module, XT. = Xenon (Interstage)Tanker, CHEM = Chemical Module, HAB = Habitat

The center of gravity (CG) of the stack migrates significantly over the course of the mission. This is mitigated somewhat by each element having its own RCS pods since each element is a free flyer at some point in the mission. Based on the available elements and the location of the estimated CG, different pairs of RCS thrusters can be actuated such that pure rotations and/or precise 3 DOF translations can occur.

4.5.3.2 Environmental Disturbance Torques

Environmental torques are estimated using well established analytical models. Atmospheric torque modeling utilizes a "calibrated" exponential atmospheric density profile, ρ, and is modeled by:

Equation 7 $$\boldsymbol{T_{ATM} = \frac{1}{2}\rho v^2 \cdot C_D A_{ATM} \cdot \Delta r}$$

Where A_{ATM} is the projection of the spacecraft geometry onto a plane which is perpendicular to the spacecraft velocity vector, C_D is the coefficient of drag, and Δr is the distance from the center of pressure and the center of mass of the spacecraft.

Gravity gradient torques assume two-body orbital dynamics. The vector representation of the gravity gradient Torque is shown below:

Equation 8 $$\boldsymbol{T_{GG} = \frac{3\mu}{r^3}(n \times Jn)}$$

Where r is the distance between the center of the central body and the center of mass of the spacecraft, J is the principal moment of inertia tensor, and $\boldsymbol{n}$ is a unit vector pointing Nadir in the principal frame.

Solar radiation pressure (SRP) torque utilizes the following model

Equation 9 $$\boldsymbol{T_{SRP} = \frac{P_0}{c} \cdot A(1 + C_R) \cdot k\cos(\delta) \cdot r}$$

Where P_0 is the solar power flux at a specific planetary distance, c is the speed of light in a vacuum, A is the projection of the spacecraft geometry onto a plane which is perpendicular to the sun-spacecraft line, C_R is the coefficient of reflectivity, k is an arbitrary scalar (set to 1 nominally), δ is the planar projection offset from 90 degrees to the sun-spacecraft line, and r is the distance from the center of pressure and the center of mass of the spacecraft.

Table 4-34 shows the "worst case" magnitudes of disturbance torques expected from SRP, aerodynamic drag, and gravity gradient (GG) torques for various phases of the mission.

Table 4-34 Environmental Disturbance Torques at Various Phases

Stage Configuration	Mission Phase	Gravity Gradient (Nm)	Aero Drag (Nm)	SRP (Nm)
NPM|XT1|XT2|XT3|CHEM	LEO: 500km	5E-1	1E-3	---
NPM|XT1|XT2|XT3|CHEM	LEO: 1100km	9E-1	1E-6	3E-3
NPM|XT1|HAB|CHEM	NRHO	2E-2	---	3E-3
NPM|XT1|HAB|CHEM	Post TMI	---	---	3E-3
NPM|XT1|HAB|CHEM	Post Mars Capture	4E-2	---	1E-3
NPM|XT1|HAB	Post Chem Jettison	---	---	8E-4
NPM|XT1|HAB	EOM	1E-2	---	2E-3

Gravity Gradient torques are calculated at periapsis points where its effect, depending on spacecraft attitude, is highest. Additionally, the Gravity Gradient torque assumes the spacecraft is oriented such that the reactor points in the direction of the velocity vector. This attitude is not stable, and thus requires active attitude control. SRP torques shown in Table 4-34 assume the worst case orientation of the spacecraft for SRP torque. Aerodynamic drag is only expected to be encountered in a meaningful capacity near Earth. This includes the 500 km staging orbit as well as

perigee passes when in the LDHEO. The aero drag torque estimates shown assume the reactor points in the direction of the velocity vector.

4.5.4 Risk Inputs

The stack is long at the departure stage, comparable to the ISS. The ISS exhibits known structural flex due to propulsive effectors, thermal effects, etc. This structural flex causes parts of the vehicle to displace and rotate non-negligibly relative to other parts of the vehicle. It is important to design the control system with knowledge of the natural modal frequencies of the stack structure for various configurations such that the control system does not impart energy into the flex modes. Additionally, the inertial navigation equipment and attitude sensors should be somewhat isolated from these effects, or sufficient knowledge of the flex must be known to correct sensor measurements.

The attitude of the spacecraft can be controlled via the dual gimballed EP thruster platforms in conjunction with running the EP thrusters. However, orienting the platforms to generate torques about the yaw and pitch axes increases thruster plume impingement on the truss and possibly the radiator assembly on the nuclear power element. Further analysis detailing how long increased impingement lasts for phases such as spiral-out and spiral-in should be done.

4.5.5 System Design

The stack is composed of several independent vehicles, each must maintain knowledge of its attitude and inertial state in between ground updates. Additionally, each element must have the capability to affect its orbit, either to maintain a desired orbit, enter into another orbit, or rendezvous with other elements.

4.5.5.1 Element Navigation and Attitude Determination Hardware

The NEP Module is required to correct its insertion orbit, and as such, it has GNC sensors and effectors that are typically found on free flying spacecraft. The NEP Module contains:

- 2 IMUs
    - Three single axis rate gyros to measure vehicle body rates
    - Three single axis accelerometers to measure vehicle body accelerations
- 4 Star Trackers
    - Determine inertial attitude
    - 2 data processing units each with 2 optical heads
- 8 sun sensor assemblies
    - Coarse attitude determination
    - Knowledge of direction to sun for safe mode

The NEP Module is the passive element while the Xenon Interstage is docking to it in the 500 km staging orbit. The NEP Module contains passive navigation aids on the docking port that are used by active RPOD hardware on the Xenon Interstage to allow for a successful docking between the two elements. These navigation aids consist of:

- 3 perimeter reflector targets (PRT)
- 1 peripheral docking target (PDT)
- 1 centerline docking target (CDT)

A representative picture of the navigation aids is below in Figure 4-45. It is assumed that the Xenon Interstage contains an identical set of navigation aids on its passive docking port to allow other Xenon Interstages and the Chemical Module to dock to it.

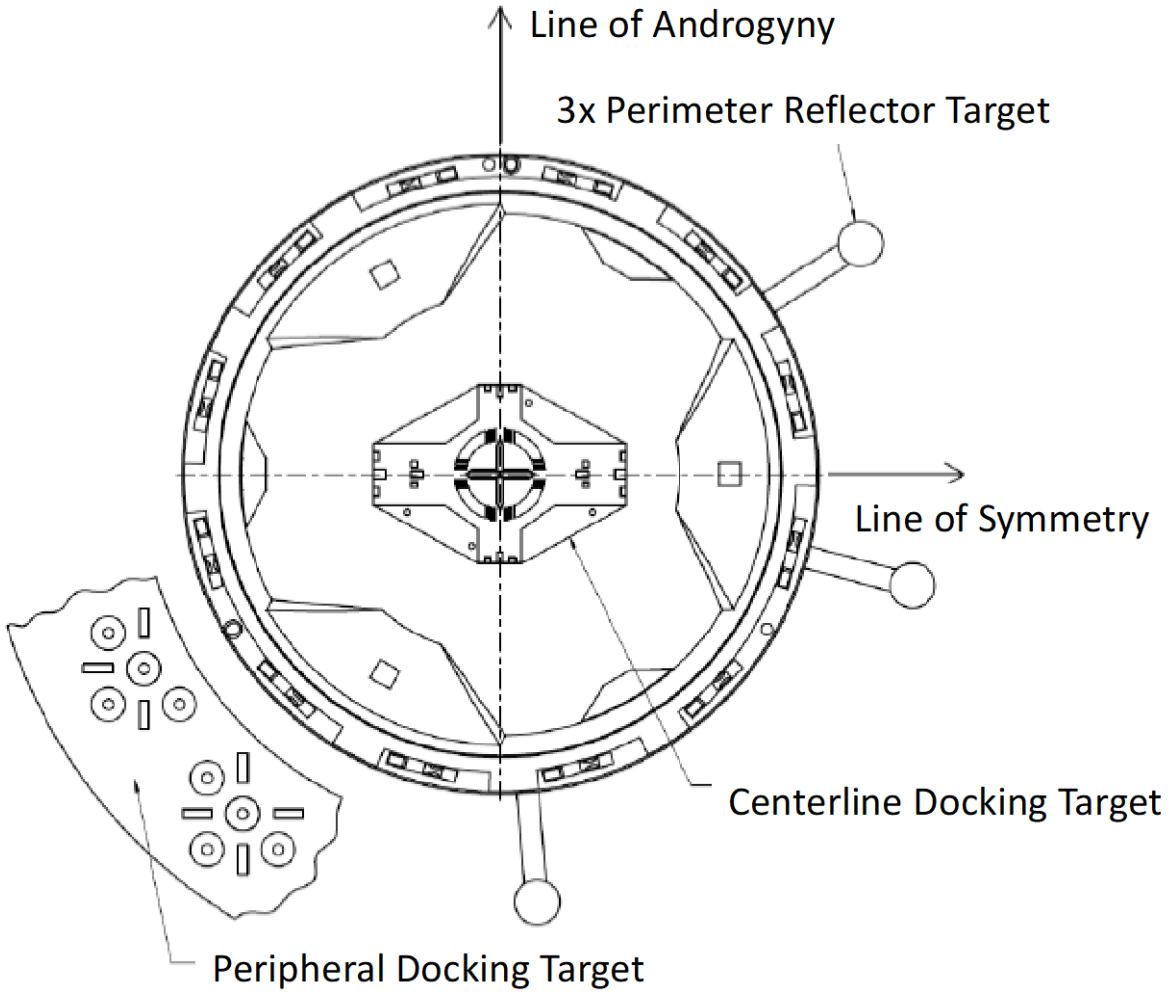

Figure 4-45 Passive Navigation Aids

The Xenon Interstages and Chemical Module contain active RPOD hardware to allow for autonomous, yet monitored, docking. This hardware consists of:

- 2 LIDARs
- 2 Docking Cameras
- 2 Docking Lights

During rendezvous, the relative state estimation between the NEP Module and the first Xenon Interstage is derived by onboard state vector differencing between the two elements. At a range of ~400 km, range and range rate measurements between the passive and active vehicles are provided by S-band radios, which are held in the communication subsystem MEL. At closer ranges, the docking cameras and the LIDAR provide visual cues and relative position and attitude respectively. This process is repeated for the next two Xenon Interstages as well as for the Chemical Element, except each incoming vehicle will dock to the end of the stack.

There is a “re-shuffling” of elements in the NRHO. During which, the Chemical Element will loiter behind or in front of the stack while the Habitat docks to the first Xenon Interstage while the second and third Xenon Interstages undock and enter into heliocentric disposal trajectories. The Chemical Element will then dock to the passive end of the remaining Xenon Interstage. Orion is the active vehicle during RPODU operations and docks to the radial port on the Habitat. Similarly, the Mars Lander and ascent vehicle rendezvous with the stack at Mars and are the active elements.

4.5.5.2 Attitude and Attitude Control Strategies

In all phases of the mission, firing two jets located on pods at the front of the NEP Module will result in obtaining a 0.05°/s rotation about the highest moment of inertia axis in ~10 sec. Cancelling the coupled translation requires firing a coupled pair of RCS jets located on the Chemical Module, or on the remaining Xenon Interstage once the Chemical Module has been jettisoned. Fine attitude control can be obtained from firing RCS jets closer to the CG, i.e., the thrusters located at the aft end of the NEP Module and/or the thrusters located at the forward end of the Chemical Module. Assuming a minimum on time of 50 ms, the minimum rotational rate about the lowest moment of inertia axis (roll axis) is ~35 μ°/s at the end of the mission.

The attitude control is baselined to be handled by the dual gimbal EP platforms. The platforms are assumed to gimbal in 40° in two axes, allowing for attitude control about all three body axes. Achieving a 0.05°/s rotational rate about the yaw/pitch axes in ~65 sec at the start of the mission requires both platforms operating 9 thrusters and oriented such that the resultant force from the thrusters generates a torque about either the yaw or pitch axes. The torques generated in this manner easily overcome environmental disturbance torques encountered when the EP thrusters are active. The following list provides possible strategies that seek to reduce propellant consumption and schedule corrections for "transient" disturbance torques:

- Low Earth Orbit Operations
  - Free flying elements will perform independent orbital maintenance and attitude control using their RCS thrusters
  - NPM/Xe stack will maintain a 500 km orbit while awaiting the Chem element.
  - Orientation of Stack should be either nose-to-nadir or nose-pointed-ram for attitude stability purposes. Offsets from these attitudes produce large gravity gradient torques, and it may be infeasible to find a Torque Equilibrium Attitude (TEA) that balances aero torques with GG torques since presenting sufficient frontal area to "the wind" requires a large attitude deviation.
  - RCS used to maintain tight attitude during orbit raising maneuver to get to 1100 km circular orbit
  - Combination of roll control and pitch (coinciding with orbital mean motion) to maintain solar pointing if in RAM orientation in 1100 km orbit
- Spiral to NRHO
  - Orientation will keep reactor pointed RAM to coincide with guidance solution
  - Attitude controlled via gimballed EP thrusters
- NRHO and LDHEO Operations
  - Orientation keeps reactor pointed at Sun to minimize solar radiation torques
  - "Transient" Gravity gradient torques incurred during perigee passes and perilune passes corrected on a per-orbit basis
- Outbound Phase
  - Attitude controlled via gimballed EP thrusters during burn arcs and RCS otherwise
  - Orientation will be nose-to-sun for coasting arcs to reduce attitude disturbance torques
  - Orientation will be nose-to-RAM for burn arcs
- Mars Orbit Operations
  - Periapsis passes are brief, and gravity gradient torques are reduced due to the smaller body being orbited along with a lower Stack moment of inertia, post chem stage jettison. Attitude should be selected based on surface comm needs and Earth relay
- Inbound Phase similar to Outbound Phase

4.5.6 Recommendation(s)

It is recommended the following studies and strategies be assessed or employed:

- Perform an integrated assessment of sensitivity of attitude determination sensor measurements due to structural flex induced by low frequency of oscillation of complete Stack. Mitigating efforts include: "slow" slew maneuvers (on the order of tens of minutes), and selection of control effector rates that do not coincide with structural modes.
- Maintain torque equilibrium attitudes for quiescent phases to reduce propellant costs associated with fighting against attitude perturbations.

4.5.7 Master Equipment List

Table 4-35 ADC Guidance, Navigation, & Control NEP Module MEL

Description Case 3_SLS_Chem NEP_Chem_Vehicle_Family CD-2020-181	QTY	Unit Mass	Basic Mass	Growth	Growth	Total Mass
Attitude Determination and Control			71.6	13%	9.2	80.8
Guidance, Navigation, & Control			71.6	13%	9.2	80.8
IMU	2	9.6	19.2	18%	3.5	22.7
Star Tracker Optical Head	4	1.0	4.0	18%	0.7	4.7
Star Tracker Electronics Unit	2	9.8	19.6	18%	3.5	23.1
Sun Sensors	8	0.1	0.8	18%	0.1	0.9
Perimeter Reflector Target	6	2.0	12.0	5%	0.6	12.6
Peripheral Docking Target	2	4.0	8.0	5%	0.4	8.4
Centerline Docking Target	2	4.0	8.0	5%	0.4	8.4

Table 4-36 ADC Interstage MEL

Description Case 3_SLS_Chem NEP_Chem_Vehicle_Family CD-2020-181	QTY	Unit Mass	Basic Mass	Growth	Growth	Total Mass
Attitude Determination and Control			101.6	14%	14.6	116.2
Guidance, Navigation, & Control			101.6	14%	14.6	116.2
IMU	2	9.6	19.2	18%	3.5	22.7
Star Tracker Optical Head	4	1.0	4.0	18%	0.7	4.7
Star Tracker Electronics Unit	2	9.8	19.6	18%	3.5	23.1
Sun Sensors	8	0.1	0.8	18%	0.1	0.9
LIDAR	2	12.0	24.0	18%	4.3	28.3
Docking Camera	2	2.0	4.0	18%	0.7	4.7
Docking Lights	2	1.0	2.0	18%	0.4	2.4
Perimeter Reflector Target	6	2.0	12.0	5%	0.6	12.6
Peripheral Docking Target	2	4.0	8.0	5%	0.4	8.4
Centerline Docking Target	2	4.0	8.0	5%	0.4	8.4

Table 4-37 ADC Chemical Stage MEL

Description Case 3_SLS_Chem NEP_Chem_Vehicle_Family CD-2020-181	QTY	Unit Mass	Basic Mass	Growth	Growth	Total Mass
Attitude Determination and Control			73.6	18%	13.2	86.8
Guidance, Navigation, & Control			73.6	18%	13.2	86.8
IMU	2	9.6	19.2	18%	3.5	22.7
Star Tracker Optical Head	4	1.0	4.0	18%	0.7	4.7
Star Tracker Electronics Unit	2	9.8	19.6	18%	3.5	23.1
Sun Sensors	8	0.1	0.8	18%	0.1	0.9
LIDAR	2	12.0	24.0	18%	4.3	28.3
Docking Camera	2	2.0	4.0	18%	0.7	4.7
Docking Lights	2	1.0	2.0	18%	0.4	2.4

4.6 Command & Data Handling (C&DH)

The NEP-Chem vehicle Command & Data Handling (C&DH) subsystem is responsible for the general avionics, command & control, and health management of the spacecraft. All components used within this analysis are based on military/space rated commercially available products from verified aerospace system vendors. Each component in this design has a high TRL level. Included in this assessment are the preliminary study requirements, system assumptions, analytical methods used, design, recommendations, and the MEL.

4.6.1 C&DH Requirements

The vehicle C&DH baseline study requirements are as follows:

1. All Avionics equipment, including flight computers, memory units, IO interface boards, motor drivers and actuators, other control units and harnessing shall be rated for 100 kRad Total Ionizing Dose (TID) and have Single Event Upset (SEU)/Single Event Functional Interrupt (SEFI) detection and reset for the duration of the mission.
    a. *Rationale*: The Avionics equipment will be exposed to external space and internal reactor radiation sources. The enclosures will dampen but not entirely eliminate the radiation exposure to the devices.
2. All Avionics equipment in this study shall be single fault tolerant with cold backups.
    a. *Rationale*: In the event an SEU/SEFI or an unrecoverable anomaly occurs in the Avionics system, backups are necessary to safely maintain nominal operations during the mission.
3. Avionics shall provide command, control & health management to the NEP Module, Xenon Interstage and chemical stage of the vehicle.

4.6.2 System Assumptions

The C&DH baseline study assumptions are as follows:

- All non-COTS (commercial off the shelf) hardware is rated for 100 k TID.
- Command & control of the reactor and guidance, navigation, and control (GN&C) systems are handled by their respective subsystems with interfaces to the C&DH system.
- Power requirements for motor drivers and actuators.
- Data budgets and software requirements.
- 100% wire mass growth and 30% equipment growth was used based on the AIAA guidelines.

- Waste heat from driving the motors and actuators was considered negligible to average power consumption. This is justified by the long timeframes of the power modes and the infrequent use of the motors.
- 3U form-factor compact peripheral component interconnect (cPCI) compatible system assumed for consistent avionics.

4.6.3 System Trades

There were no specific C&DH system trades for this design.

4.6.4 Analytical Methods

A suite of avionics software was used to estimate the mass and power usage of the C&DH system. This suite contains a motor driver mass/power estimator, an avionics enclosure dimension/mass estimator and a wire harnessing mass estimator. Each of these tools are described and results are given in the following sections.

The C&DH baseline study analytical methods are as follows:

4.6.4.1 Motor Driver Estimation

The motor drivers were estimated by separately calculating the waste heat and area of each form-factor printed circuit board (PCB), using Moog's Servo Motor Controller [40] as reference. The waste heat is calculated from the equation:

Equation 10
$$\boldsymbol{Waste\ Heat = \frac{Motor\ Power}{Driver\ Power\ Supplied} * driver\ dissipation * motor\ count}$$

The area required by the PCB is similar to the waste heat calculation:

Equation 11
$$\boldsymbol{Area = \frac{Motor\ Power}{Driver\ Power\ Supplied} * area\ per\ channel * \frac{motor\ count}{100}}$$

The area required is then used to calculate the 3U cPCI card count. Table 4-38 shows an example result.

Table 4-38 Xenon Interstage motor driver estimation example

Actuator Name	Peak Power/Actuator	Number of Actuators	Waste Heat	PCB Area Required (cm^2)	Mass Required (kg)	Number of 3U cPCI Required	Total 3U cPCI
Docking Hard Capture	10	24	9.4	137.1	0.4	0.857142857	4
Docking Soft Capture	20	12	9.4	137.1	0.4	0.857142857	
Pumps	50	4	7.9	114.3	0.4	0.714285714	
Xenon System Valves	20	22	17.3	251.4	0.8	1.571428571	

4.6.4.2 Wire Harnessing Estimation

Wiring Harness Estimation

A Monte Carlo method based software estimation tool was used to estimate the mass of the wiring required to interface between the peripherals of the NEP vehicle and the avionics box. The Monte Carlo method is used for drawing a sample at random from an empirical distribution. The method then performs an unbiased risk analysis by creating a model of possible solutions around a probability distribution. As applied to a wire mass simulation, the Monte Carlo method is used for drawing a random length of wire from a distribution between estimated minimum and maximum wire lengths. The mean-value Monte Carlo method is used in this analysis to determine wire mass and is represented in the equation below.

Equation 12 $$\widehat{\boldsymbol{\theta}} = \frac{\mathbf{1}}{\boldsymbol{B}} * \sum_{\boldsymbol{b=1}}^{\boldsymbol{B}} \boldsymbol{f(u_b)}$$

In this equation, $\hat{\theta}$ represents the solution for the mass of the wire harness, B is the number of samples, and the function $\sum_{b=1}^{B} f(u_b)$ represents the summation of the samples in the distribution. An example run is shown in the following table.

Table 4-39 chemical stage wire harnessing 1 run Monte Carlo example

Unit	Wire Protocol	kg/m	Number of cables	Min Length (m)	Max Length (m)	Run1
Sensors	24 AWG	0.0022	300	10	15	7.55
RCS Pumps/Valves	22 AWG	0.0035	48	10	15	2.08
Press. Valves	24 AWG	0.0022	120	10	15	3.39
Pyro Valves	24 AWG	0.0022	12	10	15	0.39
Thruster Valves	22 AWG	0.0035	144	10	15	5.78
Docking Hard Capture	22 AWG	0.0035	36	4	7	0.57
Docking Soft Capture	22 AWG	0.0035	18	4	7	0.40

4.6.5 Risk Inputs

Risk Statement: The radiation environment external and internal to the vehicle may cause Single Event Effects (SEEs) on electronics as well as long-term damage from ionizing doses of radiation. Due to single-fault tolerant electronics, there is a low risk of an SEU interrupting critical operations.

Mitigation Strategy: For long-term damage from ionizing doses, select parts with a TID tolerance > 100 kRad. For SEUs, combine multiple mitigation techniques such as triple mode redundancy (TMR) with voting in code, error detection and correction (EDAC), hardened memory cells and data scrubbing.

4.6.6 System Design

The C&DH avionics packages are designed around the AiTech SP0 Single Board Computer (SBC) [41] and adhere to single-fault tolerant requirements. Each computer is responsible for the C&DH of all subsystems including most actuator controllers, and each package contains a set of standard/analog IO interface cards and motor drivers. The propulsion module includes a Gimbal Control Electronics [40] unit to drive the gimbals for the electric propulsion engine decks. Each unit attached to the compact Peripheral Component Interconnect (cPCI) backplane adheres to the 3U avionics card size standard, and the cPCI handles all DC-to-DC power conversion required by the avionics package. Each SP0 SBC operates with 8 GB of storage, which will contain the Real Time Operating System (RTOS), C&DH specific flight software (not modelled) and any emergency backup storage required. The system also maintains 128 GBs of SwRI Mass Memory [42] for each system, allowing for data recording/storage prior to transfer to the Habitat. All components are radiation tolerant up to 100k TID.

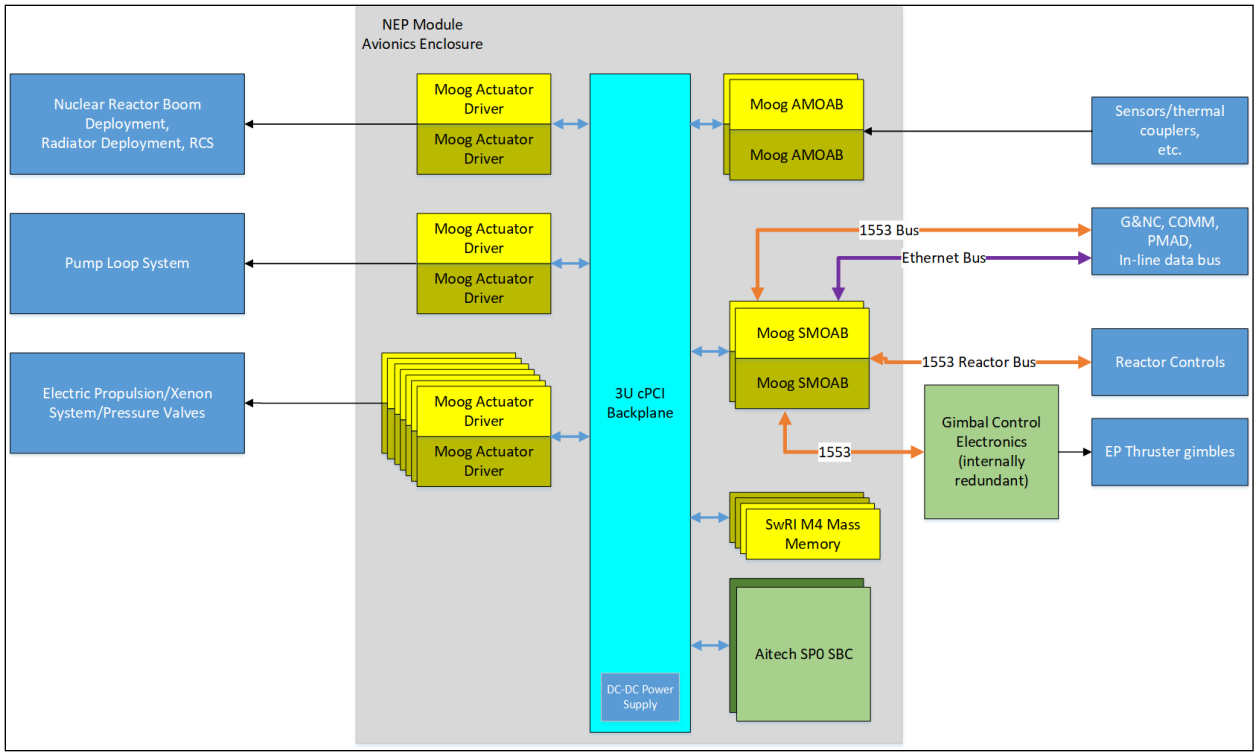

Figure 4-46 NEP Module Avionics Enclosure Block Diagram

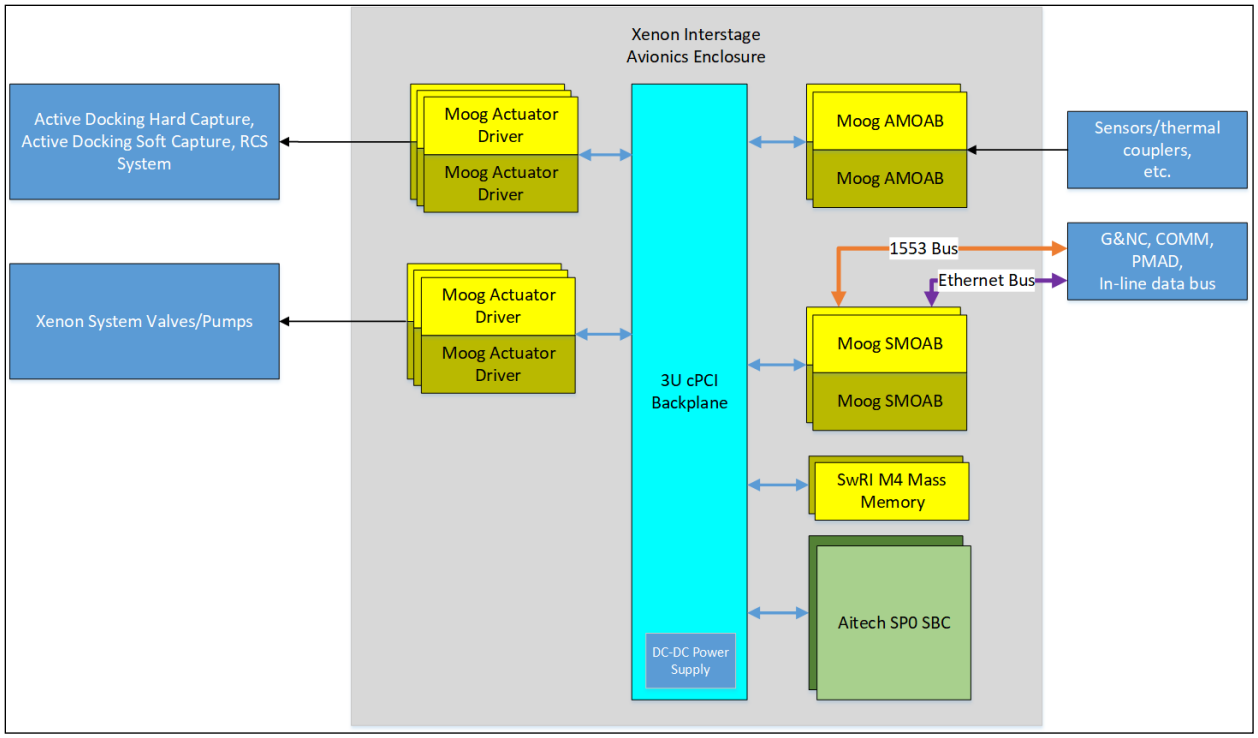

Figure 4-47 Xenon Interstage Avionics Enclosure Block Diagram

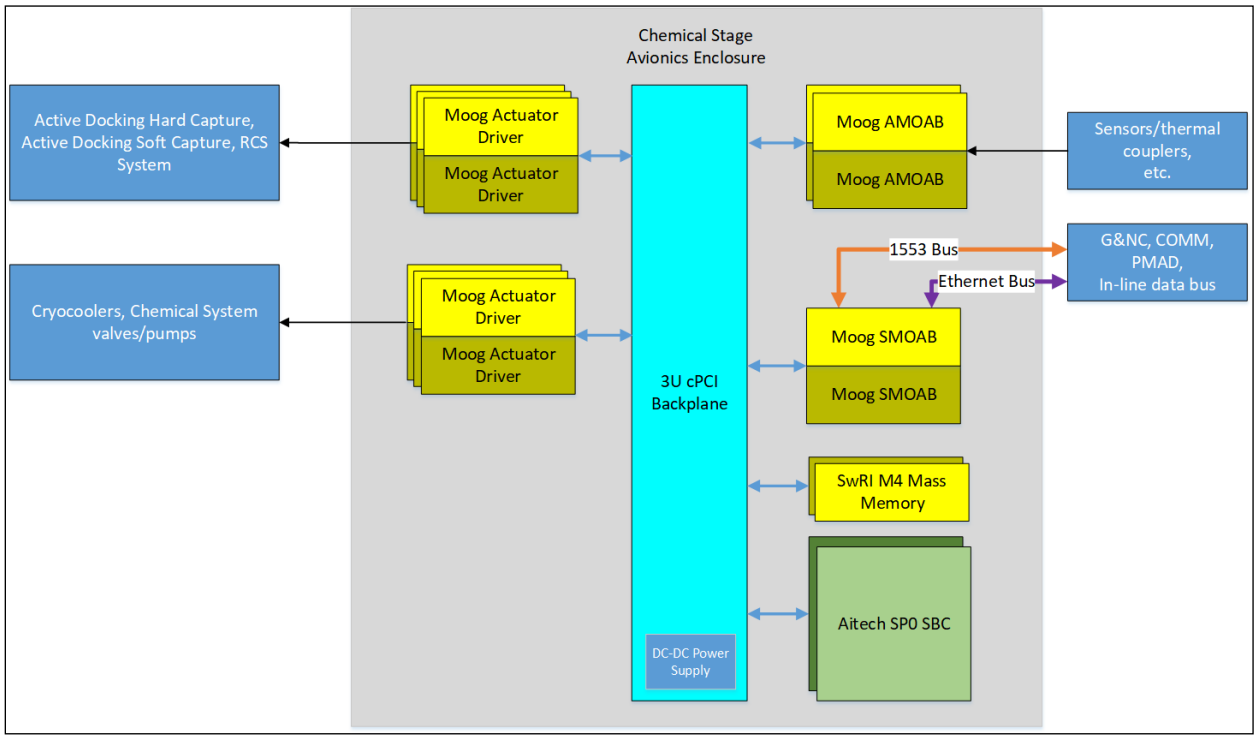

Figure 4-48 Chemical Stage Avionics Enclosure Block Diagram

The spacecraft will utilize both the Ethernet and 1553 communication standards for all digital interfaces. The IDSS Docking Standard specifies Ethernet and 1553 digital interconnects which will both be used as a single fault tolerant spacecraft data/control bus between all modules.

The following list is comprised of the main avionics components as input to the MEL shown below in Section 4.6.8, Master Equipment List.

1. AiTech SP0 Main computers [41]
2. Moog Standard (SMOAB)/Analog (AMOAB) IO cards [43]
3. Moog Actuator controller cards
    a. Refer to Propulsion System for high controller power requirements
4. SwRI M4 Mass Memory [42]
5. Gimbal Control Electronics unit [40]
    a. Controls EP thruster gimbals, power requirements estimated
6. Avionics Enclosure
    a. Houses main C&DH avionics package
7. Wire Harnessing

4.6.7 Recommendation(s)

The C&DH Compass team recommends the following improvements to the study:

- 6U form-factor with flight computer trades for a more robust system.
  - *Rationale*: Design was conducted using the 3U form-factor. A future system trade should be conducted to inspect the usage of 6U components with different COTS flight computers.
- The addition of camera equipment throughout the vehicle.
  - *Rationale*: This study was conducted without cameras mounted internal to the vehicle. Given the size of the vehicle, cameras should be used throughout to ensure proper health monitoring.
- Estimate the software effort months/lines of code required for the mission.

4.6.8 Master Equipment List

Table 4-40 C&DH NEP Module MEL

Description Case 3_SLS_Chem NEP_Chem_Vehicle_Family CD-2020-181	QTY	Unit Mass	Basic Mass	Growth	Growth	Total Mass
Command & Data Handling			**79.4**	**68%**	**53.9**	**133.3**
C&DH Hardware			**36.4**	**30%**	**10.9**	**47.3**
AiTech SP0 SBC	2	0.4	0.7	30%	0.2	0.9
Moog AMOAB	4	0.4	1.6	30%	0.5	2.1
Moog SMOAB	4	0.4	1.6	30%	0.5	2.1
Moog Actuator Driver	18	0.5	9.0	30%	2.7	11.7
Avionics Enclosure	1	17.7	17.7	30%	5.3	23.0
SwRI M4 Mass Memory	4	0.5	2.0	30%	0.6	2.6
Gimbal Control Electronics	1	3.8	3.8	30%	1.1	4.9
Instrumentation & Wiring			**43.0**	**100%**	**43.0**	**86.0**
Wire Harnessing	1	43.0	43.0	100%	43.0	86.0

Table 4-41 C&DH Interstage MEL

Description Case 3_SLS_Chem NEP_Chem_Vehicle_Family CD-2020-181	QTY	Unit Mass	Basic Mass	Growth	Growth	Total Mass
Command & Data Handling			**48.1**	**62%**	**30.0**	**78.1**
C&DH Hardware			**25.8**	**30%**	**7.7**	**33.5**
AiTech SP0 SBC	2	0.4	0.7	30%	0.2	0.9
Moog AMOAB	4	0.4	1.6	30%	0.5	2.1
Moog SMOAB	4	0.4	1.6	30%	0.5	2.1
Moog Actuator Driver	12	0.5	6.0	30%	1.8	7.8
Avionics Enclosure	1	14.9	14.9	30%	4.5	19.4
SwRI M4 Mass Memory	2	0.5	1.0	30%	0.3	1.3
Instrumentation & Wiring			**22.3**	**100%**	**22.3**	**44.6**
Wire Harnessing	1	22.3	22.3	100%	22.3	44.6

Table 4-42 C&DH Chemical Stage MEL

Description Case 3_SLS_Chem NEP_Chem_Vehicle_Family CD-2020-181	QTY	Unit Mass	Basic Mass	Growth	Growth	Total Mass
Command & Data Handling			**49.3**	**65%**	**32.2**	**81.5**
C&DH Hardware			**24.5**	**30%**	**7.4**	**31.9**
AiTech SP0 SBC	2	0.4	0.7	30%	0.2	0.9
Moog AMOAB	4	0.4	1.6	30%	0.5	2.1
Moog SMOAB	2	0.4	0.8	30%	0.2	1.0
Moog Actuator Driver	12	0.5	6.0	30%	1.8	7.8
Avionics Enclosure	1	14.4	14.4	30%	4.3	18.7
SwRI M4 Mass Memory	2	0.5	1.0	30%	0.3	1.3
Instrumentation & Wiring			**24.8**	**100%**	**24.8**	**49.6**
Wire Harnessing	1	24.8	24.8	100%	24.8	49.6

4.7 Communications Subsystem

An NEP-Chem Vehicle with space hardware assembly starting at an altitude of 500 km/28.5º inclination LEO orbit, subsequently transferring to an NRHO orbit, and finally to a Mars orbit, requires communication links (a) between docking module pairs, (b) from each module directly to DSN-34m facility at Goldstone and (c) from each space module to/from any one of TDRS satellites.

4.7.1 Communications Subsystem Requirements

The NEP-Chem Vehicle Communications subsystem requirements are to provide (a) redundant proximity and tracking S_1-band full-duplex links between two adjacent space modules for docking purposes, (b) two separate Single Fault Tolerant Direct-To-Earth (DTE) high data rate links at X-band on each space module for a total of three, and (c) redundant emergency full-duplex S_2-band links for use between each of three space modules and one of many TDRS satellites.

4.7.2 Communication Subsystem Assumptions

The communications subsystem design for the NEP-Chem Vehicle will consist of the following components per module:

(a) One Single-Fault-Tolerant *X-band Communications (Comm)* Subsystem with 1-Meter Fixed 2.5º Half-Power-Beamwidth Antennas for Direct-To-Earth (DTE) communications,

(b) One Single-Fault-Tolerant *S_1-band Comm* Subsystem with Omni (±45°) Antennas for Proximity communications, and one Single-Fault-Tolerant *S_1-band Comm* Subsystem with Active Patch (±33º) Antennas for Docking communications.

(c) One Single-Fault-Tolerant *S_2-band TDRS Comm* Subsystem with Helical (±90º) Antennas capable of hemispherical coverage.

Further assumptions for the NEP-Chem Vehicle are a minimum downlink data rate of 18 kbps with an EIRP of 59.5 dBW at a separation distance of 2.5 AU and 99.99% Annual Link Availability (ALA) at a 10º-Elevation Angle, Single Fault Tolerant, i.e., redundant components for communications subsystem electronics and a 3 dB link margin, which is included in the communications link for the link budget analysis. A 3 dB link margin is typical for space design applications due to the uncertainty of the components' performance and available EOL effective isotropic radiated power (EIRP). DVB-S2 QPSK [1/4] at 10^{-7} BER modulation/coding has been chosen with an implementation/coding loss of -3.5 dB, unless otherwise specified.

4.7.3 Communications Subsystem Trades

(a) Information rates using a Low Noise Amplifier (LNA) versus no LNA at the receiver's front end for the S_1-band proximity/tracking/docking links between neighboring space modules, and

(b) Information rates at X-band DTE vs Ka-band DTE from each of three space modules.

4.7.4 Analytical Methods (Link Budgets)

The communications subsystem design for higher information rates is a function of the transmitted power, the atmospheric absorption (gas/cloud/rain fade), and the modulation/coding scheme.

Link budget analyses of the X-, Ka-, and S-bands were performed, with two radio frequency (RF) power options at X-band for average & worst-case scenarios, plus with LNA versus w/o LNA options at S_1-band. Using the link budget that is in this report for the best information rate with a variation of EIRP, LNA, Atmospheric Losses, and modulation/coding schemes is shown in the Table 4-43 X, Ka, and S-band Link Budgets below.

Table 4-43 X, Ka, and S-band Link Budgets

	X/Omni to Earth	X/HGA to Earth	Ka/HGA to Earth	S-Band with LNA	S-Band w/o LNA	TDRS Return SSA
Carrier Frequency (GHz)	8.4	8.4	32	2.3	2.3	2.3
Carrier Wavelength [λ=c/f](cm)	3.57	3.57	0.94	13.04	13.04	13.04
Available RF Power (W)	30	300	300	5	5	5
Available RF Power (dBW)	14.8	24.8	24.8	7	7	7
Tx Antenna Diameter (m)	–	1	3	0.056	0.056	–
Tx-3dB Beamwidth [70λ/d] (°)	±45°	2.5	0.21875	±45°	±45°	±90°
Tx Antenna Efficiency (%)	–	55	55	–	–	–
Tx Antenna Gain (dBi)	0	36.3	57.4	0	0	0
Transmission Loss (dB)	-1.5	-1.5	-1	-1	-1	-0.3
EIRP (dBW)	13.3	59.5	81.2	6	6	6.7
Distance (km)	480,000	2.5 AU	2.5 AU	100	100	40,000
99.99% ALA Atmospheric Loss (dB)	-3	-3	Set to Zero	N/A (0)	N/A (0)	N/A (0)
Depolarization (dB)	0	0	0	0	0	0
Rx Antenna Diameter (m)	34	34	34	0.056	0.056	–
Rx-3dB Beamwidth [70λ/d] (°)	0.07	0.07	0.02	±45°	±45°	±22°E/W; ±28°N/S
Rx Antenna Gain (dBi)	66.9	66.9	78.5	0	0	–
G/T (dB/K)	46.6	46.6	58.2	-21.3	-25.7	9.5
DVB-S2 QPSK (1/4) 10^{-7} BER	266 kbps	18 kbps	4 Mbps	4.9 Mbps	1.8 Mbps	14* kbps
Implementation/Coding Loss (dB)	-3.5	-3.5	-3.5	-3.5	-3.5	-3.5
Link Margin (dB)	3	3	4.3	3	3	3
						* QPSK (Conv:½)

Furthermore it is feasible to increase the RF power output at X-band from 300 to 1,000 W, if so warranted at a distance of 2.5 AU, to increase the rate of 18 kbps by more than 5 dB (to 60 kbps).

For much higher information rates (~4 Mbps), a 32 GHz down-link would need to be established with the 34 m Goldstone antenna tracking station (Latitude: 35.35ºN, Longitude: -116.8833ºW). If this configuration is desirable, choosing an atmospheric attenuation of zero results in a Link Margin of 4.3dB. **At an Elevation Angle of ≥10º** it has been estimated for this configuration that a Link Margin of 7.8 dB is required (~1.8Mbps) for a 99% Annual Link Availability (ALA), whereas only 3.4 dB is required (~4 Mbps with 0.9 dB Link Margin) for a 95% ALA. **At an Elevation Angle of ≥60º** performance improves somewhat; a Link Margin of 6 dB is required (~2.7 Mbps) for a 99.9% Annual Link Availability, whereas only 2.1 dB is required (~4 Mbps with 1.2 dB Link Margin) for a 99% ALA.

4.7.5 Risk Inputs

Risk Statement: The main risk factor identified for the communications subsystem is based upon available RF power ***subject to*** atmospheric attenuation, antenna pointing, component aging, and the requirement for higher information rates; moreover, any generated plasma cloud from the RCS may temporarily disable communications (blackout period).

Strategy: The current mitigation strategy is to increase X-band transmit power and/or transmit frequency (Ka-band). A longer-term solution could be to design flight hardware to overcome the bottleneck effect on downlink data rates by using a dual feed antenna such that X-band is only used to receive TT&C data from ground and Ka-band is only used to transmit data to the ground and/or increasing the Ka-band dish diameter with deployable means. Plasma-induced communications blackouts are generally of short duration.

4.7.6 System Design

The subsystem design shown below in Figure 4-49 consists of S_1-band Proximity Communications at 100 km space module separation or less via Omni antennas that radiate 6 dBW (EIRP) to the opposite side, capable of 4.9 Mbps with an LNA, or just 1.8 Mbps without the LNA at the receiver's front end. The Omni antenna coverage is ±45º as shown below.

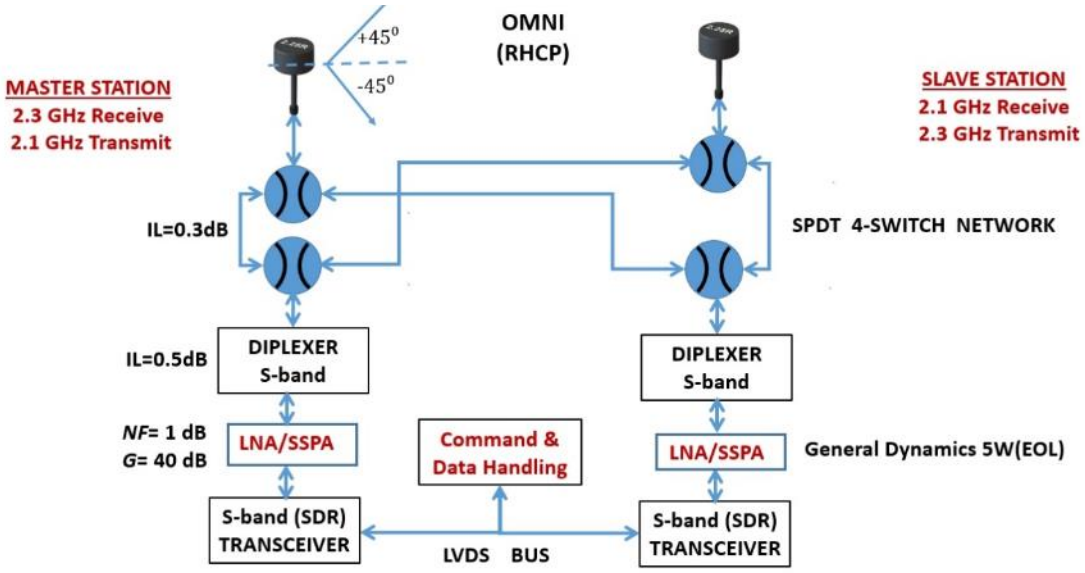

Figure 4-49 S_1-band Proximity Communications

The subsystem design shown below in Figure 4-50 consists of S_1-band Docking Communications at 100 km space module separation or less via active patch antennas that radiate >6dBW (EIRP) to the opposite side, capable of >4.9 Mbps with an LNA, or >1.8 Mbps without the LNA at the receiver's front end. The active patch antenna coverage is ±33º as shown below. The active patch antenna has a half-power beamwidth (±33º) gain of 8 dBi.

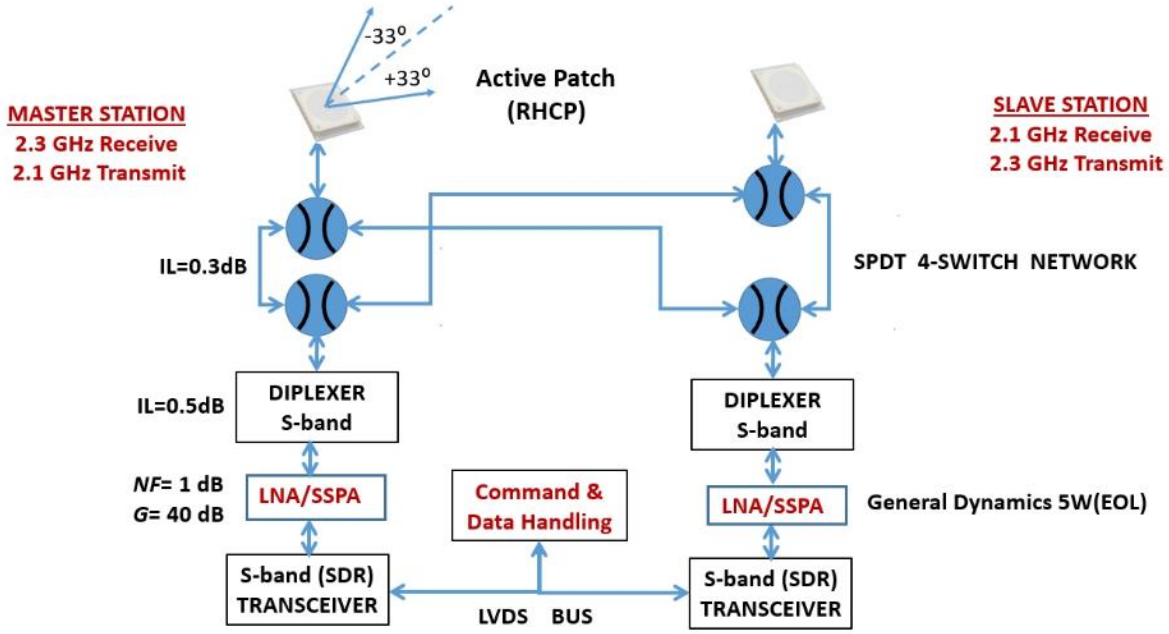

Figure 4-50 S_1-band Docking Communications

The subsystem design shown below in (Figure 4-51) consists of X-band Direct-From-Earth (DFE) for TT&C capability and X-band Direct-To-Earth (DTE) high data rate transmit system with 300 Watts of RF power for a 2.5 AU range, an atmospheric attenuation of 3dB (>99.99% Annual Link Availability at Goldstone) and 36.3 dBi antenna gain for 1 meter antenna dish. The receive system is a 34-m Goldstone dish (or equivalent) with 66.9 dBi antenna gain. Using a Solid State Transmitter Amplifier of 1,000 RF Watts at X-band would require a selection of an appropriately rated SPDT RF Failsafe Switch with low insertion loss, and additionally ensuring maximum compatibility with the X-band diplexer.

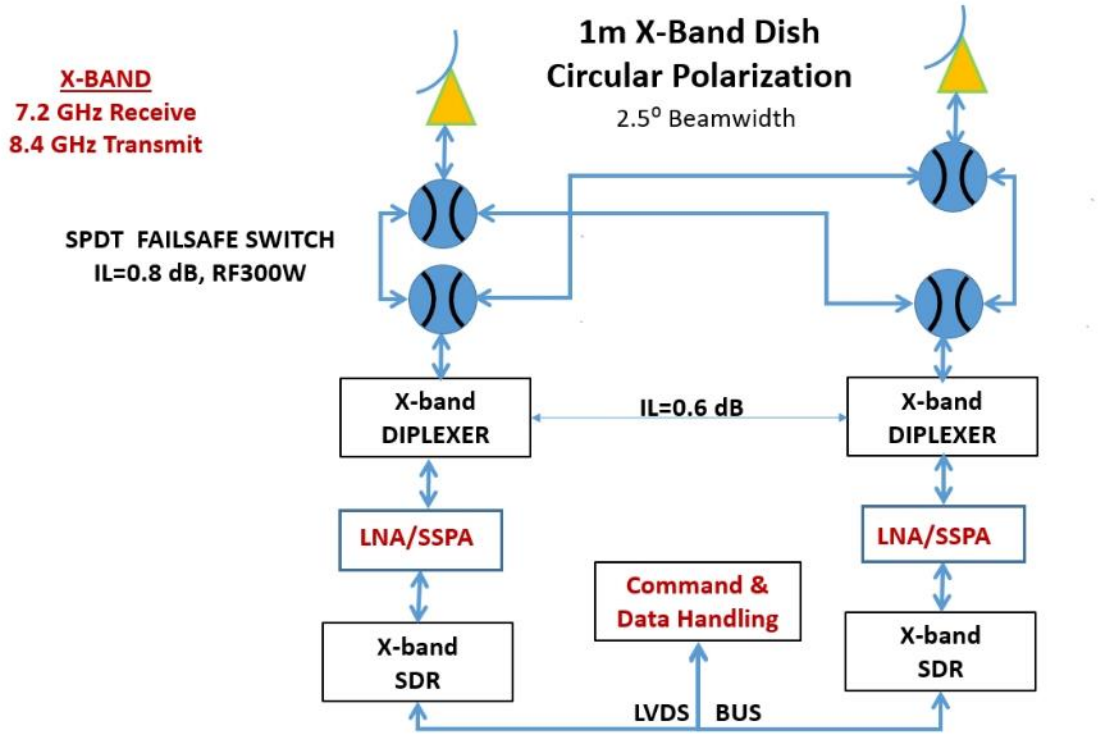

Figure 4-51 X-band DTE Communications

The subsystem design shown below in Figure 4-52 consists of X-band Direct-From-Earth (DFE) receive system for TT&C capability, X-band Direct-To-Earth (DTE) high data rate transmit system with 300 Watts of RF power for a 2.5 AU range, and Ka-band DTE higher data rate transmit system with 300 Watts of RF power for a 2.5 AU range. Details for the X-band subsystem have been discussed under the previous section, whereas details of the Ka-band subsystem have been discussed under ***Analytical Methods (Link Budgets)*** above. Adding a gimbal to the 1-m dish could be an option. For full redundancy, four (4) SPDT switches would have to be included for X-band (instead of just one used in Figure 4-52) and four (4) SPDT switches for Ka-band (instead of the one being used in Figure 4-52). Because of the full redundancy requirement, a second 1-meter dish would also have to be added below.

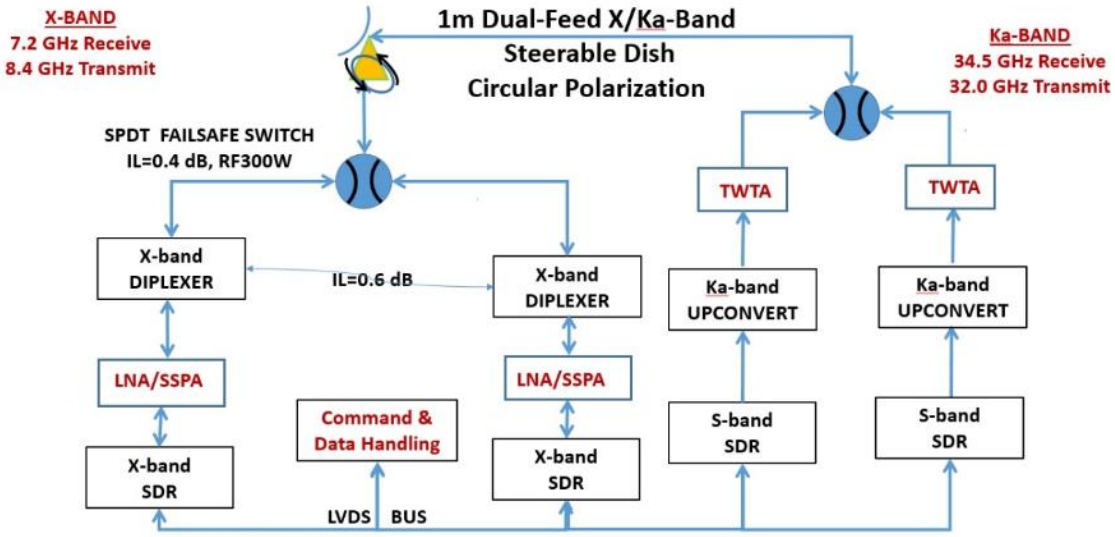

Figure 4-52 X-band and Ka-band Communications with Fixed or Steerable Dual-Feed System Dish

The subsystem design shown below in Figure 4-53 consists of S_2-band TDRS Communications at 40,000 km separation or less via two helical antennas that radiate -0.3 dBW (EIRP) towards the TDRS satellite, capable of 14 kbps when using QPSK modulation with ⅓-Rate Convolutional Coding at 10^{-7} BER. The helical antenna half-power beamwidth coverage is ±90º (hemispherical), as shown below.

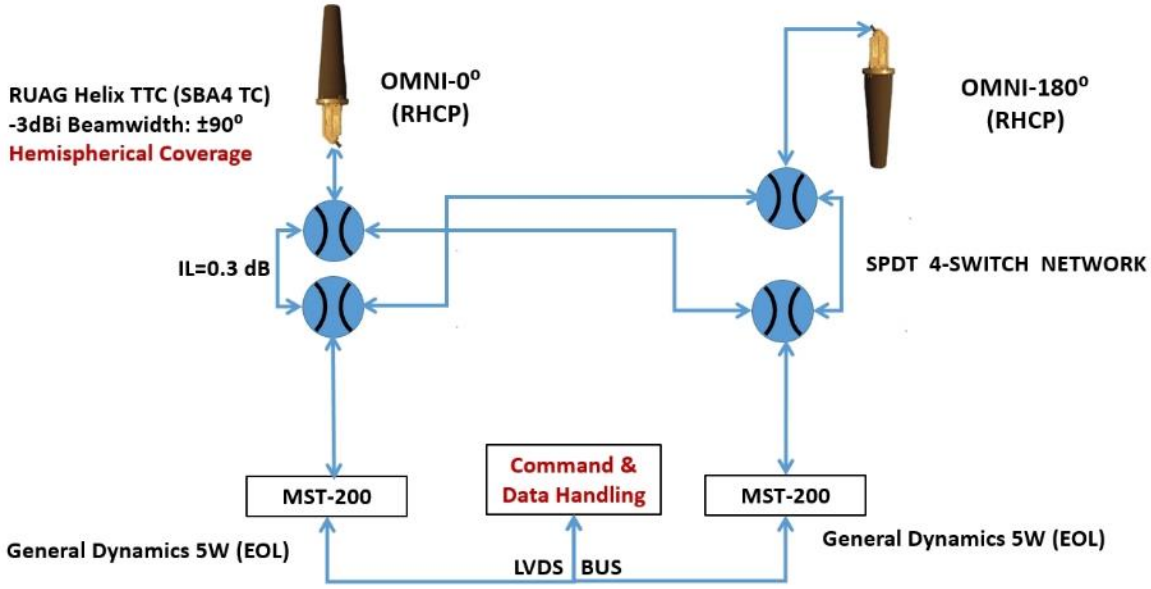

Figure 4-53 S_2-band TDRS Communications

4.7.7 Recommendation(s)

The Compass Team recommends investigating the use of a dual-feed Ka-band antenna system for X-band DTE/DFE and Ka-band DTE and/or increasing the Ka-band dish diameter with deployable means.

4.7.8 Master Equipment List

Below in Table 4-44, Table 4-45, and Table 4-46 are the Communications Subsystem Master Equipment list for the NEP-Chem vehicle.

Table 4-44 Communication Subsystem – NEP Module MEL

Description Case 3_SLS_Chem NEP_Chem_Vehicle_Family CD-2020-181	QTY	Unit Mass	Basic Mass	Growth	Growth	Total Mass
Communications and Tracking			**42.0**	**10%**	**4.2**	**46.2**
X Band System			**22.3**	**10%**	**2.2**	**24.5**
REFLECTOR	2	2.5	5.0	10%	0.5	5.5
SPDT	4	0.1	0.5	10%	0.1	0.6
DIPLEXER	2	2.2	4.4	10%	0.4	4.9
LNA	2	0.1	0.2	10%	0.0	0.2
SSPA	2	5.6	11.2	10%	1.1	12.3
SDR	2	0.2	0.4	10%	0.0	0.4
CABLE	2	0.3	0.6	10%	0.1	0.7
S Band System			**12.8**	**10%**	**1.3**	**14.1**
OMNI	2	0.1	0.1	10%	0.0	0.1
SPDT	8	0.1	1.0	10%	0.1	1.1
DIPLEXER	4	0.5	2.0	10%	0.2	2.2
SSPA	4	2.0	8.0	10%	0.8	8.8
SDR	4	0.1	0.4	10%	0.0	0.4
LNA	4	0.1	0.3	10%	0.0	0.3
ACTIVE PATCH	2	0.1	0.2	10%	0.0	0.2
CABLE	4	0.2	0.8	10%	0.1	0.9
TDRS Comm System			**6.9**	**10%**	**0.7**	**7.6**
TDRS-OMNI	2	0.2	0.5	10%	0.0	0.5
SPDT	4	0.1	0.5	10%	0.1	0.6
TDRS S-RADIO	2	2.8	5.5	10%	0.6	6.1
CABLE	2	0.2	0.4	10%	0.0	0.4

Table 4-45 Communications Subsystem – Interstage MEL

Description Case 3_SLS_Chem NEP_Chem_Vehicle_Family CD-2020-181	QTY	Unit Mass	Basic Mass	Growth	Growth	Total Mass
Communications and Tracking			**54.8**	**10%**	**5.5**	**60.3**
X band Communications System			**22.3**	**10%**	**2.2**	**24.5**
REFLECTOR	2	2.5	5.0	10%	0.5	5.5
SPDT	4	0.1	0.5	10%	0.1	0.6
DIPLEXER	2	2.2	4.4	10%	0.4	4.9
LNA	2	0.1	0.2	10%	0.0	0.2
SSPA	2	5.6	11.2	10%	1.1	12.3
SDR	2	0.2	0.4	10%	0.0	0.4
CABLE	2	0.3	0.6	10%	0.1	0.7
S Band Communications System			**25.7**	**10%**	**2.6**	**28.2**
OMNI	4	0.1	0.2	10%	0.0	0.3
SPDT	16	0.1	2.0	10%	0.2	2.2
DIPLEXER	8	0.5	4.0	10%	0.4	4.4
SSPA	8	2.0	16.0	10%	1.6	17.6
SDR	8	0.1	0.8	10%	0.1	0.9
LNA	8	0.1	0.6	10%	0.1	0.7
ACTIVE PATCH	4	0.1	0.4	10%	0.0	0.5
CABLE	8	0.2	1.6	10%	0.2	1.8
TDRS Comm system			**6.9**	**10%**	**0.7**	**7.6**
TDRS-OMNI	2	0.2	0.5	10%	0.0	0.5
SPDT	4	0.1	0.5	10%	0.1	0.6
TDRS S-RADIO	2	2.8	5.5	10%	0.6	6.1
CABLE	2	0.2	0.4	10%	0.0	0.4

Table 4-46 Communications Subsystem – Chemical Stage MEL

Description Case 3_SLS_Chem NEP_Chem_Vehicle_Family CD-2020-181	QTY	Unit Mass	Basic Mass	Growth	Growth	Total Mass
Communications and Tracking			**42.0**	**10%**	**4.2**	**46.2**
X Band System			**22.3**	**10%**	**2.2**	**24.5**
REFLECTOR	2	2.5	5.0	10%	0.5	5.5
SPDT	4	0.1	0.5	10%	0.1	0.6
DIPLEXER	2	2.2	4.4	10%	0.4	4.9
LNA	2	0.1	0.2	10%	0.0	0.2
SSPA	2	5.6	11.2	10%	1.1	12.3
SDR	2	0.2	0.4	10%	0.0	0.4
CABLE	2	0.3	0.6	10%	0.1	0.7
Antenna 2			**12.8**	**10%**	**1.3**	**14.1**
S-OMNI	2	0.1	0.1	10%	0.0	0.1
SPDT	8	0.1	1.0	10%	0.1	1.1
S-DIPLEXER	4	0.5	2.0	10%	0.2	2.2
S-SSPA	4	2.0	8.0	10%	0.8	8.8
S-SDR	4	0.1	0.4	10%	0.0	0.4
S-LNA	4	0.1	0.3	10%	0.0	0.3
S-ACTIVE PATCH	2	0.1	0.2	10%	0.0	0.2
CABLE	4	0.2	0.8	10%	0.1	0.9
Antenna 3			**6.9**	**10%**	**0.7**	**7.6**
TDRS-OMNI	2	0.2	0.5	10%	0.0	0.5
SPDT	4	0.1	0.5	10%	0.1	0.6
TDRS S-RADIO	2	2.8	5.5	10%	0.6	6.1
CABLE	2	0.2	0.4	10%	0.0	0.4

4.8 Habitat Element

A representative habitation module mass was calculated and assumed to be known for the duration of the study. That is to say that the Compass team did not design a habitat for this study and did not add additional MGA or margin to the habitat we were provided. It is worth noting that the habitat masses provided include a combined 30% MGA and mass margin. The starting wet mass of the habitat departing Earth is assumed to be 45.3 t. The 26.4 t operational mass of the empty habitat, as stated in the ground rules and assumptions, is included with approximately 18.6 t of logistics, payload, crew and consumables mass. The habitat mass is tracked in the systems integration sheet and mission calculations, rather in the MEL which captures elements designed by the Compass Team.

4.8.1 System Requirements

The habitat is required to return to NRHO/Gateway for reuse, regardless of what the rest of the vehicle does after completing its primary mission. Additionally, the NEP-Chem vehicle must provide 20 kW of power to the habitat whenever crew is present.

4.8.2 System Assumptions

The habitat is assumed to be launched on two CLV. The operational empty mass is assumed to be 26.4 t. Additional mass assumptions include:

- 4 Crew, totaling 328 kg
- Payloads and research, totaling 1000 kg
- Propulsion and RCS expendables, totaling 337 kg
- Logistics, totaling 18.6 t
- Trash dump of 11.13 kg/day

5.0 Lessons Learned and Next Steps

5.1 Lessons Learned

The 1.2 NEP-Chemical conceptual design solved the red team and habitat team issues with the 1.1 design. The red team was concerned with the large number of CLV tankers needed to fuel the vehicles at NRHO. The tanker fleet was reduced by assembling and fueling up the vehicles in low earth orbit and then using the NEP vehicle to lift itself (with all the required xenon propellants) and the fueled chemical stage to NRHO where the habitat element is integrated. This allows using the higher NEP I_{SP} to deliver the NEP-Chemical vehicle to NRHO. Compared to 1.1 assembling at NRHO starting in LEO reduces the CLV launch fleet from ~30 heavy CLVs down to only five super heavy CLVs (alternately use of only heavy CLVs to LEO would probably require on the order of 10 heavy CLVs).

The spiral from LEO to NRHO is not without impacts on the mission since the spiral takes about 14 months and about 100 t of xenon. This almost doubles the required amount of Xenon for the mission and pushes the Hall thruster xenon throughput to about 13 t each. Use of a magnetically shielded design (based on the AEPS thruster) should allow this. Alternatively, additional thrusters could be added. An additional ~50 t of chemical propellant is needed to lift the NEP vehicle before the reactor is started to 1100 km. This fuel requires an additional super heavy CLV 'top off' at 1100 km.

Two potential issues with the spiral include orbital debris and Van Allen belt radiation. By assembling the vehicle at 500 km and using MMOD shielding on important components (radiator fluid lines, propellant tanks…) the risk is minimized. The subsequent spiral from 1100 to 2000 km (major orbital debris orbits) happens over a couple of months which minimizes the risks. Tracking and avoiding major debris (like ISS) will also help reduce the risks. The Van Allen Belt radiation was assessed and it was found that assuming 10 mm of shielding on the electronics (primarily by packaging most the electronics inside the elements, near the propellant tanks) only 10 krad of radiation would be incurred.

The second major challenge addressed in 1.2 was the ground rule by the habitat team to not pass power or propellants through the habitat. The first solution was to put the thrusters on two long booms to try and eliminate the sputter and deposition impact from the electric thrusters. Analyses showed that this would be problematic and would constantly change as the habitat design changed. Next a concept to pass power around the habitat by deploying cable or using an arm was discussed but again, it would require some interface/interactions with the habitat. In the end, the electric thrusters were placed on the nuclear power element facing back towards the reactor. Analyses showed that with a 1 mm layer of pyrolytic graphite on the boom the sputter and deposition (back onto the radiators) would be minimized. This approach also removes constant changes in the electric propulsion system as habitats, or indeed other cargoes, are integrated to the NEP Module. The NEP Module becomes a complete power and propulsion system ready to push xenon interstages, habitats, landers, chemical stages, or whatever is needed. This creates an all-in-one NEP vehicle (albeit launched with limited Xe propellant <50 t). In addition, there are no high power or coolant lines to other docked elements required. The main drawback is that reuse of the NEP Module will be more challenging if thruster changeout is needed for subsequent missions.

Given the combining of the nuclear power and electric propulsion into one element only a single Xe tank could be carried (~44 t of xenon) on that element. Thus, additional xenon will need to be carried – more for some missions than others. The Xenon Interstage element was the solution to this. Launching two large COPV tanks allows launching almost 85 t of xenon in a dockable, free flyer element using a super heavy CLV. For the 2039 mission three Xenon Interstages are needed but two are dropped after the earth spiral so their empty tank mass is not carried to Mars and back.

The final element was the chemical stage which could be topped off and refueled on-orbit for the 2039 mission. Due to the ~200 t propellant load the SLS was chosen as a representative way to launch the chemical stage for the mission. The stage could be easily topped off using super heavy CLVs (especially for CLVs which use the same propellants). For some easier opposition and conjunction missions the 200 t stage might be oversized and smaller stages could be used. This suggests that using multiple stages for even the 2039 opposition mission is possible but integrating those stages was outside the scope of this study. In addition, given the commercial capabilities of chemical stages it is recommended that other chemical stage configurations be explored.

There are many ways to use NEP-Chemical elements for cargo missions, including just using the main chemical stage to deliver one lander, to just using the NEP Module alone to deliver all three landers. One NEP option would meet up with the cargos in NRHO (each cargo is launched using one SLS and boosted to NRHO using two heavy

CLVs) and spiral up to meet them in NRHO where the NEP vehicle could take them directly to Mars in ~500 days. The launch fleet for the NEP vehicle (not including the cargos) would only be one SLS, one Super Heavy, and one heavy CLV to deliver all three 65 t landers from NRHO to Mars about 19 months before the crew arrives. Use of the NEP vehicle does push the first flight of the NEP vehicle up by a year to 2036 compared to the all chemical cargo option.

5.2 Next Steps

The final NEP-Chemical point design and the trades that went into it suggest many next steps. The trajectory designers identified some interesting options for both the piloted and the cargo options that should be further evaluated. These include sending two landers with the crew on an NEP-Chemical vehicle for a conjunction opportunity and reusing an NEP cargo vehicle as a haven and taxi for crew at mars, or even an alternative return vehicle from Mars.

To develop a point design, only preliminary trades were made on technology selection. Especially in the electric propulsion and reactor/power conversion areas there are other technology approaches that could be evaluated against the baseline design.

The NEP Module has a long extendable boom and large deployable radiators. It is recommended that the assembly options be explored in more detail and even assess the use of commercial crew missions to the NEP Module at 500 km to assist in construction of the NEP-Chemical vehicle.

More refinement of the subsystem designs is needed in several areas. First, a more detailed definition of the nuclear power system itself is needed for the deployable systems (i.e., boom/radiator/coolant line/power line layouts). For the reactor itself, a more detailed design of operations, safety, and shielding is required (is the assumed re-entry shield needed for the assembly at 500 km?). A more detailed layout for the power conversion system and trades of building block sizes should be made. Trades of alternate radiator layouts should be explored. Finally, the launch of the NEP Module assumed a ~10 t strongback to mitigate launch loads and vibrations—a further investigation of this is recommended.

Lastly, the size, number of launches, and cost of the transportation system is significant. For comparison purposes it is highly recommended that both all chemical and SEP-Chemical options be explored to completely capture the advantages and relative challenges of an NEP system.

6.0 Bibliography

[1] Oleson, Steven R.; Burke, Laura; Dudzinski, Leonard; Fittje, James; Mason, Lee S.; Packard, Packard; Schmitz, Paul; Gyekenyesi, John; and Faller, Brent, "A Combined Nuclear Electric and Chemical Propulsion Vehicle Concept for Piloted Mars Opposition Class Missions," in *ASCEND 2020*, Virtual Event, 2020.

[2] McGuire, Melissa L; Oleson, Steven R.; Burk, Laura; McCarty, Steven; Newman, J. Michael; Martini, Michael; and Smith, David, "NASA GRC Compass Team conceptual point design and trades of a hybrid Solar Electric Propulsion (SEP)/Chemical Propulsion Human Mars Deep Space Transport (DST) Vehicle," in *2018 Aiaa SPACE and Astronautics Forum and Exposition*, Orlando, FL, 2018.

[3] Oberth, Hermann, Ways to Spaceflight, Enlish language translation of the German Language Original "Wege zur Raumschiffahrt" ed., Tunis, Tunisia: Agence Tunisienne de Public Relations, 1970 (1920).

[4] NASA Human Exploration Office (HEO), *Human Exploration Office (HEO) XM-M14282020A margin memorandum,* National Aeronautics and Space Administration (NASA), 2020.

[5] AIAA, "Standard: Mass Properties Control for Space Systems (ANSI/AIAA S-120A-2015 (2019))," AIAA, Reston, VA, 2019.

[6] LaPointe, Michael; Oleson, Steven; Pencil, Eric; Mercer, Carolyn; Di Stefano, Salvador; Gilland, James; and Mason, Lee , "MW-Class Electric Propulsion System Designs for Mars Cargo Transport," in *AIAA SPACE 2011 Conference & Exposition*, Long Beach, CA, 2011.

[7] NASA, "Space Technology MIssion Directorate - Kilopower," NASA, 28 JAN 2021. [Online]. Available: https://www.nasa.gov/directorates/spacetech/kilopower. [Accessed 23 FEB 2021].

[8] R. Taylor, ""Prometheus Project: Final Report,"," Jet Propulsion Laboratory, Pasadena, CA, 2005.

[9] Palac, Donald T., "Fission Surface Power Systems (FSPS) Project Final Report for the Exploration Technology Development Program (ETDP)," NASA Glenn Research Center, Cleveland, OH, 2011.

[10] Northrop Grumman, "Spacecraft Components," 2020. [Online]. Available: https://www.northropgrumman.com/space/spacecraft-components/.

[11] SolAero Technologies, "IMM-alpha Preliminary Data Sheet," April 2018.

[12] Panasonic Batteries, "NCR-18650B Product Data Sheet".

[13] K. Bozak, Y. De Jesus-Arce, J. Soeder, B. Gardner, J. Csank and K. Boomer, "Advanced Modular Power System (AMPS) Project 101," NASA Technical Reports Server, Cleveland, OH, 2020.

[14] K. J. Metcalf, "Power Management and Distribution (PMAD) Model Development: Final Report," NASA Technical Reports Server, Canoga Park, CA, 2011.

[15] National Institute of Standards and Technology, "NIST Chemical WebBook, SRD 69," National Institute of Standards and Technology, 2018. [Online]. Available: https://webbook.nist.gov/chemistry/fluid/. [Accessed 2020].

[16] Yim, John T., ""“A Survey of Xenon Ion Sputter Yield Data and Fits Relevant to Electric Propulsion Spacecraft Integration,”," in *35th International Electric Propulsion Conference*, Atlanta, GA, 2017.

[17] Tuskanom, et al., "Component tests of a LOX/methane full-expander cycle rocket engine: Single-shaft LOX/methane turbopump," in *8th European Conference for Aeronautics and Space Sciences (EUCASS)*, 2019.

[18] Moog, Inc., "Pressure Management Assembly," 2016. [Online]. Available: https://www.moog.com/content/dam/moog/literature/Space_Defense/spaceliterature/propulsion/moog-pressure-management-assembly-datasheet.pdf. [Accessed 11 2020].

[19] Bushway III, E., et al., "A Xenon Flowrate Controller for Hall Current Thruster Applications," in *International Electric Propulsion Conference*, Pasadena, CA, USA, 2001.

[20] Ariane Group, "Bipropellant Thrusters Brochure," [Online]. Available: https://www.space-propulsion.com/brochures/bipropellant-thrusters/bipropellant-thrusters.pdf. [Accessed 12 2020].

[21] Northrop Grumman, "PMD Tanks Data Sheets," 2020. [Online]. Available: https://www.northropgrumman.com/space/pmd-tanks-data-sheets-sorted-by-volume/. [Accessed July 2020].

[22] ARDE, "ARDE Performance Under Pressure," [Online]. Available: https://www.ardeinc.com/copv.html. [Accessed July 2020].

[23] J. R. Buckius and R. O. Howell, Fundamentals of Engineering Thermodynamics, New York: McGraw Hill, 1992.

[24] Ariane, "Ariane Group 300 L Helium Tank (MPCV)," [Online]. Available: https://www.ariane.group/wp-content/uploads/2019/01/11_300LHE_MPCV.pdf. [Accessed 11 2020].

[25] J. Stoltzfus, M. Shoffstall and K. Rosales, "Oxygen Hazards Analysis of Space Shuttle External Tank Gaseous Oxygen Pressurization System," in *Flammability and Sensitivity of Materials in Oxygen-Enriched Atmospheres: 10th Volume*, West Conshohocken, PA, ASTM International, 2003, pp. 230-244.

[26] N. Brugge, "Evolution of Pratt & Whitney's cryogenic rocket engine RL-10," [Online]. Available: https://www.b14643.de/Spacerockets/Specials/P&W_RL10_engine/index.htm. [Accessed 10 2020].

[27] US Military, "Digital Time Division Command/Response Multiplex Data Bus," United States Air Force Life Cycle Management Center - Aircraft Systems, 2018.

[28] Electronic Industries Alliance, *ANSI/TIA/EIA-422-B Electrical Characteristics of Balanced Voltage Differential Interface Circuits,* American National Standards Institute (ANSI), 1975/2005.

[29] Moog, Inc., "Modular Linear Electromechanical Actuators," 2018. [Online]. Available: https://www.moog.com/content/dam/moog/literature/Space_Defense/Space_Access_Integrated_Systems/SAIS_Modular_EMA_Rev_0315.pdf. [Accessed 11 2020].

[30] *Nuclear Technology Heat-Pipe Heat Exchangers for Salt-Cooled Fission and Fusion Reactors to Avoid Salt Freezing and Control Tritium: A Review Heat-Pipe Heat Exchangers for Salt-Cooled Fission and Fusion Reactors to Avoid Salt Freezing and Control Tritium:.*

[31] S. Dye, A. Kopelove, and G.L. Mills, "Integrated and Load Responsive Multilayer Insulation," in *American Institute of Physics (AIP) Conference Proceedings 1218, 946 (2010)*, 2010.

[32] Quest Product Development Corporation, "MMOD-IMLI: Integrated Thermal Insulation and Micrometeoroid/Orbital Debris Protection NASA SBIR Phase 1 Final Report," NASA, 2011.

[33] Quest Thermal Group, "Integrated MLI," 2018. [Online]. Available: https://www.questthermal.com/products/integrated-mli. [Accessed 09 March 2021].

[34] Department of Defense, Composit Materials Handbook, vol. 2, Department of Defense, 2002.

[35] Agarwal, B. D. and Broutman, L. J., Analysis and Performance of Fiber Composites ISBN 0-471-05928-5, New York: John Wiley & Sons, Inc., 1980.

[36] Collier Research Corporation, "HyperSizer," 1995. [Online]. Available: http://hypersizer.com. [Accessed 13 October 2020].

[37] NASA, "Structural Design and Test Factors of Safety for Spaceflight Hardware," NASA, Washington, 2016.

[38] Federal Aviation Administration, Metalic Materials Properties Development and Standardization (MMPDS) Handbook - 11, Columbus, OH: Battelle Memorial Institute, 2016.

[39] Heinemann, Jr., W., "Design Mass Properties II: Mass Estimating and Forecasting for Aerospace Vehicles Based on Historical Data," NASA Johnson Space Center, Houston, TX, 1994.

[40] "Spacecraft Controllers," Moog Inc., [Online]. Available: https://www.moog.com/products/controllers-controls-software/spacecraft-controllers-software.html.

[41] "SP0 | Radiation Tolerant 3U CompactPCI SBC," Aitech, [Online]. Available: https://aitechsystems.com/product/sp0-rad-tolerant-3u-compactpci-sbc/.

[42] "Solid State Recorders," Southwest Research Institute, [Online]. Available: https://www.swri.org/industry/space-engineering/solid-state-recorders.

[43] "Spacecraft Avionics," Moog, Inc., [Online]. Available: http://www.moog.com.

[44] B. G. Drake, *Technical Memorandum XM-M14282020A: Mass Margins for Human Exploration Strategic Assessments,* NASA Exploration Mission Planning Office (XM), 2020.

[45] Space Environment, Effects, and Education System (SPENVIS), "Trapped particle radiation models," SPENVIS, 27 April 2018. [Online]. Available: https://www.spenvis.oma.be/help/background/traprad/traprad.html. [Accessed 25 March 2021].

[46] De Santis, Cristian & Bigazzi, Alberto & Berrilli, F. & Casolino, M. & Del Moro, Dario & Picozza, Piergiorgio & Sparvoli, R. & Vergata, Tor., "A New Debris Detection Algorithm for Orbiting Solar Telescopes.," *Researchgate,* 2021.

[47] Space Environment Information System (SPENVIS), "Grun Model," SPENVIS, 12 March 2018. [Online]. Available: https://www.spenvis.oma.be/help/models/grun.html#. [Accessed 09 March 2021].

[48] L. A. Jackson, Lee's Awesome Book About Editing, Cleveland, OH: NASA GRC Publishing, 2020.

[49] Orbital ATK, "Orbital ATK Space Propulsion Products Catalog," Orbital ATK, Elkton, MD 21921, 2012.

[50] Meisl, Claus J., *"NASA Lewis Research Center Task Order 17, Cost Estimating Relationships (CERs) for Nuclear Power and Propulsion",* Cleveland, OH: NASA Glenn Research Center, 1991.

[51] MOOG, "Spacecraft Manifolds & Propulsion Subsystems," MOOG, 2021. [Online]. Available: https://www.moog.com/products/propulsion-controls/spacecraft/spacecraft-propulsion-components/manifolds-propulsion-subsystems.html. [Accessed 24 March 2021].

[52] MOOG Space and Defense Group, "Moog Pressure Management Assembly (PMA)," Moog, 2016. [Online]. Available: https://www.moog.com/content/dam/moog/literature/Space_Defense/spaceliterature/propulsion/moog-pressure-management-assembly-datasheet.pdf. [Accessed 24 March 2021].

APPENDIX A Ground Rules and Assumptions

A.1 Ground Rules and Assumptions

The NEP-Chem Vehicle design was completed at the request of the Mars Transportation Assessment Study Team and was subject to a number of Ground Rules and Assumptions. A comprehensive list of is below.

A.2 Mars Mission

The following ground rules were applied to the Mars Mission.

- Boots on Mars no later than 2036
- No less than 30 days surface stay time
- Total crew time away from Earth: ~2 years or less
- Propulsion performance and vehicle capabilities must envelope 2039 mission under the same ground rules

The following assumptions were applied to the Mars Mission.

- Orbit insertion, departure, rendezvous maneuvers need to be included in Mars total orbit time (in addition to surface stay time), 2 Mars orbital periods on either side.
- 760 days or less from Trans-Mars Injection to Earth Orbit Capture

A.3 Launch Vehicles

The following ground rules and assumptions were applied to launch vehicles.

A.3.1 General

The use of launch vehicles must be integrated with the campaign launch requirements of the lunar activities.

A.3.2 Space Launch System (SLS)

The following ground rules apply to the SLS.

- Nine (9) SLS 1B launch vehicles need to be expended before the SLS 2 performance is available, as part of the total Moon to Mars campaign.
- An average of 1 SLS cargo per year to support Mars activity, can surge to two in one year.
- Surge to two cargo SLS in a single year must be followed by a year with only one cargo SLS launch.
- SLS cargo launch cadence includes Orion crew launched per year.
- Twelve (12) Orion are available to be used.

A.3.3 Commercial Launch Vehicles

The following assumptions apply to the use of commercial launch vehicles.

- Heavy and super heavy class are assumed to be available. Representative C3 curves were supplied to the team.
- There is no limitation assumed on the CLV launch rate, though there is a desire to minimize peaks in launch demand
- CLV boost stage or service module to move elements around for aggregation must be developed

A.4 Crew Vehicle Payloads

A.4.1 Deep Space Habitat (DSH)

The following ground rules apply to the DSH.

- The Deep Space Habitat is deployed by CLV to NRHO. It can be self-sufficient in NRHO or near Gateway, but does not have propulsive capability to move away from NRHO.
- DSH is launched on two CLVs without logistics to cis-lunar space.
- DSH must return to NRHO/Gateway post Mars mission.
- No power and propellant pass through DSH
- DSH power system is sized to provide 20 kWe EOL power at 1AU; DST must provide power (at least) to make up for the shortfall in power as it goes beyond 1AU
- DSH must be able to easily dock/undock from the transportation elements
- DSH must be able to support docking with Orion while attached to the transport vehicle
- Operational empty mass of 26.4

A.4.2 Logistics and Outfitting

The following ground rules apply to logistics and outfitting.

- Logistics Mass is estimated based on mission time
- Logistics/spare mass based on duration, co-manifested on Orion launch if possible, additional CLV resupply if required.
- 4 Crew: 328 kg
- Payloads and research: 1000 kg
- Propulsion and RCS expendables: 337 kg
- Trash Dump: 11.1 kg/day

A.5 Crew Safety

No crew radiation dose limits were provided for use in this study.

A.6 Cargo Vehicle Payloads

A.6.1 Mars Landers

The following ground rules apply to Mars Landers.

- Mid-latitude landing site: +35 deg
- Three 65 t landers for each crew mission launched on three SLS Block 2 with 8.4 m shroud to high Earth orbit based on SLS performance curve
- The first lander supporting the crew mission will successfully land on Mars before the second lander is launched. Remaining landers supporting the crew mission must be in Mars orbit 18 months prior to crew departure.
- The third lander will transport crew to the surface
- All landers must be delivered to Mars to support a direct sub-perigee landing based on the landing site selection
- The crew DST will arrive at Mars to rendezvous with the Crew lander and support the direct sub-perigee landing of the crew lander from the parking orbit

- Crew Transportation system will position itself at the proper orientation to support a direct, due-East ascent from the MAV for rendezvous

The following assumptions apply to Mars Landers.

- Architecture should minimize the time the landers spend in High Earth Orbit to reduce the MMOD/radiation/thermal risk to the vehicle
- The lander arrival parking orbits will be determines by MTAS trade study with the Lander Element Team
- The crew DST arrival parking orbit will be determined by MTAS trade study with Lander Element Team
- The MAV ascent parking orbit will be determined by MTAS trade study with the Lander Element Team

A.6.2 Mars Surface Payload

The lander payload mass is ground ruled to 25 t.

A.7 Solar Power

The following assumptions apply to the use of solar power.

- Minimum 32% efficient solar cells (IMM or similar)
- Large area solar cells (60 to 80 cm^2)
- For deployed solar arrays, use flexible blanket array technologies
- For body-mounted solar arrays use rigid panel array technologies
- Use UltraFlex®/MegaFlex® for deployed solar arrays with high strength requirements (>0.05 g)

A.8 Electric Propulsion

The following assumption applies to the use electric propulsion. Single thruster power level not to exceed ground test capability of existing facilities with pumping augmentation or new EP test chamber based on existing high-vacuum technology.

A.8.1 Hall Thruster Performance Characteristics

The following assumptions apply to Hall thruster performance.

- 100 kW single thruster power level
- 2600 seconds I_{SP}
- 60% thruster efficiency
- 8 ton propellant throughput
- Xenon propellant
- Alpha: 3.3 kg/kW (thruster/DDU/XFC/harness w/o growth)
- 99% DDU efficiency (direct drive discharge)
- 650 VDC direct drive from PMAD to DDU

A.9 NEP Power

The following assumptions apply to NEP power.

- NEP power system consists of reactor, shield, power conversion, heat rejection, and PMAD.
- System operational life is 2 years at full power, allowing for at least one-round trip mission with residual life for contingencies.
- Reference reactor includes pumped lithium heat transport, 19.75% enriched UN fuel, refractory cladding/structure, and 1200 K reactor outlet temperature.

- Primary reactor trade study variables include coolant type, fuel type, uranium enrichment, and reactor outlet temperature.
- The lithium heat transport loop includes 8 separate Li-to-HeXe heat exchangers that service individual Brayton power converters
- Reactor thermal power is based on required Brayton thermal input power to achieve desired system electric power output.
- Reactor control utilizes negative-temperature reactivity feedback to permit automatic thermal load following and control rod position adjustment to permit reactor outlet temperature management.
- Reference shield is LiH/W truncated cone with 70 m payload separation, 26 deg cone half angle, reactor radiation less than 1E11 n/cm^2 and 25 krad at payload after 2 years at full power.
- Primary shield trade study variables include payload separation distance, half angle, and payload radiation limits.
- Reference power conversion is closed cycle, recuperated Brayton with 8 independent converters providing 12.5% power per converter.
- Primary trade study variables include turbine inlet temperature, compressor inlet temperature, working fluid, number of converters and sparing approach.
- Total Brayton output power is based on summation of EP thruster loads, spacecraft housekeeping loads, and NEP power system parasitic loads (PMAD, pumps, drive motors, etc.)
- Reference design assumes supercritical CO_2 Brayton with 1150 K turbine inlet.
- Other power conversion technologies such as Stirling, Rankine, thermoelectric, and thermionic are not considered in the current trade-space due to performance and/or technical maturity deficiencies.
- Reference heat rejection includes pumped NaK heat transport and deployable, composite radiator panels with embedded H_2O heat pipes.
- Each Brayton converter has a dedicated NaK cooling loop and radiator segment. Reference design assumes 8 independent NaK cooling loops providing 12.5% heat rejection per loop.
- Overall radiator sizing is based on producing maximum system power with 4 K thermal sink and 10% radiator area margin. System power will vary based on thermal sink.
- Radiator stowed volume and corresponding radiator area is based on launch vehicle payload fairing geometric limits. Reference radiator packaging concept permits up to 2500 m^2 radiator in SLS payload fairing. Alternative radiator packaging concepts may be considered.
- Radiator is integrated with deployable boom that extends reactor to specified separation distance to achieve shield radiation limits. Reference boom includes nested, telescoping trusses that accommodate radiator fluid lines and power transmission cabling.
- Reference PMAD includes power cabling, power conditioning, power control, and switchgear to supply electric power to a one 650 VDC EP bus and one 120 VDC spacecraft bus. EP bus voltage may be varied depending on EP thruster selection.
- Each Brayton converter has a dedicated power transmission channel that terminates at the switchgear. Reference design assumes 8 independent 960 Vac transmission channels providing 12.5% power per channel. Brayton transmission voltage may be varied based on EP bus voltage.
- PMAD power conditioning includes power electronics to convert AC transmission voltage to required DC bus voltages.
- PMAD power controls include channelized parasitic load radiator to regulate Brayton unit operating speed and power output.

- PMAD power controls include NEP power system health monitoring and control with functionality for system startup, full power operation, part power operation, power standby, and shutdown.
- NEP power system parasitic loads including reactor pumps, reactor control drives, radiator pumps, and health monitoring are fed by 120 VDC spacecraft bus.

A.10 Cryogenic Systems

A.10.1 Overall Design Description: Oxygen or Methane Storage

The following assumptions apply to Oxygen or Methane storage.

- Baseline assumes metallic tanks.
- AL 2090-T83 or similar; AL 2195; or similar
- Mass of tank internals (Liquid Acquisition Devices, slosh baffles, TVS*, mass gauge) estimated as 10 to 12% of metallic tank mass
- *A TVS system is assumed to be required for robust tank pressure control until zero boil-off storage is activated.
- The use of spray-on foam insulation (SOFI) can be traded versus a dry nitrogen purge of the MLI.
- The oxygen and methane tanks will be insulated with load bearing MLI (LB-MLI)
- The tank will be actively cooled with a single-stage distributed cooling system [i.e., Broad Area Cooling, (BAC)], utilizing tubing to carry cooled gas around each tank and appropriate structure and plumbing interfaces to intercept heat before it reaches, or remove heat from, the propellant.
- Includes an approximately 90 K tube on tank stage (neon gas working fluid).
- The 90 K shield will be supported by an “inner” LB-MLI blanket
- An LB-MLI blanket will be attached to the tank and will have MMOD materials integrated with it.
- An outer aluminum MMOD shield will be attached to the external layer of the outer LB-MLI blanket.
- The 90 K refrigerators will be reverse turbo-Brayton (RTB) cycle cryocoolers (specifications below) which include refrigerant gas circulation.
- The 90 K distributed cooling system will also intercept heat from the conductive loads to the tank (structural support, plumbing, and instrumentation connections to the tank).

A.10.2 Insulation and Shield Details

The following assumptions apply to insulation and shielding.

- Figure 6-1: Methane and Oxygen Tank MLI and Shield Stack up.

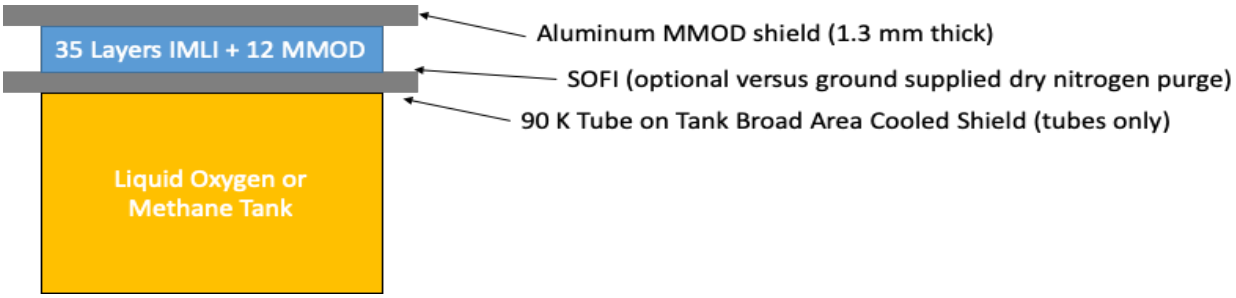

Figure 6-1 Methane and Oxygen Tank MLI and Shield Stack Up

A.10.3 MLI/MMOD: 9.4 cm Thickness

The following assumptions apply to the MLI/MMOD design.

- 47 layers of reflectors/MMOD material total
- MMOD layers – each replaces a reflector
- 6 layers of Nextel (Typical NASA MMOD)
- 6 Layers of Kevlar (Typical NASA MMOD)
- Mass of MMOD layers assume MMOD material mass plus LB-MLI layer (below)
- Any changes in MMOD due to traded CONOPS should be consistent with NNX11CG46P final report results.
- 35 reflector layers
- Heat flux between 90 K (CBT) and 255 K (WBT) = 0.16 W/m^2
- 0.07 kg/m^2/layer

A.10.4 MMOD Aluminum Shield

- An outer MMOD shield of typical NASA design is attached to the exterior of the outer MLI.
- Thickness: 1.3 mm

A.10.5 Propellant Loss dues to Leakage: Hydrogen, Oxygen, and Methane

- Metal tankage assumed as baseline
- Valve leakage is assumed to be dominated by through the valve pathways.
- Typically tank isolation valve leakage is into the coupler plumbing or the reactor
- Fill, Vent and relief valves leak out of the system
- Automated coupler leakage is assumed to be radial out of the system
- With tank isolation valves closed, the coupler leakage is ignored
- Valve leakage rates for estimating losses from key components are as given in the table. The per-valve leakage should be multiplied by the number of valves at each size that has a pathway external of the vehicle and the duration the valve is pressurized with hydrogen to determine total leakage.
- Valves used for leakage calculation have liquid cryogen against the seals.

A.11 Programmatic Considerations

A.11.1 Overarching Goals

The following ground rules apply to the overarching goals.

- Reference case is to be “minimally viable”
- Propulsion system for the first mission will not be reused
- Minimize crew time away from Earth
- Identify potential assets, capabilities, systems, and subsystems, required to conduct current Lunar program can be used, within stated limits, to support the Mars transportation development and ConOps

The following assumption applies to the overarching goals.

- Identify technology to improve performance, mitigate risk, and/or reduce cost

A.11.2 Figures of Merit

The following figures of merit are assumed.

- Safety and Mission Success
- Redundancy
- Abort Options
- Loss-of-Campaign Risk
- Program Robustness
- Policy & Change Resilience
- Affordability
- Development Risk
- Logistics Risk
- Technology Development Cost
- DDT&E Cost
- Facilities Cost
- Operations Cost

A.11.3 Element Need

The following ground rule must be met: perform an in-space habitation and propulsion system shakedown mission prior to first crew mission departure

A.12 Risk Posture

A.12.1 Mars Operations

- Pre-position of return elements/propellant for crew transportation is an acceptable risk trade

A.12.2 Orbital Maneuvering - Earth Orbit

- 90 Day launch window for crew prior to TMI.
- 30 Day launch window for crew post EOI.

A.12.3 Orbital Maneuvering - Mars Orbit

- 2 rendezvous opportunities after MOI with crew lander.
- 2 rendezvous opportunities prior to TEI with ascent stage.

A.12.4 Margin Strategy

Mass Margin

- Align with HEO XM-M14282020A margin memorandum [44].
- Manager’s reserve is book-kept with payload elements and launch vehicles; no additional manager's reserve applied to transportation system
- Propellant Residuals:
    - 2.5% High thrust chemical systems.
    - For electric propulsion systems, residual mass is calculated by multiplying the density of electric propellant (at the lowest rated operating pressure of the feed system modules and a nominal temperature) by the tank volume. It is not a straight percentage of the used propellant plus the margin xenon propellant load

    - RCS residuals covered by High Thrust Chemical Systems

Performance Margin:

- High Thrust Chemical Systems:
    - 5% ΔV margin on all ΔV maneuvers
    - 10% propellant reserve on all ACS maneuvers
- Low Thrust Electrical Propulsion Systems
    - 6% carried as propellant margin.
    - No fixed coasting period assumed for crewed missions.

System Redundancy

- All systems must be single fault tolerant except propellant tanks and structures.
- Mission must close with single fault return from Mars on all turbomachinery systems e.g., rocket engines (not EP thrusters), cryocoolers, Braytons

APPENDIX B NEP Cargo Option

B.1 Introduction

An opposition Mars mission by nature has only a roughly one month stay on the surface of Mars. While this reduces the landed infrastructure mass, the mission still requires three 25 t landers (a Mars Ascent Vehicle, a Cargo lander, and the crew lander with rover) each with a delivered on-orbit mass requirement of 65 t (includes the aero-descent landing system in addition to the landed cargo.) The Cargo GR&A are summarized below.

B.2 Cargo Ground Rules and Assumptions

- Mid-latitude landing site: +35 degrees
- Three (3) 65 t landers for each crew mission launched on (3) SLS Block 2 with 8.4 m shroud to high Earth orbit based on SLS performance curve
    - The lander payload mass is 25 MT while the landing system is 40 MT.
- Two of the three landers must be pre-deployed to Mars and arrive at least 18 months prior to crew arrival.
- The third lander will transport the crew to the surface.
- Architecture should minimize the time the landers spend in HEO to reduce the MMOD/radiation/thermal risk to the vehicle.
- All landers must be delivered to Mars to support a direct sub-perigee landing based on the landing site selection.
- The lander arrival parking orbits will be determined by MTAS trade study with the Lander Element Team.
- The crew DST will arrive at Mars to rendezvous with the Crew lander and support the direct sub-perigee landing of the crew lander from the parking orbit.
- The crew DST arrival parking orbits will be determined by MTAS trade study with the Lander Element Team.
- Crew Transportation system will position itself at the proper orientation to support a direct, due-East ascent from the MAV for rendezvous.
- The MAV ascent parking orbit will be determined by MTAS trade study with the Lander Element Team.

B.3 NEP-Chemical Cargo Options

In order to simplify the architecture and save cost, it was preferred to use elements of the NEP-Chemical transportation system to deliver the cargos to Mars. Thus the elements under consideration were the Nuclear Electric Propulsion Element, the Xenon Interstage Element, and the Chemical Stage. These vehicles can be used in in several ways depending upon where the landers are placed by the SLS for pickup and what combination of NEP and chemical stages would be used. At the two extremes are 1) all chemical, and 2) all NEP. The all chemical case would require many propellant stages and/or tanker launches while the all NEP would require launching the cargos to low earth orbit and spiraling to escape. While the all NEP option should be evaluated the impact of Van Allen belt radiation on the landers as well as the placement of the landers in LEO should be assessed first. Another all NEP option would be to spiral to the medium Earth orbits (MEO) and pick up the landers there. Unfortunately, the landers require three years of SLS launches and keeping them in the MEO orbit would be costly from aspects of orbit maintenance and radiation. For this quick mission assessment it was decided to use CLV stages to push the landers from MEO to NRHO where they could be more benignly stored while an NEP Module spiraled up from LEO to NRHO.

The selected NEP option would only require an SLS launched NEP Module, a super heavy CLV launched Xenon Interstage and six CLV heavy upper stages to push the landers for storage in NRHO (an additional CLV stage would be needed to push the NEP vehicle to 1100 km for reactor startup.) The NEP Module would be the same as that used

by the piloted mission and the Xenon Interstage would be similar except for the addition of two more docking ports to allow carrying three lander cargoes.

B.4 NEP Cargo CONOPS

A cargo vehicle CONOPS is described below to support a piloted 2039 mission. The customer wanted to 'test' the first lander so it had to be sent using a copy of the piloted vehicle chemical stage (which provides a good demonstration flight for the long duration chemical stage).

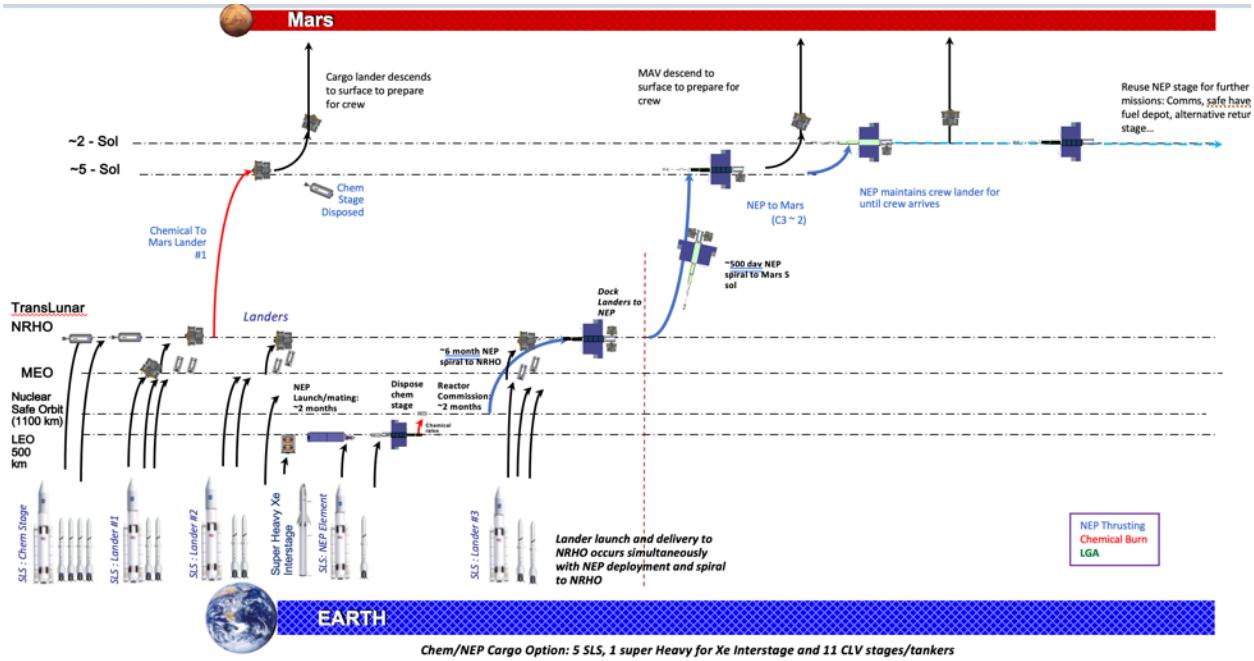

Figure 6-2 NEP Cargo to Mars (2037)

Figure 6-2 above shows the top-level CONOPS for a 2037 Conjunction 'one-way' cargo mission to deliver a first lander with the chemical stage and the second and third 65 t landers to a Mars 2 sol orbit using an NEP Module. CONOPS phases are further defined below for each specific element (Nuclear Electric Propulsion, Xenon Interstages, and Cargo Landers). The landers will be launched to MEO using three SLS cargo launchers. From there, each lander will be boosted by two heavy CLV stages to NRHO to wait for the NEP delivery vehicle. This NEP vehicle is identical in design to the crew NEP Module. An additional Xenon Interstage with side docking ports to attach two landers is also required in addition to a heavy class CLV launched chemical stage to lift the NEP Module to 1100 km for reactor commissioning. The Xenon Interstage carries the xenon to spiral the NEP Module and its Mars xenon propellant to NRHO to pick up the landers. Due to the late study baseline change of sending the first lander separately the NEP cargo stage is still sized to carry an additional 65 t of payload. (It was originally designed to carry three landers.) Further studies should explore whether a spare lander, additional propellants, or spare habitat should be carried. The NEP cargo vehicle could then provide an alternate path home for the crew.

The CONOPS figure illustrates that the assembly and fueling of the NEP transportation vehicle could be quick. The spiral out of the transportation system to NRHO (where it meets up with the cargoes) will take only six months exclusively using the NEP system. This spiral will be a 'shakedown' cruise for the NEP Module system.

Launch and Assembly Phase (~6 months): A 500 km, 28.5° orbit was chosen for commissioning and fueling due to its benign qualities of low orbital debris and Van Allen belt radiation. In addition, 500 km is a sufficiently low orbit to allow commercially launched crew to assist in assembly of the NEP vehicle if needed. Only one SLS launch will be required to launch the NEP Module. Simultaneously one super heavy CLVs will launch a Xenon Interstage (fully fueled). Both elements will have sufficient propulsion, power, and docking equipment to loiter at 500 km LEO and dock to each other. At some point the NEP Module will deploy its reactor boom and electric thruster booms but not will not start its reactor.

Boost to Nuclear Safe Orbit (1-2 days): Once the NEP Module and the Xenon Interstage are docked, a CLV stage will be docked to the two elements and will perform two burns to lift the transportation stack to an 1100 km nuclear safe orbit. This phase should only take a day or so to complete.

Reactor Commissioning Phase in Nuclear Safe Orbit (1-2 weeks): Once at 1100 km the reactor will be started using the commissioning solar arrays for power. For startup, the control system will activate the control rod ~1 kW for 1 hour while simultaneously warming up the power systems. The Brayton's will be rotated using ~10 kWhr of energy over 4 hours. The radiators will be deployed in sections (pointed at the sun) as they receive the hot Brayton coolants. Once the reactor and the electric propulsion system have been checked out, the NEP Module and Xenon Interstage will begin their spiral to NRHO.

Spiral to NRHO (6 months): The spiral to NRHO will exclusively use the NEP system for thrusting. The integrated transportation system includes all the xenon propellants for the subsequent Mars mission, eliminating any fueling at NRHO. Analyses of the Van Allen radiation belt impact show that only ~5 krad of radiation on the electronics, mainly from the proton belts, is expected assuming proper shielding (~10 mm). (See Section 4.3, Thermal Control System for further analyses.)

Docking of the two landers at NHRO (1-2 weeks): Once in the NRHO, the two landers will rendezvous and dock with the NEP stack at the two side-docking ports. Options for filling the third, inline docking port slot are left for future studies. The NEP Module provides power and communications for all cargos all the way to Mars.

Mars Mission (~2 years) Phase: Once assembled the NEP vehicle and cargoes will directly depart for Mars. An approximately 500 day transfer to Mars occurs using only electric propulsion. The vehicle captures and spirals down to a 2 SOL elliptical orbit where it deploys one of the two landers (the MAV) to allow it to prepare for the crew landing 19 months later. The last lander for the crew is kept attached to the NEP vehicle until the crew arrive to use it for descent to the surface.

- SLS Chemical Stage Launch to NRHO 2033
    - Chemical stage loaded with four CLVs in NRHO (2033-2034)
- Assumes all three cargos launched with SLS and moved to NRHO using CLV stages
    - #1 lander in Mid 2034
        - #1 lander pushed to Mars using chemical stage in 2035
    - #2 lander in 2035
    - #3 lander in 2036
- Super Heavy launch: Xenon Interstage (88 t Xe), CLV: Boost chem stage (~25 t propellant), SLS: NEP Module
- NEP launches Jan. 2036 on SLS
    - NEP vehicle departs 1100 km June 2036
    - NEP vehicle arrives in NRHO Nov 2036
    - NEP vehicle takes itself and fuel to NRHO
        - ~40 t of Xe spiral, ~55 t of Xe interplanetary, 5 months
    - NEP meets with Landers in NRHO Nov 2036
    - NEP with cargo departs from Earth Dec 2036
- Last two cargos arrive at Mars May 2038 using NEP

At this point the NEP vehicle's primary mission is complete but with additional propellants and equipment this large, high power asset with multiple docking ports could be used for a multitude of uses. Some uses may require that additional elements be added to the vehicle and transferred to Mars.

- Crew Haven: NEP vehicle provides a backup orbital habitat for the crew starting with the first mission.
- Crew Taxi: Would allow the NEP cargo vehicle to spiral down to low Mars orbit to wait for the crew ascent in low orbit and shuttle them to the crew NEP vehicle in the higher, 2 sol orbit. (Would significantly reduce the size of the MAV – allowing all it to fit on one lander without needing refueling.)
- Alternate Return Vehicle: With sufficient xenon and habitat it could provide an alternate return path to Earth.
- Propellant Depot: Could deliver, maintain, and disperse propellants to piloted vehicles.
- Storage for ascent vehicle re-use: Could provide a platform to dock the used ascent vehicle, re-fuel, and refit it for further use.

B.5 Cargo Variant Propulsion System

The cargo variant of this design requires some changes to the propulsion system, primarily the chemical propulsion module. The EP thrusters, xenon feed system, DDUs, and RCS on the nuclear power module remain unchanged. One Xenon Interstage module is required, which is also same as the baseline variant in terms of propellant tanks and feed system operability, but is structurally modified to add two passive docking systems. The chemical propulsion module, however, is much smaller than the baseline design. It is only required to carry 23.4 t of chemical propellant to raise the vehicle stack to 1100 km, where it is jettisoned. It is also required, however, to bring 940 kg of RCS propellant and 15 t of xenon. This is accomplished with a modified Flacon Heavy upper stage carrying additional RCS and xenon tanks. It also utilizes its existing chemical propulsion system for the boost to 1100 km. When docked with the vehicle stack, the additional xenon tank is plumbed into the xenon feed system as if it were another Xenon Interstage module. This allows for the inter-tank xenon transfer, via the compressor located in the nuclear power module, to be accomplished prior to the stage being jettisoned.

B.6 Cargo Reference Cases

Both all-Chemical and all-NEP cargo cases were analyzed for this study. Landers meant to be prepositioned on the surface are captured into 5-sol orbits. Since the crewed vehicle descends from a 2-sol orbit, the crewed lander will need to capture into a 2-sol orbit. ΔVs to reach both of these orbits were provided for each mission option.

Both the all-Chem and all-NEP cases were designed to arrive prior to the crewed vehicle in 2039. The all-Chem cargo mission departs during the 2035 opportunity. Forcing the all-NEP cargo mission to arrive 2 years prior to the crewed mission similar to the chemical case results in undesirable mission timing. Delivering cargo via all-NEP during the 2035 opportunity requires an early delivery of the NEP cargo vehicle to the NRHO limiting the development timeline. Cargo delivered during the 2037 opportunity relaxed the NEP Module development timeline but the optimal cargo mission arrives at Mars in mid-2038, only ~1.5 years prior to crew arrival. Constraining the mission to arrive exactly two years before the crewed mission is very costly. Instead, the decision was made to target a spring arrival for the cargo in 2038.

The chemical cargo mission departs Earth in June, 2035 from the SLS injected orbit. For a 65 t lander this is approximately a 185 x 16,000 km orbit. Following TMI from this orbit, the vehicle coasts during transit until the required Deep Space Maneuver (DSM) after which the cargo vehicle continues the coast until reaching Mars and performing the MOI burn to capture into orbit. The transit from Earth to Mars takes approximately 280 days, arriving in April, 2036. The chemical mission was envisioned to deliver a single lander. The burns were modeled impulsively. The ΔVs provided in Table 6-1 can be used to approximate the propellant load required to deliver any number of landers.

Table 6-1 2035 All-Chem Cargo ΔVs to 2-sol and 5-sol Orbits

	ΔV (m/s)
185 x 16,000 km to 5-sol	3178
185 x 16,000 km to 2-sol	3233

Unlike the all-Chemical cargo vehicle, the 1.9MW all-NEP cargo vehicle was designed to deliver all three 65 t landers into Mars orbit in a single mission. Two landers will be delivered into a 5-sol orbit and one lander plus the NEP cargo vehicle will insert into a 2-sol orbit to await rendezvous with the crew. The all-NEP cargo case departs directly from the NRHO with all three landers on December 9, 2036. The NEP system will thrust during the interplanetary transit and then spiral into the 5-sol orbit. After dropping off 2 landers in this orbit the NEP cargo vehicle and remaining lander will spiral down to the 2-sol orbit. This trajectory was constrained such that arrival in the 2-sol orbit is no later than April 1, 2038 in order to extend the time between cargo delivery and crew arrival as much as possible without increasing the ΔV drastically. The all-NEP cargo ΔVs are provided in Table 6-2.

Table 6-2 All-NEP Cargo ΔVs to 2-sol and 5-sol Orbits

	ΔV (m/s)	Arrival Date
NRHO to 5-sol orbit	6950	May 15, 2038
5-sol orbit to 2-sol orbit	265	May 31, 2038

APPENDIX C Radiation in Orbit

The Van Allen belts that encircle the earth are composed of high energy protons and electrons. The radiation dose within these belts can be significant depending on the amount of time the spacecraft resides within the belts during its transit from LEO to NRHO. The radiation belts are composed of two segments and inner belt composed mainly of high energy protons and lower energy electrons and an outer belt composed of high energy electrons, as illustrated in Figure 6-3. The inner belt extends from approximately 500 km altitude to 13,000 km altitude. The proton energies within the inner belt are greater than 10 MeV. There is also a low energy electron belt residing within this altitude range. The low energy electrons have energies between 1 and 5 MeV. The outer belt consists of high energy electrons and extends from approximately 16,000 to 45,000 km altitude. The electrons within this belt have energies between 10 and 100 MeV.

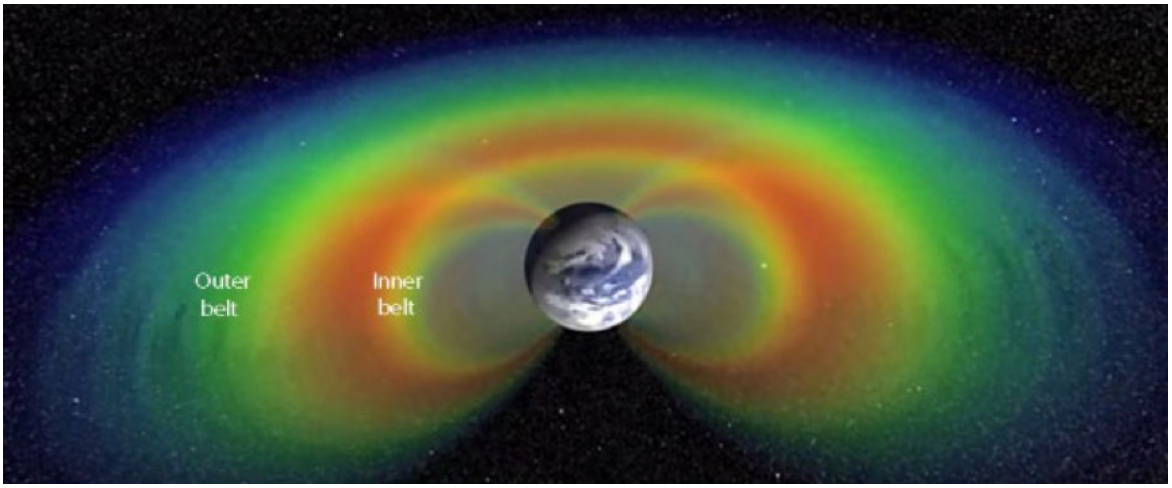

Figure 6-3 Van Allen Radiation Belts

As seen in Figure 6-3, the belts form a torus surrounding earth. The belts follow the magnetic field lines of the Earth dropping down into the atmosphere near the poles, which is the source of the northern lights. Because of the shape of the belts the intensity will vary with both altitude and the orbit inclination. The particle energy for both the inner and outer belts is shown in Figure 6-4.

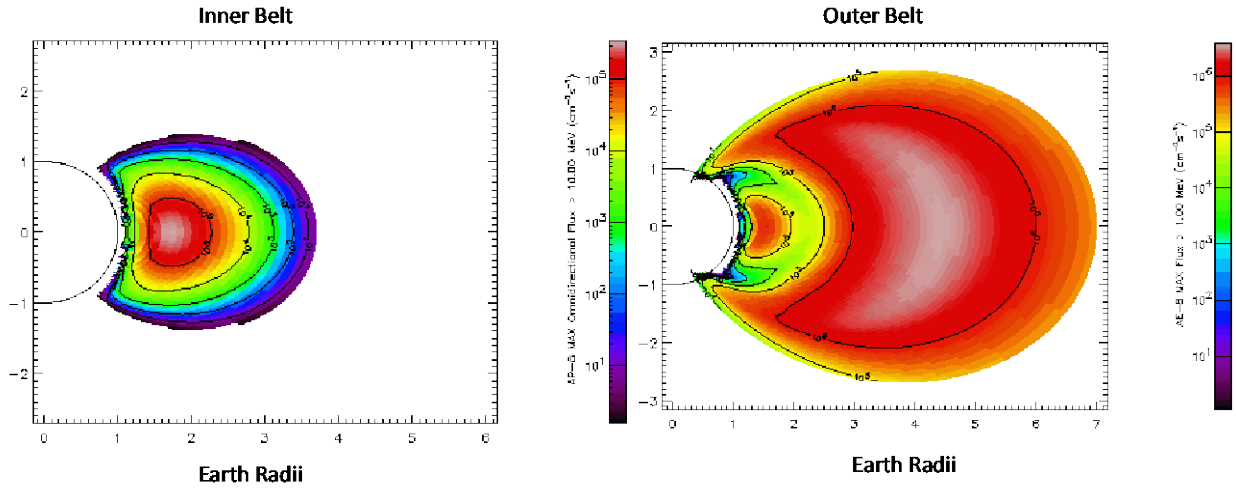

Figure 6-4 Inner and Outer Radiation Belt Particle Energies [45]

It should be noted that although a larger portion of the outer belt has higher energy particles because it is mainly made up of electrons, the damage done is less than for the inner belt which is mainly composed of heavier protons. For an uncrewed vehicle, the main concern for damage is silicon-based electronics. Electronic devices are susceptible to radiation damage and usually have lifetime dose exposure limits of 100 kRads for space-rated components.

The sun goes through a cycle every eleven years on average. This cycle, termed the solar cycle, affects the strength of the Van Allen radiation belts surrounding Earth. The magnetic field strength of the sun along with the intensity of solar particles emitted from the sun vary with the cycle. This cycle also effects the sunspots visible on the sun and is also called the sunspot cycle (Figure 6-5). The variations in the solar cycle cause variations in the strength and position of the Van Allen radiation belts. These factor into the total dose experienced as the spacecraft traverses through the belts. The analysis performed on the radiation dose from the belts was done for both solar minimum and solar maximum conditions. These represent the two extremes within the solar cycle. The actual dose will be between these two extremes depending on the state of the cycle when the spacecraft is traversing the belts.

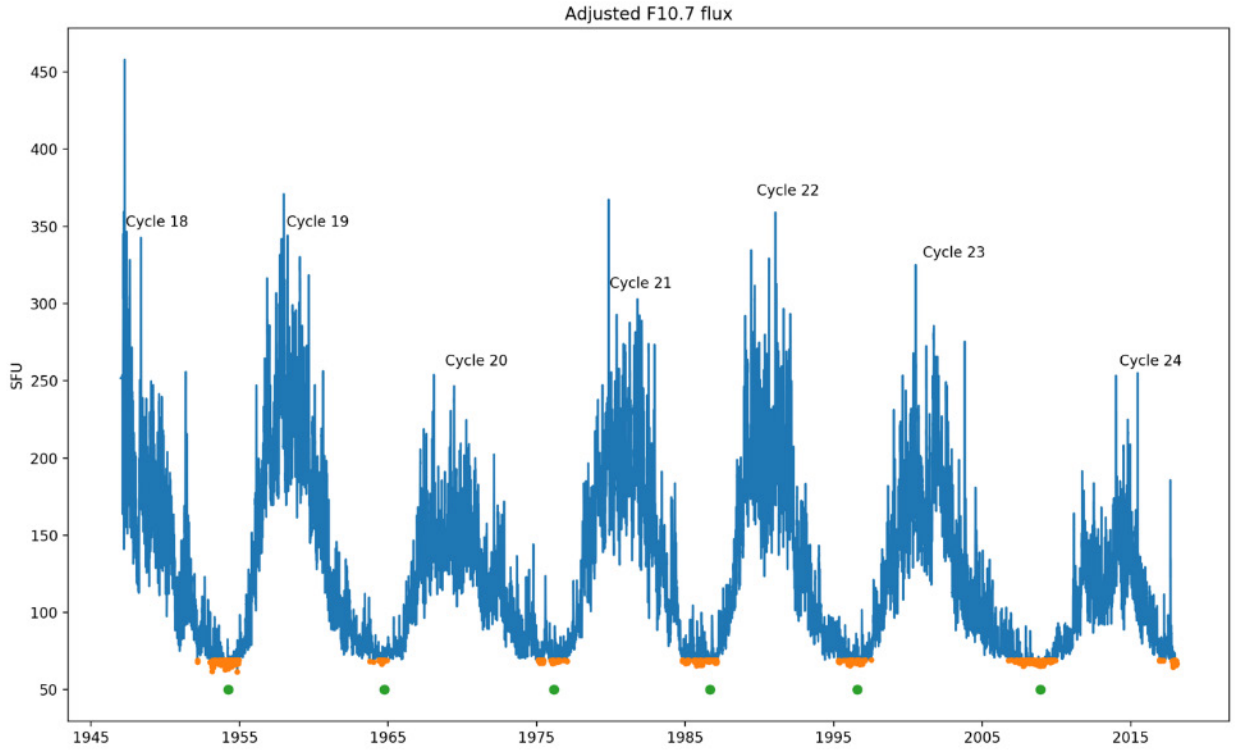

Figure 6-5 Graph of Solar Cycle Based on F10.7 Flux Output

The NEP spacecraft will spiral out from its buildup LEO to NRHO. The inclination of this transfer orbit as well as the duration of the spiral out from LEO to NRHO will determine the dose that is experienced by the electronics during transit. Seven different orbits were evaluated for the radiation dose that the electronics would experience in transit. Table 6-3 Case Orbit Specifications lists these orbits. The orbits were all generated from an initial 2,000 km circular Earth orbit with 70 N total thrust and an I_{sp} of 2,600 s.

Table 6-3 Case Orbit Specifications

Case	Spacecraft Mass (tons)	Orbit Inclination	Transfer Time (days)	Delta V (km/s)
1	260	28.5°	274	5.693
2	260	51.6°	330	5.989
3	370	28.5°	431	5.695
4	370	51.6°	453	5.988
5	285	28.5°	190	5.672
6	405	28.5°	189	6.076
7	450	28.5°	507	6.107

The radiation dose experienced by the silicon-based electronics was calculated by utilizing various modeling codes with the analysis tool SPENVIS. The modeling tools used include:

- Orbit generator developed by the European Space Agency (ESA)/European Space Operations Center (ESOC): This tool specifies the orbit based on a number of input parameters. Orbits are generated incrementally as the spacecraft spirals outward. Orbits are generated at 10 day increments during the spiral and used for the radiation and dose analysis.
- Trapped Proton Model AP-8 developed by the National Space Science Data Center (NSSDC): This model is used to determine the proton flux for the specified orbit. Cases are run for both solar maximum and minimum conditions.
- Trapped Electron Model AE-8 developed by NSSDC: This model is used to determine the electron flux for the specified orbit. Cases are run for both solar maximum and minimum conditions.
- Ionizing Dose Radiation Model SHELDOSE-2 developed by NIST is used to determine the dose on the silicon electronics over a range of aluminum shielding thickness. This dose is based on the trapped proton and electron fluxes previously determined.

Case 7 was used as the transfer orbit for this spacecraft transfer from LEO to NHRO. The results for this case are shown below.

Case 7: 450 ton, 28.5° Inclination

The case 7 orbit is shown in Figure 6-6 and Figure 6-7. The spacecraft leaves the belts after approximately 360 days. The spacecraft leaves the inner radiation belt after approximately 226 days then enters the outer belt at 248 days. It then remains in the outer belt for 109 days leaving after 360 days from the beginning of the transit.

The orbital parameters and the dose experienced in ten-day increments in the transfer through the belts is show in Table 6-4 for solar minimum and Table 6-5 for solar maximum. The dose rates are also graphed in Figure 6-8 and Figure 6-9 respectively. The dose rates shown are for 3 mm of aluminum shielding. This is the typical amount of shielding associated with standard electronics boxes and spacecraft installation structure. To reduce the dose, rate the shielding thickness can be increased. The dose rates and total dose for 1 cm of aluminum shielding are shown in Table 6-6 and Table 6-7, and Figure 6-10 and Figure 6-11 for the solar minimum and maximum, respectively.

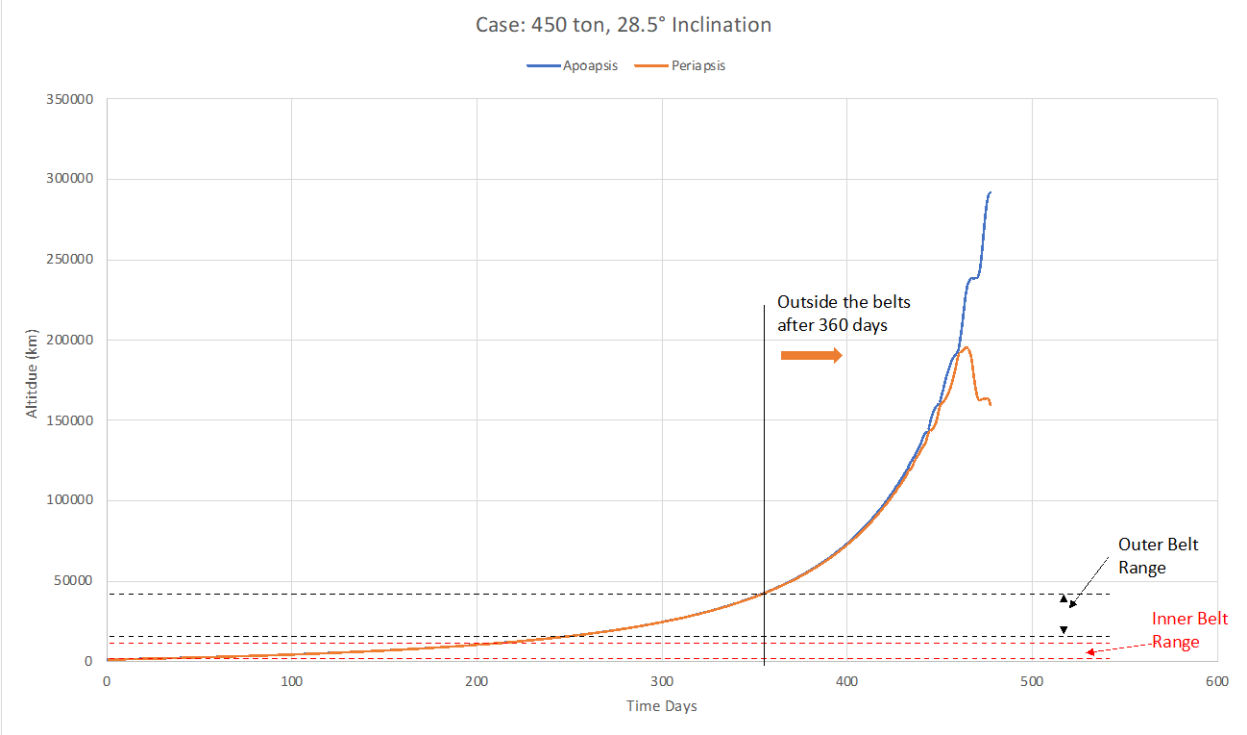

Figure 6-6 Case 1 Orbit from 2000 km Altitude to NRHO

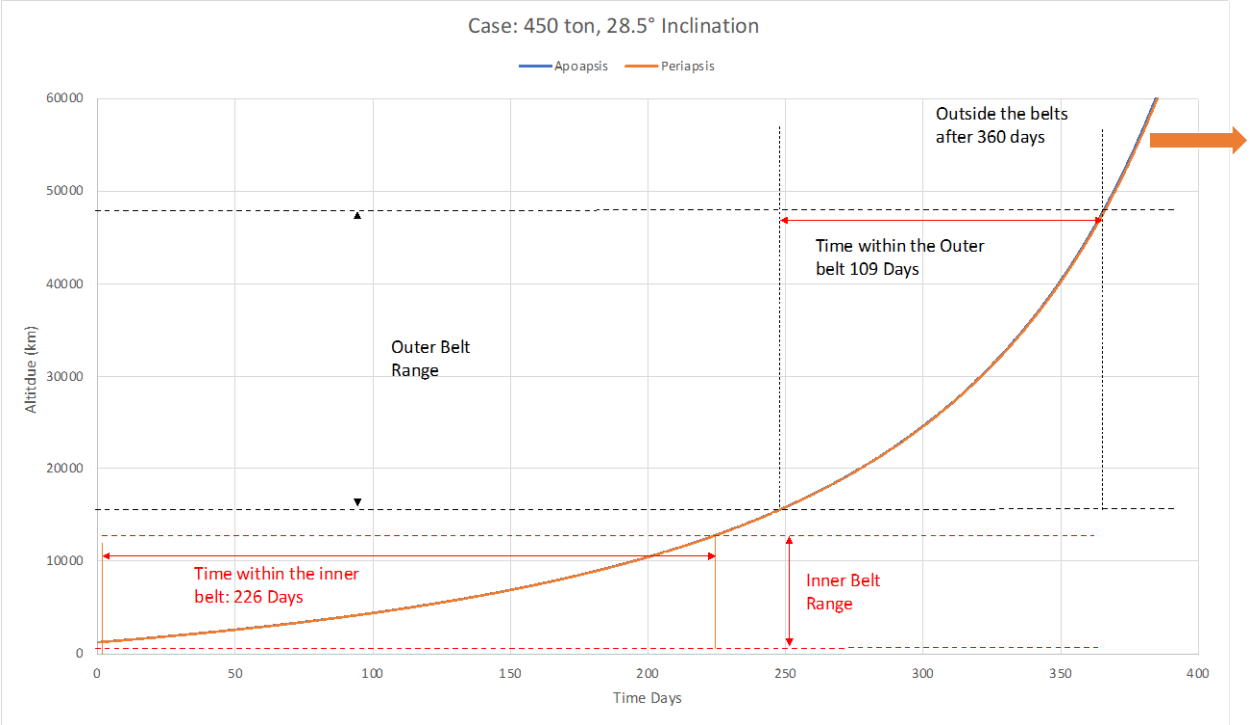

Figure 6-7 Case 1 Orbit Showing Duration Within the Radiation Belts

Table 6-4 Case 7 Orbital Parameters, Dose Rate and Total Dose for Solar Minimum with 3 mm of Aluminum Shielding

Time (Days)	Perigee (km)	Apogee (km)	Inclination	Right Ascension Node	Argument of Perigee	True Anomaly (deg)	Rads/year	Dose Rate/Day	Dose
0.00	1202.06	1217.87	28.51	322.65	225.85	48.15	1.01E+04	27.53	0.00
10.00	1446.16	1461.34	28.51	322.65	230.34	217.39	2.43E+04	66.58	470.61
20.00	1702.42	1718.89	28.51	322.65	225.46	27.09	5.13E+04	140.60	1035.97
30.00	1973.69	1989.65	28.51	322.64	230.34	230.73	9.24E+04	253.01	1967.81
40.00	2259.71	2276.63	28.51	322.64	230.23	196.80	1.42E+05	389.86	3214.27
50.00	2562.32	2579.61	28.51	322.64	224.96	348.57	1.92E+05	525.21	4576.40
60.00	2882.66	2899.88	28.51	322.63	224.62	347.63	2.38E+05	650.96	5879.55
70.00	3222.86	3239.57	28.51	322.63	226.62	280.73	2.76E+05	755.89	7034.58
80.00	3583.07	3600.77	28.51	322.63	230.37	201.17	2.72E+05	746.03	7511.03
90.00	3965.52	3984.26	28.51	322.62	232.45	154.44	2.50E+05	684.38	7151.01
100.00	4373.73	4391.31	28.51	322.62	232.70	214.36	2.32E+05	635.89	6601.80
110.00	4806.52	4827.64	28.51	322.62	226.82	77.99	1.99E+05	545.48	5907.65
120.00	5269.89	5291.29	28.51	322.62	232.59	140.09	1.60E+05	439.45	4925.05
130.00	5764.23	5786.81	28.51	322.61	230.23	113.13	1.32E+05	361.37	4003.56
140.00	6294.13	6316.91	28.51	322.61	223.79	56.21	1.04E+05	284.93	3231.38
150.00	6863.11	6884.78	28.51	322.61	218.81	16.45	8.07E+04	221.15	2530.30
160.00	7472.06	7496.40	28.51	322.61	219.30	42.52	6.54E+04	179.18	2001.35
170.00	8129.99	8151.58	28.51	322.61	240.89	181.92	5.34E+04	146.30	1627.79
180.00	8836.94	8860.58	28.51	322.60	241.59	158.78	5.28E+04	144.55	1454.28
190.00	9600.89	9626.53	28.51	322.60	216.18	30.93	6.02E+04	164.82	1546.45
200.00	10428.16	10455.84	28.51	322.59	240.61	145.66	7.88E+04	215.86	1903.77
210.00	11332.34	11349.41	28.51	322.59	222.38	277.48	1.02E+05	278.08	2469.80
220.00	12301.89	12336.20	28.51	322.58	214.83	65.83	1.38E+05	378.90	3284.85
230.00	13378.78	13394.31	28.51	322.58	218.30	282.89	1.84E+05	503.56	4413.02

240.00	14546.30	14560.25	28.51	322.56	232.94	250.73	2.35E+05	644.38	5737.87
250.01	15812.24	15856.82	28.51	322.55	214.51	76.73	3.00E+05	822.19	7337.32
260.01	17220.18	17268.59	28.51	322.54	224.31	91.16	3.44E+05	941.64	8818.67
270.00	18777.73	18824.02	28.51	322.53	194.88	54.10	3.89E+05	1064.93	10030.82
280.01	20522.51	20530.02	28.51	322.51	157.16	347.30	4.35E+05	1192.05	11290.83
290.00	22418.24	22469.83	28.51	322.51	264.06	129.46	3.54E+05	969.04	10798.17
300.01	24551.35	24629.61	28.51	322.50	236.55	102.75	3.27E+05	895.07	9329.90
310.00	26948.70	27035.26	28.51	322.48	252.35	110.51	1.76E+05	482.19	6879.01
320.01	29679.89	29728.93	28.51	322.48	103.42	63.93	1.17E+05	320.27	4014.93
330.01	32753.45	32805.16	28.51	322.47	68.55	75.88	6.29E+04	172.33	2464.52
340.02	36207.57	36365.96	28.51	322.46	241.54	94.67	1.92E+04	52.60	1125.81
350.02	40223.53	40372.64	28.51	322.45	308.02	106.21	5.01E+03	13.72	331.34
360.04	44848.97	45043.53	28.51	322.43	329.01	102.18	4.23E+02	1.16	74.52
370.03	50188.41	50488.75	28.51	322.42	310.05	98.09	3.53E+01	0.10	6.27
380.02	56449.95	56864.92	28.51	322.39	286.93	100.28	1.08E+01	0.03	0.63
390.04	63904.70	64450.48	28.51	322.33	313.31	97.23	3.84E-01	0.00	0.15
							Total		162983.05

Table 6-5 Case 7 Orbital Parameters, Dose Rate and Total Dose for Solar Maximum with 3 mm of Aluminum Shielding

Time (Days)	Perigee (km)	Apogee (km)	Inclination	Right Ascension Node	Argument of Perigee	True Anomaly (deg)	Rads/year	Dose Rate/Day	Dose
0.00	1202.06	1217.87	28.51	322.65	225.85	48.15	6.79E+04	186.03	0.00
10.00	1446.16	1461.34	28.51	322.65	230.34	217.39	2.27E+04	62.16	1241.11
20.00	1702.42	1718.89	28.51	322.65	225.46	27.09	4.90E+04	134.33	982.54
30.00	1973.69	1989.65	28.51	322.64	230.34	230.73	9.07E+04	248.44	1913.57
40.00	2259.71	2276.63	28.51	322.64	230.23	196.80	1.42E+05	389.86	3191.40
50.00	2562.32	2579.61	28.51	322.64	224.96	348.57	1.94E+05	531.51	4607.92
60.00	2882.66	2899.88	28.51	322.63	224.62	347.63	2.41E+05	659.45	5953.51
70.00	3222.86	3239.57	28.51	322.63	226.62	280.73	2.80E+05	765.75	7126.37
80.00	3583.07	3600.77	28.51	322.63	230.37	201.17	2.75E+05	754.25	7601.46
90.00	3965.52	3984.26	28.51	322.62	232.45	154.44	2.53E+05	692.60	7233.19
100.00	4373.73	4391.31	28.51	322.62	232.70	214.36	2.35E+05	644.38	6685.36
110.00	4806.52	4827.64	28.51	322.62	226.82	77.99	2.03E+05	555.34	5999.45
120.00	5269.89	5291.29	28.51	322.62	232.59	140.09	1.65E+05	451.78	5036.02
130.00	5764.23	5786.81	28.51	322.61	230.23	113.13	1.40E+05	382.19	4169.29
140.00	6294.13	6316.91	28.51	322.61	223.79	56.21	1.16E+05	317.26	3497.12
150.00	6863.11	6884.78	28.51	322.61	218.81	16.45	1.02E+05	280.00	2986.17
160.00	7472.06	7496.40	28.51	322.61	219.30	42.52	9.59E+04	262.77	2713.43
170.00	8129.99	8151.58	28.51	322.61	240.89	181.92	1.03E+05	281.10	2719.98
180.00	8836.94	8860.58	28.51	322.60	241.59	158.78	1.31E+05	358.36	3197.34
190.00	9600.89	9626.53	28.51	322.60	216.18	30.93	1.68E+05	460.27	4092.09
200.00	10428.16	10455.84	28.51	322.59	240.61	145.66	2.33E+05	638.63	5495.52
210.00	11332.34	11349.41	28.51	322.59	222.38	277.48	3.04E+05	832.33	7355.01
220.00	12301.89	12336.20	28.51	322.58	214.83	65.83	4.06E+05	1112.88	9725.80

230.00	13378.78	13394.31	28.51	322.58	218.30	282.89	5.09E+05	1395.07	12541.69
240.00	14546.30	14560.25	28.51	322.56	232.94	250.73	5.97E+05	1634.25	15141.67
250.01	15812.24	15856.82	28.51	322.55	214.51	76.73	6.66E+05	1824.93	17306.38
260.01	17220.18	17268.59	28.51	322.54	224.31	91.16	6.78E+05	1856.99	18408.54
270.00	18777.73	18824.02	28.51	322.53	194.88	54.10	6.31E+05	1728.77	17925.09
280.01	20522.51	20530.02	28.51	322.51	157.16	347.30	5.81E+05	1592.60	16615.53
290.00	22418.24	22469.83	28.51	322.51	264.06	129.46	3.90E+05	1068.22	13295.11
300.01	24551.35	24629.61	28.51	322.50	236.55	102.75	3.28E+05	897.81	9840.00
310.00	26948.70	27035.26	28.51	322.48	252.35	110.51	1.73E+05	472.88	6846.17
320.01	29679.89	29728.93	28.51	322.48	103.42	63.93	1.15E+05	316.16	3947.76
330.01	32753.45	32805.16	28.51	322.47	68.55	75.88	6.29E+04	172.38	2444.23
340.02	36207.57	36365.96	28.51	322.46	241.54	94.67	1.92E+04	52.60	1126.08
350.02	40223.53	40372.64	28.51	322.45	308.02	106.21	5.01E+03	13.72	331.34
360.04	44848.97	45043.53	28.51	322.43	329.01	102.18	4.23E+02	1.16	74.52
370.03	50188.41	50488.75	28.51	322.42	310.05	98.09	3.53E+01	0.10	6.27
380.02	56449.95	56864.92	28.51	322.39	286.93	100.28	1.08E+01	0.03	0.63
390.04	63904.70	64450.48	28.51	322.33	313.31	97.23	3.84E-01	0.00	0.15
							Total		239374.80

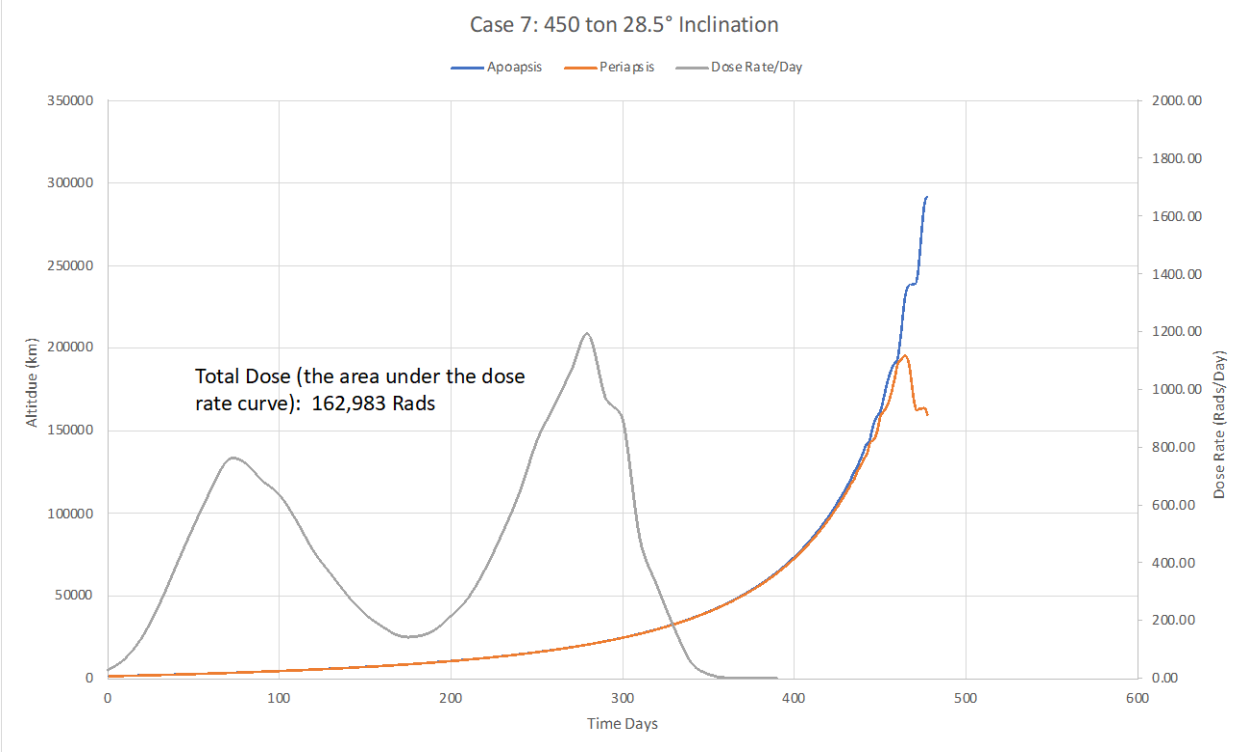

Figure 6-8 Case 7 Dose Rate During Solar Minimum with 3 mm of Aluminum Shielding

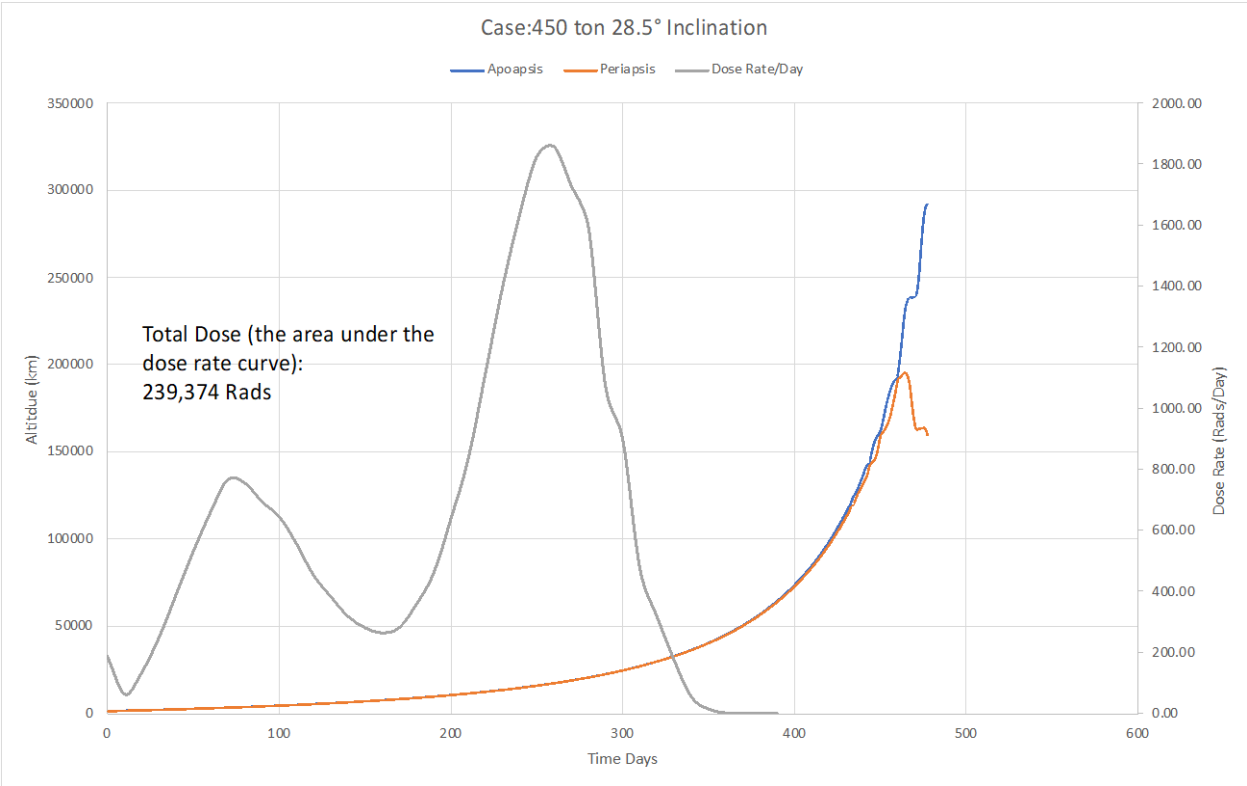

Figure 6-9 Case 7 Dose Rate During Solar Maximum with 3 mm of Aluminum Shielding

Table 6-6 Case 7 Orbital Parameters, Dose Rate and Total Dose for Solar Minimum with 1 cm of Aluminum Shielding

Time (Days)	Perigee (km)	Apogee (km)	Inclination	Right Ascension Node	Argument of Perigee	True Anomaly (deg)	Rads/year	Dose Rate/Day	Dose
0.00	1202.06	1217.87	28.51	322.65	225.85	48.15	4.90E+03	13.41	0.00
10.00	1446.16	1461.34	28.51	322.65	230.34	217.39	1.09E+04	29.86	216.41
20.00	1702.42	1718.89	28.51	322.65	225.46	27.09	2.02E+04	55.42	426.47
30.00	1973.69	1989.65	28.51	322.64	230.34	230.73	3.17E+04	86.96	711.82
40.00	2259.71	2276.63	28.51	322.64	230.23	196.80	4.22E+04	115.62	1012.84
50.00	2562.32	2579.61	28.51	322.64	224.96	348.57	4.87E+04	133.51	1245.91
60.00	2882.66	2899.88	28.51	322.63	224.62	347.63	5.19E+04	142.25	1378.47
70.00	3222.86	3239.57	28.51	322.63	226.62	280.73	5.23E+04	143.34	1428.01
80.00	3583.07	3600.77	28.51	322.63	230.37	201.17	4.62E+04	126.44	1349.16
90.00	3965.52	3984.26	28.51	322.62	232.45	154.44	3.73E+04	102.27	1143.39
100.00	4373.73	4391.31	28.51	322.62	232.70	214.36	3.02E+04	82.60	924.44
110.00	4806.52	4827.64	28.51	322.62	226.82	77.99	2.25E+04	61.75	721.88
120.00	5269.89	5291.29	28.51	322.62	232.59	140.09	1.60E+04	43.78	527.71
130.00	5764.23	5786.81	28.51	322.61	230.23	113.13	1.12E+04	30.71	372.41
140.00	6294.13	6316.91	28.51	322.61	223.79	56.21	7.22E+03	19.78	252.47
150.00	6863.11	6884.78	28.51	322.61	218.81	16.45	4.43E+03	12.15	159.65
160.00	7472.06	7496.40	28.51	322.61	219.30	42.52	2.83E+03	7.74	99.42
170.00	8129.99	8151.58	28.51	322.61	240.89	181.92	1.63E+03	4.47	61.04
180.00	8836.94	8860.58	28.51	322.60	241.59	158.78	9.90E+02	2.71	35.89
190.00	9600.89	9626.53	28.51	322.60	216.18	30.93	6.98E+02	1.91	23.13
200.00	10428.16	10455.84	28.51	322.59	240.61	145.66	6.21E+02	1.70	18.08
210.00	11332.34	11349.41	28.51	322.59	222.38	277.48	7.10E+02	1.95	18.23
220.00	12301.89	12336.20	28.51	322.58	214.83	65.83	9.91E+02	2.71	23.30
230.00	13378.78	13394.31	28.51	322.58	218.30	282.89	1.19E+03	3.27	29.90

240.00	14546.30	14560.25	28.51	322.56	232.94	250.73	1.25E+03	3.43	33.47
250.01	15812.24	15856.82	28.51	322.55	214.51	76.73	1.27E+03	3.48	34.57
260.01	17220.18	17268.59	28.51	322.54	224.31	91.16	1.26E+03	3.45	34.64
270.00	18777.73	18824.02	28.51	322.53	194.88	54.10	1.29E+03	3.53	34.88
280.01	20522.51	20530.02	28.51	322.51	157.16	347.30	1.39E+03	3.82	36.75
290.00	22418.24	22469.83	28.51	322.51	264.06	129.46	1.26E+03	3.44	36.28
300.01	24551.35	24629.61	28.51	322.50	236.55	102.75	1.33E+03	3.64	35.43
310.00	26948.70	27035.26	28.51	322.48	252.35	110.51	9.12E+02	2.50	30.64
320.01	29679.89	29728.93	28.51	322.48	103.42	63.93	7.04E+02	1.93	22.15
330.01	32753.45	32805.16	28.51	322.47	68.55	75.88	5.31E+02	1.45	16.92
340.02	36207.57	36365.96	28.51	322.46	241.54	94.67	2.57E+02	0.70	10.80
350.02	40223.53	40372.64	28.51	322.45	308.02	106.21	1.28E+02	0.35	5.26
360.04	44848.97	45043.53	28.51	322.43	329.01	102.18	3.85E+01	0.11	2.28
370.03	50188.41	50488.75	28.51	322.42	310.05	98.09	7.80E+00	0.02	0.63
380.02	56449.95	56864.92	28.51	322.39	286.93	100.28	2.83E+00	0.01	0.15
390.04	63904.70	64450.48	28.51	322.33	313.31	97.23	9.74E-02	0.00	0.04
							Total		12514.95

Table 6-7 Case 7 Orbital Parameters, Dose Rate and Total Dose for Solar Maximum with 1 cm of Aluminum Shielding

Time (Days)	Perigee (km)	Apogee (km)	Inclination	Right Ascension Node	Argument of Perigee	True Anomaly (deg)	Rads/year	Dose Rate/Day	Dose
0.00	1202.06	1217.87	28.51	322.65	225.85	48.15	4.17E+03	11.42	0.00
10.00	1446.16	1461.34	28.51	322.65	230.34	217.39	1.09E+04	29.86	206.46
20.00	1702.42	1718.89	28.51	322.65	225.46	27.09	1.82E+04	49.97	399.21
30.00	1973.69	1989.65	28.51	322.64	230.34	230.73	2.98E+04	81.59	657.72
40.00	2259.71	2276.63	28.51	322.64	230.23	196.80	4.06E+04	111.10	963.39
50.00	2562.32	2579.61	28.51	322.64	224.96	348.57	4.77E+04	130.77	1209.60
60.00	2882.66	2899.88	28.51	322.63	224.62	347.63	5.17E+04	141.56	1361.35
70.00	3222.86	3239.57	28.51	322.63	226.62	280.73	5.27E+04	144.30	1429.38
80.00	3583.07	3600.77	28.51	322.63	230.37	201.17	4.67E+04	127.89	1361.22
90.00	3965.52	3984.26	28.51	322.62	232.45	154.44	3.80E+04	104.19	1160.24
100.00	4373.73	4391.31	28.51	322.62	232.70	214.36	3.10E+04	84.99	945.95
110.00	4806.52	4827.64	28.51	322.62	226.82	77.99	2.36E+04	64.52	747.64
120.00	5269.89	5291.29	28.51	322.62	232.59	140.09	1.69E+04	46.41	554.70
130.00	5764.23	5786.81	28.51	322.61	230.23	113.13	1.22E+04	33.32	398.58
140.00	6294.13	6316.91	28.51	322.61	223.79	56.21	8.14E+03	22.30	278.07
150.00	6863.11	6884.78	28.51	322.61	218.81	16.45	5.31E+03	14.56	184.28
160.00	7472.06	7496.40	28.51	322.61	219.30	42.52	3.68E+03	10.08	123.19
170.00	8129.99	8151.58	28.51	322.61	240.89	181.92	2.42E+03	6.64	83.64
180.00	8836.94	8860.58	28.51	322.60	241.59	158.78	1.71E+03	4.68	56.59
190.00	9600.89	9626.53	28.51	322.60	216.18	30.93	1.34E+03	3.67	41.73
200.00	10428.16	10455.84	28.51	322.59	240.61	145.66	1.25E+03	3.41	35.42
210.00	11332.34	11349.41	28.51	322.59	222.38	277.48	1.37E+03	3.76	35.86
220.00	12301.89	12336.20	28.51	322.58	214.83	65.83	1.76E+03	4.83	42.96
230.00	13378.78	13394.31	28.51	322.58	218.30	282.89	2.09E+03	5.72	52.75

240.00	14546.30	14560.25	28.51	322.56	232.94	250.73	2.21E+03	6.04	58.78
250.01	15812.24	15856.82	28.51	322.55	214.51	76.73	2.22E+03	6.09	60.69
260.01	17220.18	17268.59	28.51	322.54	224.31	91.16	2.14E+03	5.87	59.79
270.00	18777.73	18824.02	28.51	322.53	194.88	54.10	2.00E+03	5.48	56.77
280.01	20522.51	20530.02	28.51	322.51	157.16	347.30	1.96E+03	5.37	54.29
290.00	22418.24	22469.83	28.51	322.51	264.06	129.46	1.52E+03	4.15	47.56
300.01	24551.35	24629.61	28.51	322.50	236.55	102.75	1.44E+03	3.95	40.56
310.00	26948.70	27035.26	28.51	322.48	252.35	110.51	9.45E+02	2.59	32.68
320.01	29679.89	29728.93	28.51	322.48	103.42	63.93	7.23E+02	1.98	22.86
330.01	32753.45	32805.16	28.51	322.47	68.55	75.88	5.37E+02	1.47	17.27
340.02	36207.57	36365.96	28.51	322.46	241.54	94.67	2.57E+02	0.70	10.89
350.02	40223.53	40372.64	28.51	322.45	308.02	106.21	1.28E+02	0.35	5.26
360.04	44848.97	45043.53	28.51	322.43	329.01	102.18	3.85E+01	0.11	2.28
370.03	50188.41	50488.75	28.51	322.42	310.05	98.09	7.80E+00	0.02	0.63
380.02	56449.95	56864.92	28.51	322.39	286.93	100.28	2.83E+00	0.01	0.15
390.04	63904.70	64450.48	28.51	322.33	313.31	97.23	9.74E-02	0.00	0.04
							Total		12800.41

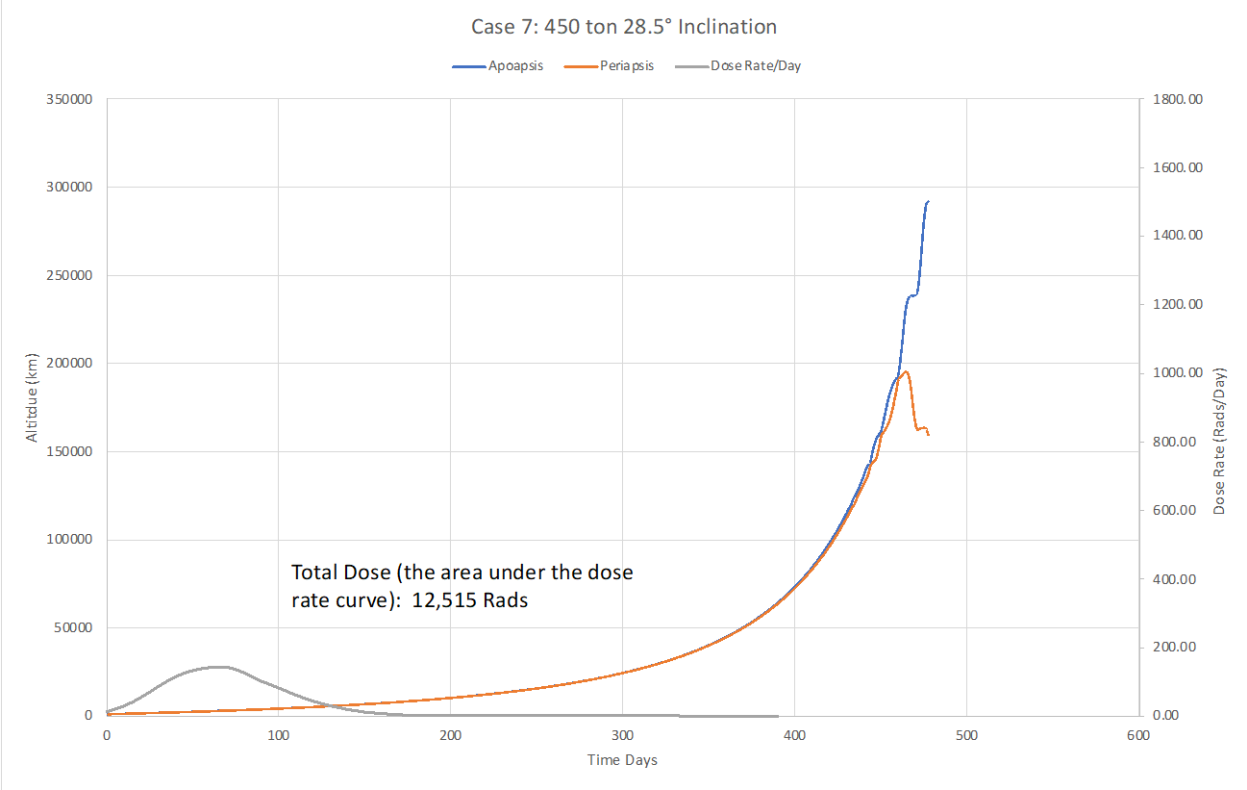

Figure 6-10 Case 7 Dose Rate During Solar Minimum with 1 mm of Aluminum Shielding

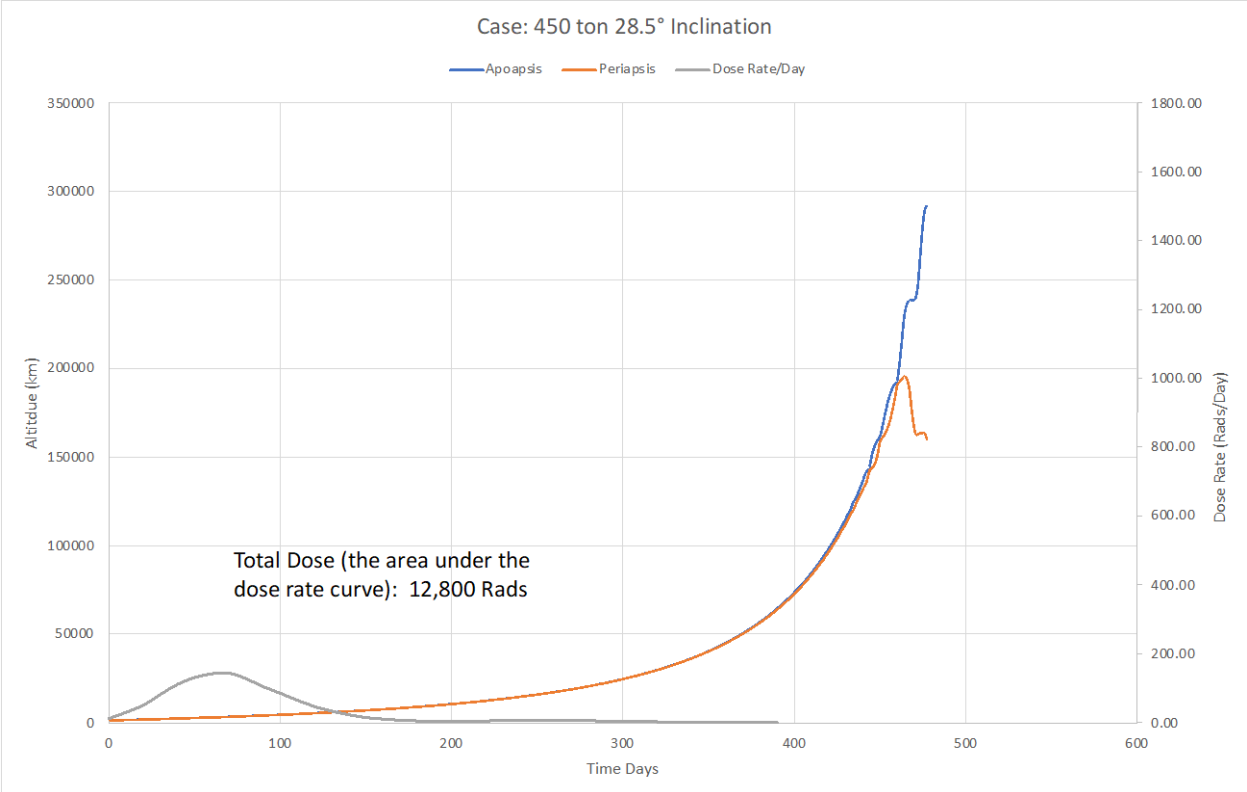

Figure 6-11 Case 7 Dose Rate During Solar Maximum with 1 mm of Aluminum Shielding

These results show that there is a significant reduction in the electronics dose by increasing the shielding thickness from 3 mm to 1 cm. The majority of this reduction occurs due to the effect the thicker shielding has on reducing the dose from the electrons primarily in the outer belt. This is because the lower mass electrons cannot penetrate the thicker aluminum shield thereby reducing the dose on the electronics. The relationship between dose and shielding thickness for this orbit transfer was also produced. This is shown in Figure 6-12 for both the solar maximum and minimum dose rates.

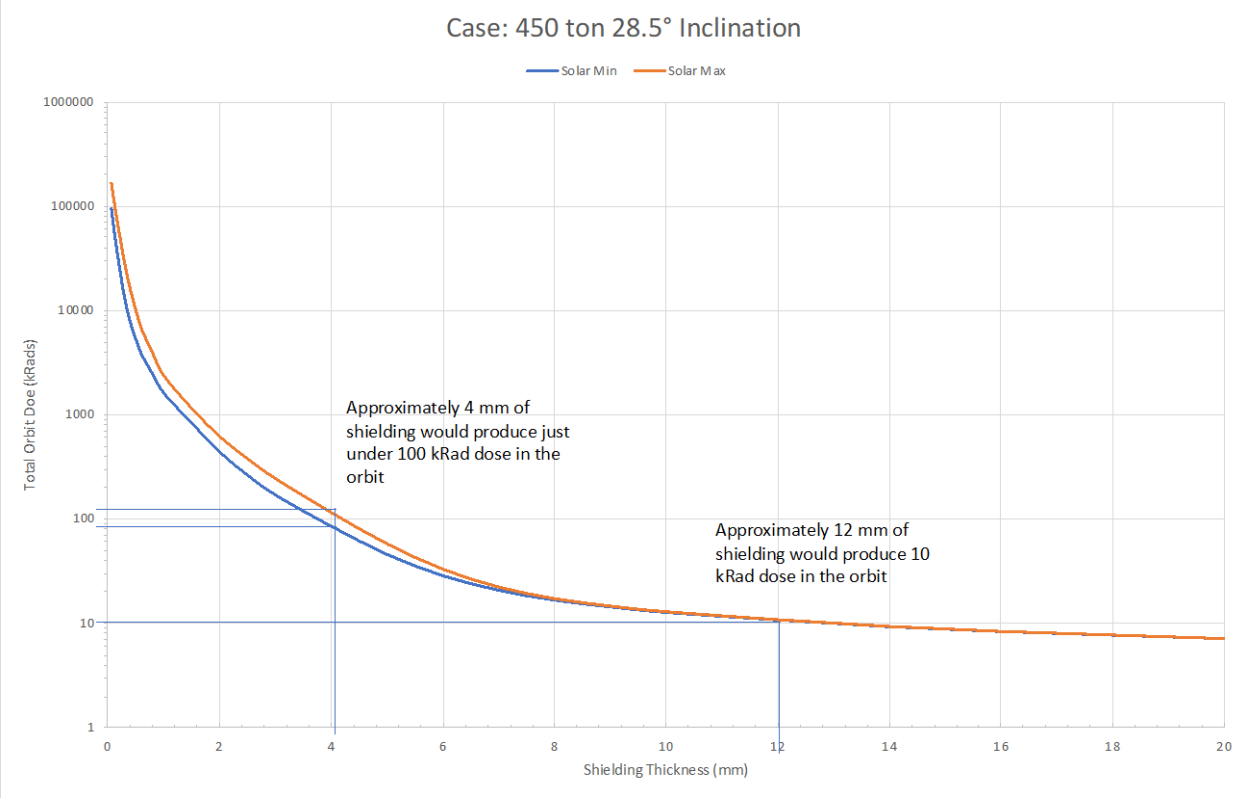

Figure 6-12 Total Electronics Dose as a function of the Aluminum Shielding Thickness

These results show that a shielding thickness of 4 mm will limit the dose to approximately 100 krad during the transit. This is the total expected lifetime dose for the electronics. To reduce this to 10% of the lifetime does the shielding thickness would need to be increased to 1.2 cm.

APPENDIX D Micrometeor and Orbital Debris Protection

Because the spacecraft will spend a considerable amount of time in LEO during buildup, the issue of impact with MMOD is a concern. The buildup altitude was selected as 500 km and it was estimated that the buildup time would take one year. The MMOD evaluation was done to determine what level of shielding, if any, would be needed to reduce the probability of impact that would cause damage to a critical component of the spacecraft to 0.1% or less. The component of the spacecraft that is most susceptible to damage is the Xenon tanks. This is due to their size, structural wall thickness and that a puncture of the tank wall will cause a critical failure of the tank. Therefore, the protection of the Xenon tanks from MMOD impacts was used as a proxy for protecting the complete spacecraft.

There are a number of different models that predict the MMOD density or flux as a function of altitude. Particles larger than 10 cm can be tracked by radar. Their distribution is shown in Figure 6-13 for altitudes up to 2,000 km and at a larger scale in Figure 6-14 for altitudes up to 50,000 km. The densities of particles this size or larger usually correspond to a known breakup of a spacecraft.

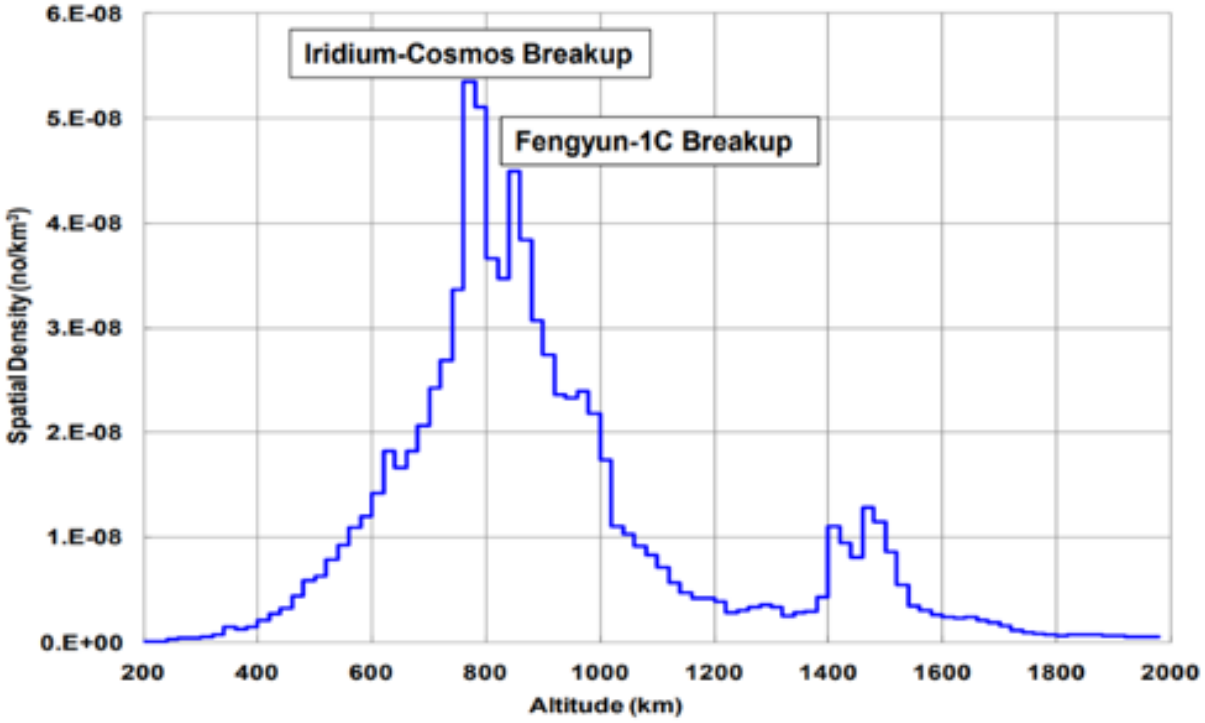

Figure 6-13 Observed Spatial Density for Particles Larger Than 10 cm in Size Up to Altitudes of 2,000 km

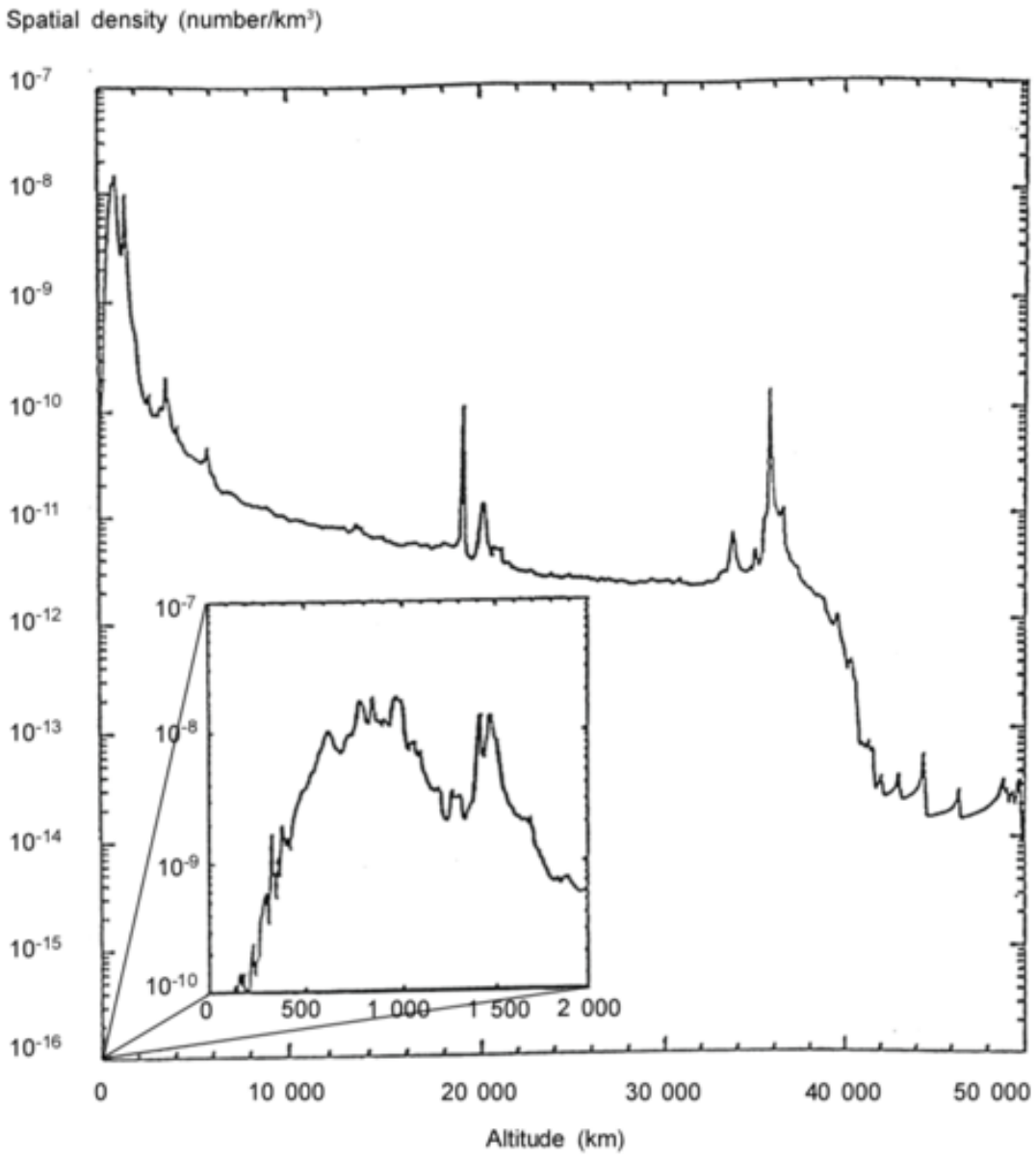

Figure 6-14 Observed Spatial Density for Particles Larger Than 10 cm in Size Up to Altitudes of 50,000 km

For particles smaller than 10 cm models are used to estimate their spatial density. The ESA model for particles greater than 1 mm in size is shown in Figure 6-15. This figure shows that the estimated special density of MMOD particles greater than 1 mm in size at 500 km is approximately 1.5E-5 particles per cubic kilometer. The distribution range for three orders in magnitude of particle size, less than or equal to 1 mm, 1 cm and 10 cm, compiled from a number of sources is shown in Figure 6-16.

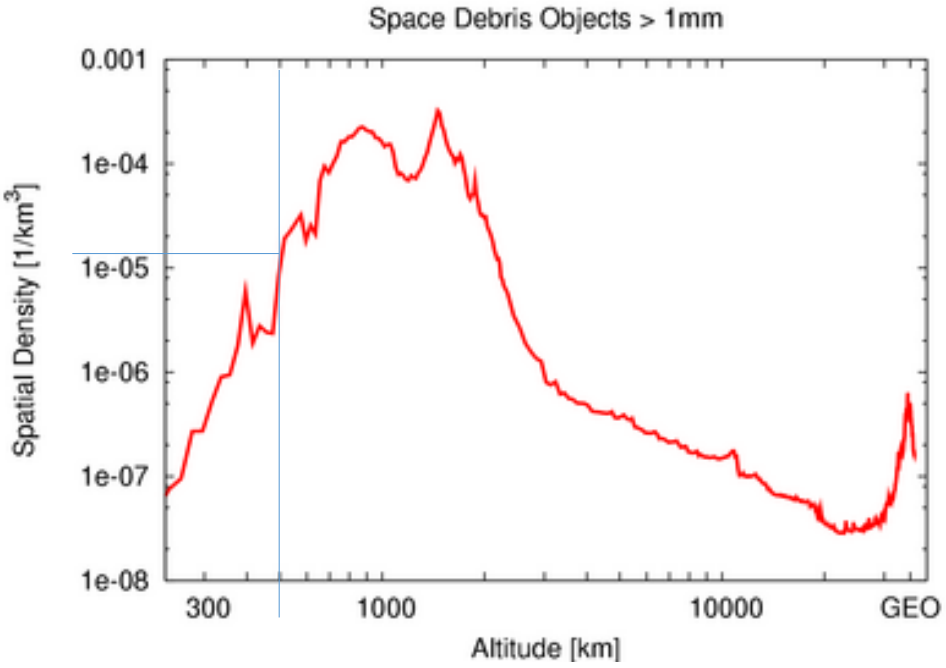

Figure 6-15 ESA [46] Model MMOD Particle Distribution as a Function of Altitude for Particles Larger than 1 mm

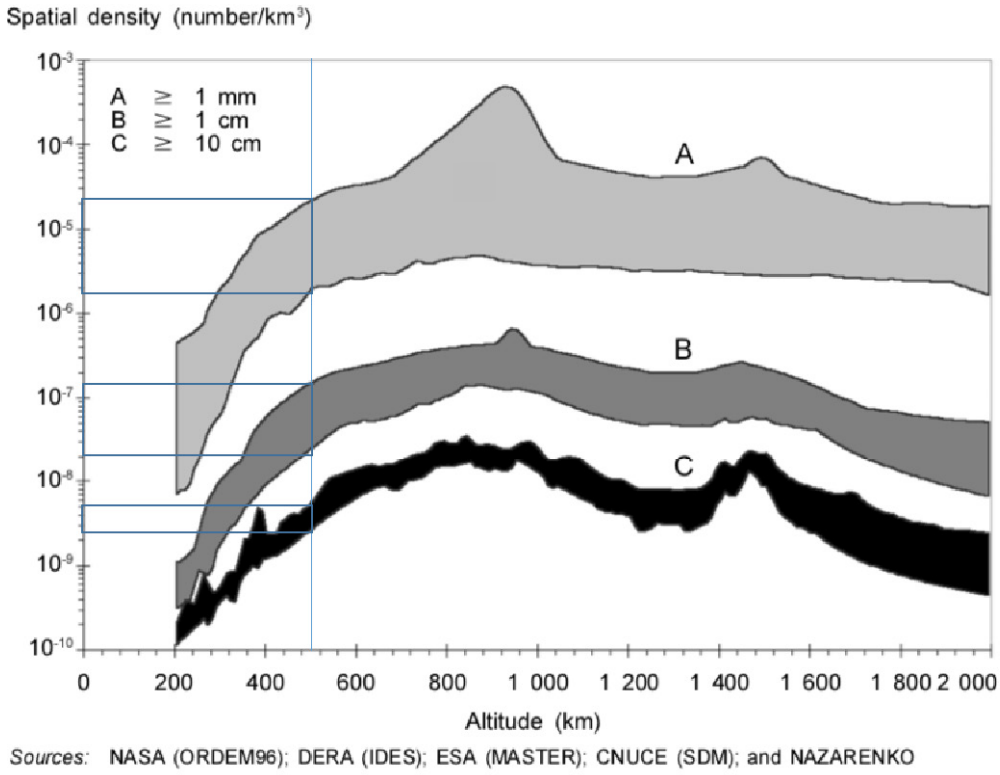

Figure 6-16 MMOD Particle Distribution as a Function of Altitude for Particles Based on Orders of Magnitude (> 1 mm, >1 cm, >10 cm)

From Figure 6-16 for the buildup altitude of 500 km the MMOD spatial density flux range is given in Table 6-8 for each class of particle size.

Table 6-8 Particle Size Class and Corresponding Spatial Density Range

Particle Size	Lower Spatial Density (Particles / km^3)	Upper Spatial Density (Particles / km^3)
>= 10 cm	$2.8X10^{-9}$	$5X10^{-9}$
>= 1 cm	$2X10^{-8}$	$1.6X10^{-7}$
>= 1 mm	$1.6X10^{-6}$	$2.1X10^{-5}$

The primary direction for the MMOD impacts on the spacecraft while in orbit is along the axis normal to the orbital velocity direction or ram direction as illustrated in Figure 6-17.

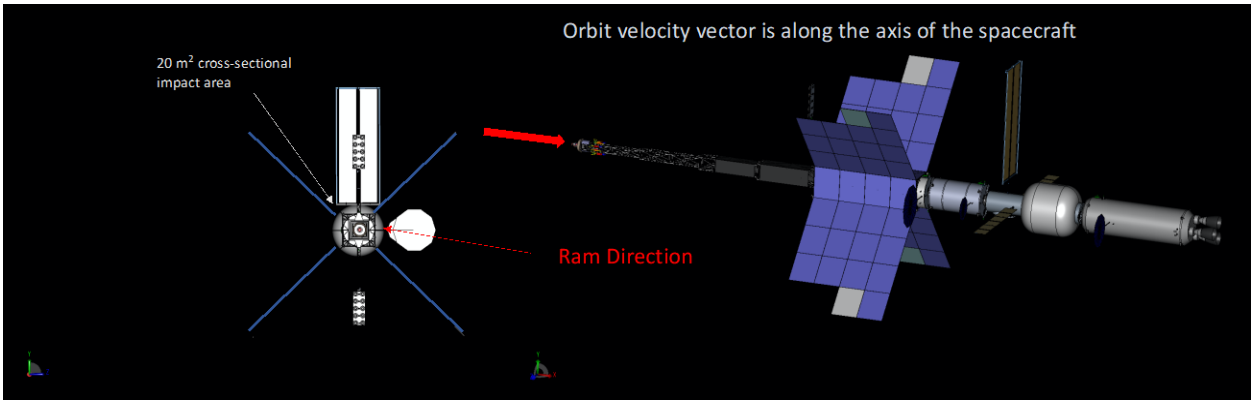

Figure 6-17 Spacecraft Orbital Flight Orientation

Since the MMOD particles are also in orbit at the flight altitude the majority will hit the spacecraft in the cross-sectional area associated with the ram flight direction. The initial Xenon tank located in the nuclear section of the spacecraft is the tank that is most at risk for impact. There is a structural bulkhead in front of this tank that can provide some shielding for the MMOD particles. This bulkhead orientation is illustrated in Figure 6-17.

The bulkhead is constructed of carbon fiber composite and is spaced a distance 14.8 cm from the tank wall. The tank is surround by MLI has a wall thickness of 28 mm and is composed of T1000 carbon composite. The frontal area that is in the primary path of the MMOD particles has a cross-sectional area of approximately 20 m^2. To evaluate the probability of an impact on the tank the flux density at the orbital location has to be determined. This flux density (particles/m^2-yr) as a function of the particle mass at the 500 km buildup altitude was calculated using the Grün meteoroid model [47]. This is shown in Figure 6-19 for particle masses up to 1 gm.

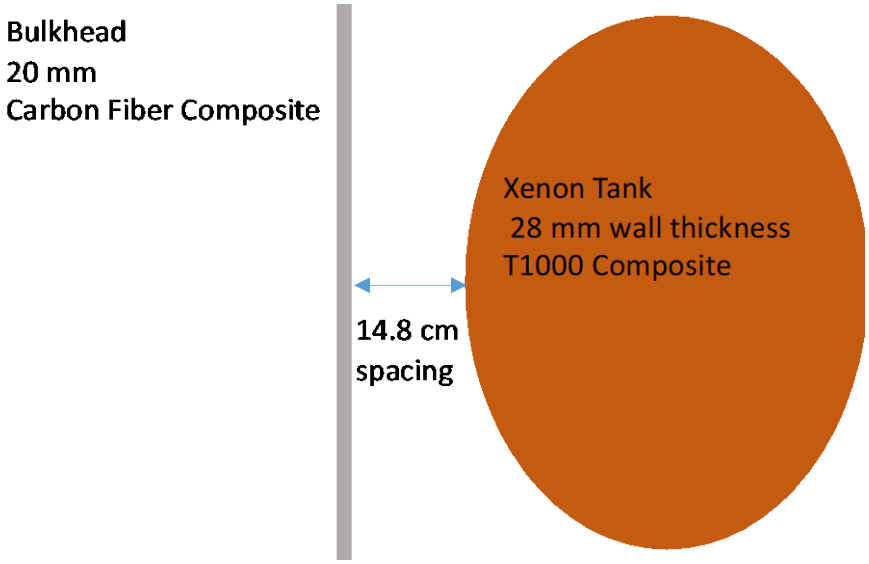

Figure 6-18 Illustration of the Initial Xenon Tank and Bulkhead

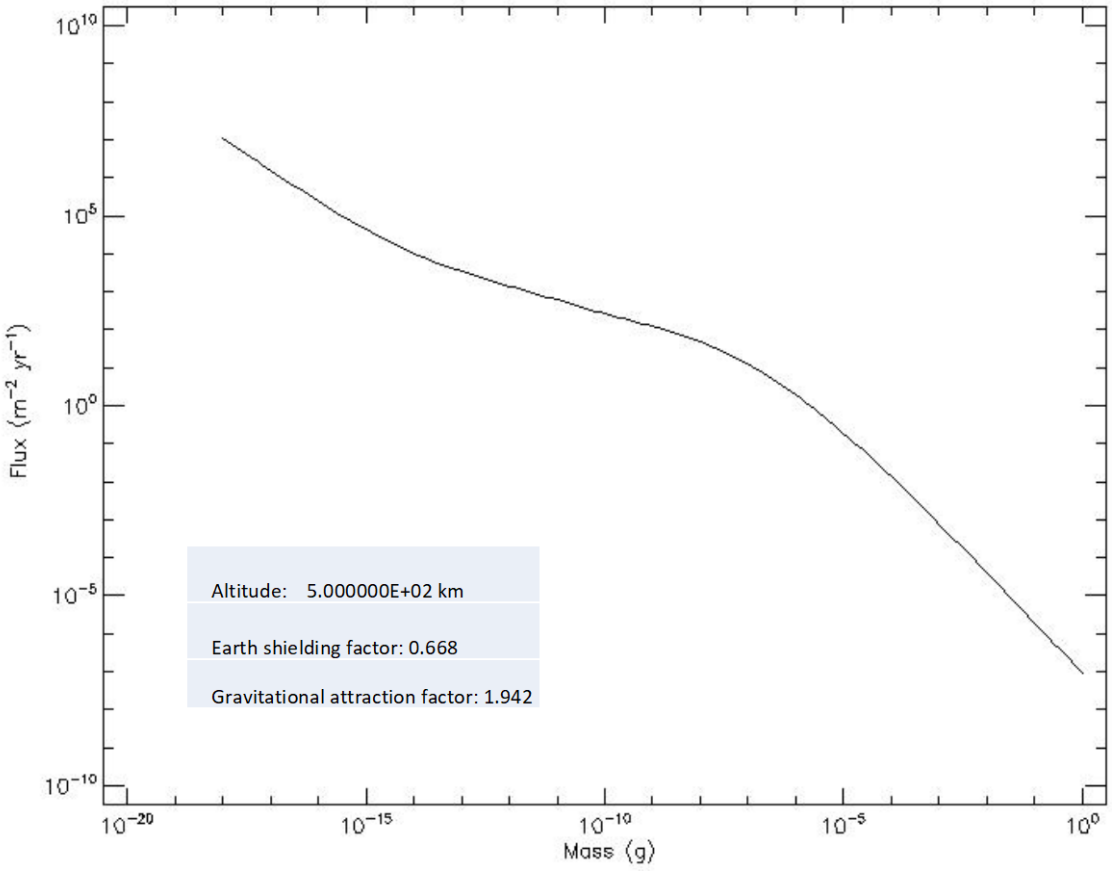

Figure 6-19 Flux Density (Particles/m^2-year) vs. Particle Mass (gm) at 500 km Altitude

The bulkhead in front of the initial tank acts as a Whipple shield breaking apart any particles that could impact the tank into smaller sizes and reducing their kinetic energy. An analysis was performed to determine the critical particle size that could penetrate the tank as a function of the particle velocity. This analysis is based on the thickness and spacing of the bulkhead and tank. The results of this analysis are shown in Figure 6-20.

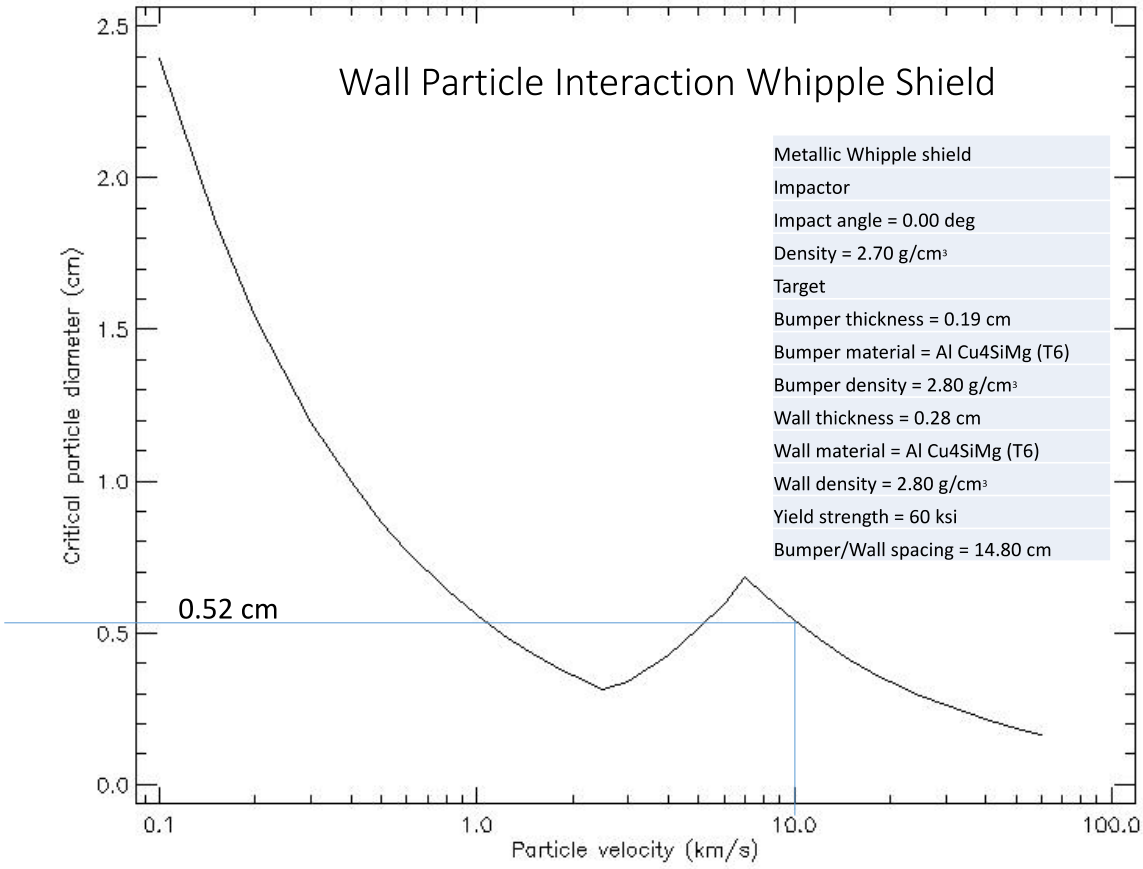

Figure 6-20 Critical Particle Size to Penetrate the Xenon Tank as a Function of Particle Velocity

Figure 6-20 shows the critical particle size for penetration into the Xenon tank. The particle size represents the size particle that can penetrate the tank and cause a failure. For this analysis an aluminum composite that had a similar density to the carbon fiber was utilized for both the bumper material as well as the tank wall. This was done because the material database for the analysis tool did not have the carbon fiber material as an option. Based on the orbit it is assumed that the impact particle velocity will be approximately 10 km/s. For the assumed material properties and geometry between the bulkhead and tank the minimum particle size that is needed to penetrate the tank is 0.52 cm.

To determine the frequency of impact for a particle of this size the flux distribution shown in Figure 6-19 has to be converted to a particle size. For the critical particle diameter analysis, it was assumed that the particle density was 2.7 g/cm^3. Using this density, the curve in Figure 6-19 can be converted to a particle diameter as a function off impacts per year for a 20 m^2 cross-sectional impact area. These results are shown in Figure 6-21.

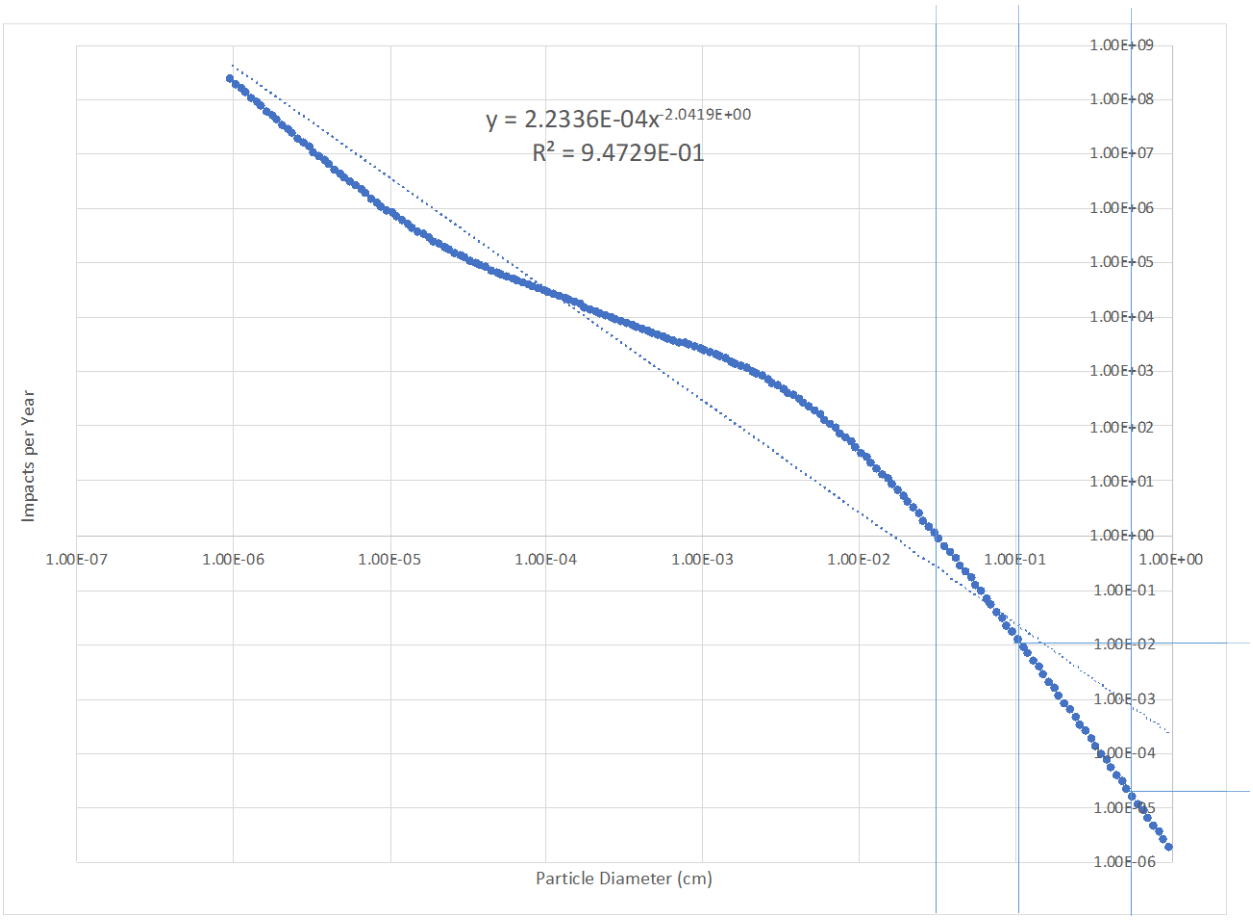

Figure 6-21 Impacts Per Year as a Function of Particle Diameter

These results show that a particle of a size less than 0.3 mm will impact this area within the 1-year buildup duration and there is a 1% chance that a particle with a size of 1 mm will impact the area. For a failure of the tank to occur, from Figure 6-20, a particle of 0.52 cm diameter would need to impact this area. Based on the results shown in Figure 6-21 this will occur 2.1×10^{-5} times per year. Which represents a 0.002% chance of an impact within the one-year buildup duration. Based on this analysis it was determined that no additional MMOD shielding would be needed to protect the tanks during the buildup period.

APPENDIX E Acronyms and Abbreviations

ΔV	Delta-V, Change in Velocity
Å	Angstroms
ACS	Attitude Control System
AD&C	Attitude, Determination & Control
AEPS	Advanced Electrical Propulsion System
AES	Advanced Exploration Systems
Ah	Ampere (or Amp) Hour
AIAA	American Institute for Aeronautics and Astronautics
AMPS	Advanced Modular Power System
Ar	Radiator Area
ARU	Array Regulator Unit
ATV	Autonomous Transfer Vehicle
AU	Astronomical Unit
BAC	Broad Area Cooling
BCDU	Battery Charge-Discharge Unit
BDCM	Bi-Directional Converter Modules
BOL	Beginning of Life
BRU	Brayton Rotating Unit
C&DH	Command and Data Handling
CAD	Computer Aided Design
CBE	Current Best Estimate
CDT	Centerline Docking Target
CER	Cost Estimating Relationships
CLV	Commercial Launch Vehicles
CG	Center of Gravity
CH_4	Methane
CH_4/O_2	methane oxygen
CM	Center of Mass
CO_2	Carbon Dioxide
CONOPS	Concept of Operations
COPV	Composite Overwrapped Pressure Vessel
COTS	Commercial Off-The-Shelf
cPCI	Compact Peripheral Component Interconnect
CTLM	Controller Module
DC	Direct Current
DCIU	Digital Control Interface Unit
DDCU	DC-DC Converter Unit
DDT&E	Design Development Test and Evaluation
DDU	Direct Drive Unit
DOD	Depth of Discharge
DOE	Department of Energy
DOF	Degrees of Freedom
DSH	Deep-Space Habitat
DSM	Deep Space Maneuver
DST	Deep Space Transport
DTE	Direct to Earth
ECM	Exploration Crew Module
EDAC	Error Detection and Correction
EDM	Earth Departure Mass
EOI	Earth Orbit Insertion
EOL	End of Life
EOM	End of Mission
EP	Electric Propulsion
EPS	Electrical Power System
ESA	European Space Agency
ESOC	European Space Operations Center
FEA	Finite Element Analysis
FOM	Figure of Merit
GG	Gravity Gradient
GN&C	Guidance, Navigation, and Control
GPa	Giga Pascal
GR&A	Ground Rules and Assumptions
GRC	Glenn Research Center

HALEU	High-Assay Low Enriched Uranium (19.75% enrichment)
Hab	Habitat
HCSM	High Current Switchgear Modules
HEO	High Earth Orbit
HEO	Human Exploration Office
HERMeS	Hall Effect Rocket with Magnetic Shielding
HEU	Highly Enriched Uranium
HeXe	Helium Xenon
HKPM	Housekeeping Power Modules
IDDS	International Docking System Standard
IMLI	Integrated Multi-Layered Insulation
IMU	Inertial Measurement Unit
I_{sp}	Specific Impulse
ISS	International Space Station
KBOO	Kuiper Belt Object Orbiter
Klbf	kilopound force
kN	kilonewton
KRAD	KiloRAD (radiation absorbed dose)
ksi	Kilo pound per square inch
kWe	Kilowatt-electric
LB-MLI	Load Bearing Multi-Layer Insulation
LCH_4	Liquid Methane
LDHEO	Lunar Distant High Earth Orbit
LEO	Low Earth Orbit
LEU	Low Enriched Uranium
LGA	Lunar Gravity Assists
Li	Lithium
LIDAR	Light Detection and Ranging
LiH	Lithium Hydride
LOX	Liquid Oxygen
LOX/LCH_4	Liquid Oxygen/Liquid Methane
LSGM	Load Switchgear Module
LV	Launch Vehicle
LVA	Launch Vehicle Adapter
m/s	Meters per second
MAV	Mars Ascent Vehicle
MBSU	Main Bus Switching Unit
MEL	Master Equipment List
MEO	Medium Earth Orbit
MGA	Mass Growth Allowance
MLI	Multi-Layer Insulation
MMH	Monomethyl Hydrazine
MMH/NTO	Monomethyl Hydrazine and Nitrogen Tetroxide Bipropellant System
MMOD	Micrometeoroid and Orbital Debris
MMPDS	Metallic Materials Properties Development and Standardization
MOI	Mars Orbit Insertion
MOI	Moments of Inertia
MOP	Mean Operating Pressure
MPa	Mega Pascal
MPCV	Multi-Purpose Crew Vehicle
Mr	Radiator Mass
MRAD	MilliRAD
mrem	millirem
MTAS	Mars Transportation Assembly Study
MW	Megawatt
MWe	Megawatts electric
NAFCOM	NASA/Airforce Cost Model
NaK	Sodium and Potassium
NEP	Nuclear Electric Propulsion
NG	Northrup Grumman
NIST	National Institute of Standards and Technology
NPM	Nuclear Power Module
NRHO	Near-Rectilinear Halo Orbit
NSSDC	National Space Science Data Center
NTO	Nitrogen Tetroxide
O_2	Oxygen
O/F	Oxidizer to Fuel Mass Ratio
ORNL	Oak Ridge National Laboratory
P&ID	Plumbing and Instrumentation Diagram

PAF	Payload Attach Fitting
PCB	Printed Circuit Board
PDT	Peripheral Docking Target
PDU	Power Distribution Unit
PEB	Energy Balance Power
PEL	Power Equipment List
PI	Principle Investigator
PLA	Payload Launch Adapter
PM	Project Management
PMAD	Power Management and Distribution
PMC	Polymer-Matrix Composite
PMD	Propellant Management Device
POC	Point of Contact
Pr	Power Rejected
PRT	Perimeter Reflector Targets
RAD	Radiation-Absorbed Dose
RCS	Reaction Control System
rem	Roentgen equivalent man (a large dose of radiation)
RPODU	Rendezvous and Proximity Operations and Docking/Undocking
RCS	Reaction Control System
S/C	Spacecraft
S&MA	Safety and Mission Assurance
SBIR	Small Business Innovation Research
$scCO_2$	supercritical carbon dioxide
SEFI	Single Event Functional Interrupt
SE&I	Systems Engineering and Integration
SEP	Solar Electric Propulsion
SEU	Single Event Upset
SLS	Space Launch System
SOL	Solar Day
SRP	Solar Radiation Pressure
SSU	Sequential Shunt Unit
STS	Space Transportation System
t	Metric Ton
TCR	Transformational Challenge Reactor
TDRS	Trackin And Data Relay Satellite
TEA	Torque Equilibrium Attitude
TEI	Trans Earth Injection
TiH_2O	Titanium in Water
TMI	Trans Mars Injection
TMR	Triple Mode Redundancy
TRL	Technology Readiness Level
TVC	Thrust Vector Control
TVS	Thermal Vent System
U	10 by 10 by 10 cm cube (Cubesat)
UMo	Uranium Molybdenum
UN	Uranium Nitride
VDC	Voltage Direct Current
W	Tungsten
WBS	Work Breakdown Structure
WSB	Weak Stability Bound
Xe	Xenon
YH	Yttrium Hydride

APPENDIX F Study Participants

NEP-Chem 1.2 Design Session			
Subsystem	**Name**	**Center**	**Email**
Design Customer POC/PI	Leonard Dudzinski	HQ	Leonard.dudzinski@nasa.gov
Design Customer POC/PI	Ave Kludze	HQ	Ave.k.kludze@nasa.gov
Compass Team			
Study Lead	Steven Oleson	GRC	Steven.r.oleson@nasa.gov
System Integration, MEL, and Final Report Documentation	Betsy Turnbull	GRC	elizabeth.r.turnbull@nasa.gov
Technical Editing	Lee Jackson	GRC	Lee.a.jackson@nasa.gov
Mission	Laura Burke Dave Smith Steven McCarty Brent Faller	GRC GRC GRC GRC	laura.m.burke@nasa.gov david.a.smith-1@nasa.gov steven.mccarty@nasa.gov brent.f.faller@nasa.gov
Configuration	Thomas Packard	GRC	thomas.w.packard@nasa.gov
Attitude, Determination & Control (AD&C)	Brent Faller Christine Schmid	GRC	brent.f.faller@nasa.gov christine.l.schmid@nasa.gov
Propulsion	Jim Fittje	GRC	james.e.fittje@nasa.gov
Electric Propulsion (EP) Thrusters	John Yim	GRC	john.t.yim@nasa.gov
Thermal Control	Tony Colozza	GRC	anthony.j.colozza@nasa.gov
Radiation	Mike Smith	DOE	smithmb@ornl.gov
Electrical Power	Brandon Klefman Lucia Tian Caroline Austin	GRC GRC GRC	brandon.klefman@nasa.gov lucia.tian@nasa.gov caroline.r.austin@nasa.gov
Nuclear Power	Lee Mason Paul Schmitz	HQ GRC	lee.s.mason@nasa.gov paul.c.schmitz@nasa.gov
Structures	John Gyekenyesi	GRC	john.z.gyekenyesi@nasa.gov
Command and Data Handling (C&DH), Software	W. Peter Simon Christopher Heldman	GRC GRC	william.p.simon@nasa.gov christopher.r.heldman@nasa.gov
Communications	Onoufrios Theofylaktos	GRC	onoufrios.theofylaktos-1@nasa.gov
Cost Estimating	Natalie Weckesser Thomas Parkey	GRC GRC	Natalie.j.weckesser@nasa.gov Thomas.j.parkey@nasa.gov